



SEDIMENTOLOGY OF THE LATE PRECAMBRIAN
MUNDALLIO SUBGROUP : A CLASTIC-CARBONATE
(DOLOMITE, MAGNESITE) SEQUENCE IN THE
MT. LOFTY AND FLINDERS RANGES, SOUTH
AUSTRALIA.

(VOLUME II)

by

ROBIN K. UPPILL, B. Sc. (Hons.) (Adelaide)
Department of Geology and Mineralogy,
The University of Adelaide.

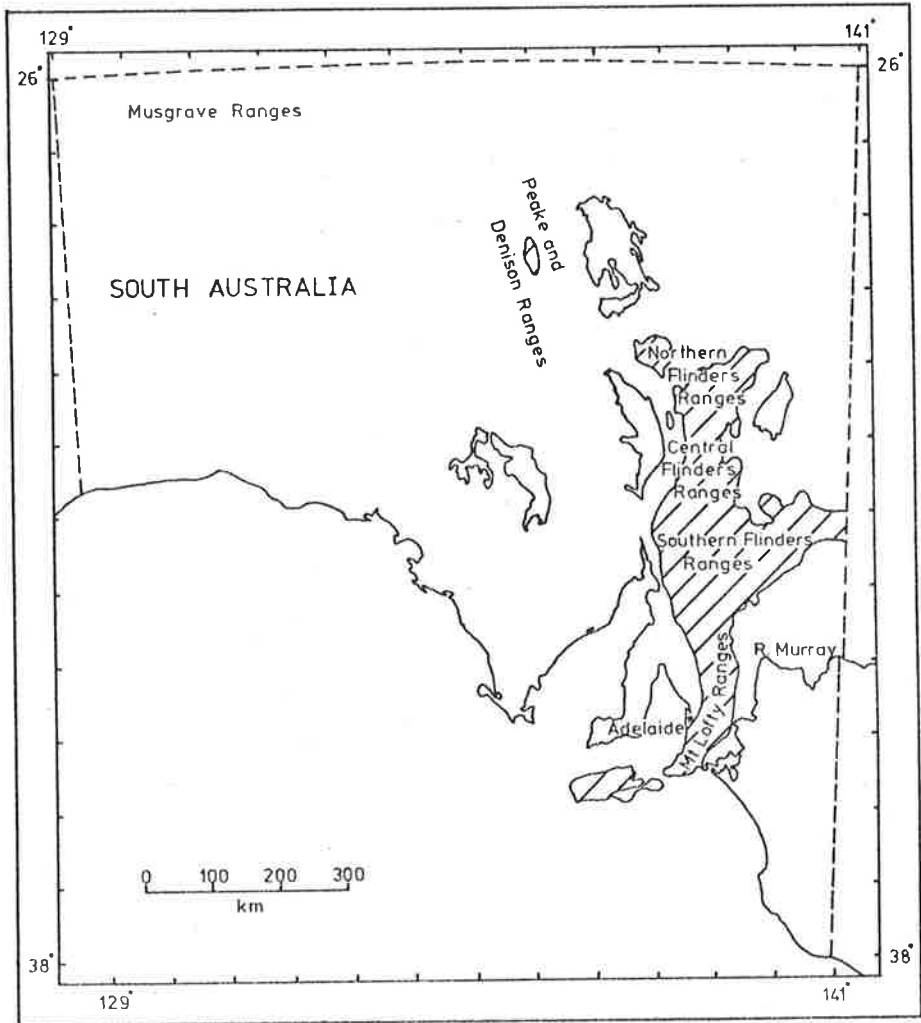
FIGURES, TABLES, PLATES AND APPENDICES

Awarded 13th June 1980

TABLE OF CONTENTS

VOLUME II

Figure	1.1		
	2.1		
Table	2.1		
Figures	3.1	to	6
	4.1	to	14
	5.1	to	3
	6.1	to	16
Table	6.1		
Figures	7.1	to	6
Tables	7.1	to	6
Figures	8.1	to	11
	9.1	to	3
Tables	9.1	to	2
Figures	10.1	to	14
Tables	10.1	to	5
Figures	11.1	to	3
	12.1	to	2
Plates	4.1	to	10
	5.1	to	3
	6.1	to	19
	9.1	to	3
	11.1	to	8
APPENDIX	1	DETAILED LOCATION MAPS OF MEASURED STRATIGRAPHIC SECTIONS	A1
	2	MARKOV CHAIN ANALYSIS: MATRICES	A8
	3	CHEMICAL METHODS	A15
		A. WHOLE ROCK ANALYSES: SHALES	A16
		B. TRACE ELEMENT ANALYSES: CARBONATES	A16
		C. DETERMINATION OF WEIGHT PERCENT MAGNESITE	A16
	4	GEOCHEMICAL DATA: CARBONATE FACIES	A19
		A. DOLOMITE FACIES	A19
		B. MAGNESITE FACIES	A30
	5	REPRINT OF THE PAPER "Stratigraphy and depositional environments of the Mundallio Subgroup (new name) in the late Precambrian Burra Group of the Mt. Lofty and Flinders Ranges".	A32



AOU79

Figure 1.1. Geographical location of study areas: northern Flinders Ranges, and southern Flinders and Mt. Lofty Ranges. Cross-hatched area represents outcrops of folded Adelaidean and Cambrian rocks and associated basement inliers.

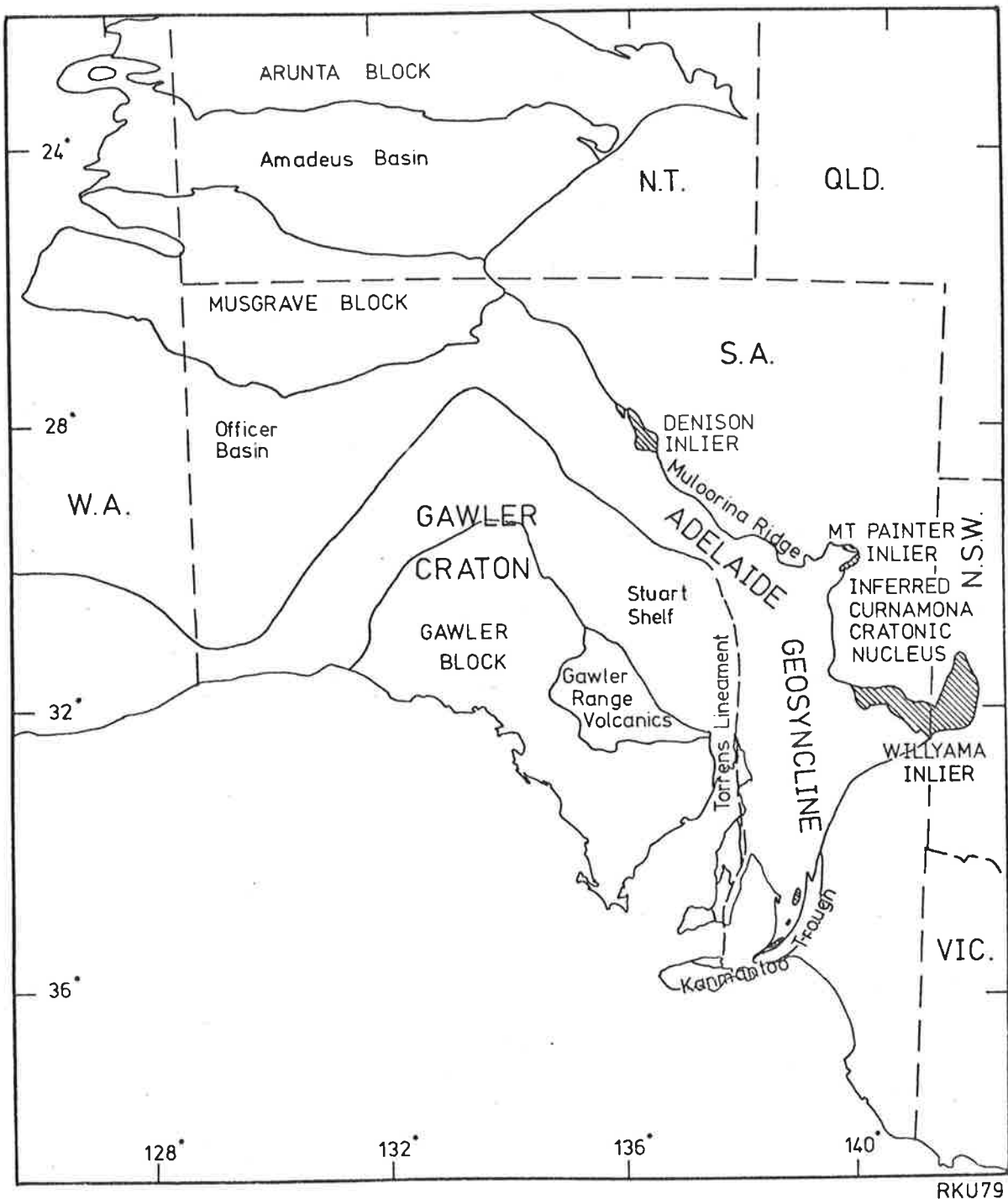


Figure 2.1. Tectonic framework of the Adelaide Geosyncline. After Thomson (1970, 1976), Geological Society of Australia (1971) and Daily et al..(1973).

Table 2.1. Summary of the sedimentary and tectonic history of the Adelaide Geosyncline.

After Ambrose and Flint (1976); Thomson *et al.* (1976); Glenn *et al.* (1977); Murrell (1977); Mancktelow (1979); Preiss (1979a); Webb (1979).

ADELAIDE GEOSYNCLINE

Sedimentation terminated by Delamerian Orogeny, c. 450-510 Ma.

Cambrian	Variable subsidence rates and water depths produced facies changes and local disconformities, transgressive phases extended onto Stuart Shelf.	Mostly shallow water sediments with both carbonates and clastics; deeper water, rapid deposition in Kanmantoo Trough.
	Minor uplift and erosion - disconformity, low angle unconformity.	
Sturtian-Marinoan	Some syndepositional tectonism - fault controlled facies changes, local disconformities, transgressive phases extended onto Stuart Shelf.	Glacial sediments, shallow water clastics and carbonates, including red beds, limestones, dolomites.
	Mild folding, uplift and widespread erosion - low angle unconformity, rarely high angle.	
Torrensian	Gentle warping of basin floor produced thickness changes, possible syndepositional folding and faulting.	Shallow water sediments, clastics, dolomites, magnesite.
	Folding and faulting, development of chaos breccias - low angle unconformity.	
Willouran	Tensional tectonics associated with basaltic volcanism.	Shallow water sediments, clastics, carbonates and evaporites, volcanics.
	Sedimentation commenced in the interval c. 800-1100 Ma	

CARPENTARIAN
BASEMENT

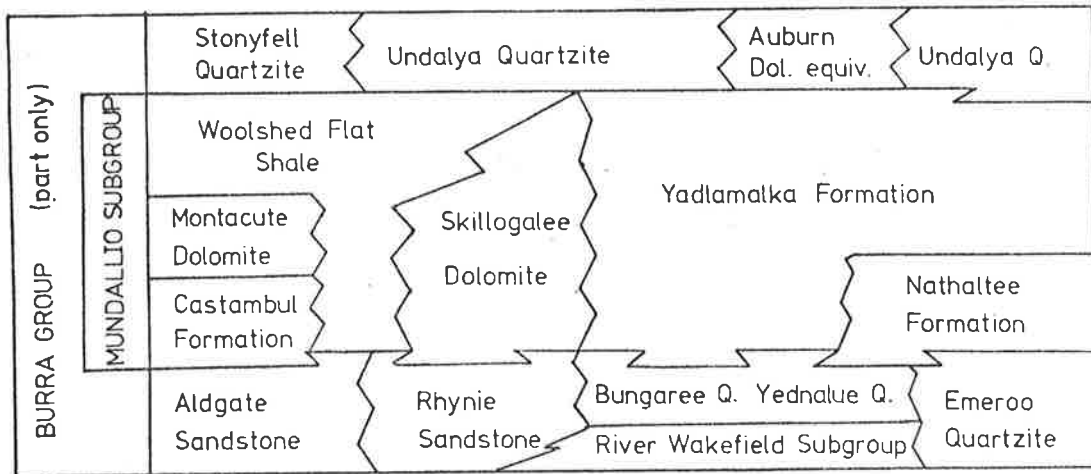
Gawler Craton
Largely stabilized in Kimban Orogeny with final stabilization in the period 1400-1575 Ma in association with post orogenic granite intrusion, and acid volcanics (Gawler Range Volcanics).

Inliers within Geosyncline
Some record of events younger than Kimban Orogeny e.g. in Peake and Denison Ranges, Houghton Inlier near Adelaide.

A.

MT. LOFTY RANGES

SOUTHERN FLINDERS RANGES
CENTRAL WESTERN

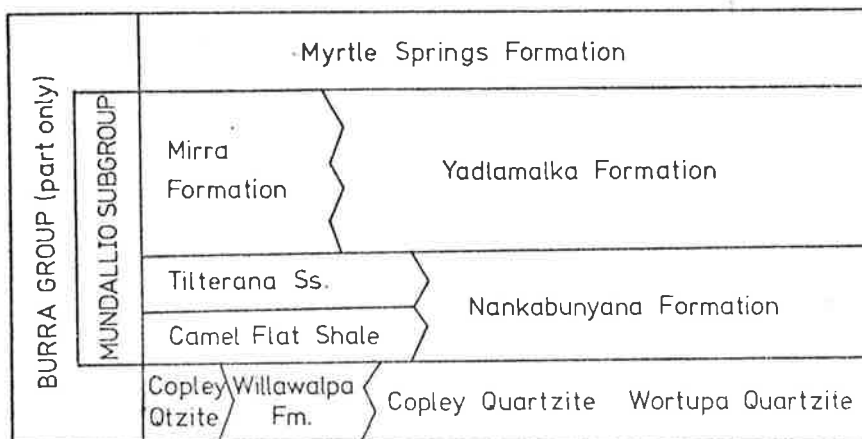


B.

WILLOURAN RANGES

COPLEY

ARKARoola



RKU79

Figure 3.1. Stratigraphy of the Mundallio Subgroup and the immediately underlying and overlying parts of the Burra Group. For complete Burra Group stratigraphy, see Forbes (1971), Murrell (1977) and Preiss (1979b).

A. Mt. Lofty and southern Flinders Ranges.

B. Northern Flinders and Willouran Ranges.

Figure 3.2: Outcrops of the Mundallio Subgroup in the Mt. Lofty and Flinders Ranges of South Australia, and distribution of constituent formations. List of locations, and their abbreviations, mentioned in text.

Northern Flinders Ranges

Willouran Ranges - W

WH Willouran Hill
 NW Norwest H.S.
 R Rischbieth Hut
 MR Mirra Bore
 MI Mirra Creek
 WW Warra Warra Mine
 CH Cadnia Hill
 WR West Rischbieth
 SH South Hill
 CO Coronation Bore
 SO Screech Owl Creek
 TM Top Mount Bore
 WH West Mount Hut
 TH Termination Hill

MS Myrtle Springs
 CP Copley
 AV Avondale
 MH Mandarin Hill

Arkaroola Region - A

BM Blue Mine Creek
 WT Wheal Turner Mine
 N The Needles
 BC Bolla Bollana Creek
 WC Wywyana Creek
 AH Arkaroola H.S.
 NH Nudlamutana Hut
 MY Munyallina Creek
 EP East of Paralana Fault


Southern Flinders Ranges

Emeroo Range


YL Yadlamalka H.S.
 DC Depot Creek
 MC Mundallio Creek
 WI Willow Creek
 YD Yednalua H.S.
 YDA Yednalua Anticline
 J Johnburgh
 C Carrieton
 YT Yatina
 WE Weekeroo H.S.
 PG Port Germein Gorge
 B Beetaloo
 CB Crystal Brook
 PP Port Pirie
 YW Yacka-west
 YE Yacka-east

Mt. Lofty Ranges

S Spalding
 BU Burra
 DT Duttons Trough H.S.
 SR Scrubby Range
 CL Clare
 SC Skillogalee Creek
 RW River Wakefield
 (west of Rhynie)
 U Undalya
 T Tarlee
 RL River Light
 (south of Stockport)
 TG Torrens Gorge
 BL Balhannah
 MB Mt. Bold Reservoir
 CR Congeratinga River


 Outcrop limits of folded Adelaidean and Cambrian sedimentary rocks

 Basement inliers

 Outcrops of Mundallio Subgroup

 Sandstone equivalent

Distribution of

 Castambul Formation and Montacute Dolomite

 Skillogalee Dolomite

 Woolshed Flat Shale

 Nathaltee Formation

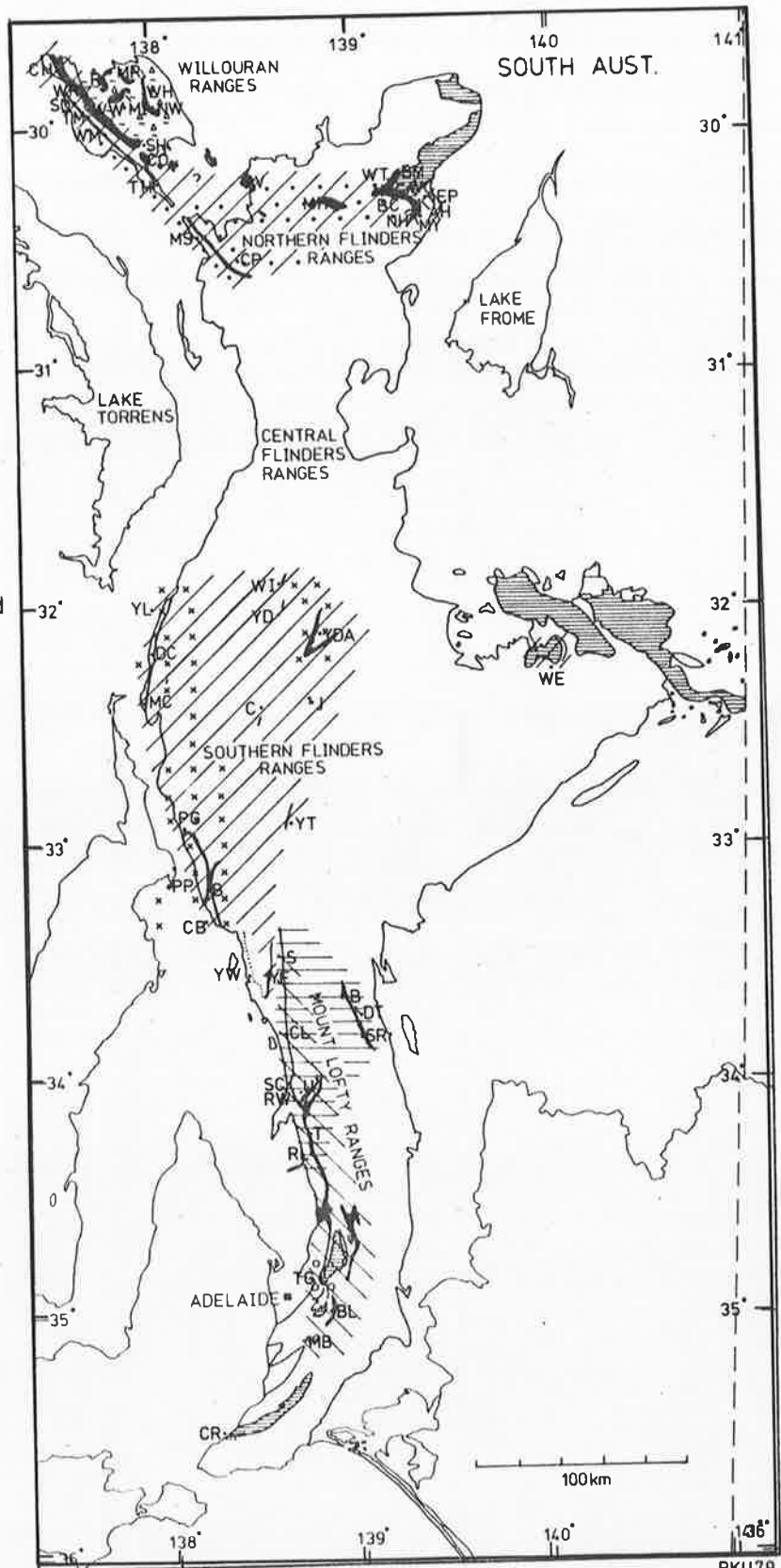
 Nankabunyana Formation

 Camel Flat Shale and

 Tilterana Sandstone

 Yadlamalka Formation

 Mirra Formation



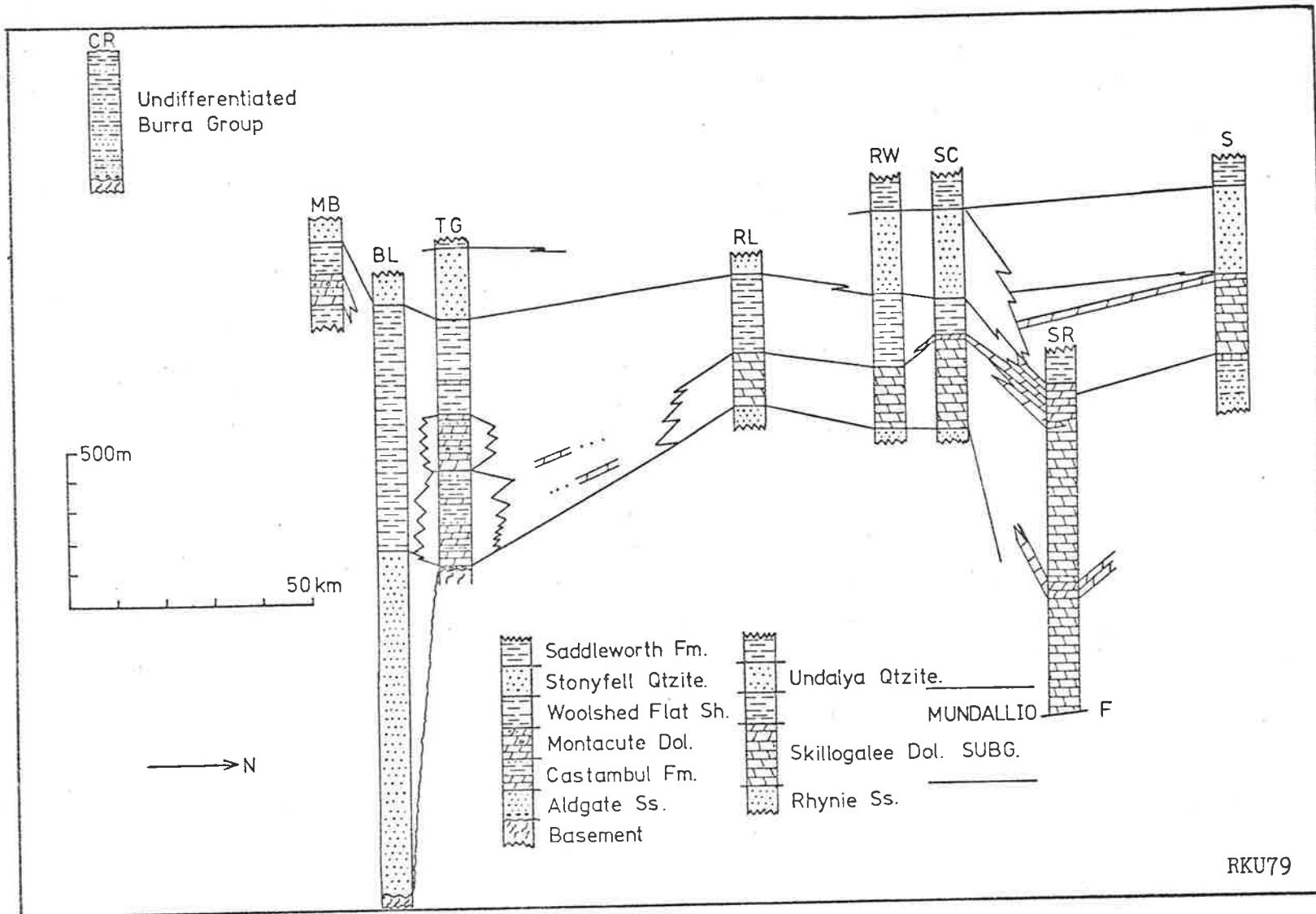


Figure 3.3. Simplified stratigraphic sections for part of the Burra Group including the Mundallio Subgroup, showing relationships between formations, Mt. Lofty Ranges. Locations as in Figure 3.2.

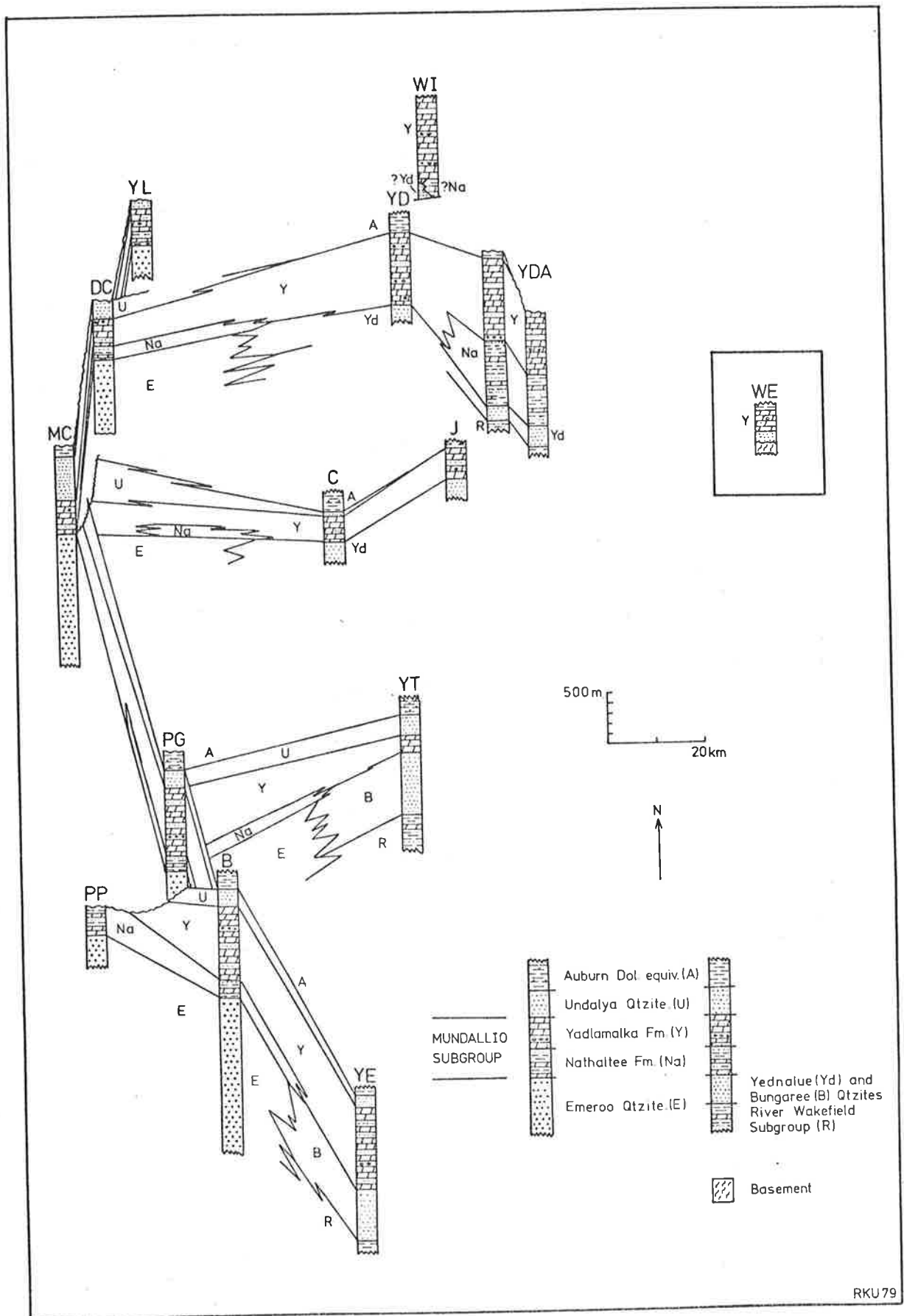


Figure 3.4. Simplified stratigraphic sections for part of the Burra Group including the Mundallio Subgroup, showing relationships between formations in the southern Flinders Ranges. Locations as in Figure 3.2. The Burra Group is unnamed in the Weekeroo area.

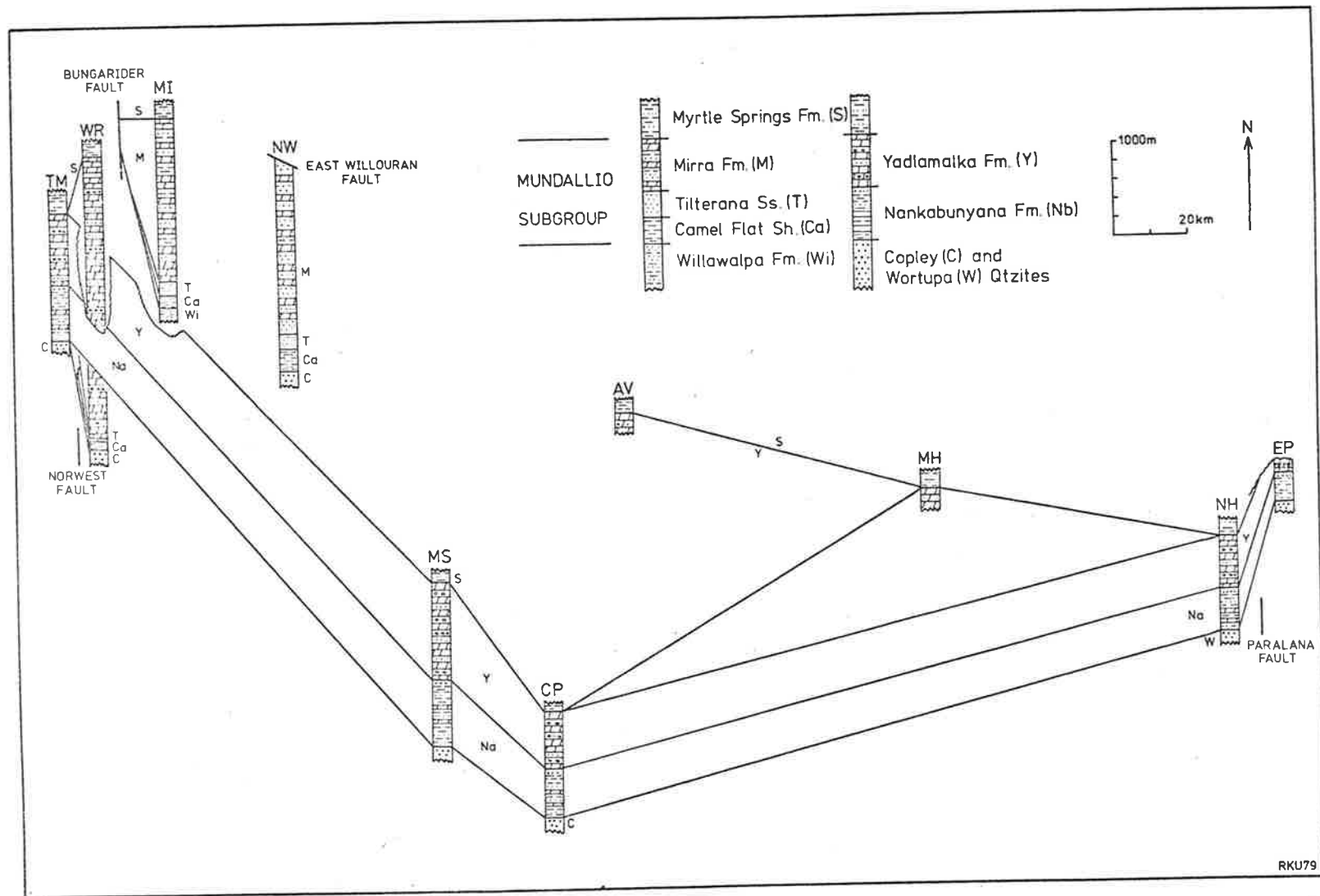


Figure 3.5. Simplified stratigraphic sections for part of the Burra Group including the Mundallio Subgroup showing the relationships between formations in the northern Flinders and Willouran Ranges. Locations as in Figure 3.2.

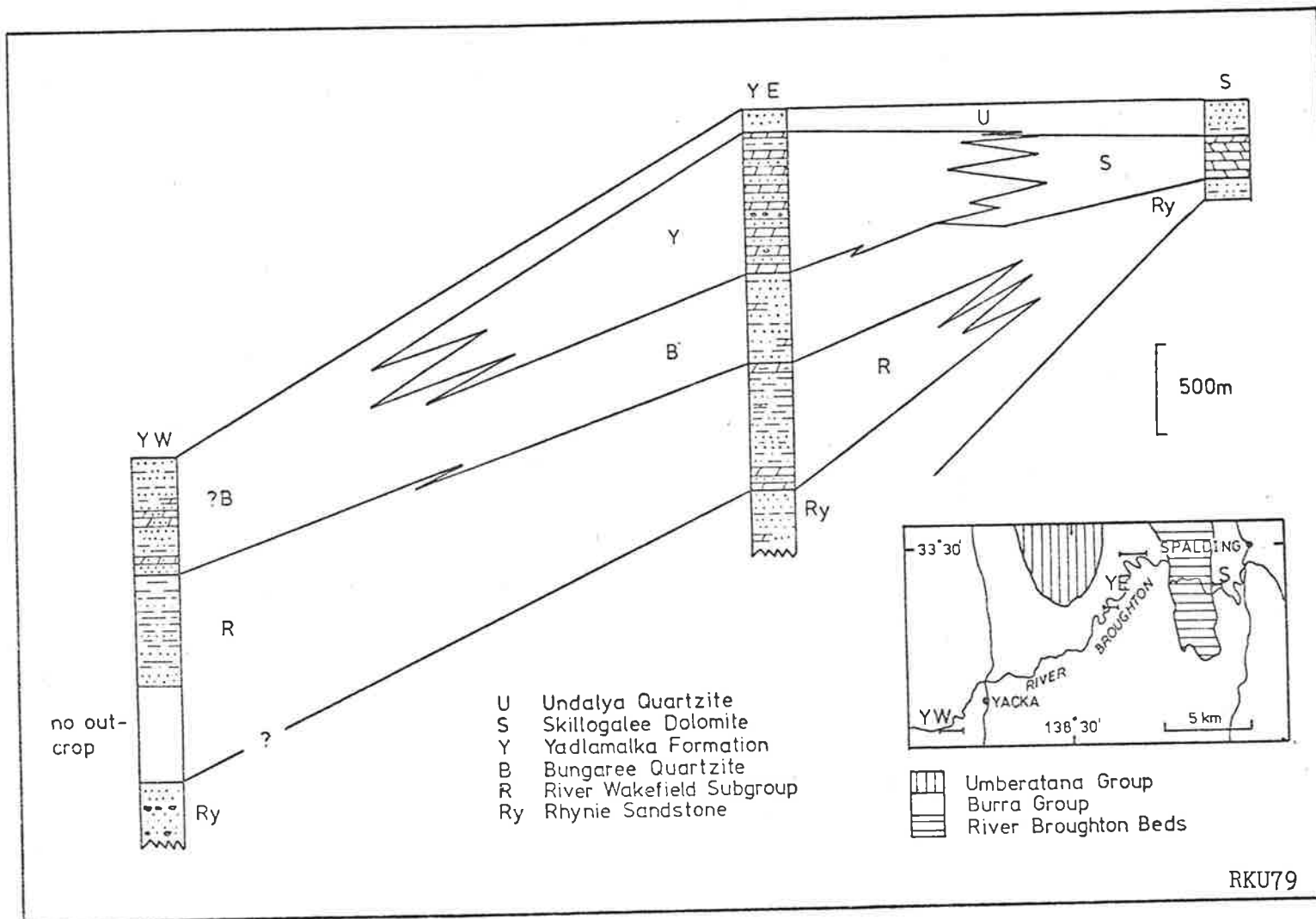
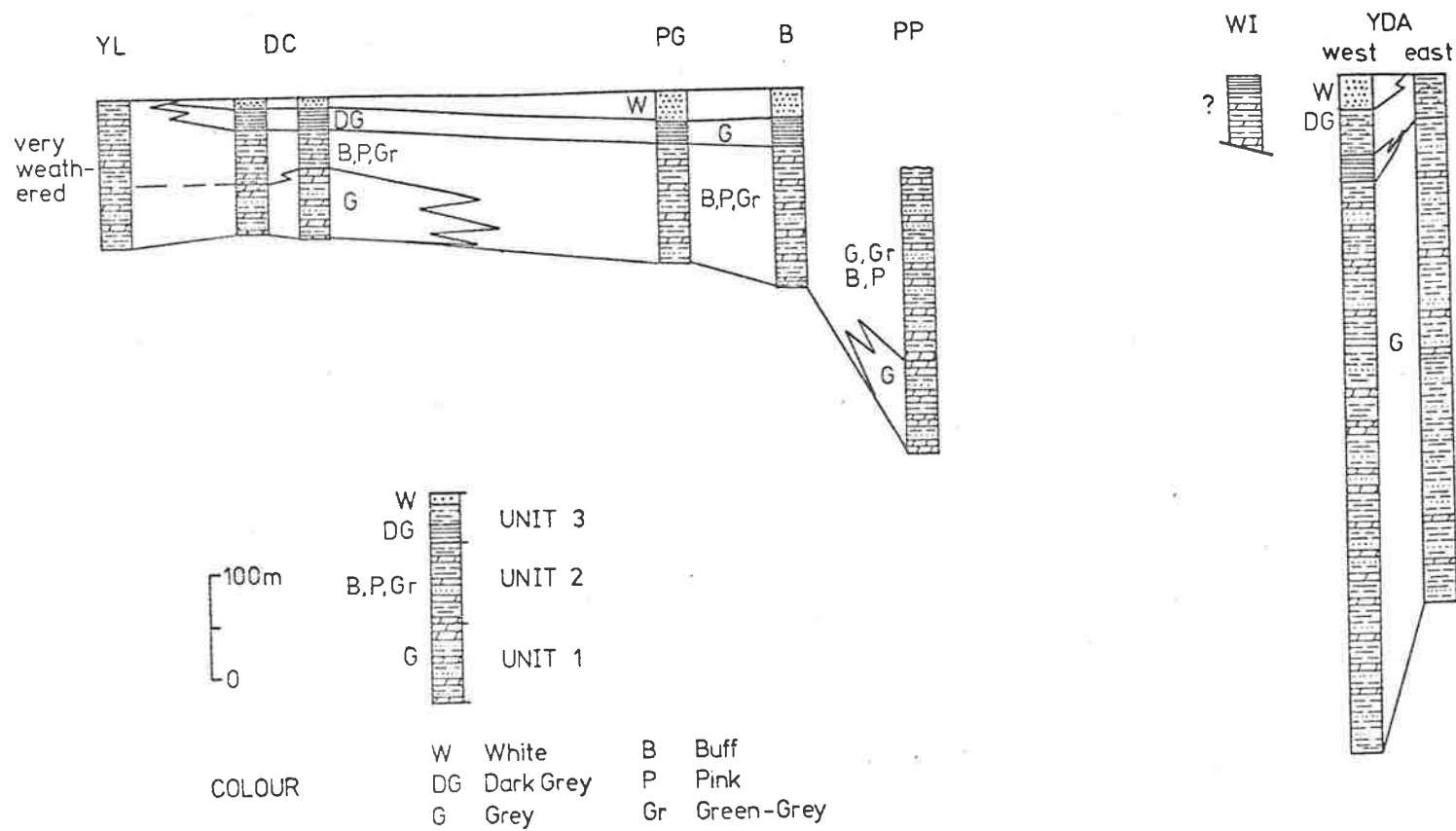


Figure 3.6. Stratigraphic sections for part of the Burra Group including the Mundallio Subgroup, in the Yacka-Spalding area, indicating the major east-west facies and thickness changes. Inset map shows section locations.

Figure 4.1. (In pocket at back)

Measured stratigraphic sections of the Nathaltee Formation at Depot Creek (DC1, DC2), Port Germein Gorge (PG), Beetaloo (B) and the Yednalue Anticline (YDA, west limb). Only the upper part of the formation is presented for YDA as the lower part is faulted and folded. The Nathaltee Formation in this area is approximately 650 m in thickness, although this varies around the anticline (see Fig. 4.2). For locations of sections, see Figure 3.2 and Appendix 1 (more detailed maps). The locations of sections DC1 and DC2 are also shown in Figure 4.3.

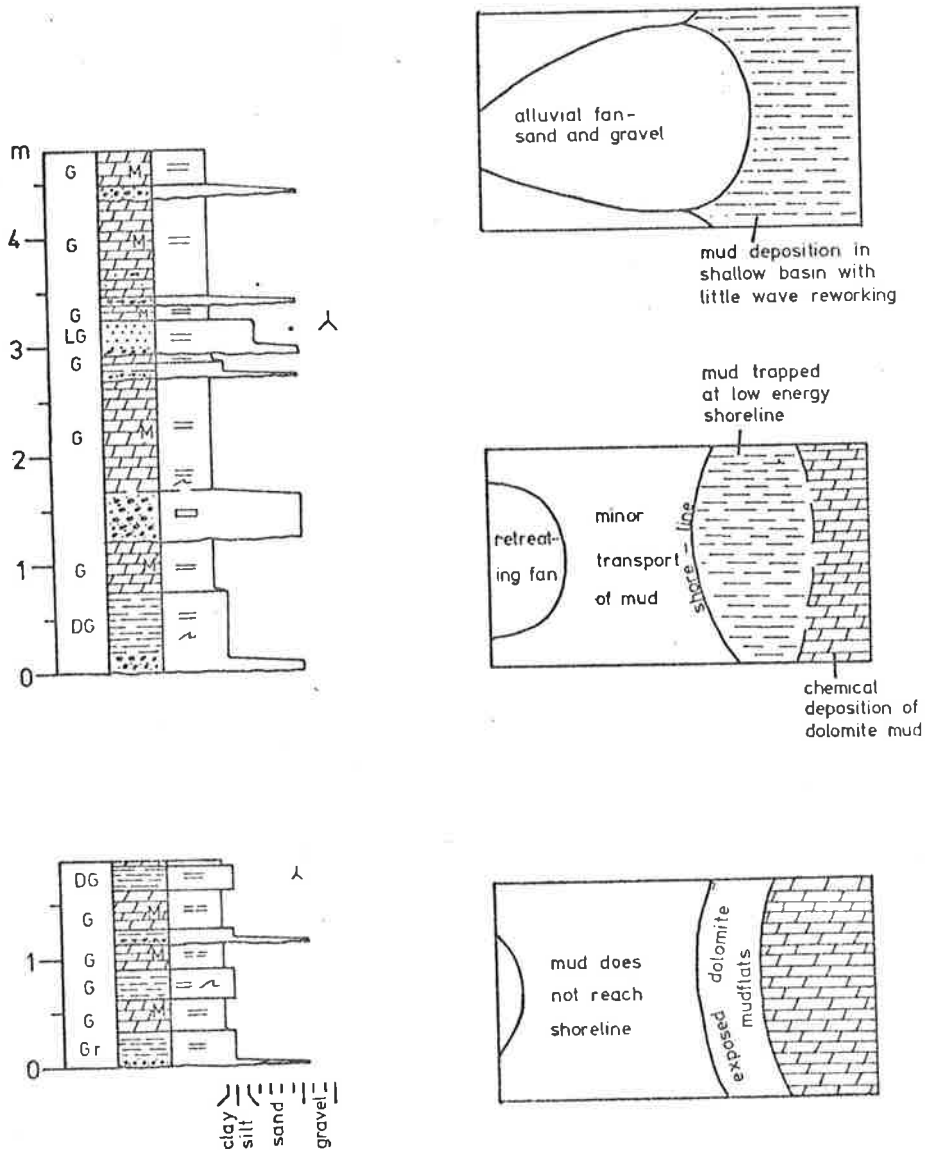


RKU79

Figure 4.2. Summary stratigraphic sections of the Nathaltee Formation in the major outcrop areas. For locations, see Figure 3.2.

Figure 4.3. (In pocket at back)

Geological map of the Mundallio Subgroup
in the Depot Creek area.



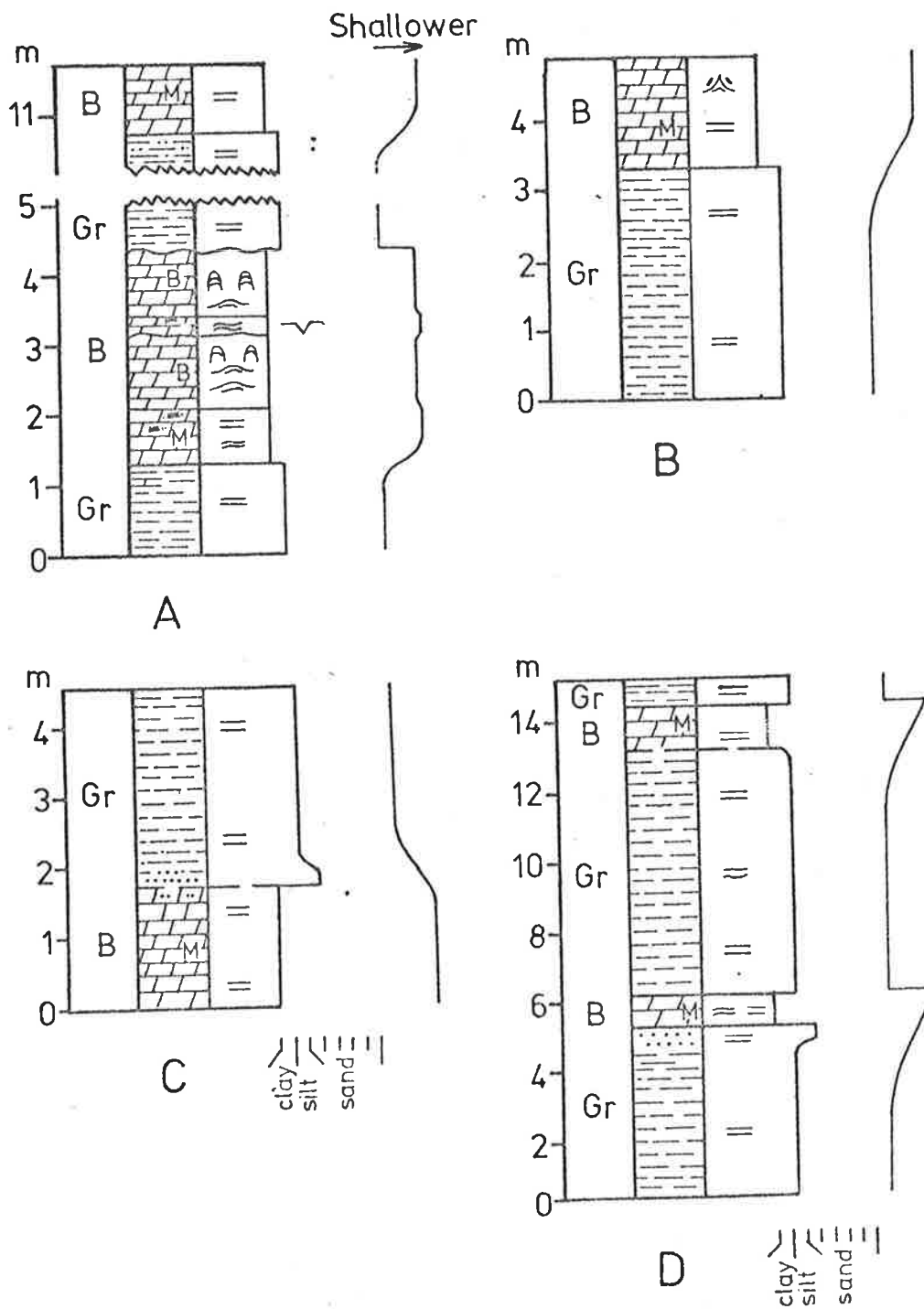
A

B

RKU79

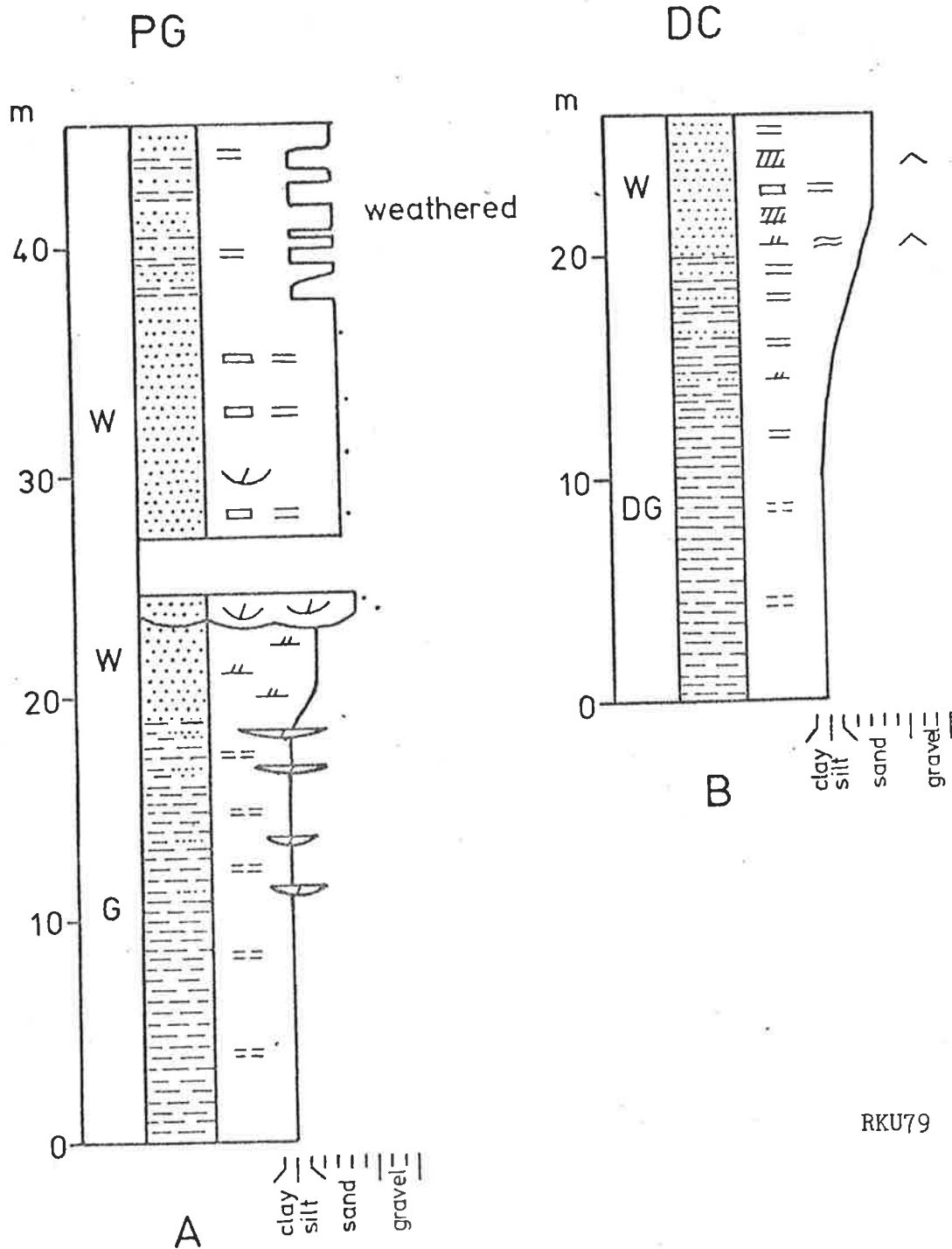
Figure 4.4. A. Detailed stratigraphic sections from part of Unit 1 (near base), Nathaltee Formation, Port Pirie area, with examples of conglomeratic sandstone-shale-dolomite mudstone cycles. For legend to sections, see Figure 4.14.

B. Interpreted origin of conglomeratic sandstone-shale-dolomite mudstone cycles (top to bottom).



RKU79

Figure 4.5. Examples of shallowing upward shale-(sandstone)-dolomite cycles, and deepening cycles (reverse) in Unit 2 of the Nathaltee Formation. A and B are from Beetaloo, C and D from Port Germein Gorge. For legend to sections, see Figure 4.14.



RKU79

Figure 4.6. Sections in Unit 3 of the Nathaltee Formation at A. Port Germein Gorge (PG), and B. Depot Creek (DC) illustrating the coarsening upward cycle. For legend, see Figure 4.14.

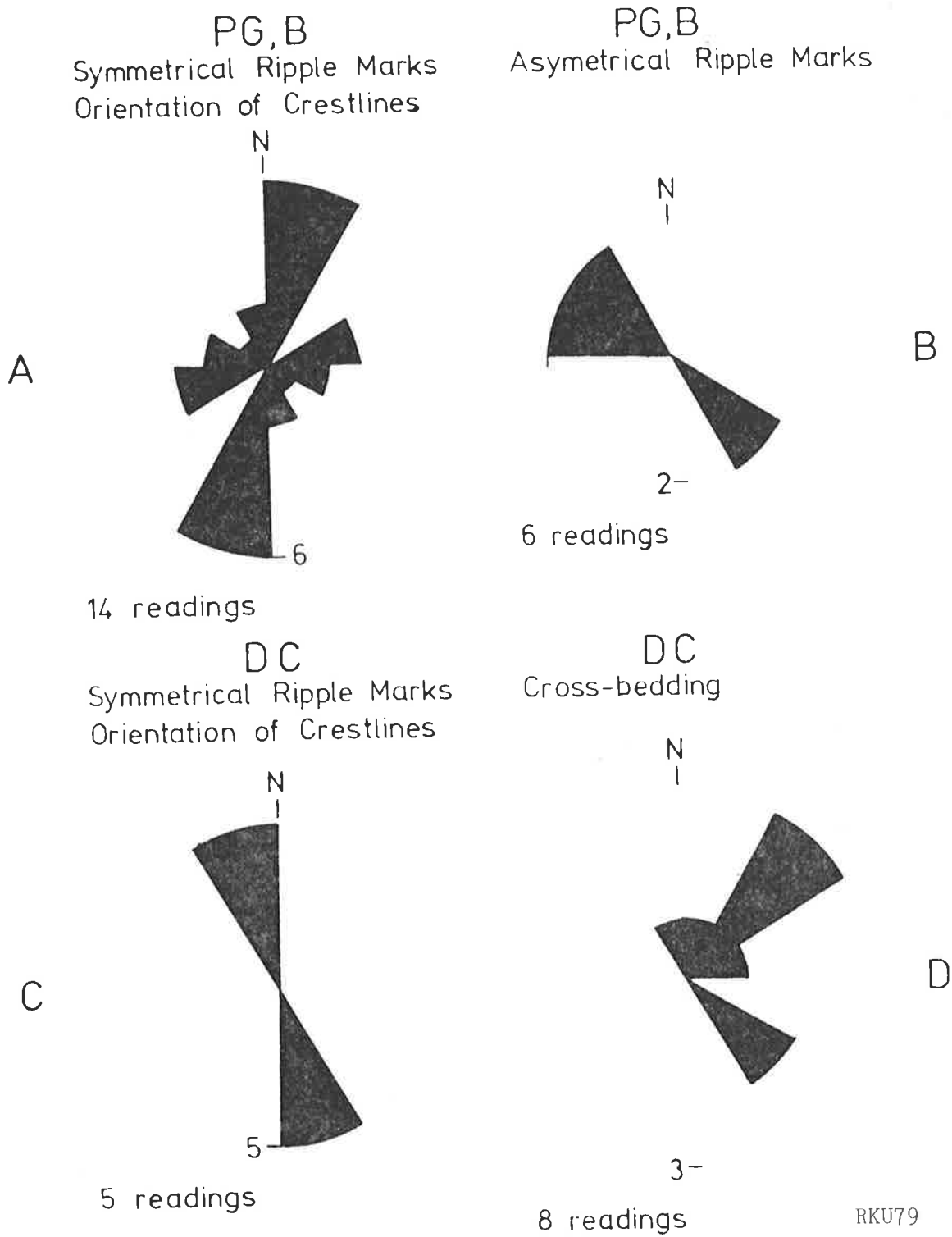


Figure 4.7. Palaeocurrent data, Nathaltee Formation.
 A and B. Upper most part of Emeroo Quartzite and Unit 2, Nathaltee Formation, Port Germein Gorge and Beetaloo.
 C and D. Unit 3, Depot Creek.

Figure 4.8. (In pocket at back)

Geological map of the Mundallio Subgroup,
Copley - Myrtle Springs area.

Figure 4.9. (In pocket at back)
Geological map of the Mundallio
Subgroup, Arkaroola area.

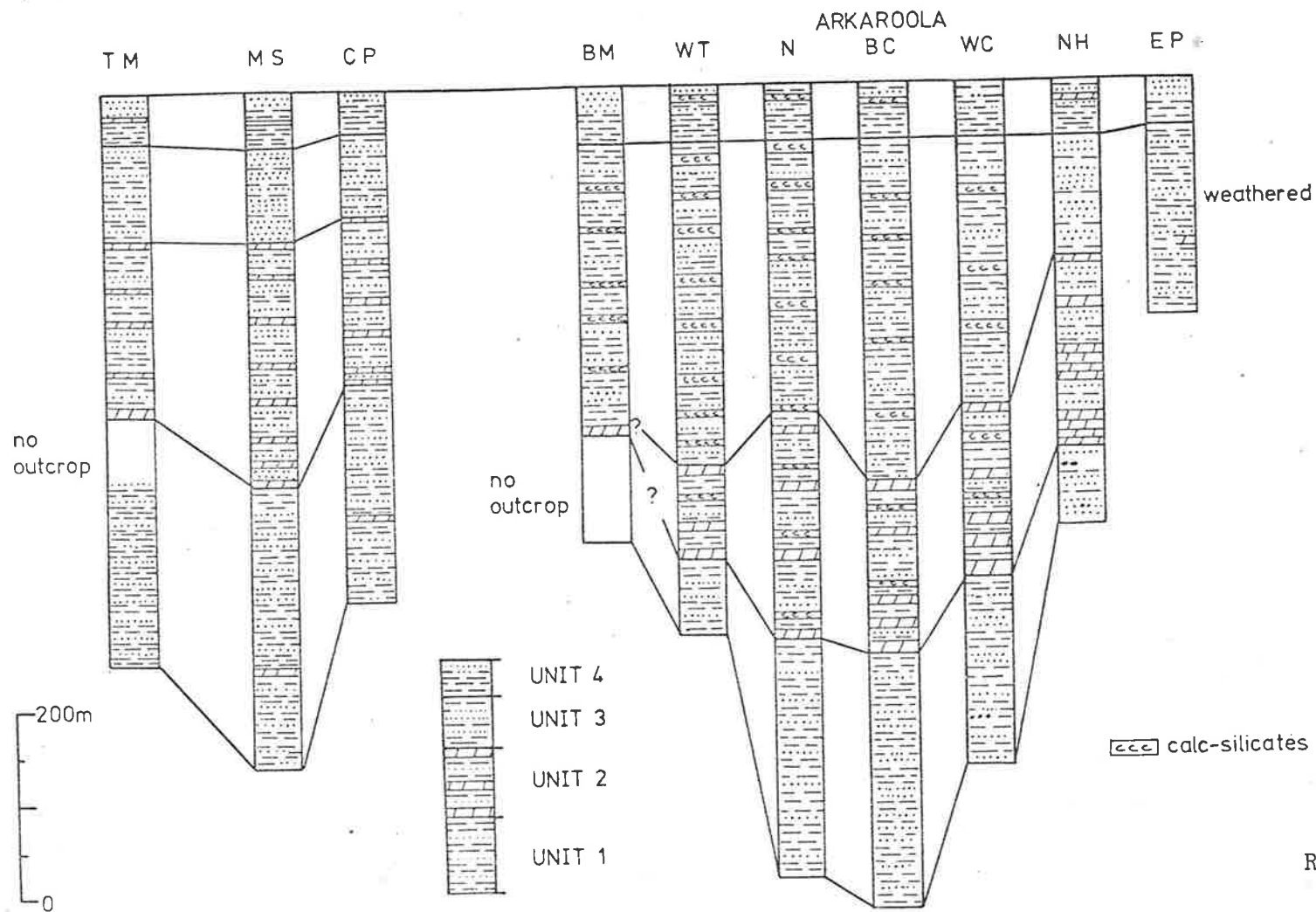
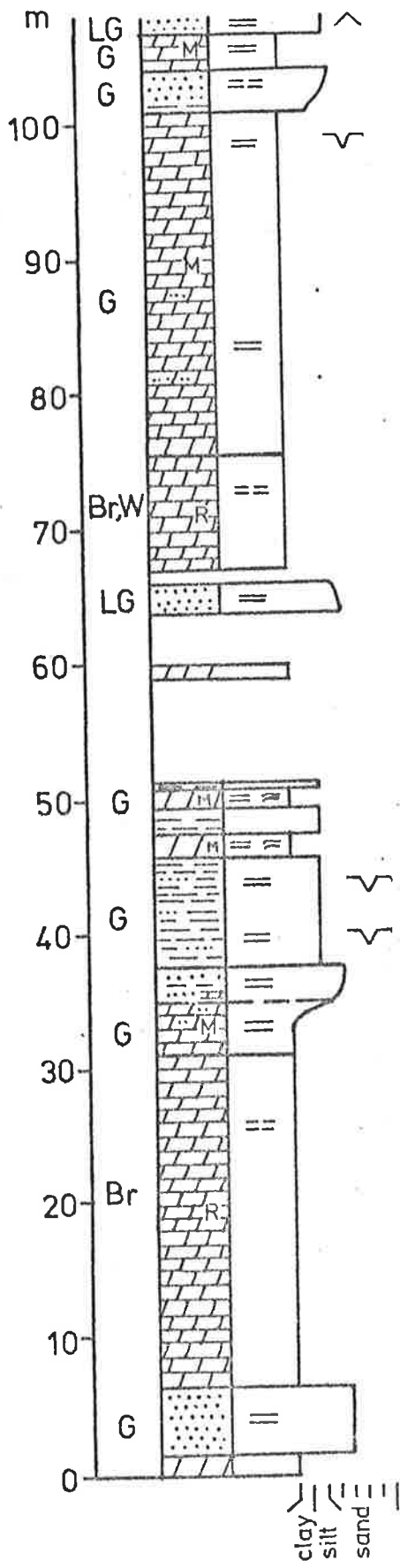


Figure 4.10. Summary stratigraphic sections, Nankabunyana Formation. For locations see Figure 3.2. Calc-silicates have formed by metamorphism of dolomitic sandstones and sandy dolomites.

RKU79

Figure 4.11. (In pocket at back)

Measured stratigraphic sections of the Nankabunyana Formation at Nudlamutana Hut (NH), Copley (CP1), Myrtle Springs (MS) and Top Mount Bore (TM); and in the Camel Flat Shale and Tilterana Sandstone at Mt. Norwest H.S. (NW). For locations of sections, see Figure 3.2 and Appendix 1 (more detailed maps). The locations of sections CP1 and MS are also shown in Figure 4.8, and NH in Figure 4.9.



massively outcropping, some very irregular lamination, minor haematite filled pods

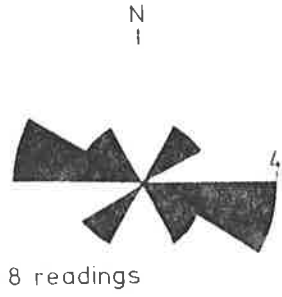
massively outcropping, very irregular lamination, irregular pods, veins and fissures infilled with reddish-brown siliceous haematite

weathered

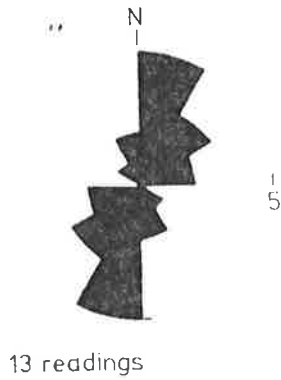
RKU79

Figure 4.12. Stratigraphic section in the lower part of Unit 2, Nankabunyana Formation, Nudlamutana Hut, illustrating the occurrence of massive, iron stained recrystallised dolomites.

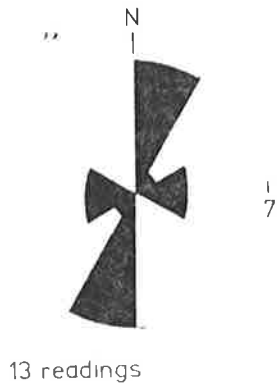
A. Symmetrical Ripple Marks -TM
Orientation of Crestlines



B. " -CP,MS



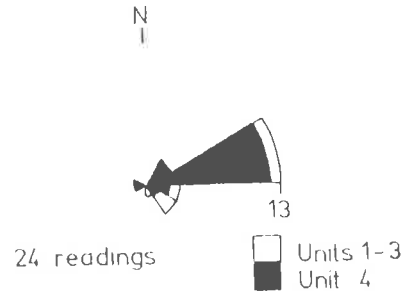
C. " -A



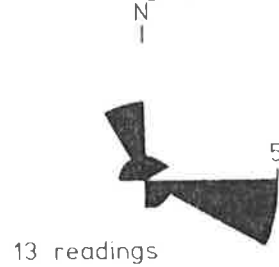
D. Cross-bedding -TM



E. Asymmetrical Ripple Marks -CP,MS



F. Cross-bedding -CP



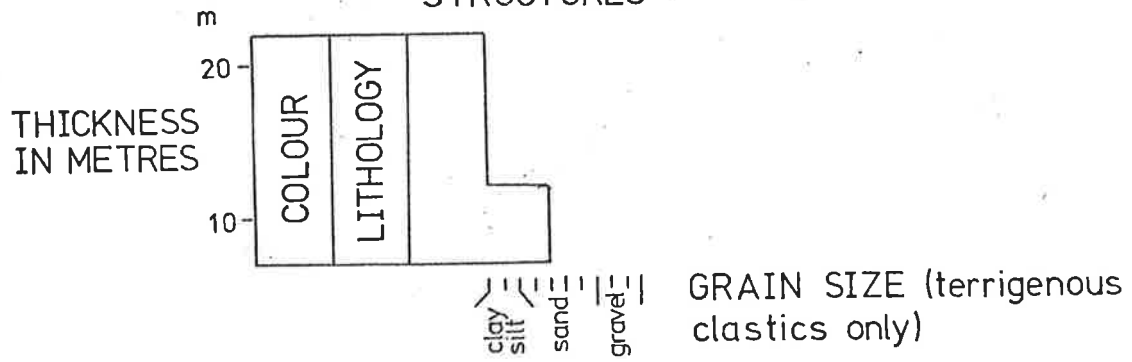
G. Asymmetrical Ripple Marks - A



RKU79

Figure 4.13. Palaeocurrent data, Nankabunyana Formation.
A. Top Mount Bore. B. Copley and Myrtle Springs. C. Arkaroola. D. Top Mount Bore.
E. Copley and Myrtle Springs. F. Copley. G. Arkaroola.

SEDIMENTARY STRUCTURES




LITHOLOGY		SEDIMENTARY STRUCTURES
	<p>Conglomerate</p> <p>Sandstone</p> <p>Siltstone, Shale</p> <p>Dolomite</p> <p style="padding-left: 20px;">M - mudstone</p> <p style="padding-left: 20px;">D - diagenetic texture</p> <p style="padding-left: 20px;">R - recrystallised</p> <p>Dolomite Intraclasts</p> <p>Dolomite Oncoids</p> <p>Dolomite Ooids</p> <p>Shaly Dolomite</p> <p>Magnesite Mudstone</p> <p>Nodular Magnesite</p> <p>Intraclastic Magnesite</p> <p>Chert Nodules</p>	<p>Massive</p> <p>= Flat lamination, thin bedding</p> <p>≅ Wavy " " "</p> <p>== Indistinct " "</p> <p>▭ Medium to thick bedding</p> <p>▨ Tabular cross-bedding</p> <p>∪ Trough cross-bedding</p> <p>∟ Ripple cross-lamination</p> <p>⋈ Climbing ripple lamination</p> <p>∩ Disrupted bedding</p> <p>∩ Load casts</p> <p>⋈ Tepees</p> <p>⋈ Inverse graded bedding</p> <p>⋈ Domal stromatolites</p> <p>A Columnar stromatolites</p> <p>∧ Symmetrical ripple marks</p> <p>∧ Asymmetrical " "</p> <p>∧ Interference " "</p> <p>∩ Desiccation Cracks</p> <p>∩ Synacresis Cracks</p> <p>∩ Evaporite pseudomorphs</p> <p>5 Maximum intraclast size in cm</p>
<p>COLOUR</p> <p>DG Dark-grey</p> <p>G Grey</p> <p>LG Light-grey</p> <p>W White</p> <p>B Buff</p> <p>P Pink</p> <p>R Red</p> <p>Br Brown</p> <p>Gr Greenish Grey</p> <p>Y Yellow</p> <p>YG Yellow Green</p> <p>C Cream</p>	<p>LITHOLOGICAL BOUNDARIES</p> <p>— Sharp</p> <p>— Gradational</p> <p>~ Irregular</p>	

Figure 4.14. Legend to stratigraphic sections.

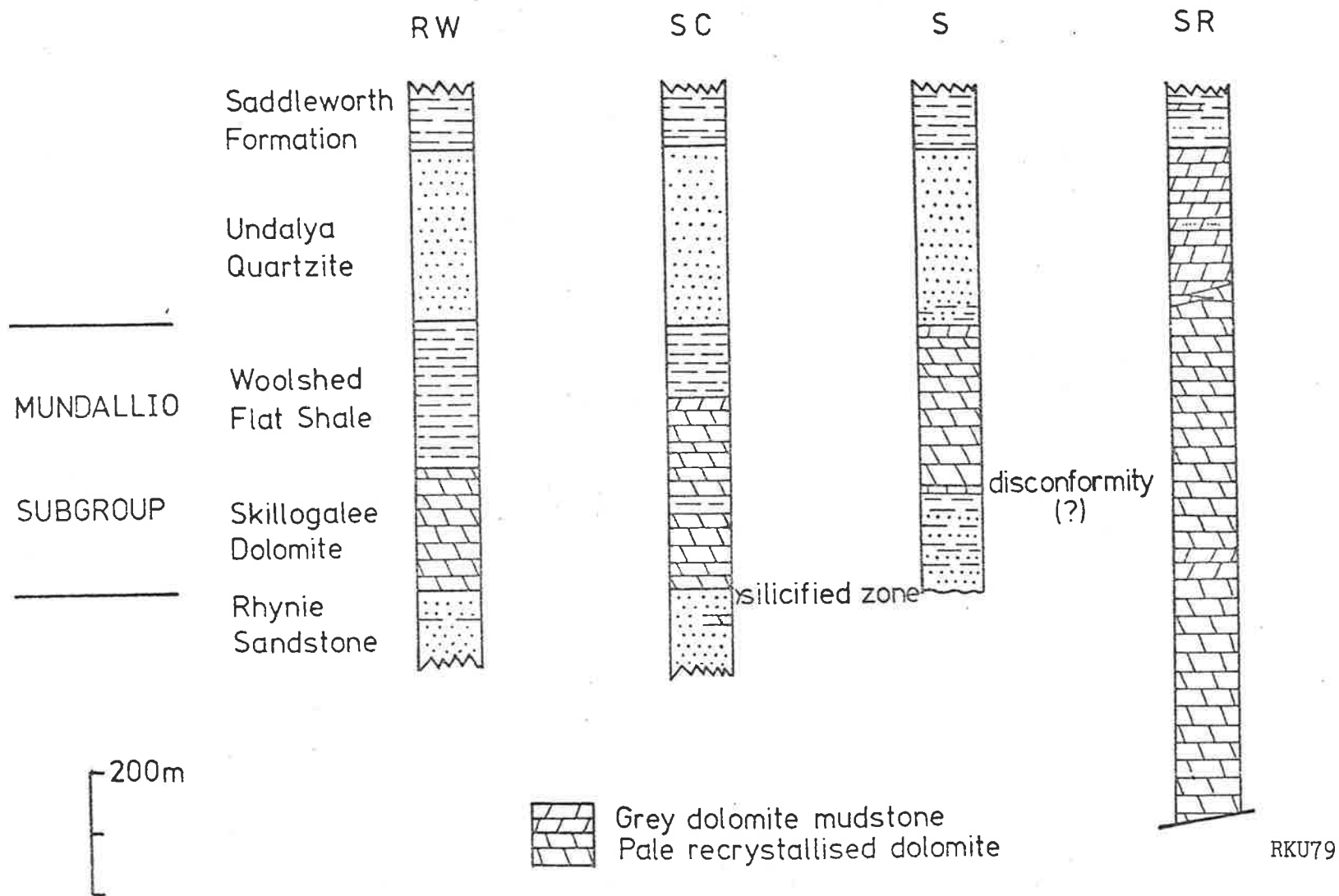


Figure 5.1. Summary stratigraphic sections in the lower Burra Group including the Mundallio Subgroup, northern Mt. Lofty Ranges, indicating the distribution of the two main dolomite facies in the Skillogalee Dolomite. For locations, see Figure 3.2.

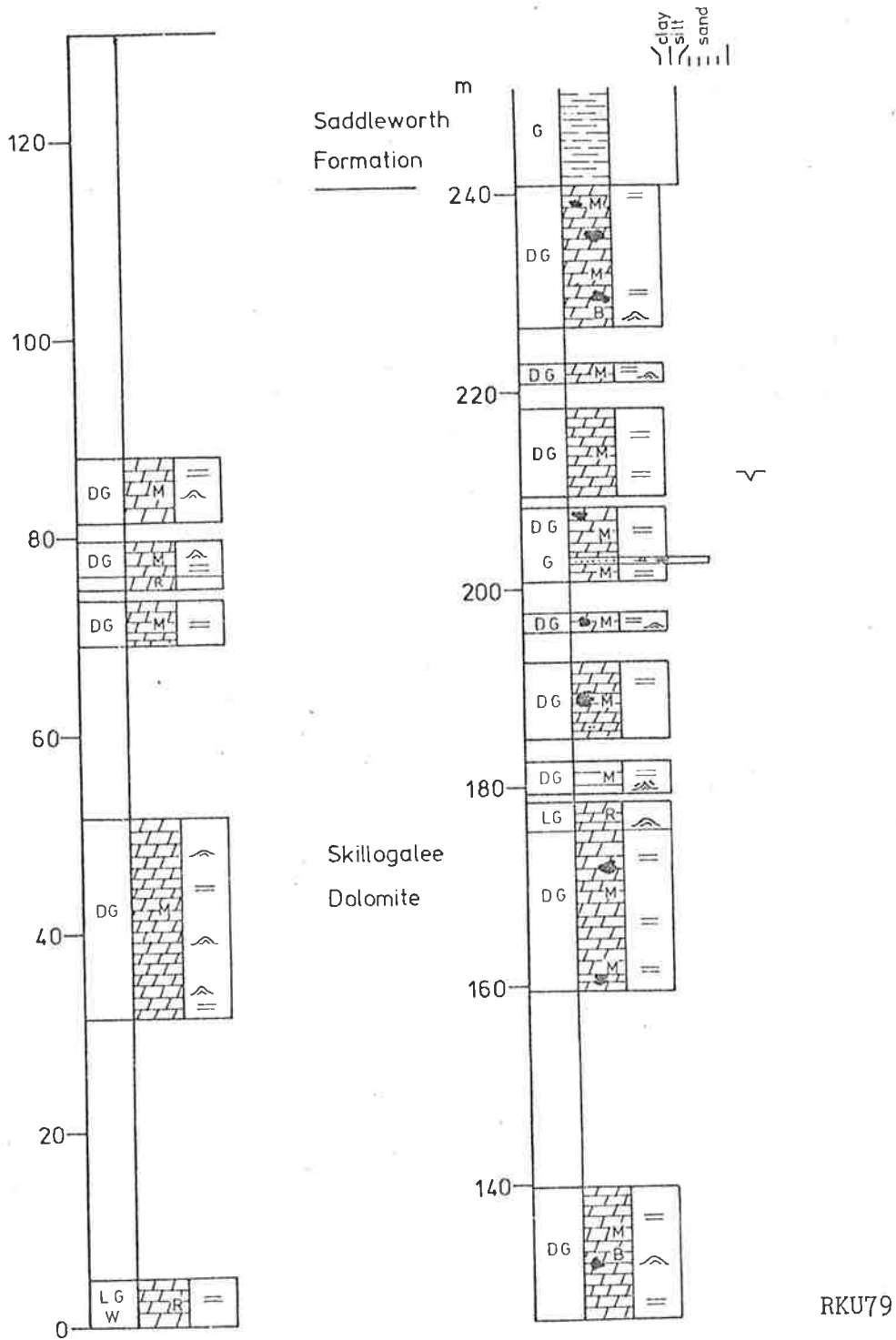


Figure 5.2. Measured stratigraphic section in upper member of dark-grey dolomites, Skillogalee Dolomite, Scrubby Range. For legend, see Figure 4.14, and for detailed location map, Appendix 1.

RKU79

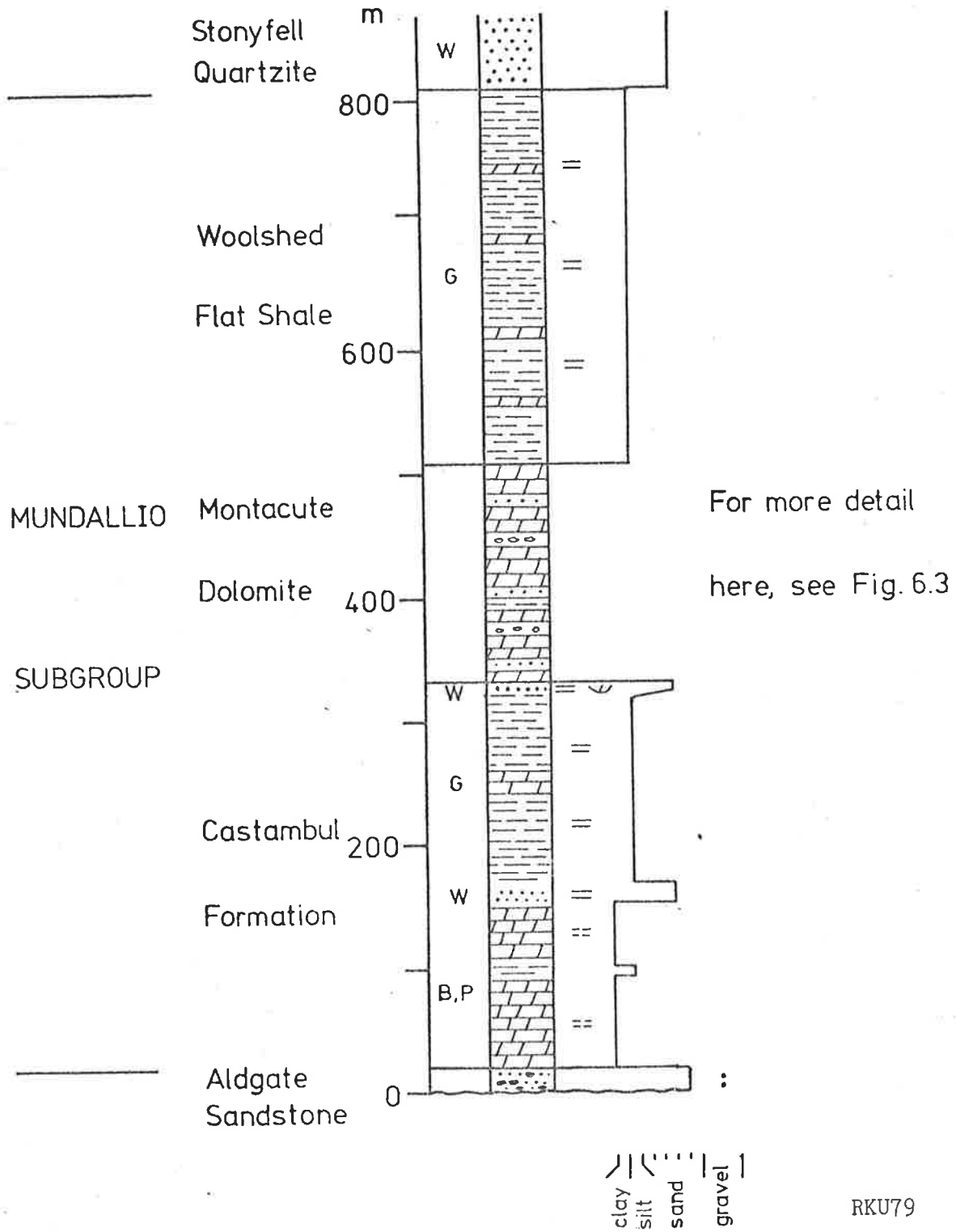
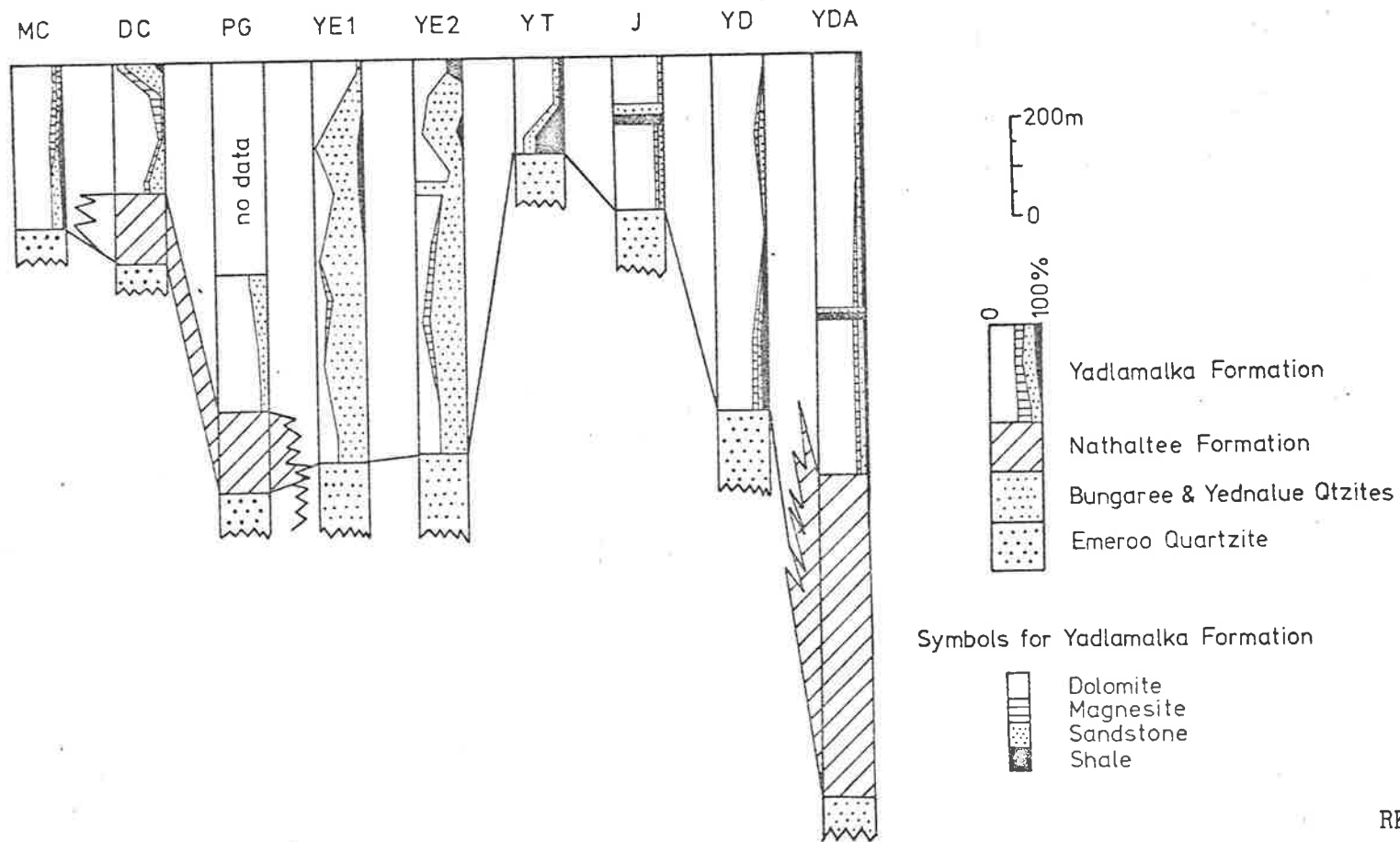
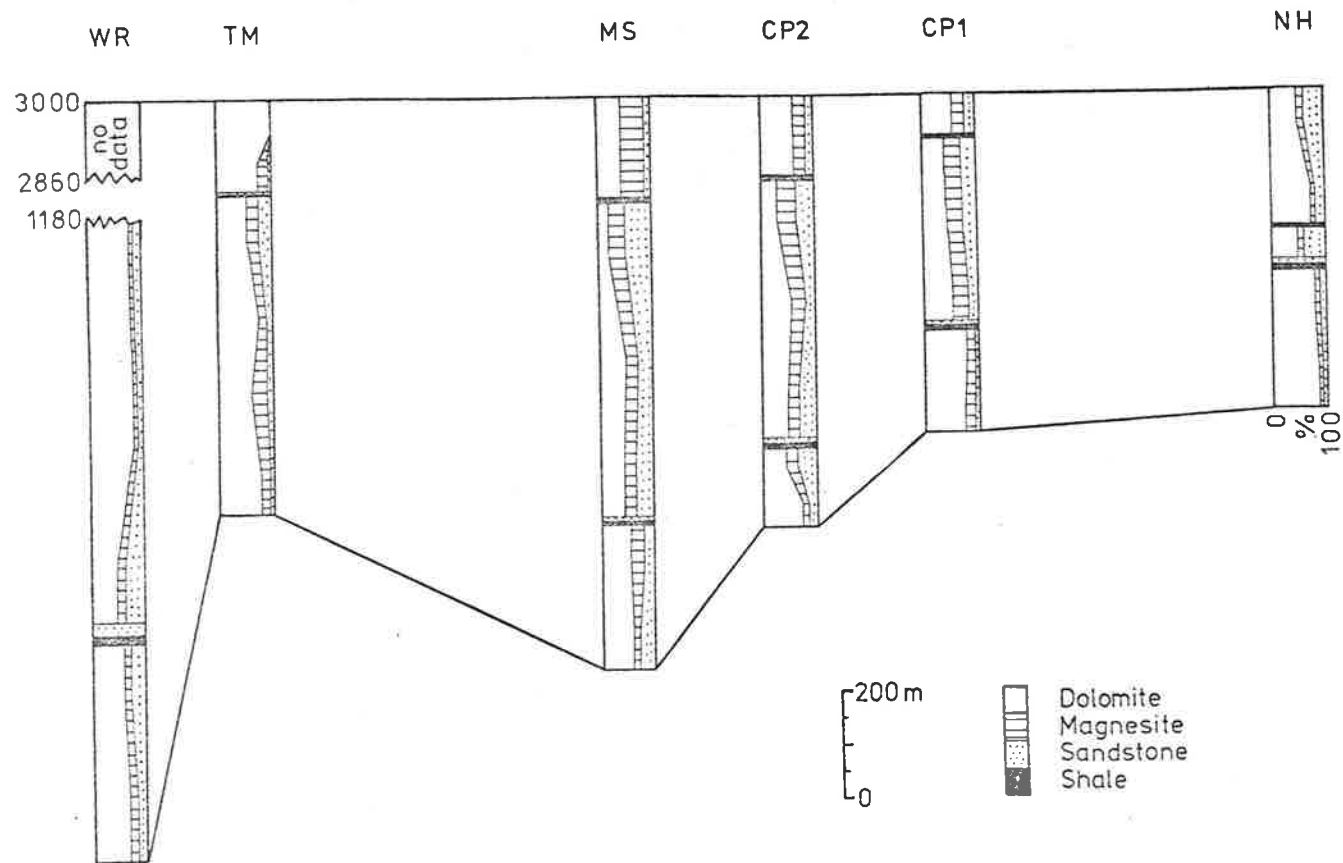


Figure 5.3. Stratigraphic section in the Mundallio Subgroup, Torrens Gorge. For legend to section, see Figure 4.14.



RKU79

Figure 6.1. Summary stratigraphic sections of the Yadlamalka Formation in the southern Flinders Ranges. For more detailed sections, see Figure 6.4, and for locations, Figure 3.2. Dolomite - all dolomite facies; magnesite - all magnesite facies; sandstones - all sandstones and minor coarse-grained siltstones; shales - all shales and siltstones, these are generally non-dolomitic except at YT.



RKU79

Figure 6.2. Summary stratigraphic sections of the Yadlamalka Formation, northern Flinders and southeastern Willouran Ranges. For more detailed sections, see Figure 6.5, and for locations, Figure 3.2. Facies as in Figure 6.1.

Figure 6.3. (In pocket at back)

Measured stratigraphic sections of the Montacute Dolomite. Section A is in Torrens Gorge (TG), and B is in the Readymix Quarry 1 km south of Torrens Gorge (for detailed location map, see Appendix 1). Section B represents the uppermost part of the Montacute Dolomite only, as the base is not exposed in the quarry. For legend, see Figure 4.14.

Figure 6.4. (In pocket at back)

Measured stratigraphic sections of the Yadlamalka Formation, southern Flinders Ranges. The sections from Mundallio Creek (MC), Depot Creek (DC1), Yatina (YT) and Johnburg (J) are shown in full. The Port Germein Gorge section (PG) is from the west limb of the Nelshaby Anticline and represents the lower part of the formation only, the upper part is not exposed. Complete sections from Yacka (YE1, YE2), Yednalue (YD) and Yednalue Anticline (west limb, YDA) are shown as % logs only (note scale difference), with representative parts in more detail. Total thickness of the Yadlamalka Formation is given for each section in brackets at the top. For the location of sections, see Figure 3.2, more detailed location maps are given in Appendix 1. The location of section DC1 is also shown in Figure 4.3.

Figure 6.5. (In pocket at back)

Measured stratigraphic sections of the Yadlamalka Formation, northern Flinders and Willouran Ranges. WR - West Rischbieth, TM - Top Mount Bore, MS - Myrtle Springs, CP1 and CP2 - Copley, NH - Nudlamutana Hut, WC - Wywyana Creek. Because of the frequent vertical facies changes in the Yadlamalka Formation and the thickness of the formation in these areas, the complete sections are given as % logs only, with representative parts in more detail. For the location of sections see Figure 3.2, more detailed location maps are given in Appendix 1. The locations of sections CP1, CP2 and MS are also given in Figure 4.8, and NH and WC in Figure 4.9.

Figure 6.6. (In pocket at back)

Section through part of the Yadlamalka Formation at Copley, representing the interval from 425-496 m, which is the most magnesite rich portion in the Yadlamalka Formation. The section is exposed in an excavation trench, and the equivalent interval intersected in the Copley Magnesite DDH1 drill core. Some discrepancies between the two sections result from the very weathered nature of some surface magnesite outcrops, and the lack of 100% recovery in parts of core, as well as real facies changes.

Figure 6.7. (In pocket at back)

Measured stratigraphic sections of the Mirra Formation at Mirra Creek (MI) and Mt. Norwest H.S. (NW). In the latter area the top of the formation is faulted. For locations see Figure 3.2, more detailed location maps are given in Appendix 1.

Submerged

Exposed

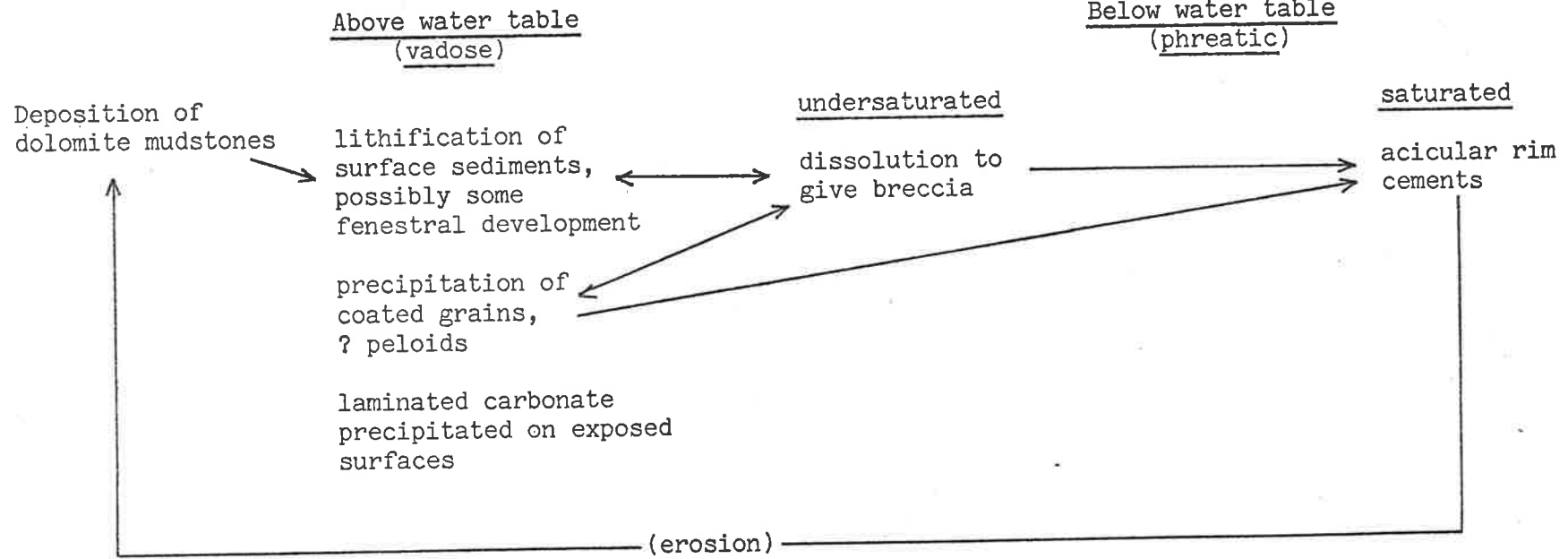
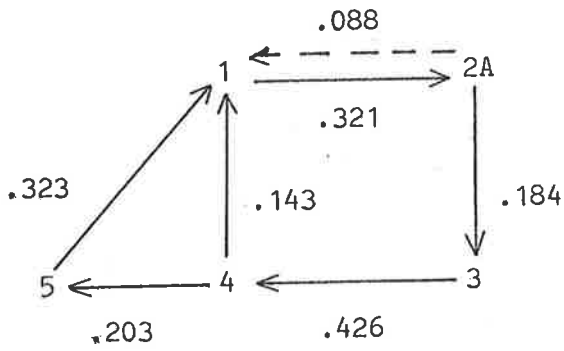


Figure 6.8. Summary of the formation of diagenetic textures in massive dolomites.

Figure 6.9. Examples of Markov Chain Analyses, with values from difference matrix determined using the method of Miall (1973).

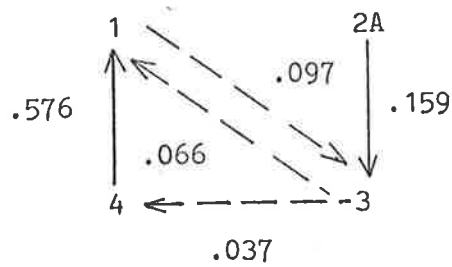
- Facies 1. Intraclastic magnesite
- 2A. Dolomitic, very fine-grained sandstone
- 2B. Dolomitic, medium-grained sandstone
- 3. Dolomite mudstone
- 4. Magnesite mudstone
- 5. Nodular magnesite
- 6. Stromatolitic dolomite.
- 7. Shales and siltstones
- 8. Dolomite grainstone

Example A. COPLEY MAGNESITE DDH1 section (Fig. 6.6)



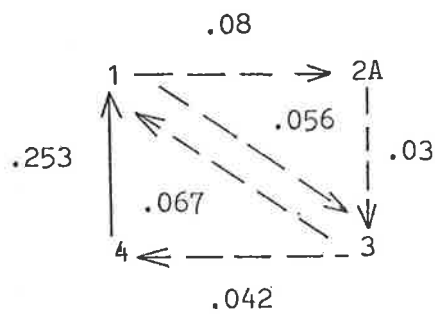
105 transitions

Example B. Copley : Section 1, 0-185.4 m



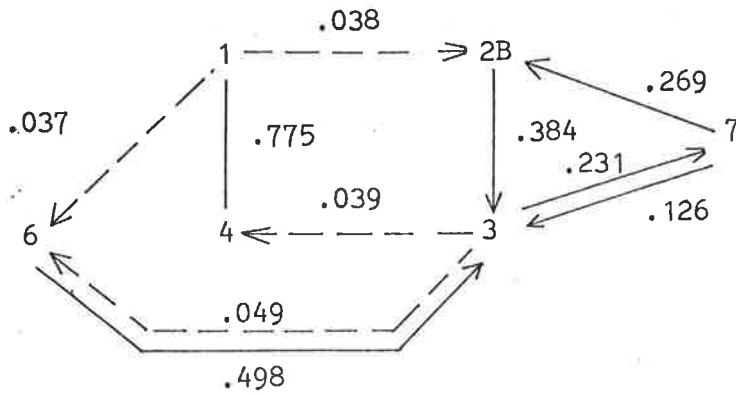
97 transitions

Example C. Copley : Section 1, 209-432 m



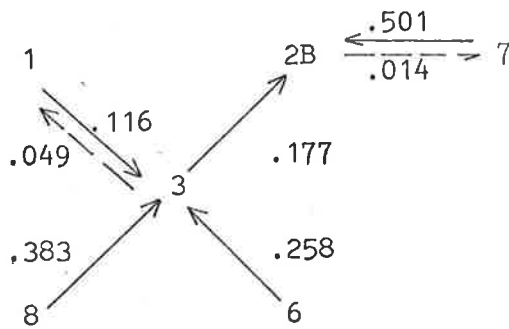
90 transitions

Example D. Yednalue Section, 0-200 m



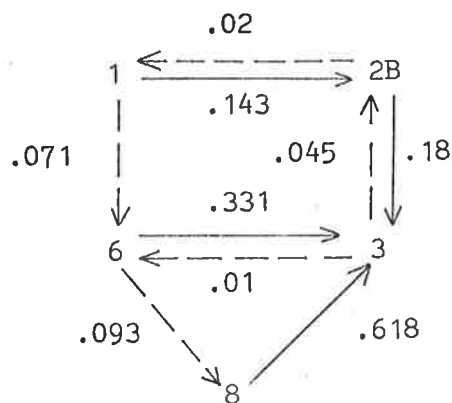
93 transitions

Example E. Depot Creek Section



202 transitions

Example F. Depot Creek Section, 0-58 m



70 transitions

Figure 6.9. (continued)

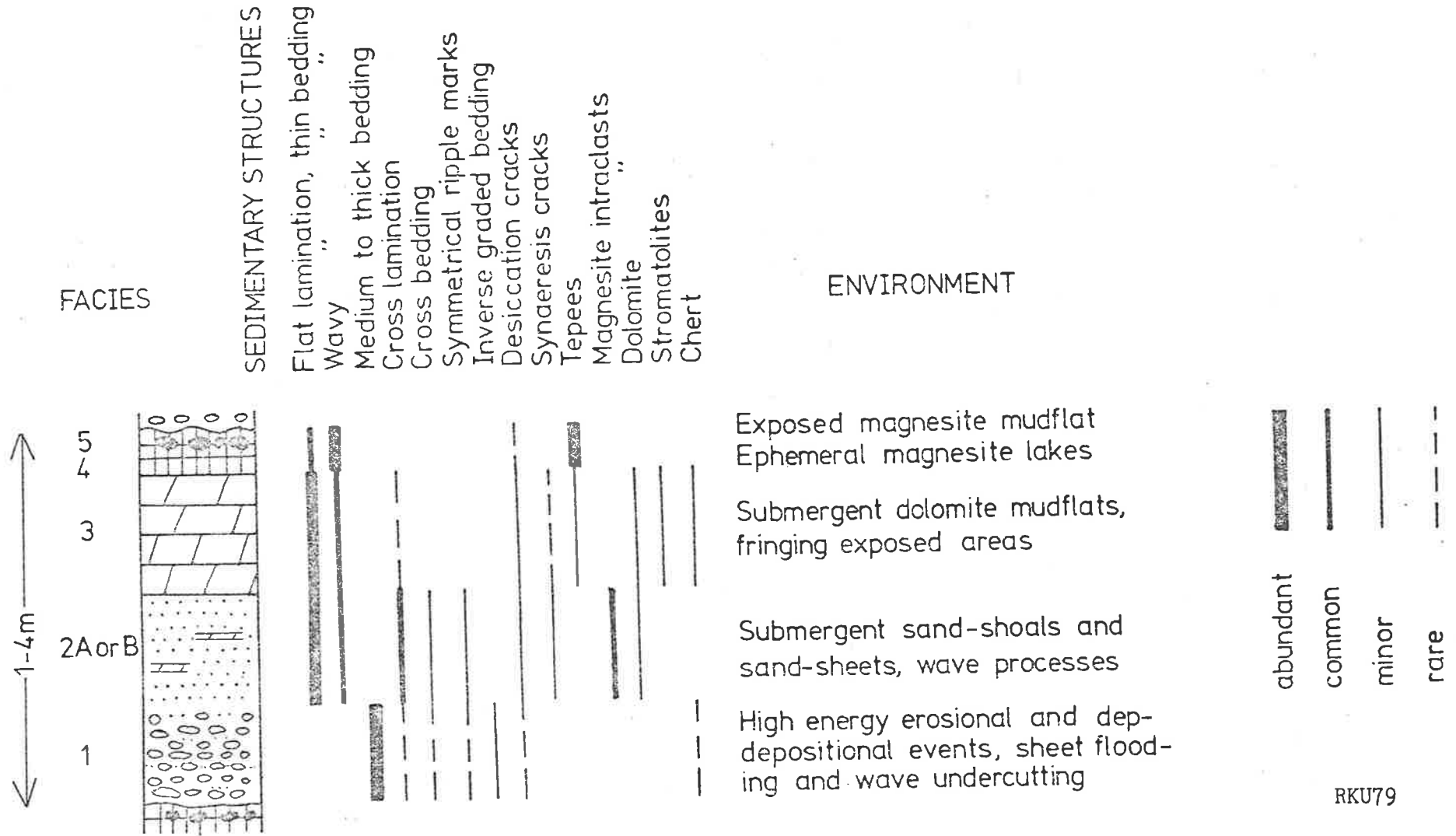
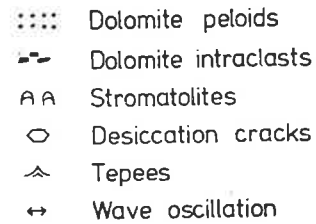
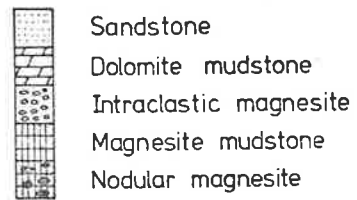
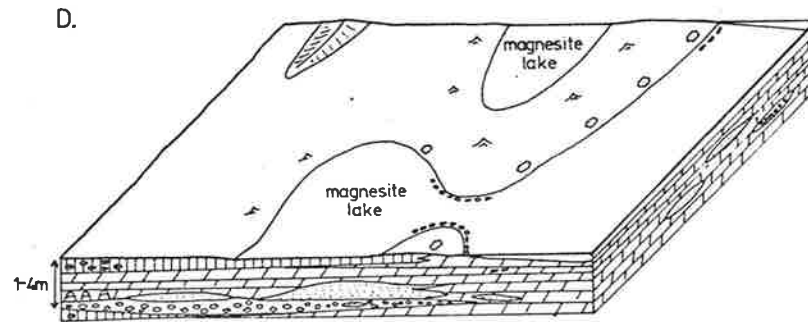
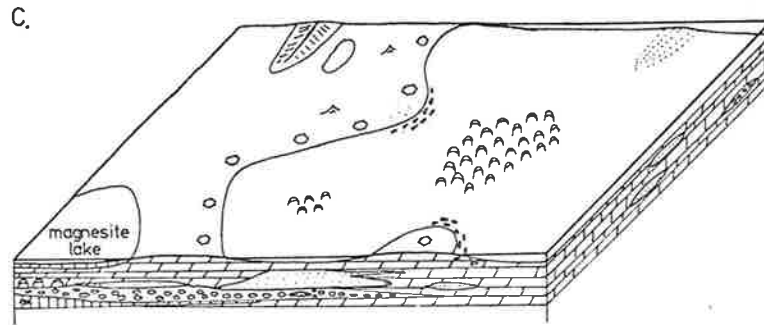
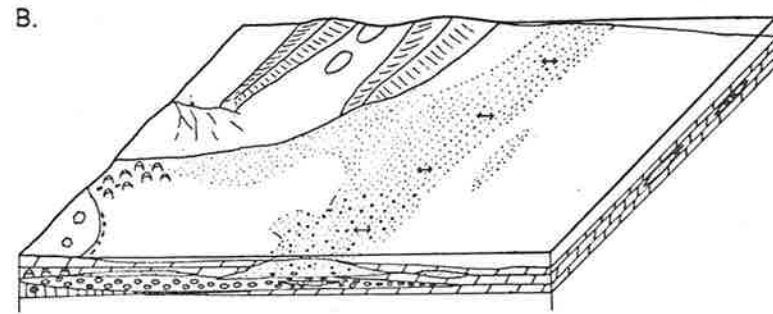
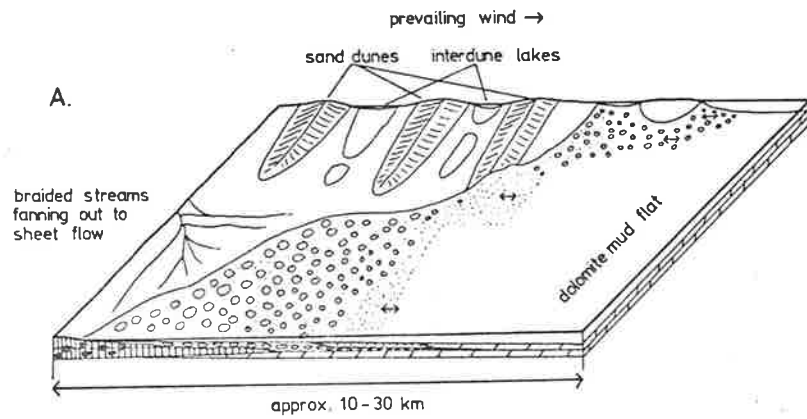


Figure 6.10. Summary of the intraclastic magnesite-dolomitic sandstone-dolomite mudstone-magnesite mudstone-nodular magnesite cycle, with the sedimentary structures of each facies and the environment of deposition.

Figure 6.11. Schematic block diagrams illustrating the formation of the major facies.

- A. Erosion of magnesite mudstones and nodular magnesite by sheet flooding and wave action as basin expands. Some introduction of sand.
- B. Magnesite mudstones now largely eroded, and sand deposition is more widespread as aeolian sand is transported into the basin where it is reworked by wave processes.
- C. Sand supply largely exhausted, and energy levels in basin lowered, resulting in the widespread deposition of dolomite muds. Minor magnesite deposition occurs in isolated lakes formed as water level falls.
- D. With continued fall in water level, magnesite deposition becomes more widespread, and there are extensive exposed mudflats.

Note vertical exaggeration.



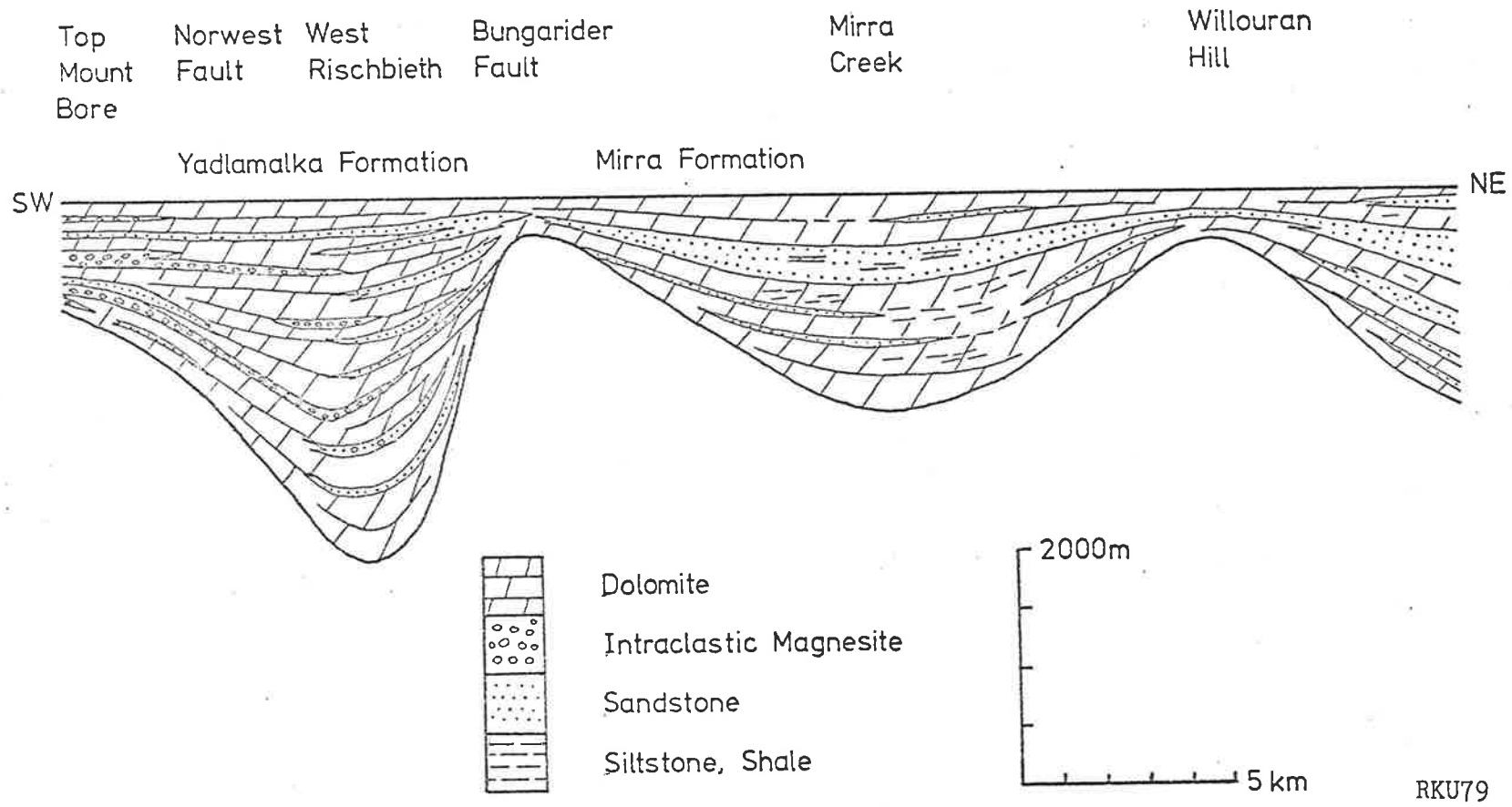
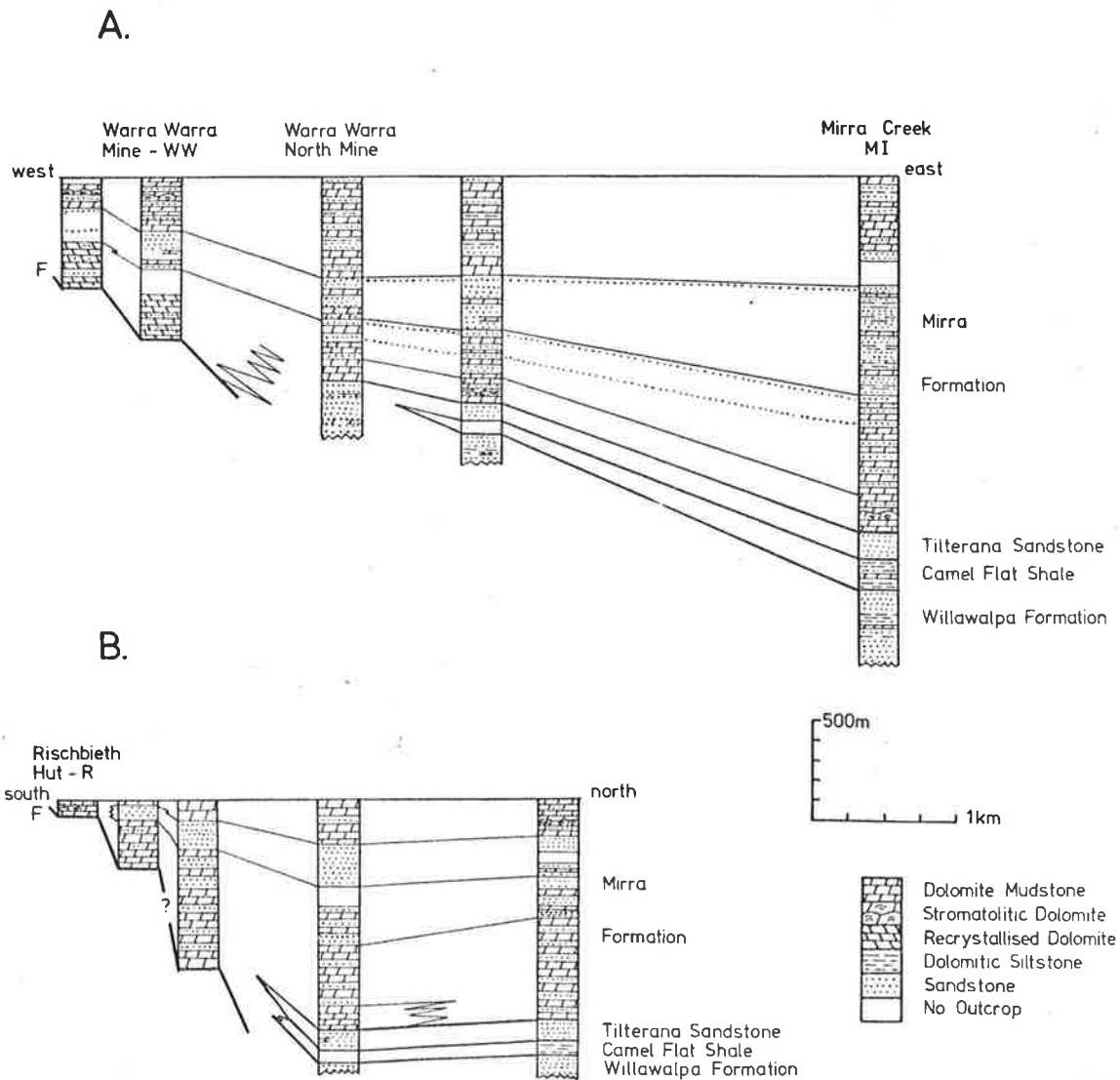


Figure 6.12. Summary of the major thickness and facies changes in the upper Mundallio Subgroup, from southwest to northeast across the Willouran Ranges.



RKU79

Figure 6.13. Stratigraphic cross sections in the Mundallio Subgroup, central Willouran Ranges, illustrating the marked thickness changes in the Mirra Formation.

- A. Warra Warra Mine to Mirra Creek
- B. Rischbieth Hut to the limits of outcrop of the Mundallio Subgroup between Withchelina and Callana Stations.

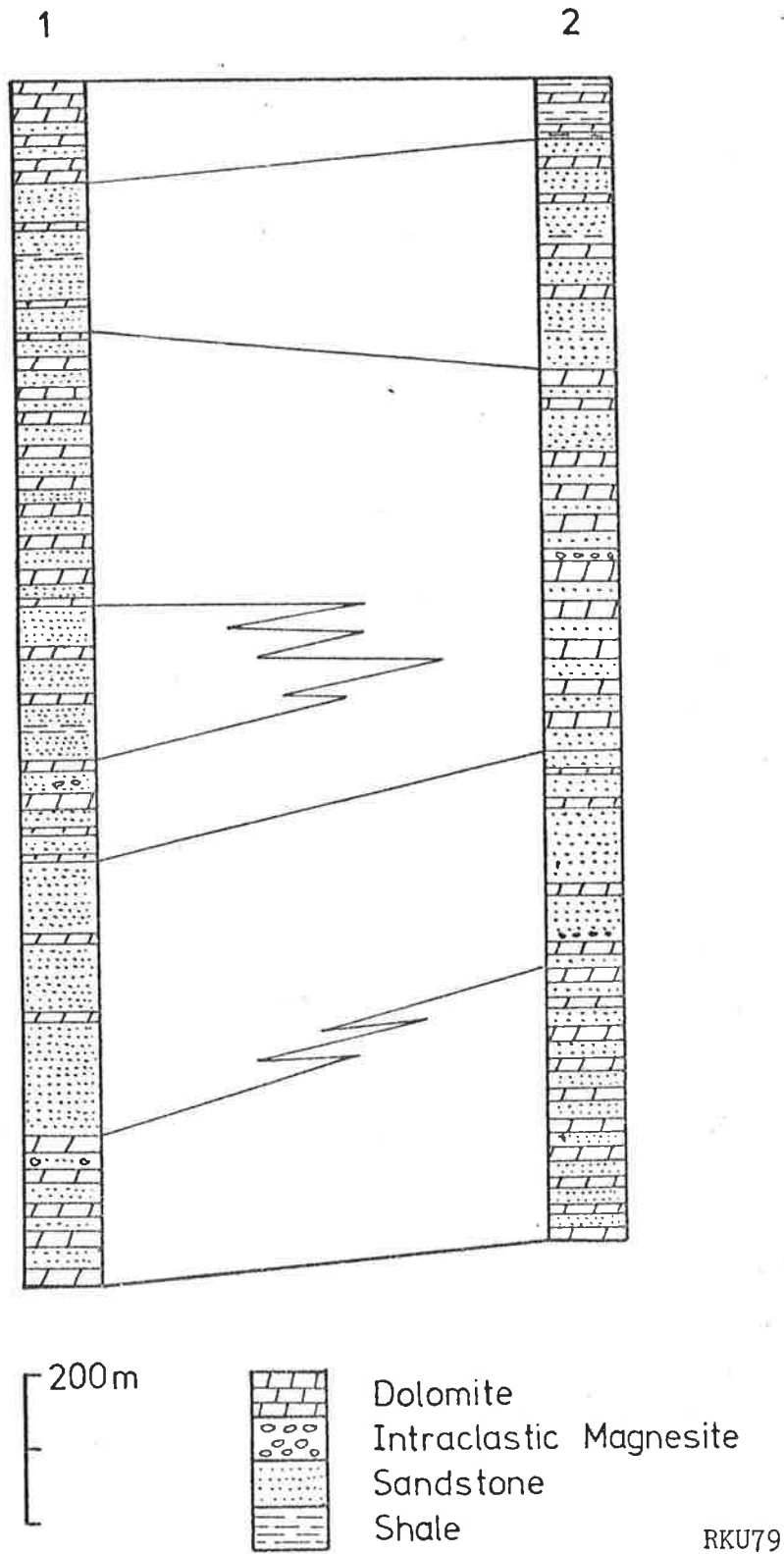


Figure 6.14. Summary stratigraphic sections in the Yadlamalka Formation, east of Yacka, illustrating the major pulses of sand influx which alternated with periods in which sandstones and dolomites (almost exclusively dolomite mudstones) were deposited in approximately equal abundance. Section 2 is on the River Broughton $7\frac{1}{2}$ km north east of Yacka, Section 1 is 3 km south of Section 1.

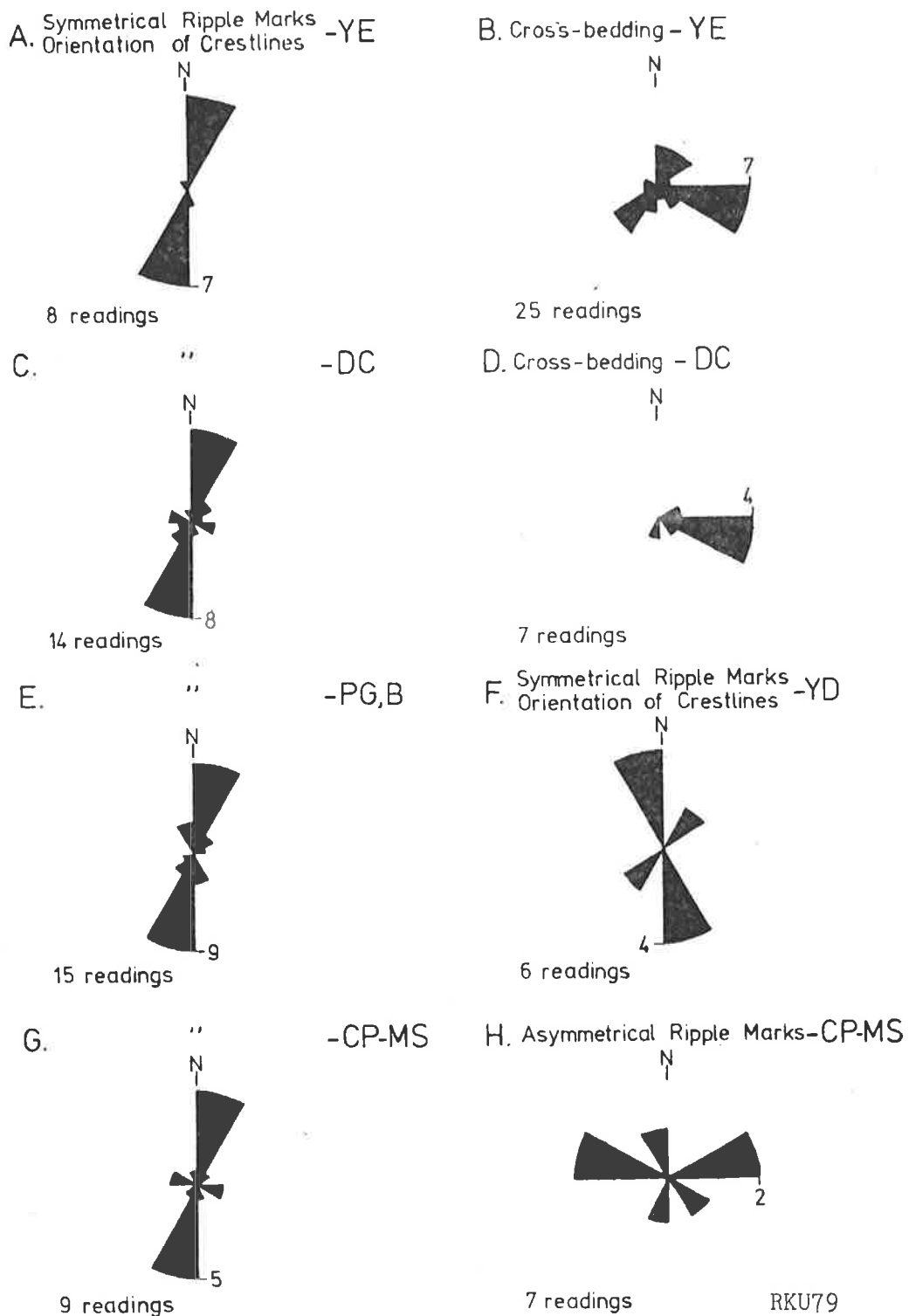


Figure 6.15. Palaeocurrent data, Yadlamalka Formation.
 A. and B. East of Yacka. C. and D. Depot Creek.
 E. Port Germein Gorge, Beetaloo. F. Yednalue.
 G. and H. Copley and Myrtle Springs.

Symmetrical Ripple Marks - Orientation of Crestlines
Willouran Ranges

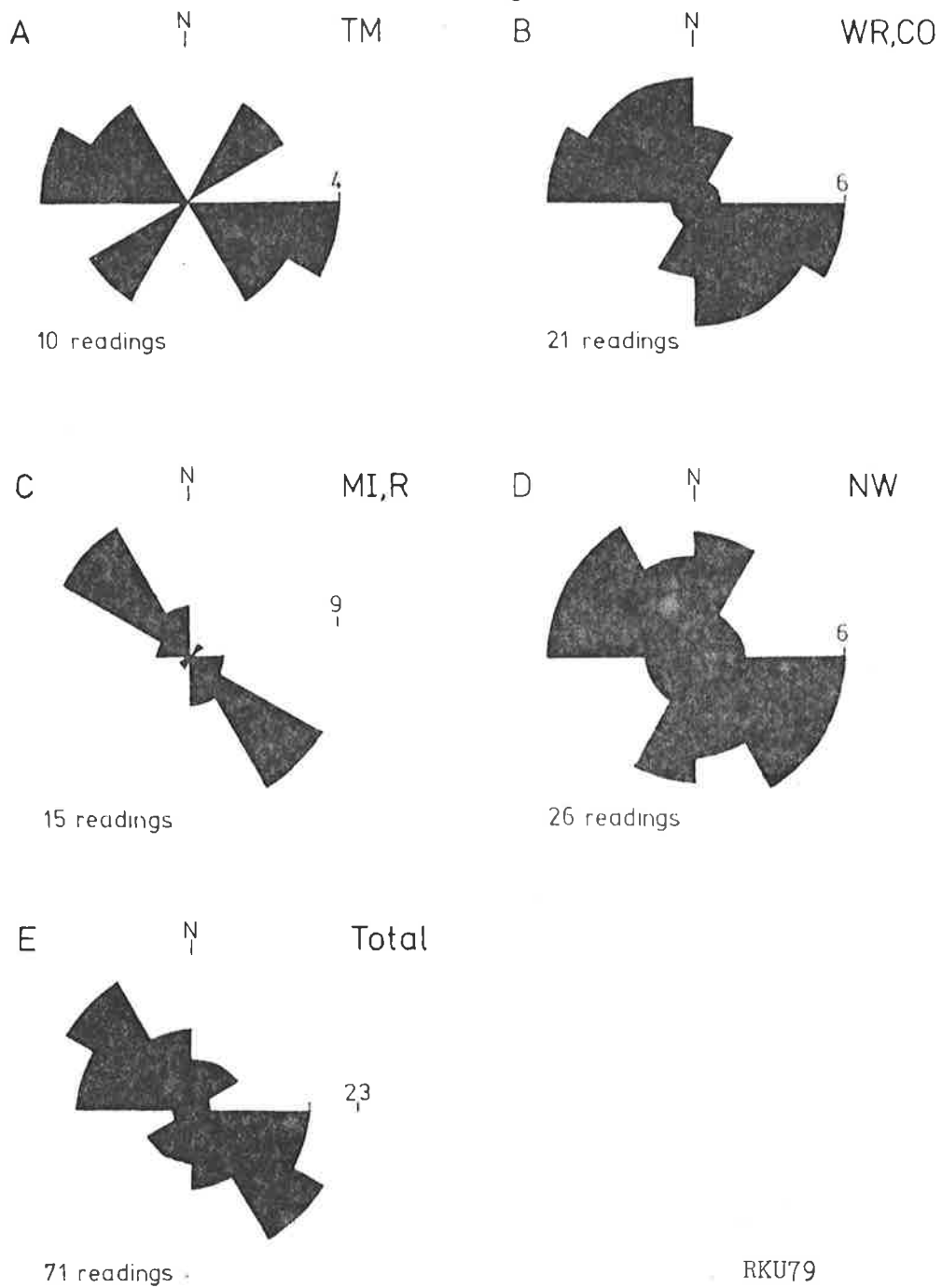


Figure 6.16. Palaeocurrent data, Yadlamalka and Mirra Formations, Willouran Ranges.
A. Top Mount Bore. B. West Rischbieth and Coronation Bore. C. Mirra Creek and Rischbieth. D. Mt. Norwest H.S. E. Total.

RKU79

Table 6.1. Distribution and abundance of magnesite facies.

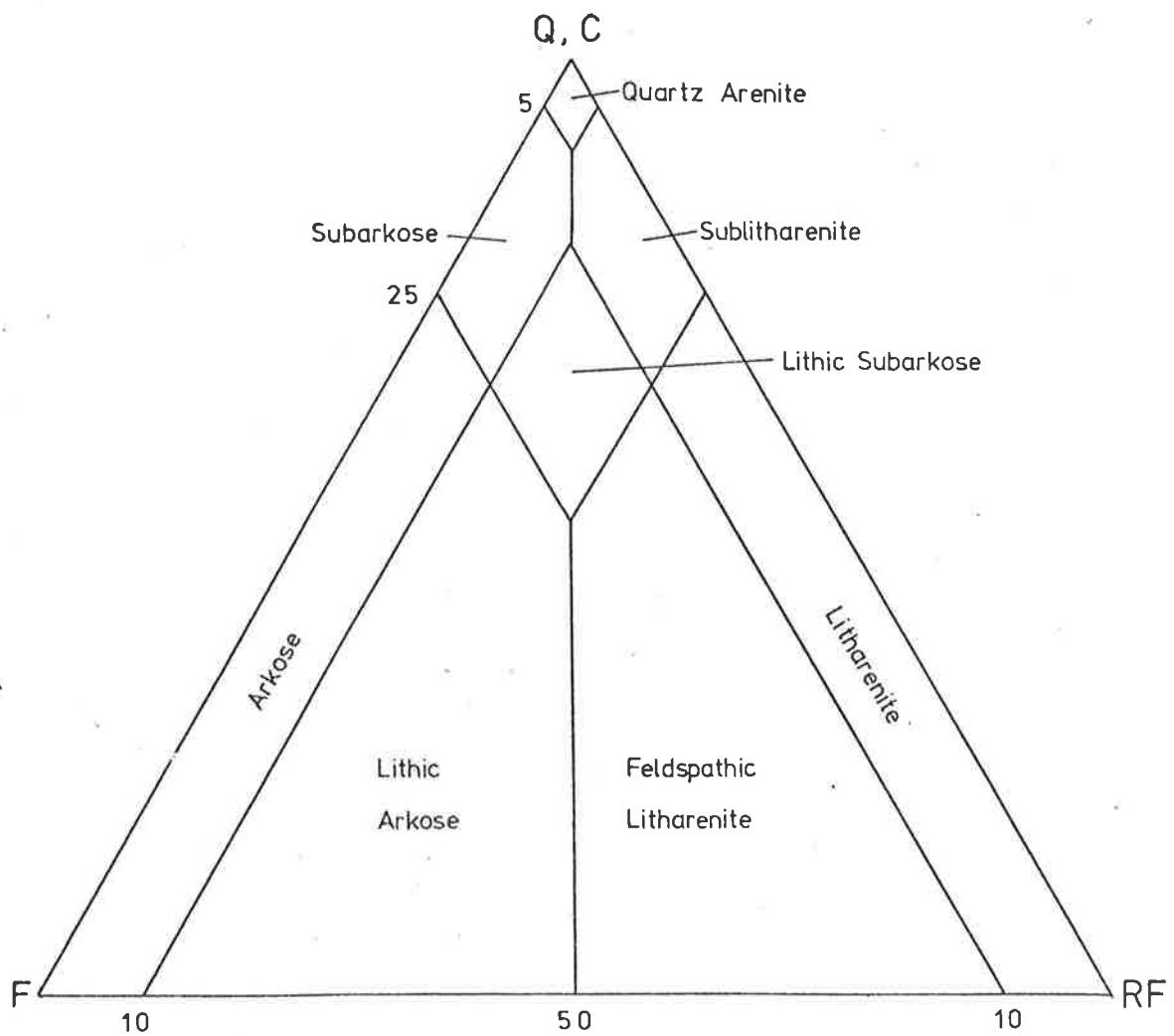
- Facies: 1 - Interlaminated magnesite-dolomite mudstones
2 - Magnesite mudstones
3 - Nodular magnesite
4 - Intraclastic magnesite

+ present; - absent (not observed);

p probably present, but outcrop very weathered

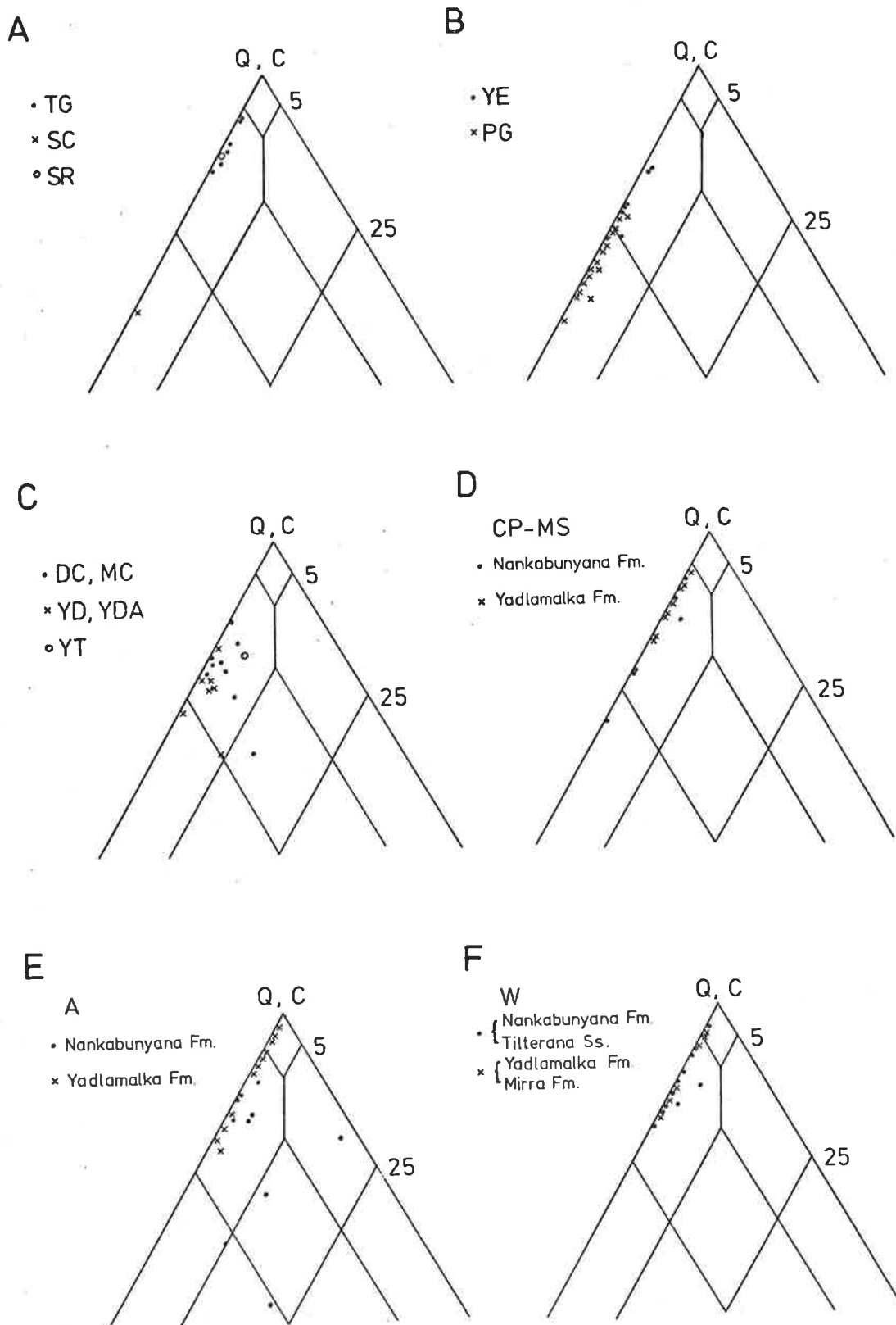
Data for percentage and thickness derived from the stratigraphic sections in Figures 6.3-7. The average thickness includes beds with more than one facies e.g. magnesite mudstone overlain by intraclastic magnesite.

	Area	Facies					% of sequence	average thickness(m)	range (m)	
		1	2	3	4					
Montacute Dol.	Torrens Gg.	+	+	+	+	1	1.3	0.28	0.15-1	
						2	9.5	0.35	0.1-0.6	
Yadlamalka Formation	Yacka	-	+	p	+		1.1	0.48	0.15-0.8	
	Beetaloo	-	-	-	+		no data			
	Port Germein Gg	-	+	p	+		0.2	0.3	0.2-0.3	
	Mundallio Creek	-	+	+	+		4.0	0.73	0.2-2.2	
	Depot Creek	-	+	+	+		11.0	0.55	0.08-2.15	
	Willow Creek	-	+	-	+		no data			
	Yednalue	-	+	-	+		1.6	0.52	0.1-1.5	
	Yednalue Ant.	-	+	-	+		2.7	0.56	0.1-1.3	
	Johnburg	-	+	-	+		3.8	0.56	0.1-1.1	
	Carrieton	-	-	-	+		no data			
	Yatina	-	-	-	+		0.2	0.2	0.2	
	Weekeroo	-	+	-	+		no data			
	Arkaroola		+	+	+	+	1	6.1	0.43	0.1-1.2
							2	5.1	0.47	0.05-1.1
	Copley		+	+	+	+	1	21.0	0.86	0.2-3.4
						2	21.2	0.96	0.2-4.9	
Myrtle Springs		-	+	+	+		18.0	0.89	0.2-3.0	
Top Mount		-	+	-	+		13.7	0.80	0.1-3.5	
West Rischbieth		-	+	-	+		3.8	0.84	0.2-3.8	
Mirra Formation	Mirra Creek	-	-	-	+		very minor		-0.7	
	Mt.Norwest H.S.	-	-	-	+		very minor		-0.5	



RKU79

Figure 7.1. Sandstone classification used in this study, and in particular Figure 7.2. After McBride (1963). Rock fragments (RF) include granitic and gneissic fragments.



RKU79

Figure 7.2. Composition of sandstones from the Mundallio Subgroup using the composition triangle shown in Figure 7.1. A. Torrens Gorge; Skillogalee Creek; Scrubby Range. B. Yacka east; Port Germein Gorge (compositions from McCarthy, 1974). C. Depot Creek; Mundallio Creek; Yednalue; Yednalue Anticline; Yatina. D. Copley-Myrtle Springs. E. Arkaroola. F. Willouran Ranges.

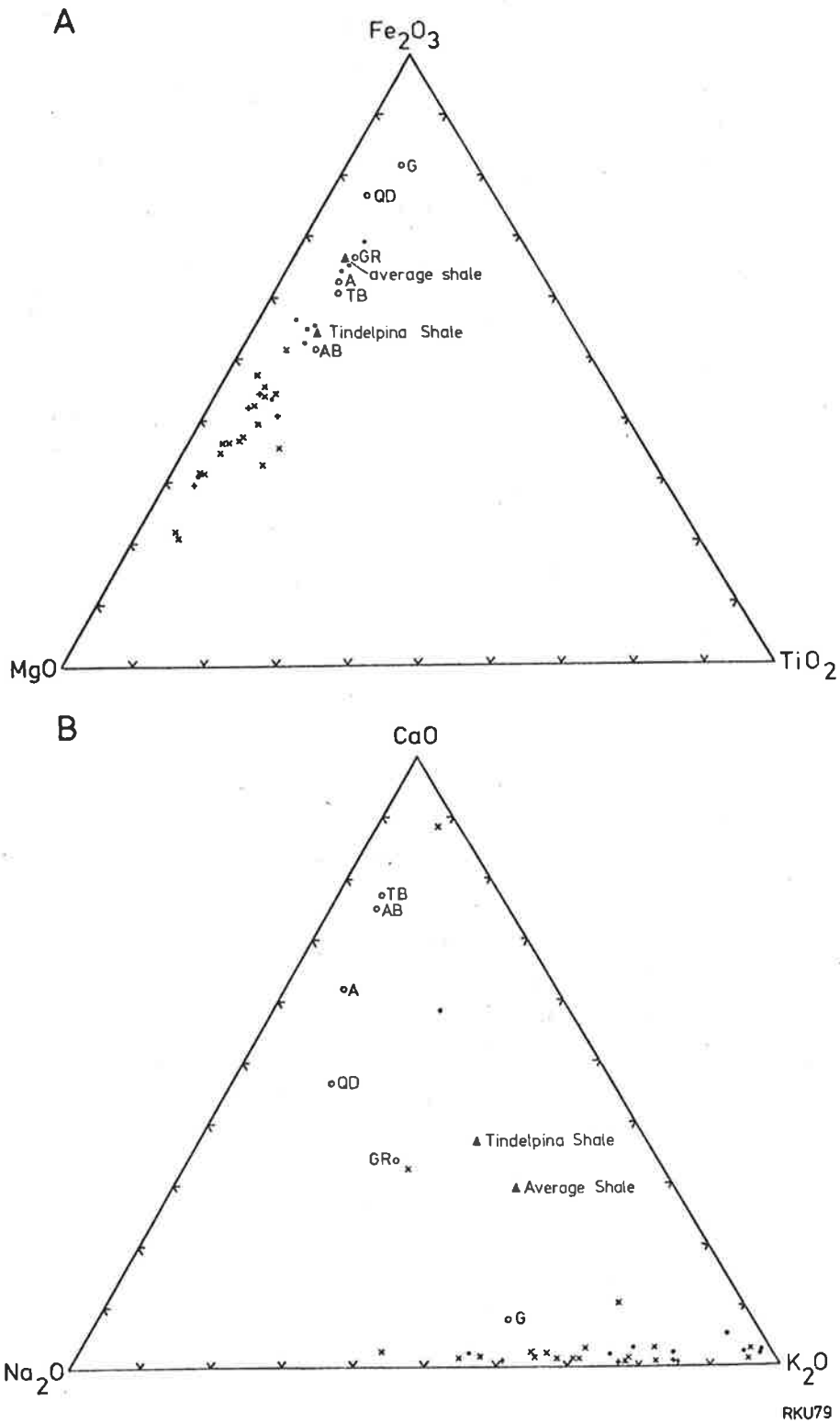
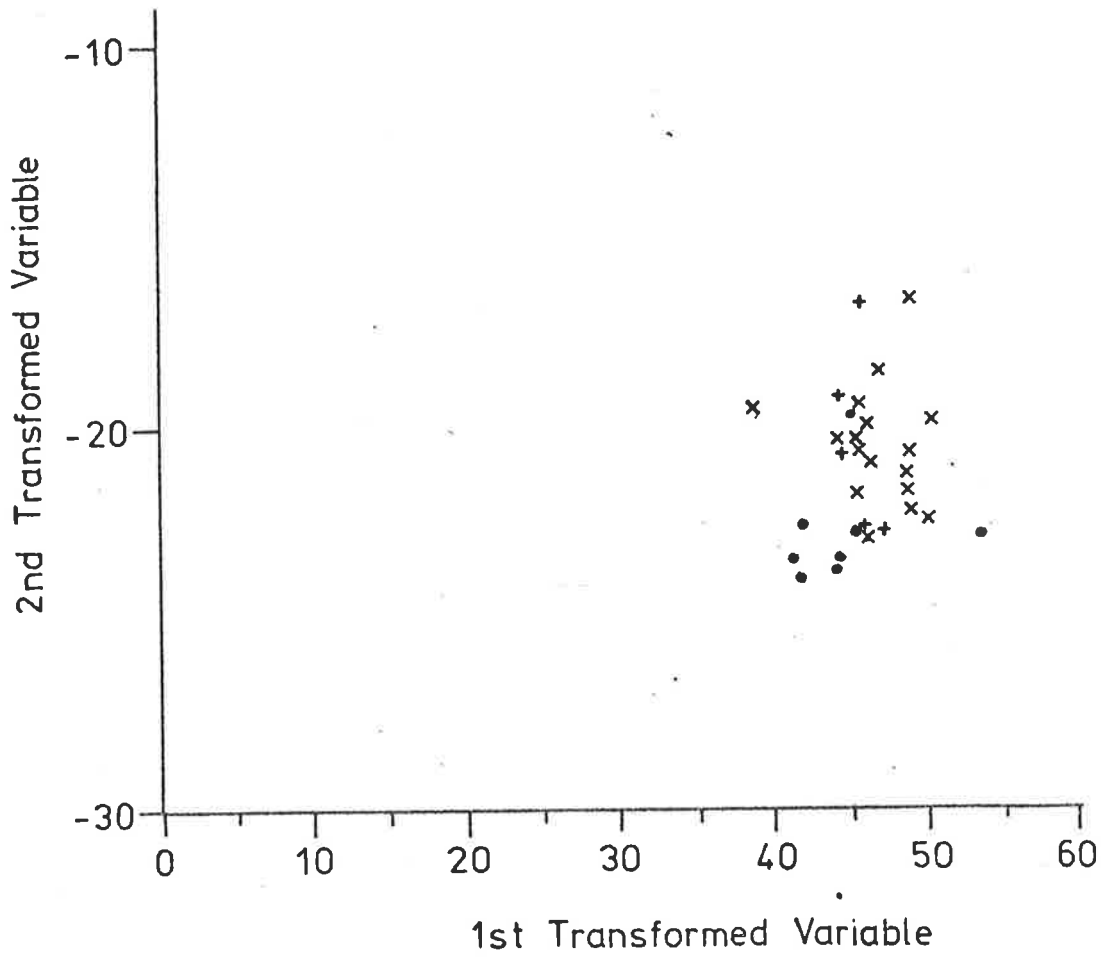
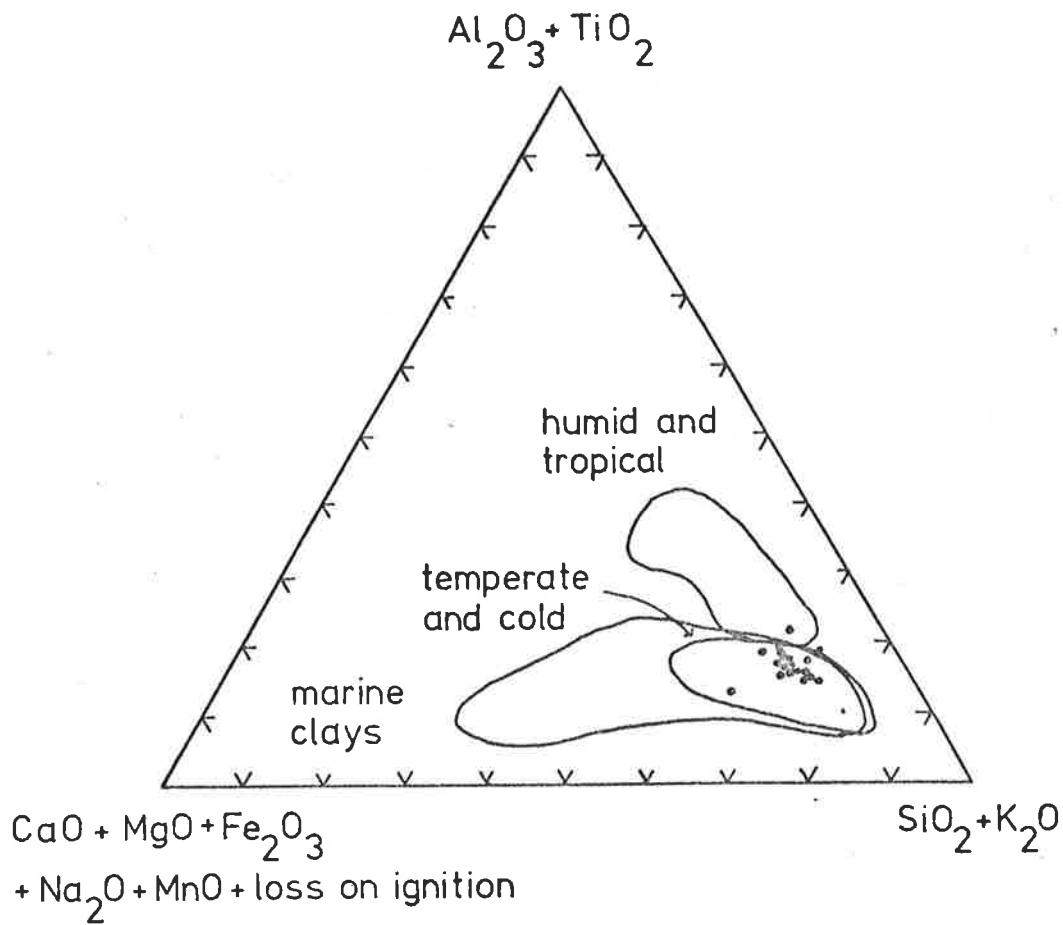


Figure 7.3. A. Fe_2O_3 - MgO - TiO_2 plot of shale compositions, where Fe_2O_3 is total iron.
 B. CaO - Na_2O - K_2O plot of shale compositions.
 x Units 1 and 2, Nathaltee Formation; Units 1, 2 and 3 Nankabunyana Formation.
 . Unit 3, Nathaltee Formation; Unit 4, Nankabunyana Formation.
 + Yadlamalka Formation.
 G : granite, GR : granodiorite, QD : quartz diorite
 A : andesite, AB : alkali basalt, TB : tholeiitic basalt - after Hyndman (1972).
 Average shale - after Wedepohl (1971); Tindelpina Shale - after Sumartojo (1974).



RKU79

Figure 7.4. Principal component analysis - plot of 2nd transformed variable versus 1st transformed variable. Symbols as in Figure 7.3.



RKU79

Figure 7.5. Compositions of shales from the three main environmental groups of Ronov and Khlebnikova (1957), showing the distribution of shales from the Mundallio Subgroup.

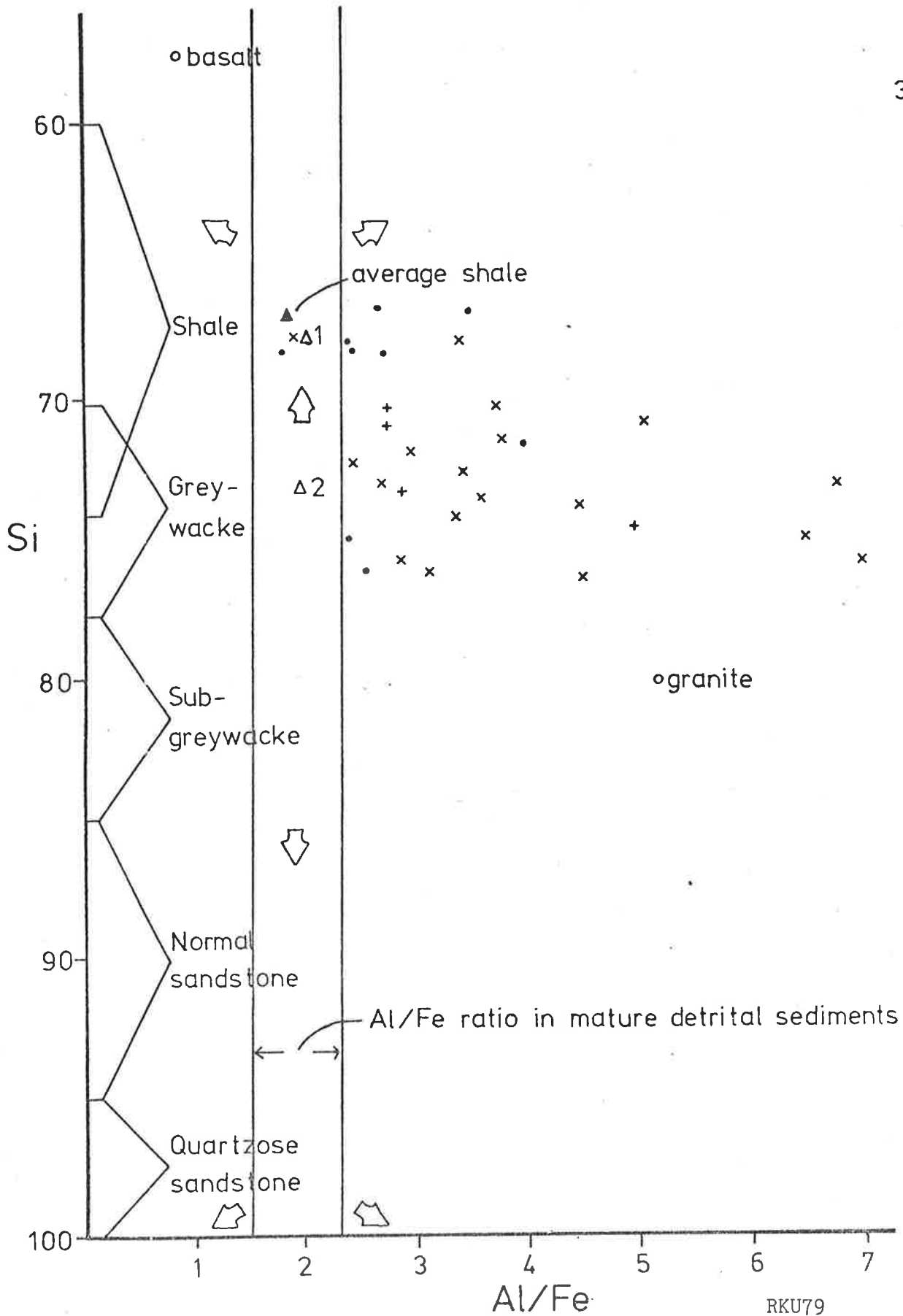


Figure 7.6. The Dennen and Moore (1971) Maturity Index of shales from the Mundallio Subgroup. Symbols as in Figure 7.3. 1=average of marine clays, 2=average of clays of cold and temperate environments, 3=average of humid and tropical clays (Ronov and Khlebnikova, 1957). Arrows show the paths of chemical change once a mature stage i.e. $Al/Fe = 1.9 \pm 0.4$, is reached.

Table 7.1. Whole rock analyses of shales and siltstones in the Mundallio Subgroup. Sample numbers beginning with A and T are from Arkaroola, with CP are from Copley and Myrtle Springs, with DC from Depot Creek, with B from Beetaloo, and with YDA from the Yednalue Anticline. Samples DC079, YDA042 and CP025 are dolomitic.

Formation		Sample	SiO ₂	Al ₂ O ₃	Fe ₂ O ₃	MnO	MgO	CaO	Na ₂ O	K ₂ O	TiO ₂	P ₂ O ₅	LOI	Total	
Nathaltee Formation	Units 1 and 2	DC023	62.59	16.08	3.57	0.00	6.29	0.19	0.16	5.92	0.16	0.05	4.36	99.82	
		DC079	29.6	4.48	1.26	0.05	14.9	18.23	0.62	1.68	0.13	0.06	29.40	100.41	
			BO14	65.04	15.64	4.87	0.02	3.98	0.22	2.56	4.91	0.56	0.07	2.56	100.43
			YDA041	58.50	16.15	6.43	0.01	6.56	0.12	2.17	4.82	0.65	0.05	3.90	99.36
			YDA044	64.03	14.34	2.44	0.01	8.09	0.13	2.08	4.03	0.63	0.06	4.09	99.93
			YDA089	66.37	16.36	1.92	0.02	2.78	0.11	4.39	5.47	0.71	0.04	1.92	100.09
		Unit 3	DC026	62.90	17.70	3.43	0.02	3.76	0.18	0.15	8.09	0.66	0.07	3.19	100.15
			DC083	59.80	17.91	5.03	0.02	3.41	0.44	0.53	8.48	0.70	0.20	3.20	99.72
			YDA042	51.11	10.65	3.40	0.15	6.95	8.08	2.51	3.30	0.44	0.10	13.23	99.92
			YDA058	61.24	16.08	6.82	0.01	4.52	0.18	2.96	3.85	0.68	0.10	3.31	99.75
Nankabunyana Formation	Units 1, 2 and 3	A028	66.95	13.95	3.44	0.02	5.57	0.22	2.52	5.24	0.53	0.05	1.55	100.04	
		A040	63.16	16.22	1.90	0.01	6.79	0.17	3.81	5.29	0.64	0.04	1.59	99.62	
		A041	62.34	17.42	3.55	0.02	5.38	0.16	2.23	5.83	0.75	0.05	1.67	99.39	
			A043	55.85	18.00	4.05	0.03	6.06	1.30	2.26	9.14	0.81	0.08	1.10	98.68
			A078	61.37	17.95	3.70	0.07	5.89	0.31	1.40	7.12	0.63	0.07	1.08	99.59
			A096	63.98	15.00	4.00	0.03	5.34	0.13	0.36	8.32	0.57	0.05	1.66	99.44
			A149	64.25	18.09	2.21	0.01	3.72	0.09	1.42	6.99	0.84	0.04	2.06	99.73
			A168	62.14	18.52	3.12	0.02	3.32	0.28	6.15	4.72	0.77	0.05	0.84	99.93
			T459	65.46	16.36	3.16	0.02	4.17	0.35	2.07	5.78	0.71	0.06	1.47	99.62
			CP001	65.25	15.48	4.39	0.02	4.69	0.09	2.14	4.76	0.63	0.05	2.77	100.27
			CP025	59.97	12.53	3.38	0.05	6.9	3.02	3.31	2.94	0.44	0.06	6.64	99.24
			CP086	65.88	15.58	3.55	0.02	3.64	0.10	1.58	6.13	0.65	0.05	2.58	99.76
			CP101	63.31	16.30	4.22	0.01	5.16	0.10	1.94	4.78	0.64	0.06	3.18	99.70
		Unit 4	A004	59.81	20.35	4.49	0.01	3.3	0.17	0.14	7.72	0.72	0.09	2.80	99.60
			A034	69.9	13.92	4.18	0.03	2.71	0.18	1.11	4.54	0.61	0.08	2.20	99.47
			A158	60.42	19.29	5.60	0.08	2.42	0.23	0.57	8.30	0.70	0.09	1.84	99.55
			CP028	62.22	18.11	5.70	0.04	2.31	0.20	1.02	6.12	0.73	0.09	3.08	99.62
		CP103	62.11	18.18	5.81	0.03	1.79	0.20	1.87	6.25	0.73	0.11	2.75	99.83	
Yadlamalka Formation		YDA066	64.41	16.17	2.51	0.01	2.97	0.10	2.20	8.16	0.65	0.03	2.45	99.69	
		A058	62.44	14.94	3.95	0.03	8.87	0.09	1.07	6.2	0.60	0.04	1.78	100.01	
		A186	60.75	16.53	4.61	0.05	5.66	0.12	3.73	5.92	0.66	0.04	1.26	99.33	
		CP113	61.36	16.28	4.55	0.03	5.03	0.10	1.28	7.70	0.67	0.04	2.95	99.99	

LOI Loss on Ignition

	(1)	(2)	(3)	(4)	(5)	(6)	(7)	(8)
SiO ₂	58.9	63.06	53.32	58.32	59.77	68.79	61.39	62.89
Al ₂ O ₃	16.7	13.53	29.79	16.60	13.65	13.54	15.96	16.65
Fe ₂ O ₃	2.8				5.45	5.18	3.91	4.04
FeO	3.7	5.25	2.46	6.13				
MnO	0.09		0.06	0.06	0.07	0.03	0.03	0.02
MgO	2.6	1.57	0.54	2.22	3.75	2.60	5.09	4.62
CaO	2.2	3.16	0.93	3.76	4.01	0.62	1.11	0.21
Na ₂ O	1.6	1.98	0.56	0.67	1.17	1.23	1.95	1.93
K ₂ O	3.6	3.97	1.24	3.07	3.35	3.76	5.89	6.23
TiO ₂	0.78	0.69	1.21	0.90	0.95	0.89	0.63	0.66
P ₂ O ₅	0.16				0.18	0.13	0.06	0.07
LOI	6.3	7.38	10.23	8.4	7.31	3.31	3.70	2.39
Total		100.6	100.34	100.13				

Table 7.2 Composition of some shales

- (1) average shale, Wedepohl (1971)
- (2) continental clays, cold and temperate belt, Ronov and Khlebnikova (1957)
- (3) continental clays, tropical belt, Ronov and Khlebnikova (1957)
- (4) marine clays, Ronov and Khlebnikova (1957)
- (5) Tindelpina Shale, Adelaide Geosyncline, Sumartojo (1974)
- (6) Sturt Tillite, Adelaide Geosyncline, Sumartojo (1974)
- (7) this study (n = 32)
- (8) this study, excluding dolomitic shales (n = 29)

A. Correlation coefficients for the complete sample group (n = 32).

	SiO ₂	Al ₂ O ₃	Fe ₂ O ₃	MnO	MgO	CaO	Na ₂ O	K ₂ O	TiO ₂	P ₂ O ₅
Al ₂ O ₃	.634									
Fe ₂ O ₃	.193	.414								
MnO	-.412	-.334	.019							
MgO	-.731	-.777	-.407	.188						
CaO	-.926	-.833	-.377	.459	.736					
Na ₂ O	.153	.013	-.183	-.027	-.076	-.107				
K ₂ O	.344	.708	.192	-.166	-.511	.529	.394			
TiO ₂	.583	.835	.296	-.303	-.714	.720	.216	.564		
P ₂ O ₅	-.150	.156	.462	.219	-.238	.061	-.296	.165	.102	
LOI	-.906	-.842	-.327	.383	.733	.980	-.181	-.565	-.766	.073

limiting value at 95% confidence level = .349

limiting value at 99.9% confidence level = .554

B. Correlation coefficients excluding three dolomitic shales (n = 29)

	SiO ₂	Al ₂ O ₃	Fe ₂ O ₃	MnO	MgO	CaO	Na ₂ O	K ₂ O	TiO ₂	P ₂ O ₅
Al ₂ O ₃	-.620									
Fe ₂ O ₃	-.438	.189								
MnO	-.211	.283	.275							
MgO	-.202	-.454	-.188	-.145						
CaO	-.510	.276	.074	.161	.068					
Na ₂ O	.088	-.095	-.256	-.157	.020	.027				
K ₂ O	-.446	.506	-.028	.349	-.200	.387	-.513			
TiO ₂	-.307	.569	.015	.094	-.376	.295	.266	.230		
P ₂ O ₅	-.320	.375	.511	.137	-.367	.345	-.328	.249	.189	
LOI	-.049	-.138	.323	-.442	.042	-.308	-.425	-.206	-.374	.235

limiting value at 95% confidence level = .365

limiting value at 99.9% confidence level = .570

Table 7.3. Correlation Coefficients

SOLUTIONS OF COVARIANCE MATRIX

EIGEN VALUES

89.7633 7.9279 2.8158 2.3400 1.5930 .6411 .1517 .0111 .0044 .0006 .0004

EIGEN VALUES AS PERCENTAGES - ABSOLUTE AND CUMULATIVE

85.2864 7.5325 2.6754 2.2233 1.5135 .6091 .1442 .0105 .0042 .0006 .0004

85.2864 92.8189 95.4943 97.7176 99.2311 99.8402 99.9844 99.9949 99.9991 99.9996 100.0000

EIGEN VECTORS

SiO ₂	.6875	-.5721	-.2141	-.1700	-.0322	-.0945	-.0291	.3320	.0645	.0079	.0048
Al ₂ O ₃	.2405	.5770	-.0264	.1784	-.1090	-.6474	-.1302	.3567	.0381	.0056	.0054
Fe ₂ O ₃	.0415	.1840	-.1575	.1624	.8296	.2960	-.0028	.3640	.0692	-.0027	.0007
MnO	-.0012	.0006	-.0025	.0020	.0002	.0118	-.0262	.0018	-.0797	.1380	.9868
MgO	-.2089	-.2005	.7662	-.3479	.1901	-.2198	-.0094	.3432	.0744	.0137	.0083
CaO	-.3583	-.1110	-.1840	.0368	-.2598	.2061	-.7370	.4092	.0559	-.0026	-.0188
Na ₂ O	.0201	-.1324	.2865	.7150	-.2991	.2481	.3430	.3431	.0477	.0136	.0069
K ₂ O	.0940	.4221	-.0479	-.5222	-.3246	.4557	.3162	.3479	.0620	.0093	.0069
TiO ₂	.0106	.0209	.0019	.0212	-.0171	.0011	-.0229	-.1691	.9815	-.0010	.0790
P ₂ O ₅	-.0002	.0046	-.0079	.0013	.0069	.0031	-.0098	-.0186	.0087	.9901	-.1380
LiO	-.5325	-.2393	-.4726	-.0790	.0050	-.3522	.4690	.2777	.0713	.0103	.0189

Table 7.4. Principal Component Analysis - Total sample group (n = 32)

SOLUTIONS OF COVARIANCE MATRIX

EIGEN VALUES

9.9266 4.1762 2.4750 2.1183 .7258 .4012 .0464 .0079 .0040 .0005 .0001

EIGEN VALUES AS PERCENTAGES - ABSOLUTE AND CUMULATIVE

49.9273 21.0051 12.4482 10.6544 3.6508 2.0178 .2335 .0395 .0202 .0025 .0007
 49.9273 70.9324 83.3806 94.0350 97.6858 99.7036 99.9372 99.9767 99.9969 99.9993 100.0000

EIGEN VECTORS

SiO ₂	.8663	-.2594	-.1411	-.0492	-.0196	-.1987	-.1824	.2591	.1391	-.0153	.0005
Al ₂ O ₃	-.3640	-.4035	.2253	-.1399	-.5066	-.4894	-.2056	.2843	.1217	-.0177	-.0017
Fe ₂ O ₃	-.1800	-.0442	-.0219	.7105	.4899	-.2513	-.2530	.2678	.1447	-.0232	-.0053
MnO	-.0015	-.0019	-.0006	-.0010	.0088	-.0115	-.0083	.0094	-.0411	.0100	.9989
MgO	-.0264	.8132	-.2180	-.2136	-.0978	-.3038	-.2307	.2587	.1511	-.0101	.0005
CaO	-.0359	.0062	.0101	-.0383	.0751	.0245	.7774	.5796	.2079	-.0855	.0100
Na ₂ O	.0902	.1409	.7947	-.1596	.1700	.3530	-.2748	.2659	.1228	-.0088	.0036
K ₂ O	-.2726	-.2901	-.4468	-.4775	.3628	.3143	-.3076	.2621	.1414	-.0131	-.0003
TiO ₂	-.0109	-.0171	.0267	-.0137	.0040	-.0096	.0638	-.4183	.9034	-.0407	.0419
P ₂ O ₅	-.0041	-.0057	-.0025	.0085	.0018	.0009	.0449	.0615	.0705	.9945	-.0072
LiO	-.0079	.0479	-.2219	.4153	-.5719	.5843	-.1632	.2433	.1449	-.0212	.0147

Table 7.5. Principal Component Analysis - Excluding dolomitic shales (n = 29)

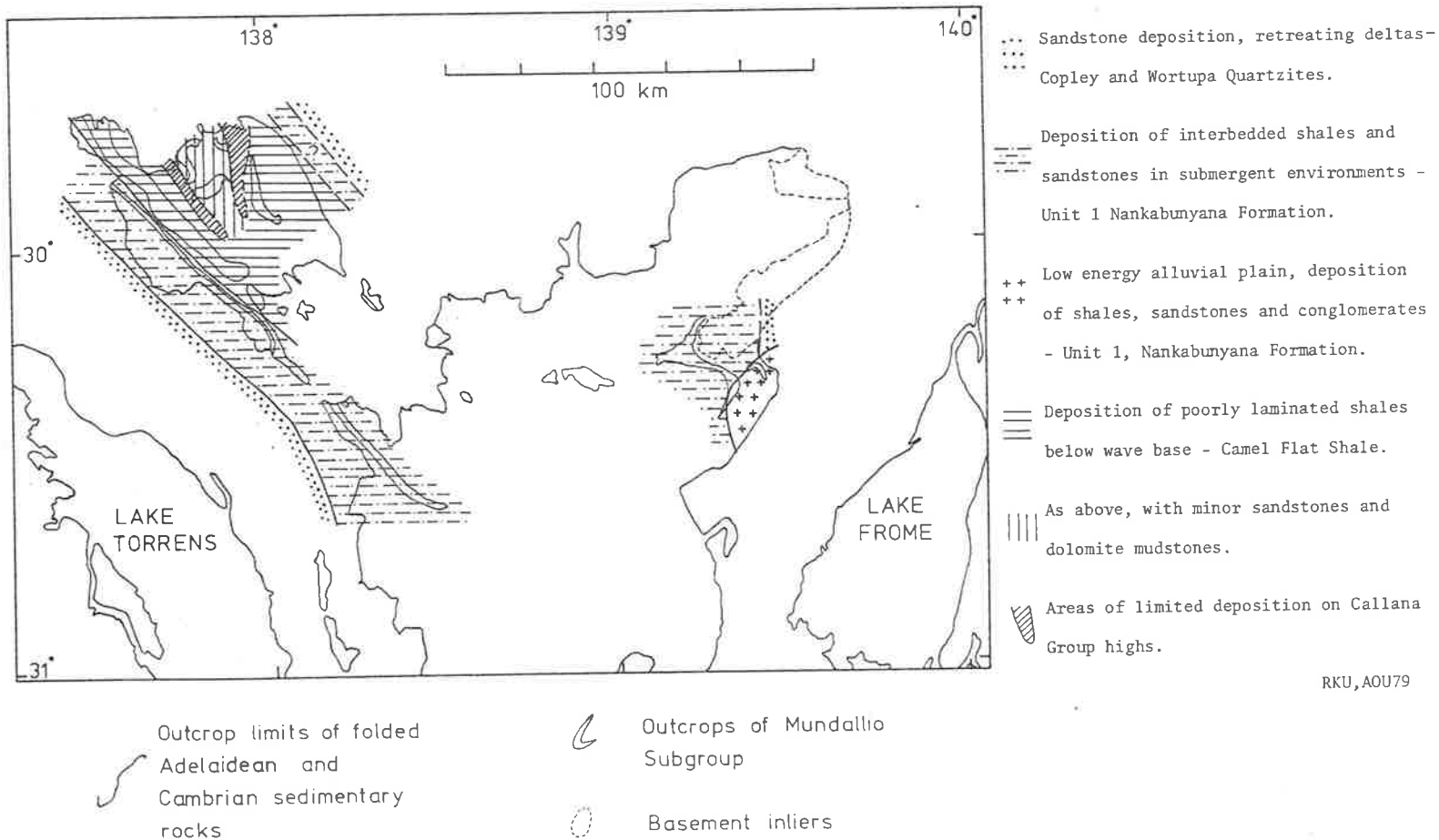
- (1) Mean value for all samples (n = 32) VI = 1.63
- (2) Mean value, excluding dolomitic shales (n = 29) VI = 1.76
- (3) Mean value - Nathaltee Formation, Units 1 and 2,
and Nankabunyana Formation, Units 1 - 3
(n = 17) VI = 1.38
- (4) Mean value - Nathaltee Formation, Unit 3,
and Nankabunyana Formation, Unit 4
(n = 8) VI = 2.73
- (5) Mean value - Yadlamalka Formation (n = 4) VI = 1.46

Values of components in Vogt Index

mol %	Al_2O_3	K_2O	MgO	Na_2O	CaO	VI
(3)	16.0	6.17	12.76	3.72	0.44	1.38
(4)	17.35	7.08	7.50	2.19	0.38	2.73
(5)	15.67	7.42	13.97	3.34	0.18	1.46

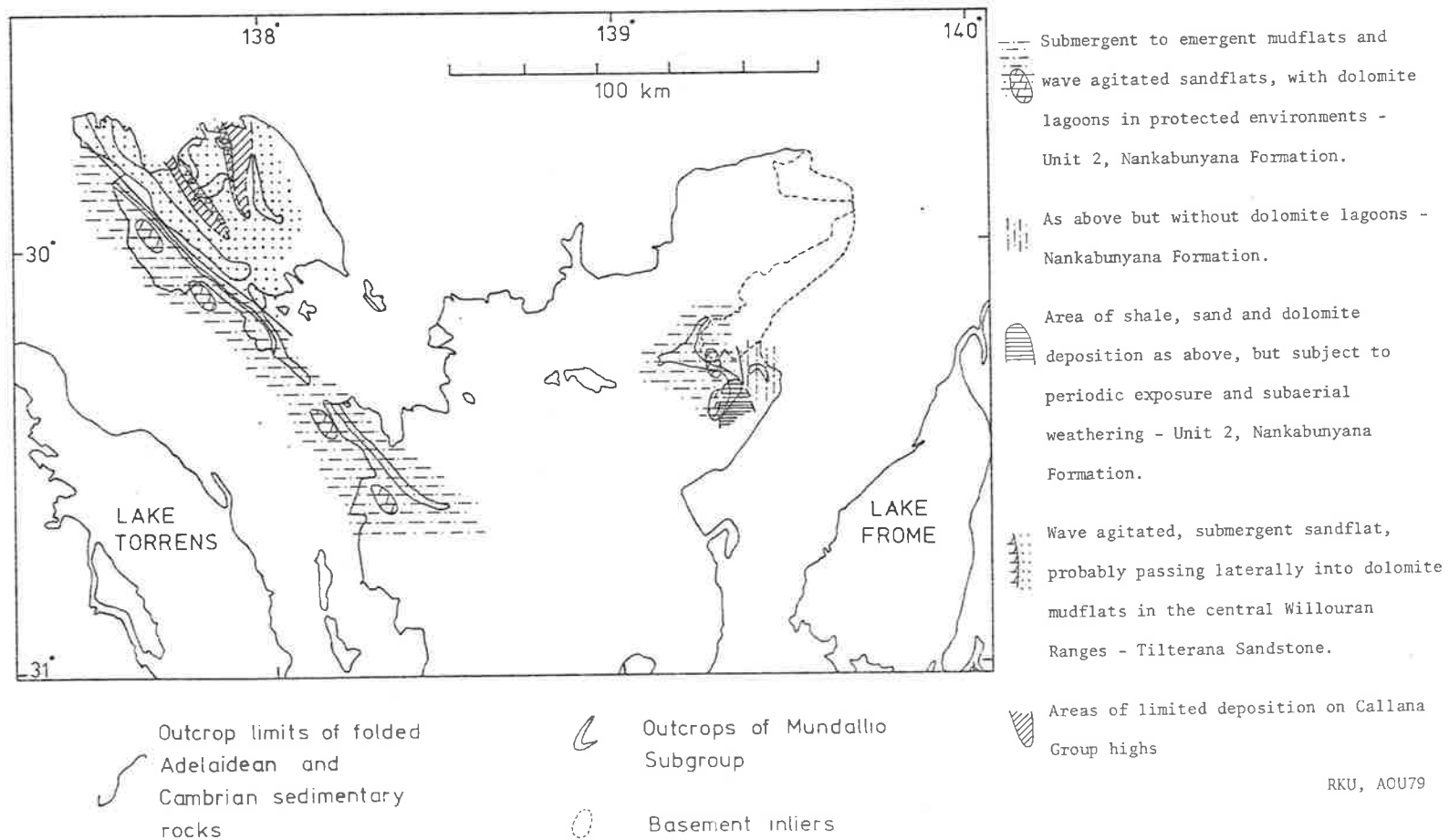
Vogt Index for an average granite	VI = 2.5
grandodiorite	VI = 1.13
andesite	VI = 0.58
basalt	VI = 0.35

Table 7.6. Vogt Indices. Values for average igneous rocks are from Hyndman (1972).



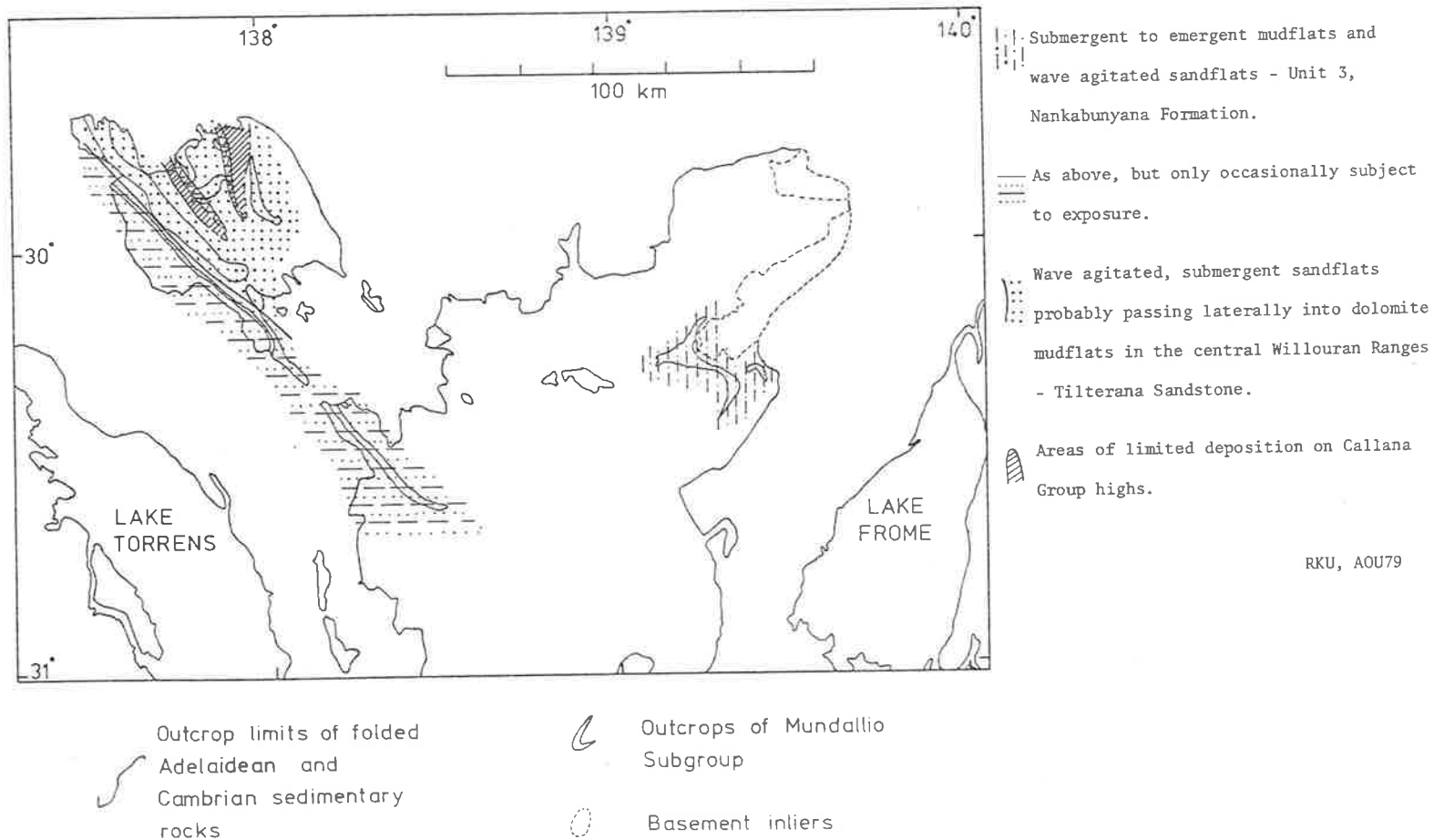
RKU, AOU79

Figure 8.1. Distribution of facies and environments, lower Mundallio Subgroup, northern Flinders and Willouran Ranges I. Unit 1, Nankabunyana Formation, Camel Flat Shale.



RKU, AOU79

Figure 8.2. Distribution of facies and environments, lower Mundallio Subgroup, northern Flinders and Willouran Ranges II. Unit 2, Nankabunyana Formation, lowermost Tilterana Sandstone.



RKU, AOU79

Figure 8.3. Distribution of facies and environments, lower Mundallio Subgroup, northern Flinders and Willouran Ranges III. Unit 3, Nankabunyana Formation, Tilterana Sandstone.

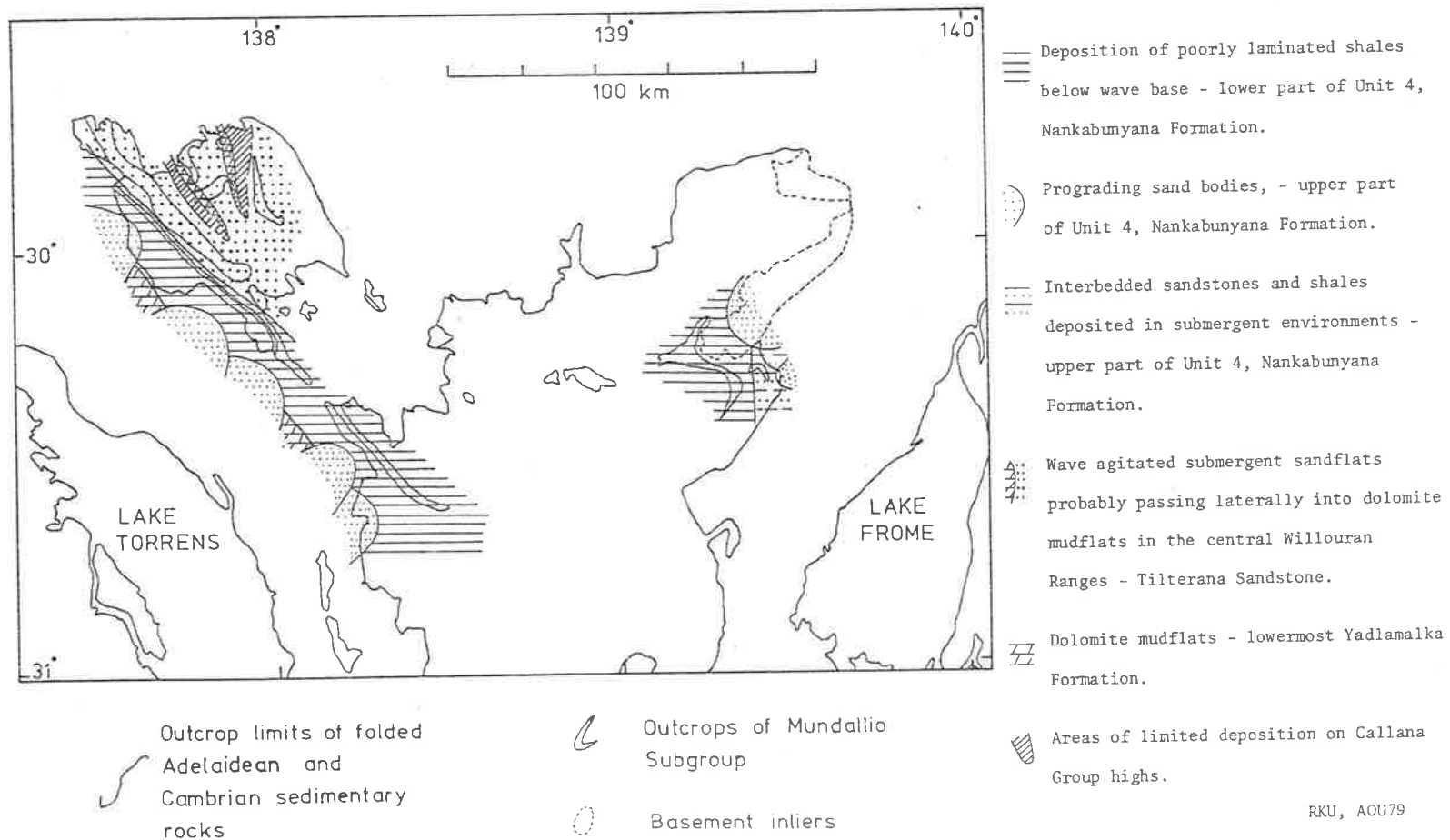
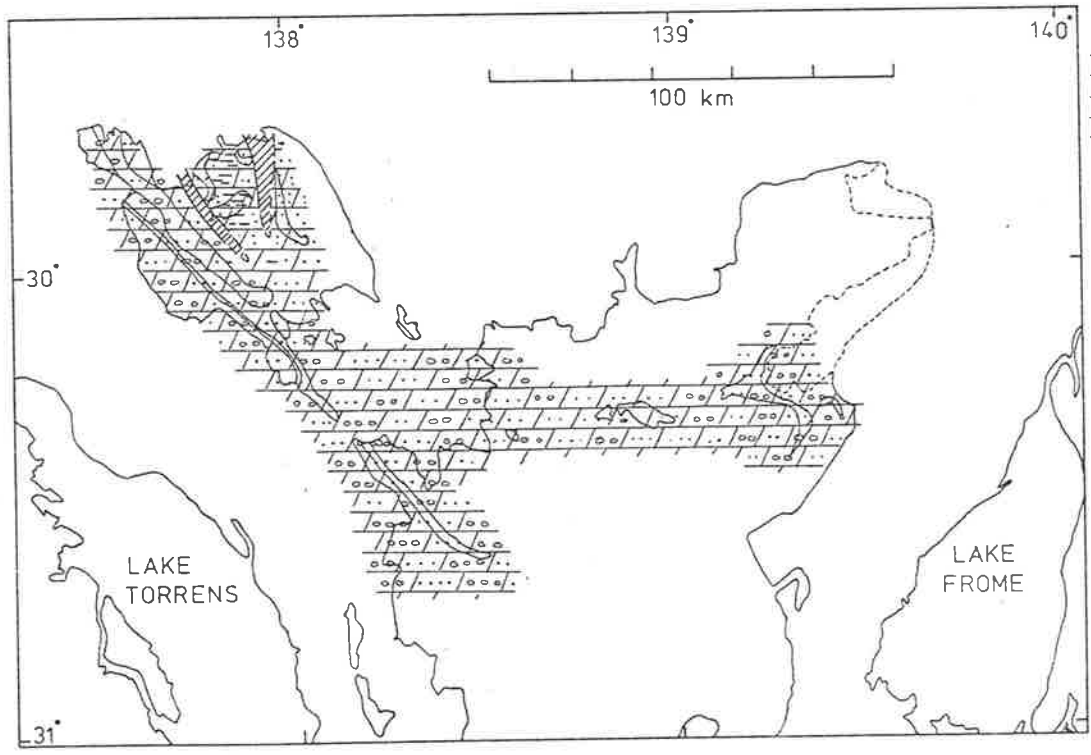
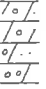
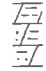
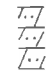



Figure 8.4. Distribution of facies and environments, lower Mundallio Subgroup, northern Flinders and Willouran Ranges IV. Unit 4, Nankabunyana Formation, uppermost Tilterana Sandstone.



-  Alternating deposition of dolomite mudstones on submergent to occasionally emergent dolomite mudflats, sandstones on wave agitated sandshoals and sand flats, magnesite in ephemeral lagoons, and intraclastic magnesite during high energy periods - Yadlamalka Formation.
-  Deposition of dolomite mudstones, sandstones and siltstones in largely submergent environments - Mirra Formation, central Willouran Ranges.
-  Deposition of sandstones and dolomite mudstones in largely submergent environments - Mirra Formation, eastern Willouran Ranges.
-  Areas of limited deposition on Callana Group highs.

-  Outcrop limits of folded Adelaidean and Cambrian sedimentary rocks
-  Outcrops of Mundallio Subgroup
-  Basement inliers

RKU, AOU79

Figure 8.5. Distribution of facies and environments, upper Mundallio Subgroup, northern Flinders and Willouran Ranges.

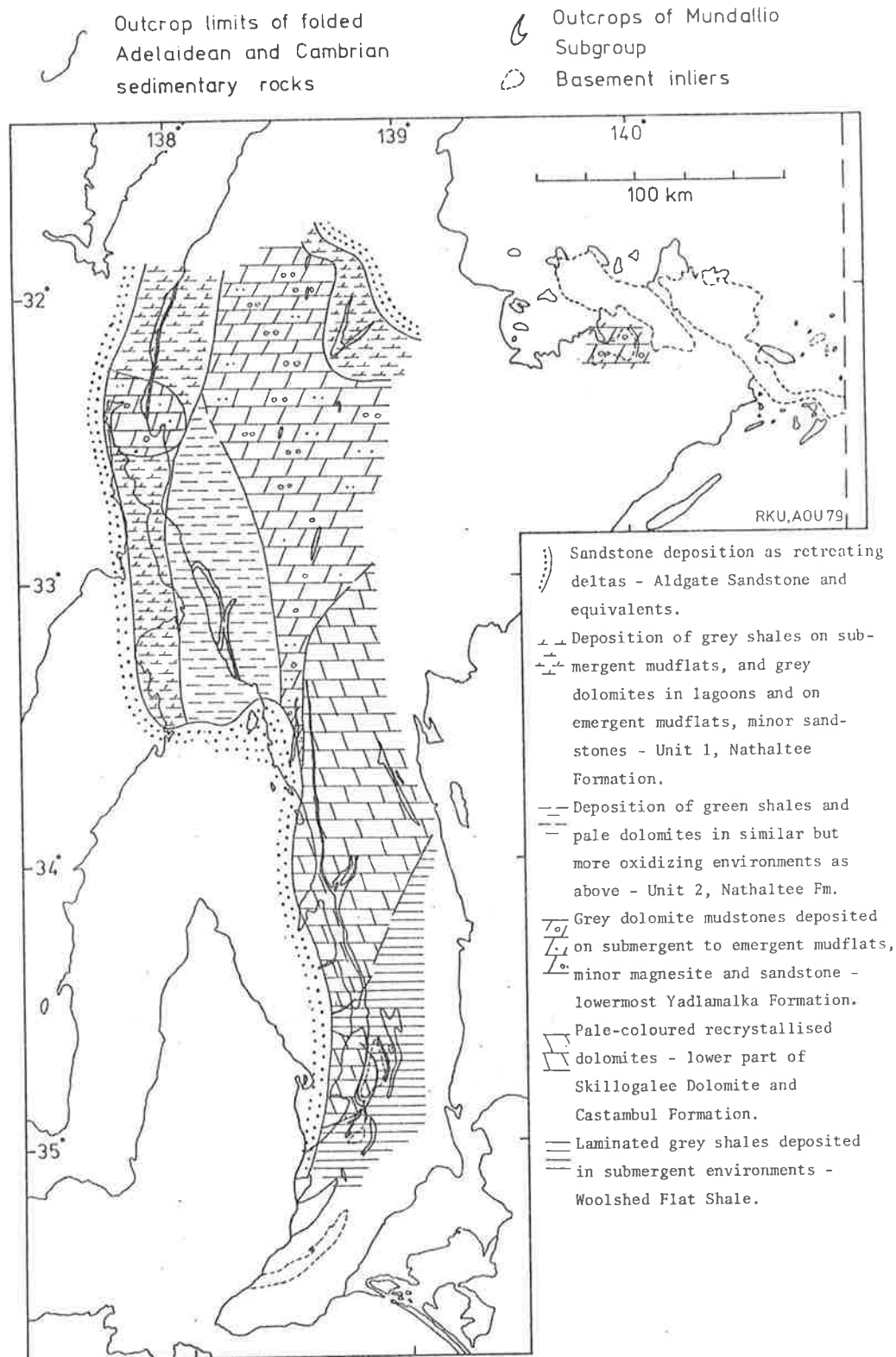


Figure 8.6. Distribution of facies and environments, lower Mundallio Subgroup, southern Flinders and Mt. Lofty Ranges I.

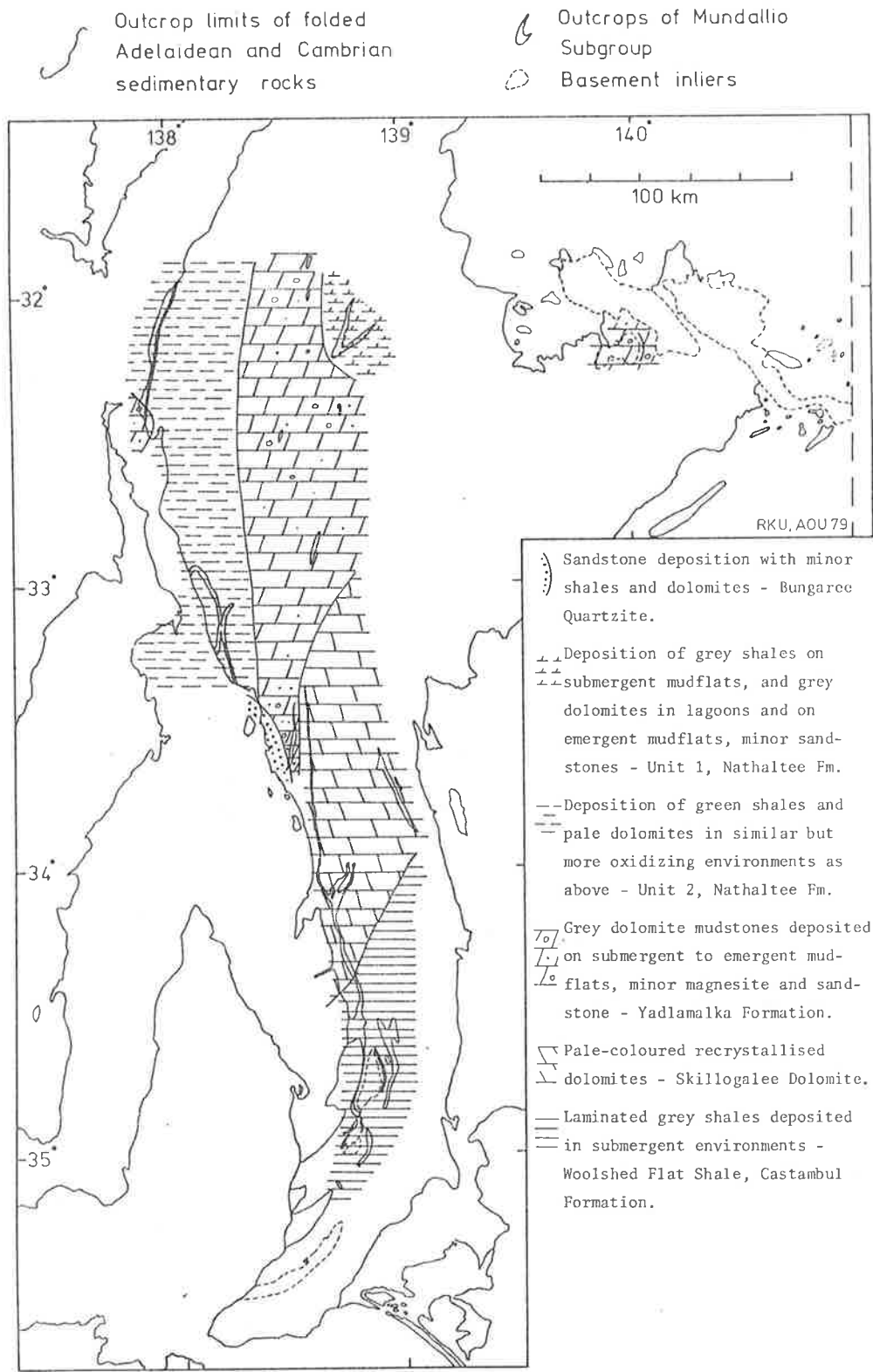


Figure 8.7. Distribution of facies and environments, lower Mundallio Subgroup, southern Flinders and Mt. Lofty Ranges II.

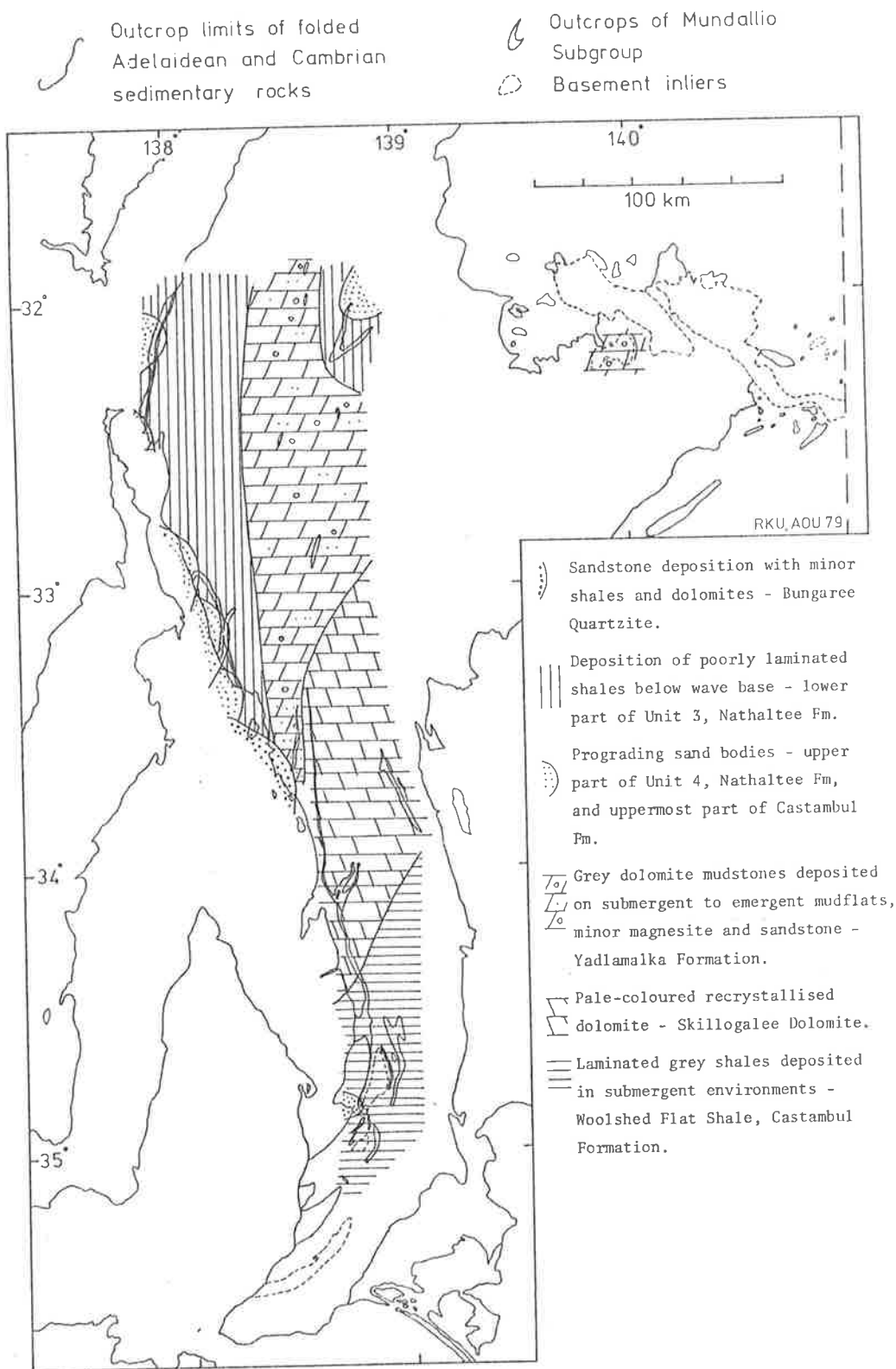


Figure 8.8. Distribution of facies and environments, lower Mundallio Subgroup, southern Flinders and Mt. Lofty Ranges III.

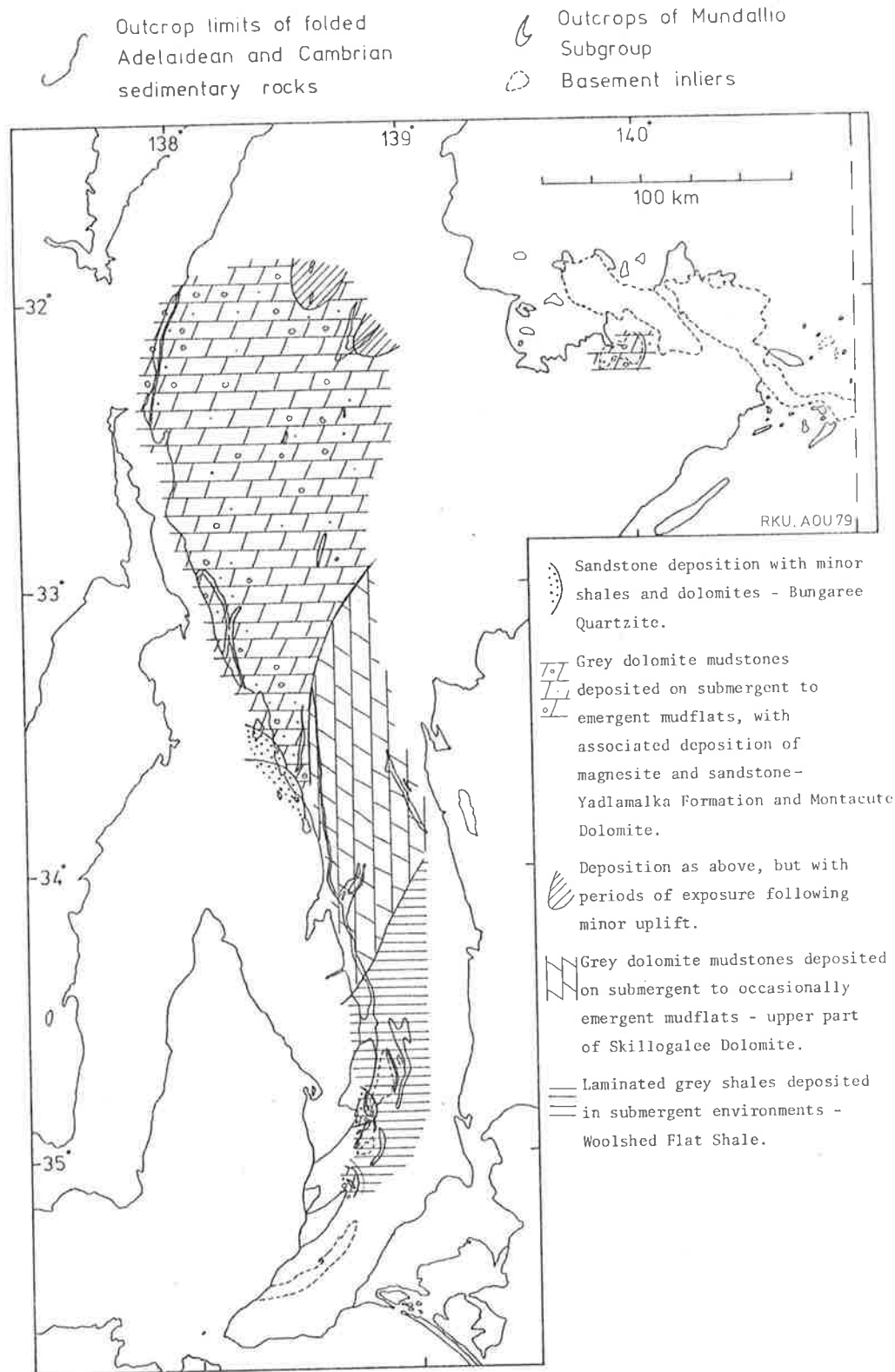


Figure 8.9. Distribution of facies and environments, upper Mundallio Subgroup, southern Flinders and Mt. Lofty Ranges.

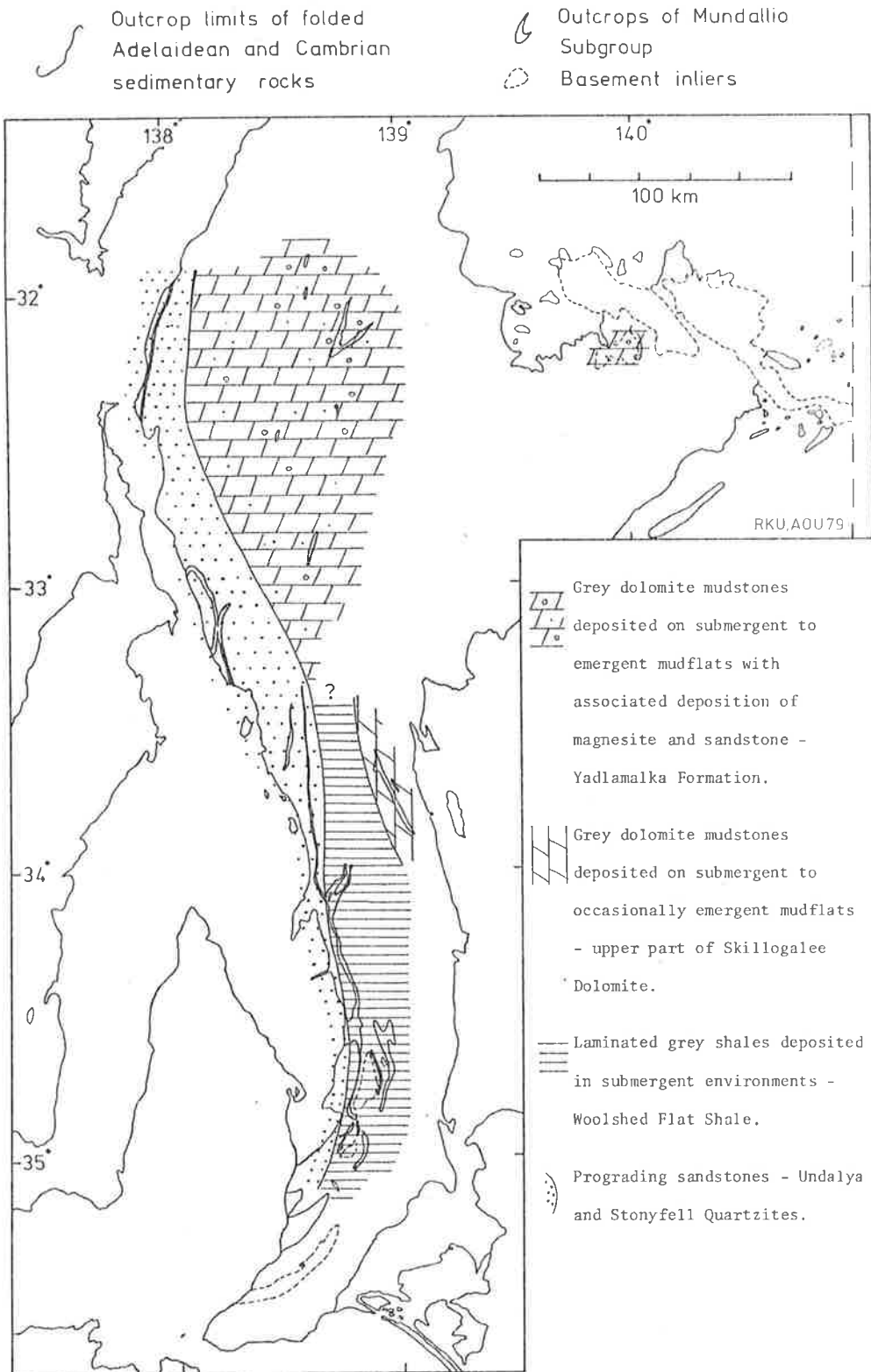


Figure 8.10. Distribution of facies and environments, uppermost and post-Mundallio Subgroup, southern Flinders and Mt. Lofty Ranges.

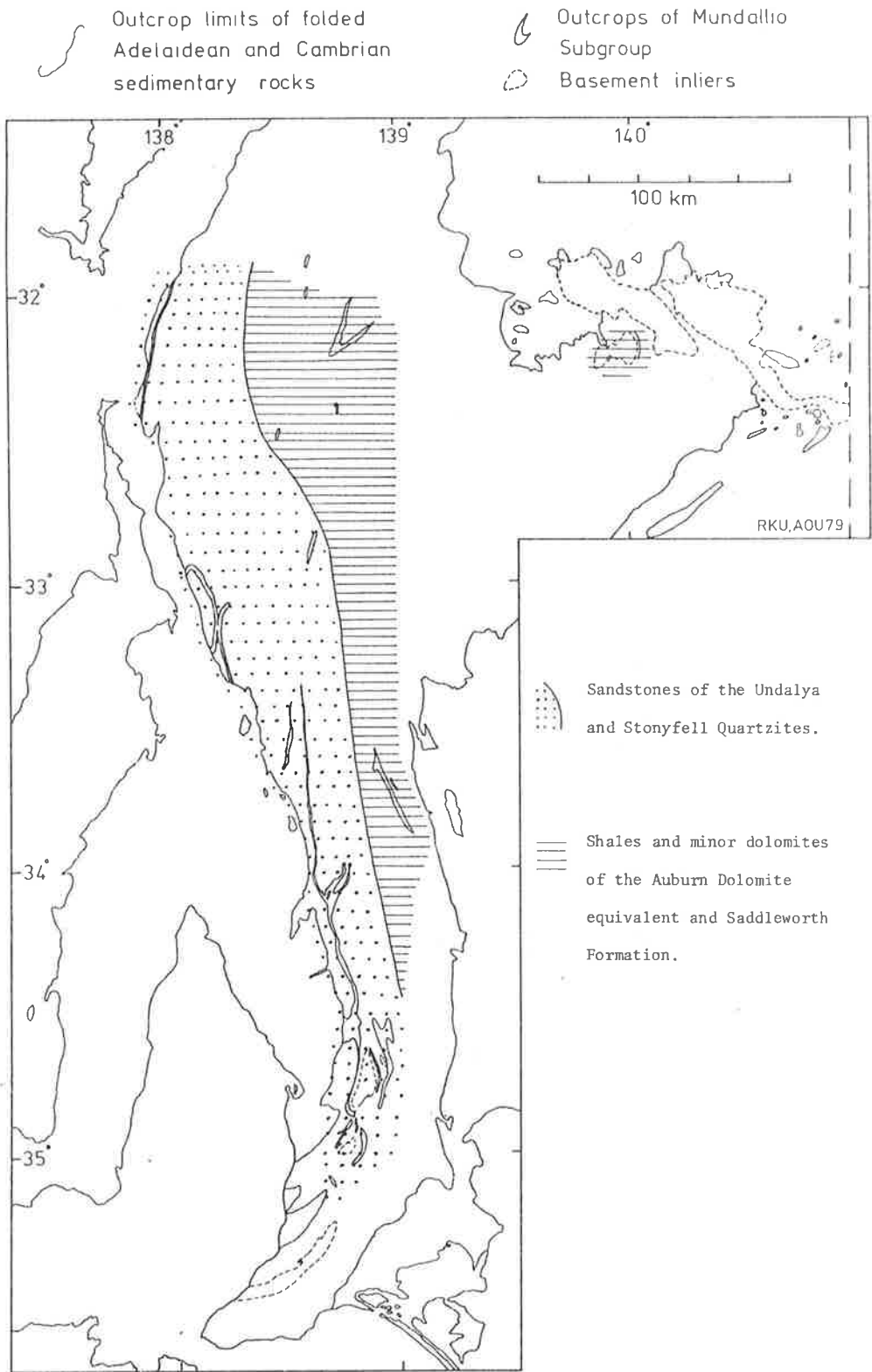


Figure 8.11. Distribution of major facies, post Mundallio Subgroup, southern Flinders and Mt. Lofty Ranges.

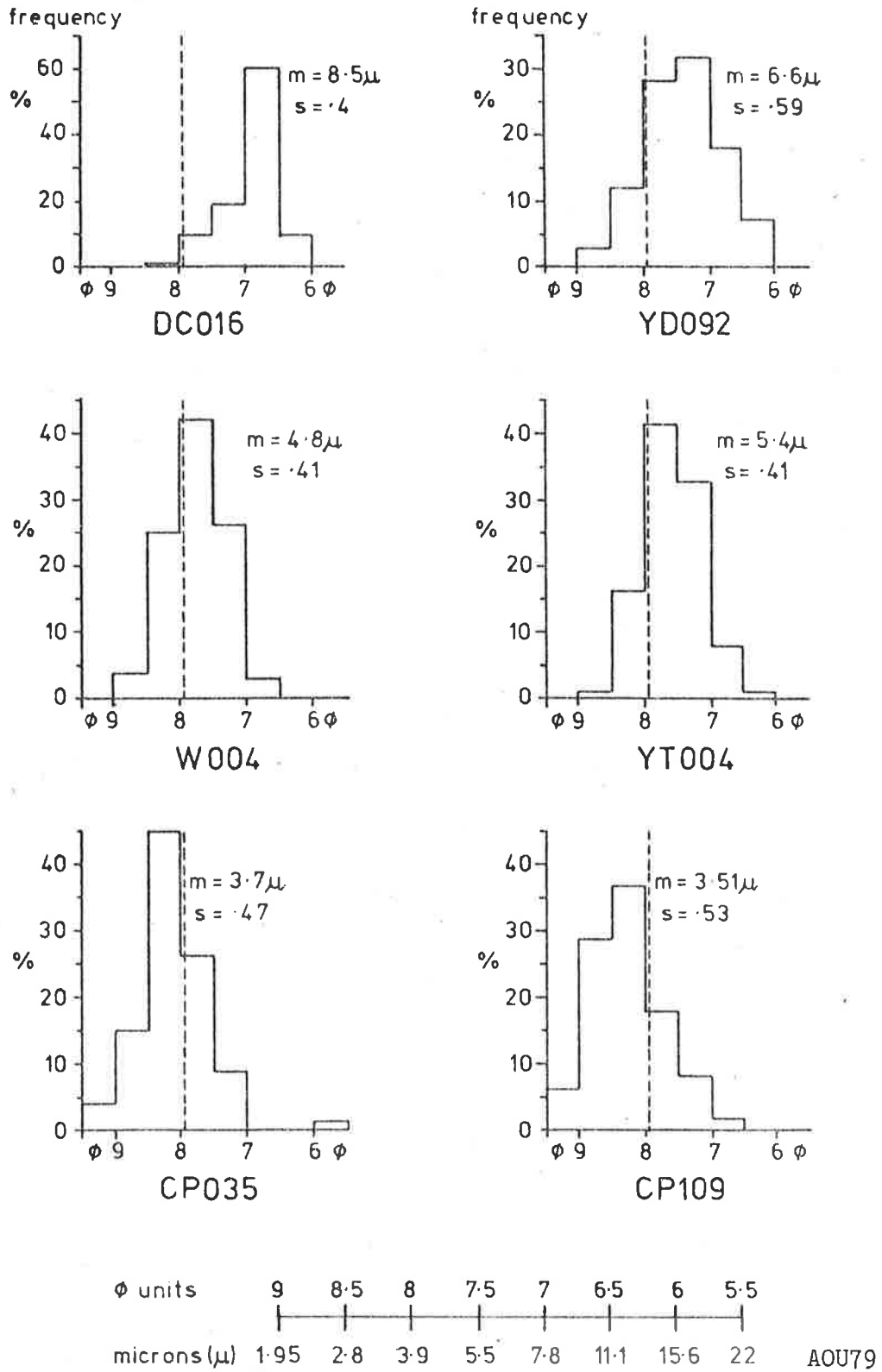


Figure 9.1. Grain size distribution of some dolomite mudstones. Dashed line is the boundary between micrite and microspar, m = mean, s = sorting.

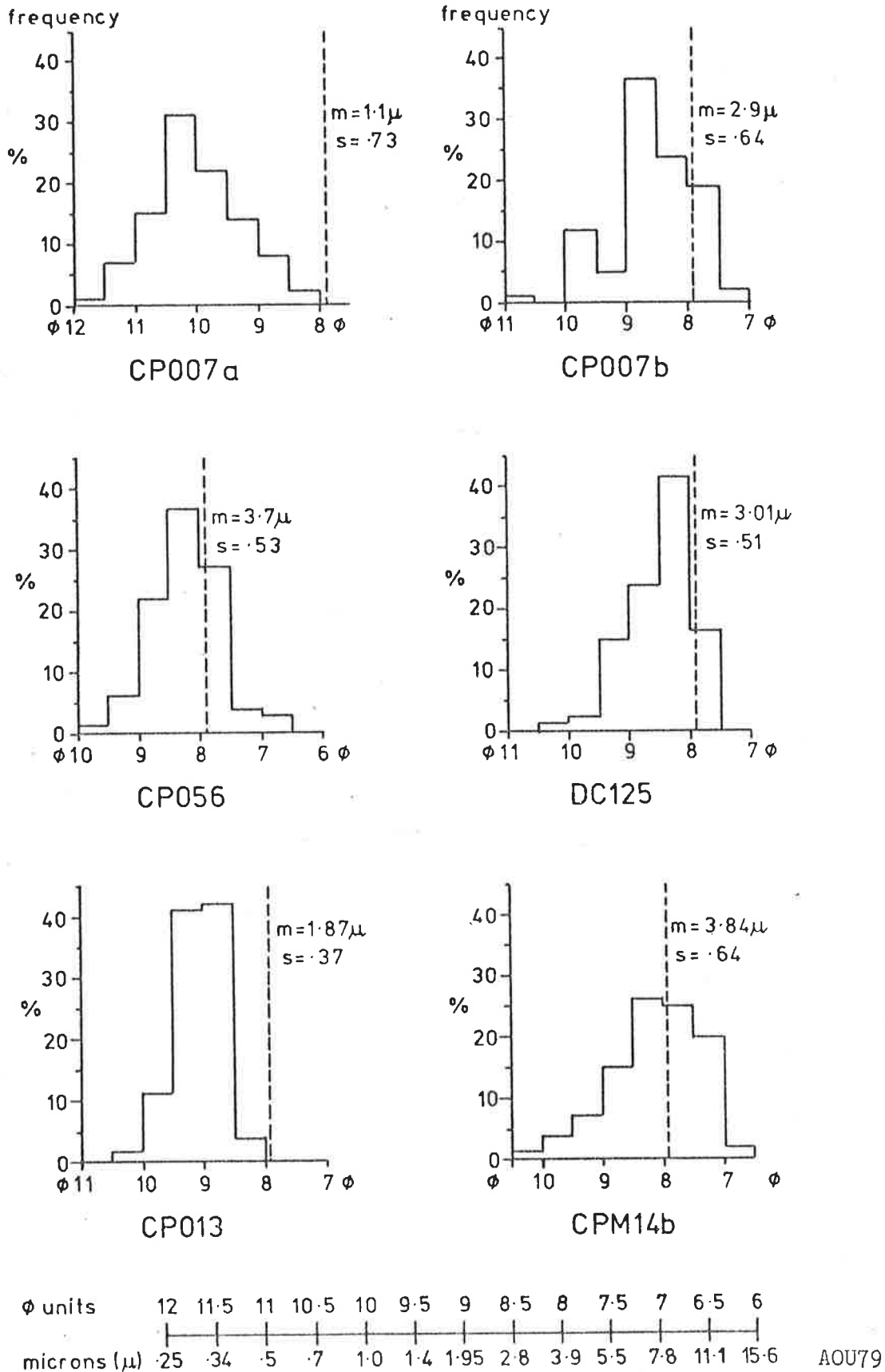


Figure 9.2. Grain size distributions of some magnesite mudstones (CP007a and b, CP056) and nodular magnesites (DC125, CP013, CPM146). Dashed line is the boundary between micrite and microspar, m = mean, s = sorting.

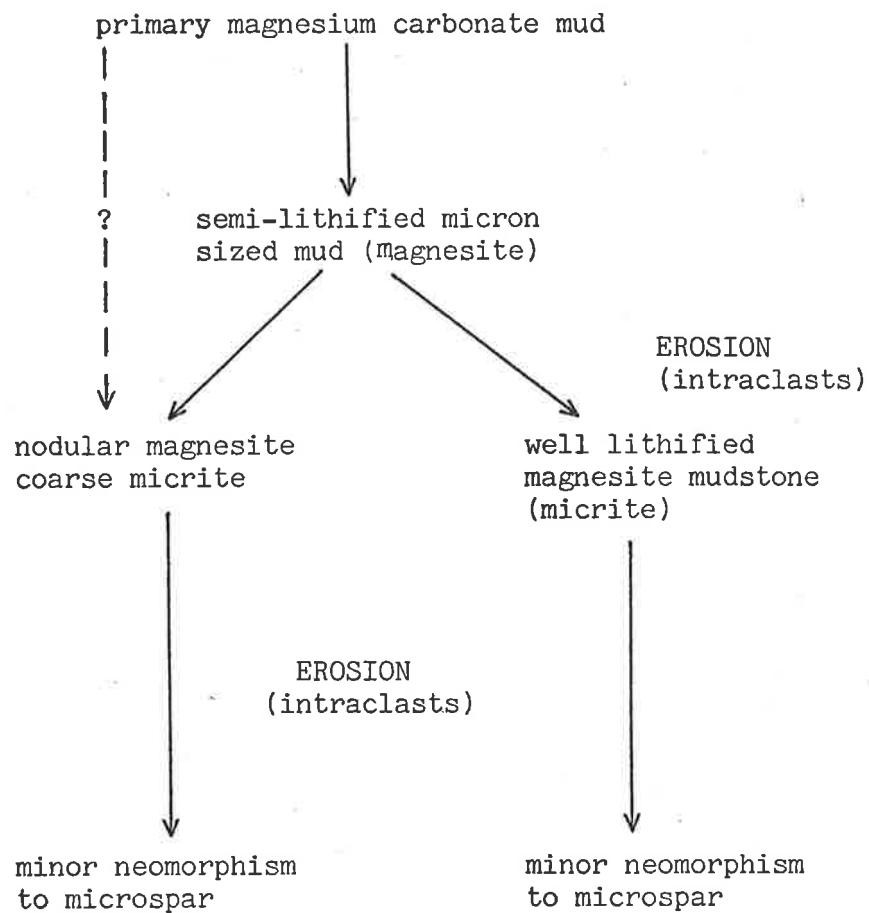


Figure 9.3. Summary of the diagenetic history of magnesite mudstones.

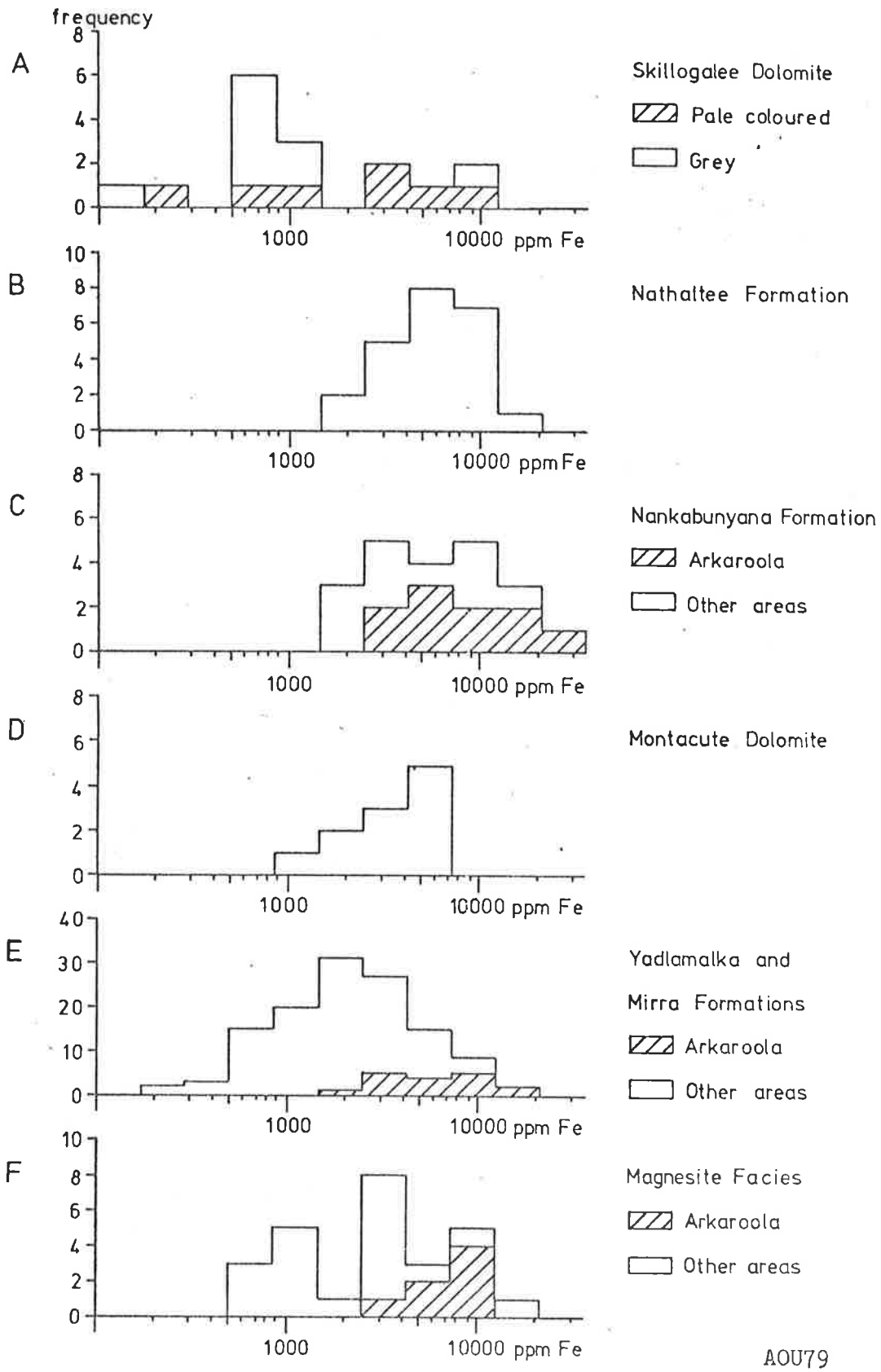
Formation	Sample Number	Average Grain Size	Sorting (s)
Nathaltee Formation	DC006	12.0	0.39
	DC016	8.5	0.40
	DC024	9.8	0.41
	DC025a	7.1	0.41
	DC025b	10.2	0.54
	YDA087	11.6	0.43
	YDA090	5.2	0.46
	YDA092	6.6	0.59
Nankabunyana Formation	W004	4.8	0.41
Yadlamalka Formation	YE014a	6.2	0.45
	YE014b	7.6	0.41
	YT004	5.4	0.41
	CP030	6.0	0.39
	CP035	3.7	0.47
	CP109	3.5	0.53
	W052	5.6	0.49

$$s = \frac{\phi_{84} - \phi_{16}}{4} + \frac{\phi_{95} - \phi_5}{6.6}$$

Table 9.1. Average grain size in microns and sorting of some dolomite mudstones. Sample numbers beginning with DC are from Depot Creek, with YDA from the Yednalue Anticline, with YE from Yacka (east), with YT from Yatina, with CP from Copley, with W from the Willouran Ranges.

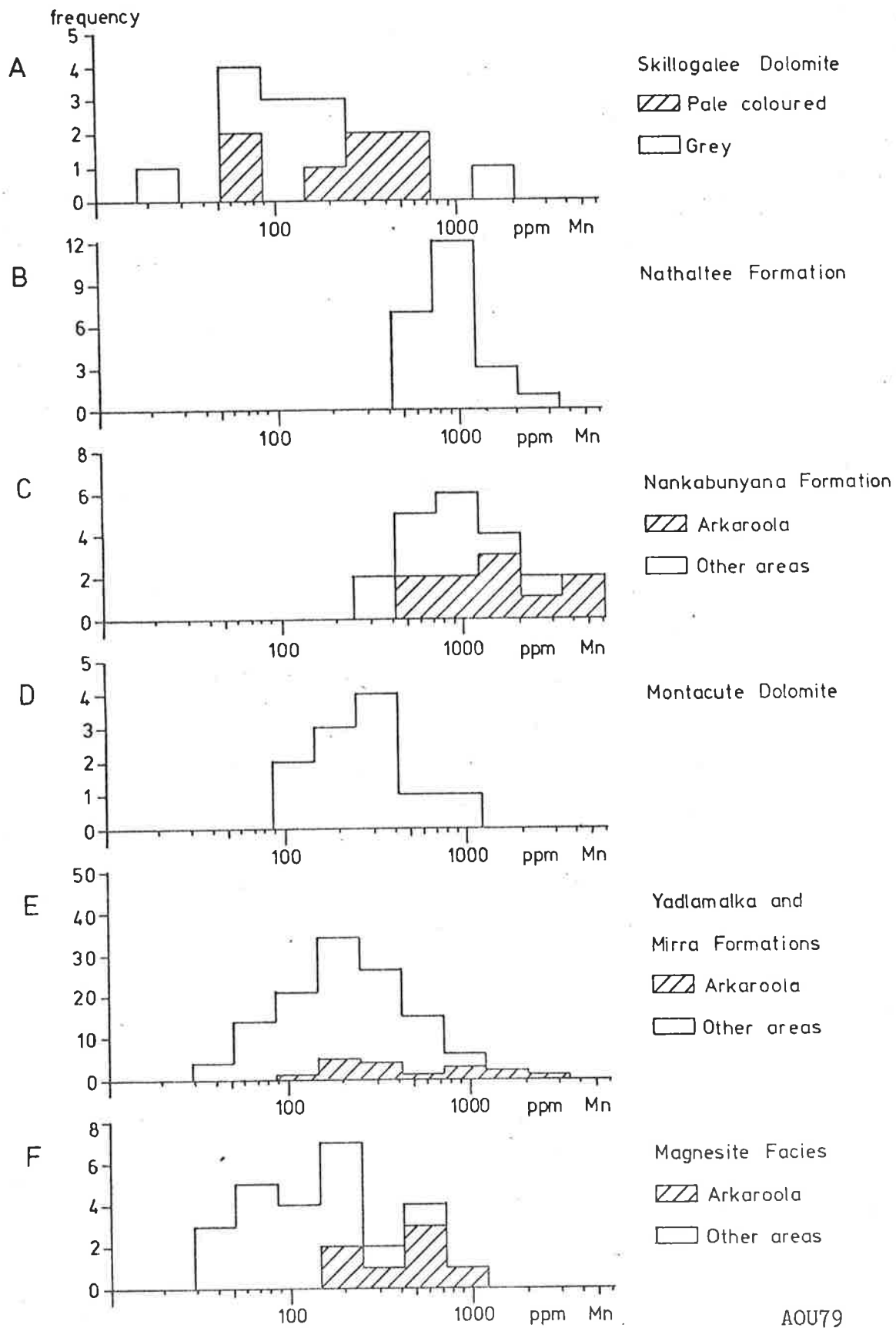
Facies	Sample Number	Average Grain Size	Sorting
Magnesite mudstone	CP007a	1.1	0.73
	CP007b	2.9	0.64
	CP007c	3.9	0.71
	CP056	3.7	0.53
	CP120A	3.3	0.56
	CPM11	2.7	0.55
	A017A	3.8	0.44
Nodular magnesite	DC125a	3.0	0.51
	DC125b	3.7	0.57
	CPM14a	3.2	0.69
	CPM14b	3.8	0.64
	CP013	1.9	0.37

Table 9.2. Average grain size in microns and sorting of some magnesite mudstones, and nodular magnesite. Sample numbers beginning with CP and CPM from Copley, with DC from Depot Creek, with A from Arkaroola.



AOU79

Figure 10.1. Frequency distribution of Fe contents for dolomite facies of each formation (A-E) and magnesite facies (F).



AOU79

Figure 10.2. Frequency distribution of Mn contents for dolomite facies of each formation (A-E) and magnesite facies (F).

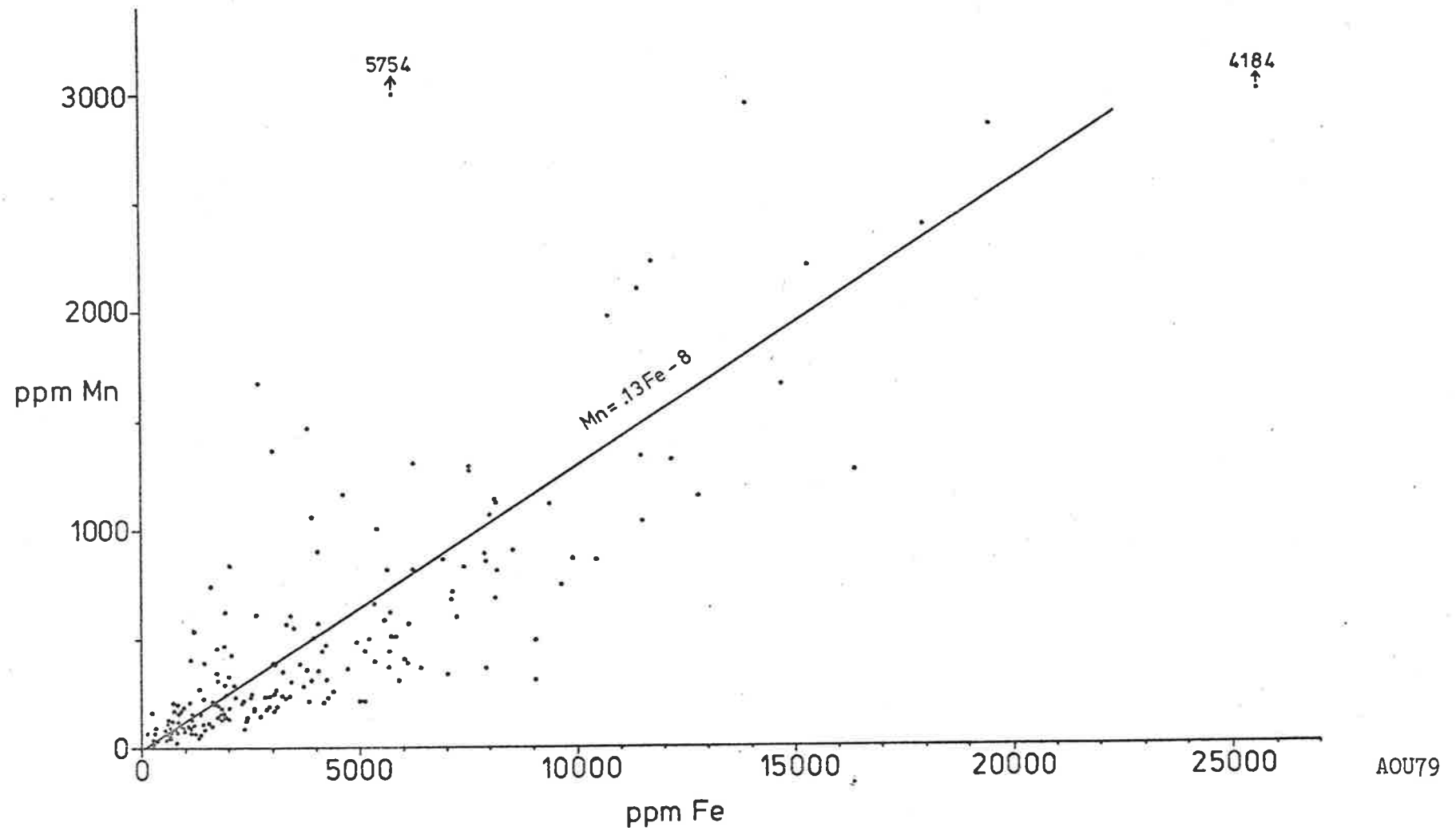


Figure 10.3. Plot of Mn versus Fe for all dolomite samples. Regression line was calculated using the reduced major axis method.

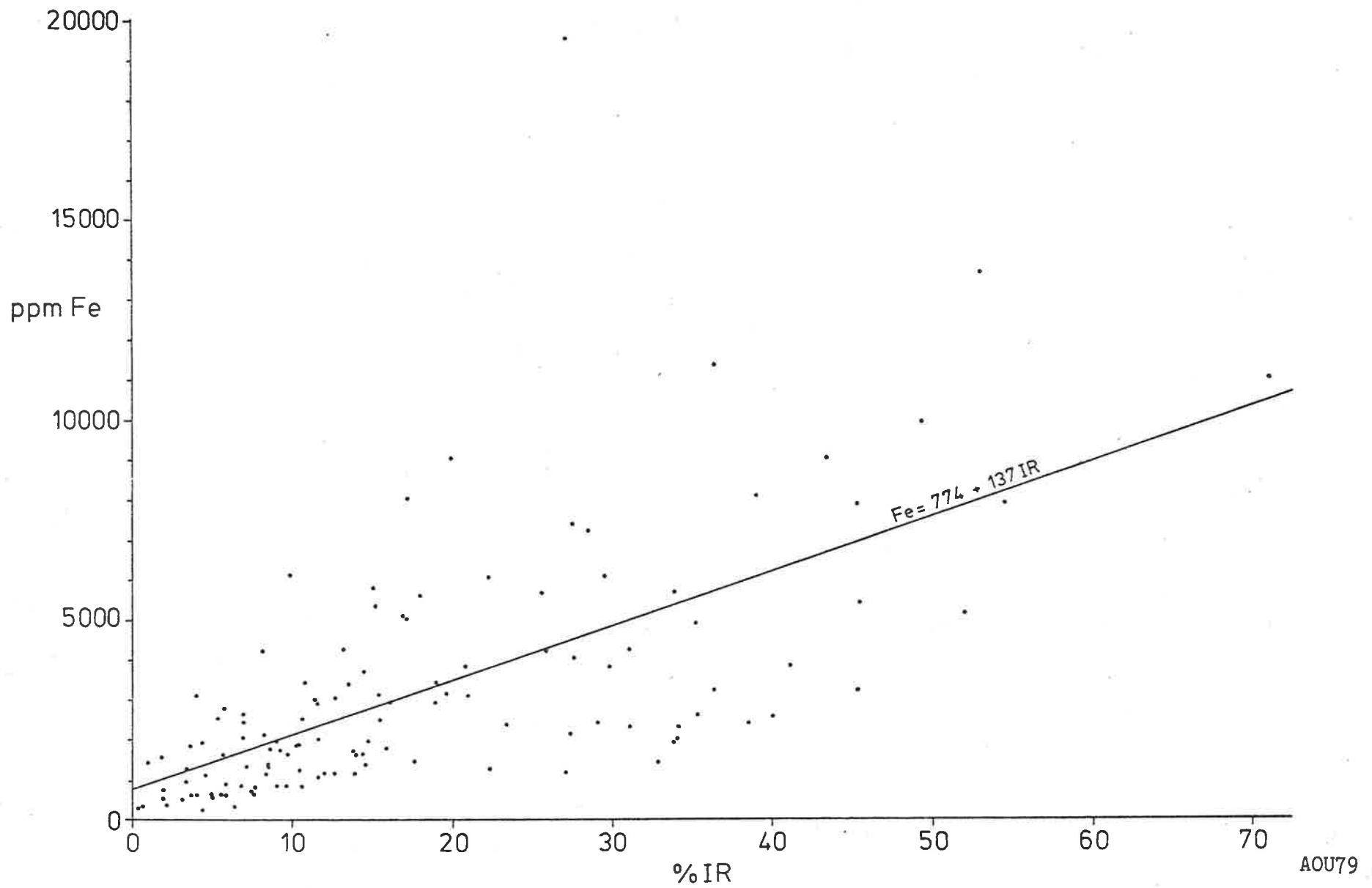
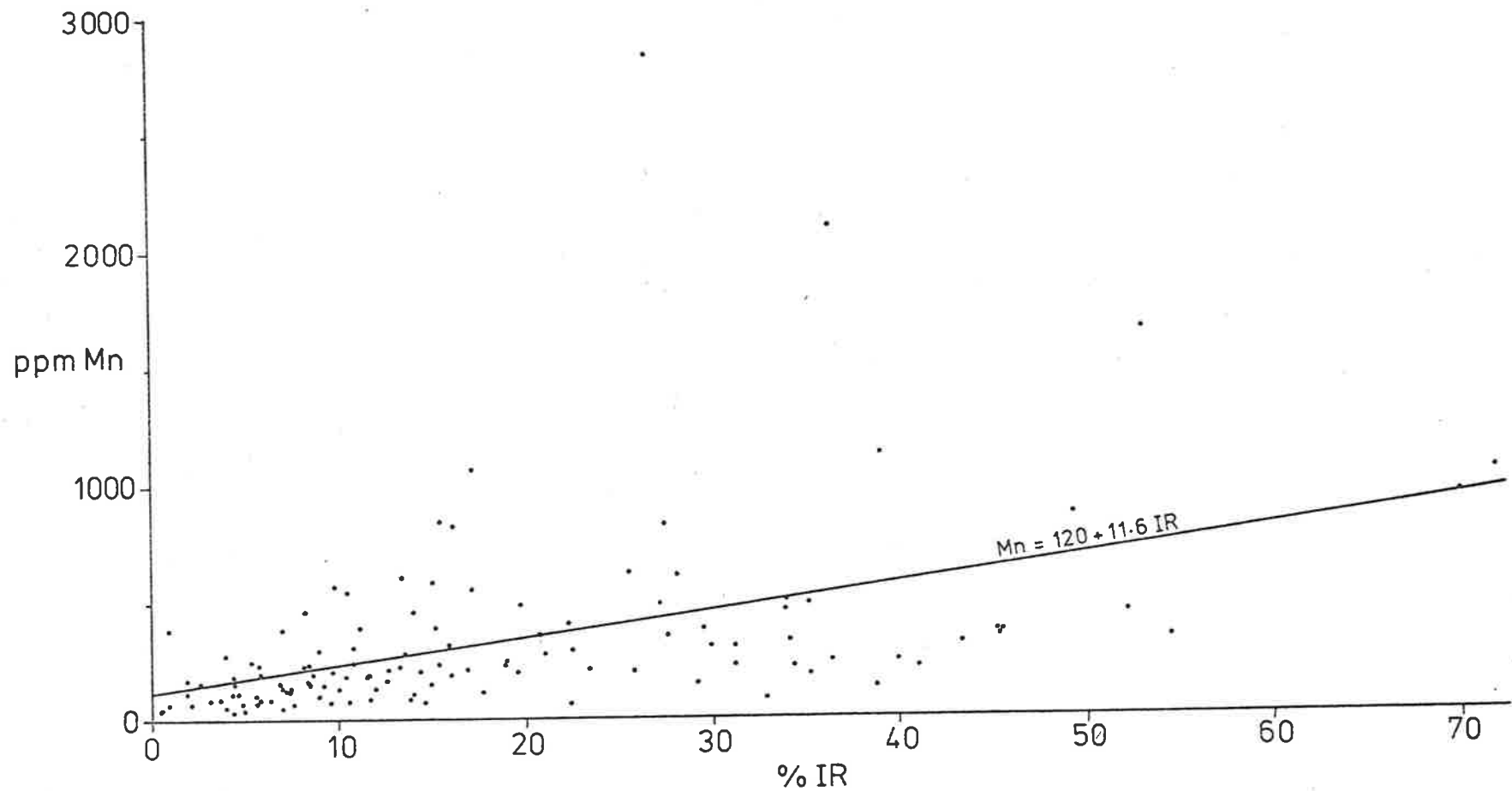
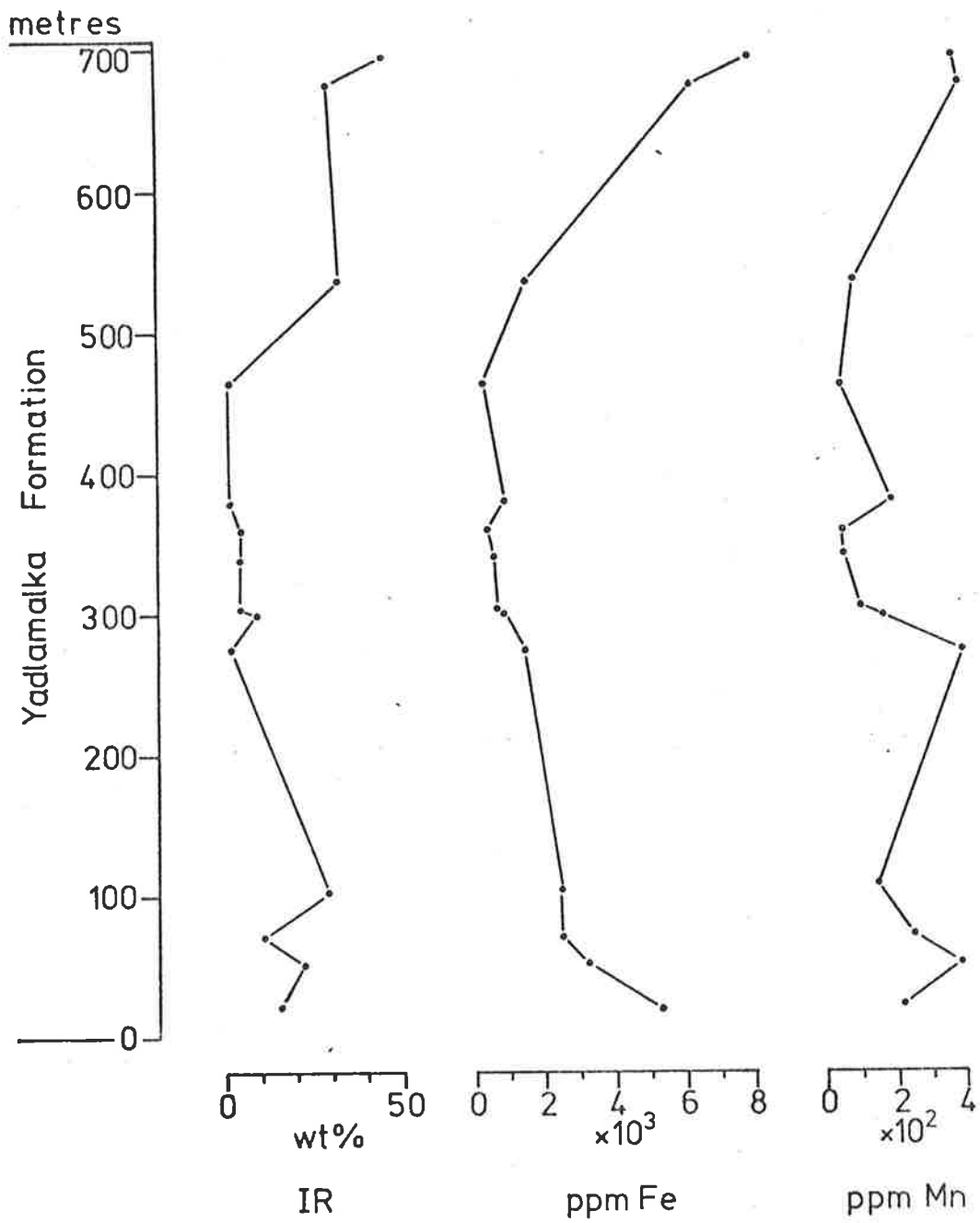


Figure 10.4. Plot of Fe versus IR for dolomite samples in the Yadlamalka and Mirra Formations. Regression line was calculated using the reduced major axis method.



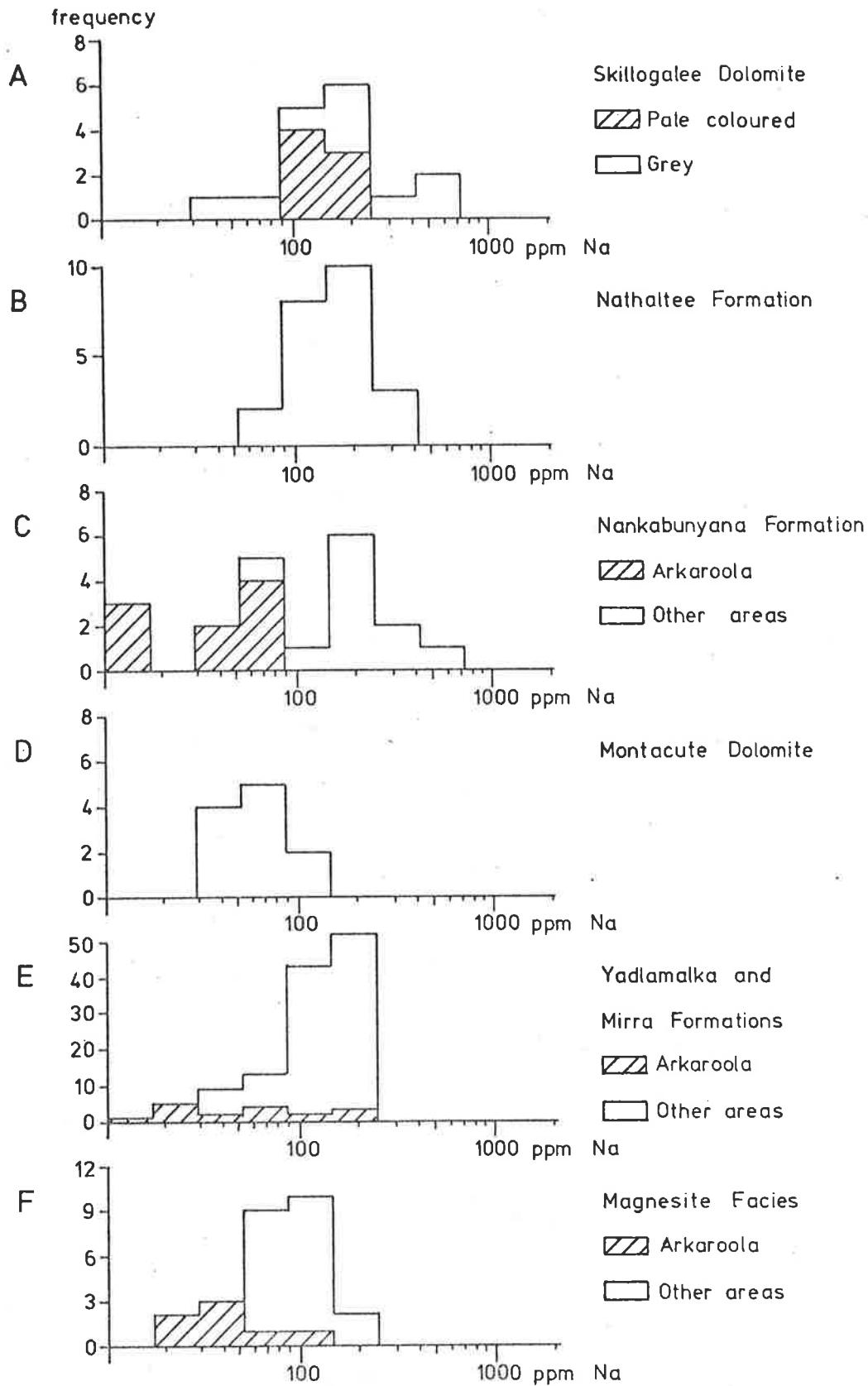
AOU79

Figure 10.5. Plot of Mn versus IR for all dolomite samples from the Yadlamalka and Mirra Formations. Regression line was calculated using the reduced major axis method.



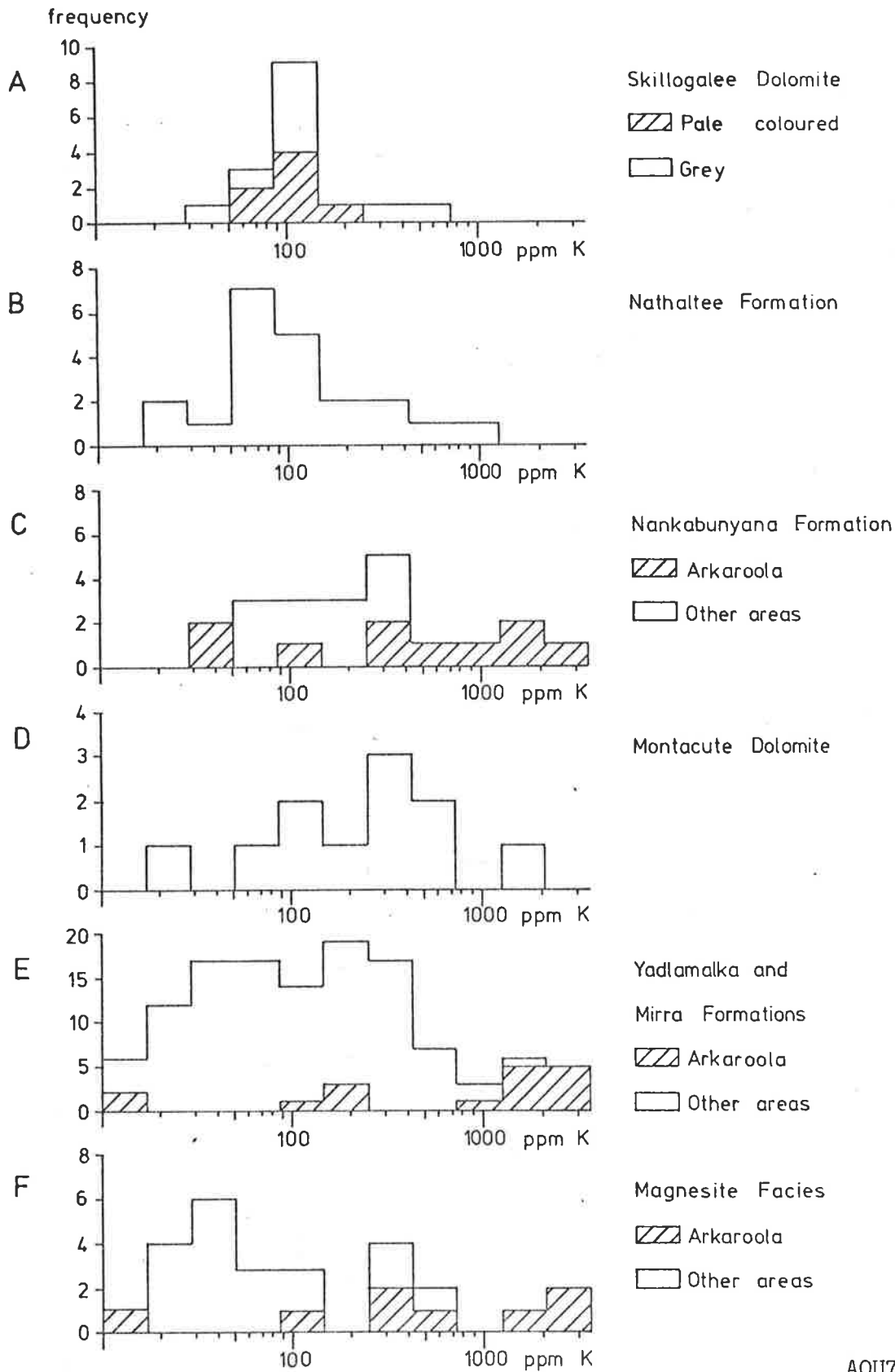
AOU79

Figure 10.6. Vertical variation in IR, Fe and Mn in the Yadlamalka Formation at Yednalue.



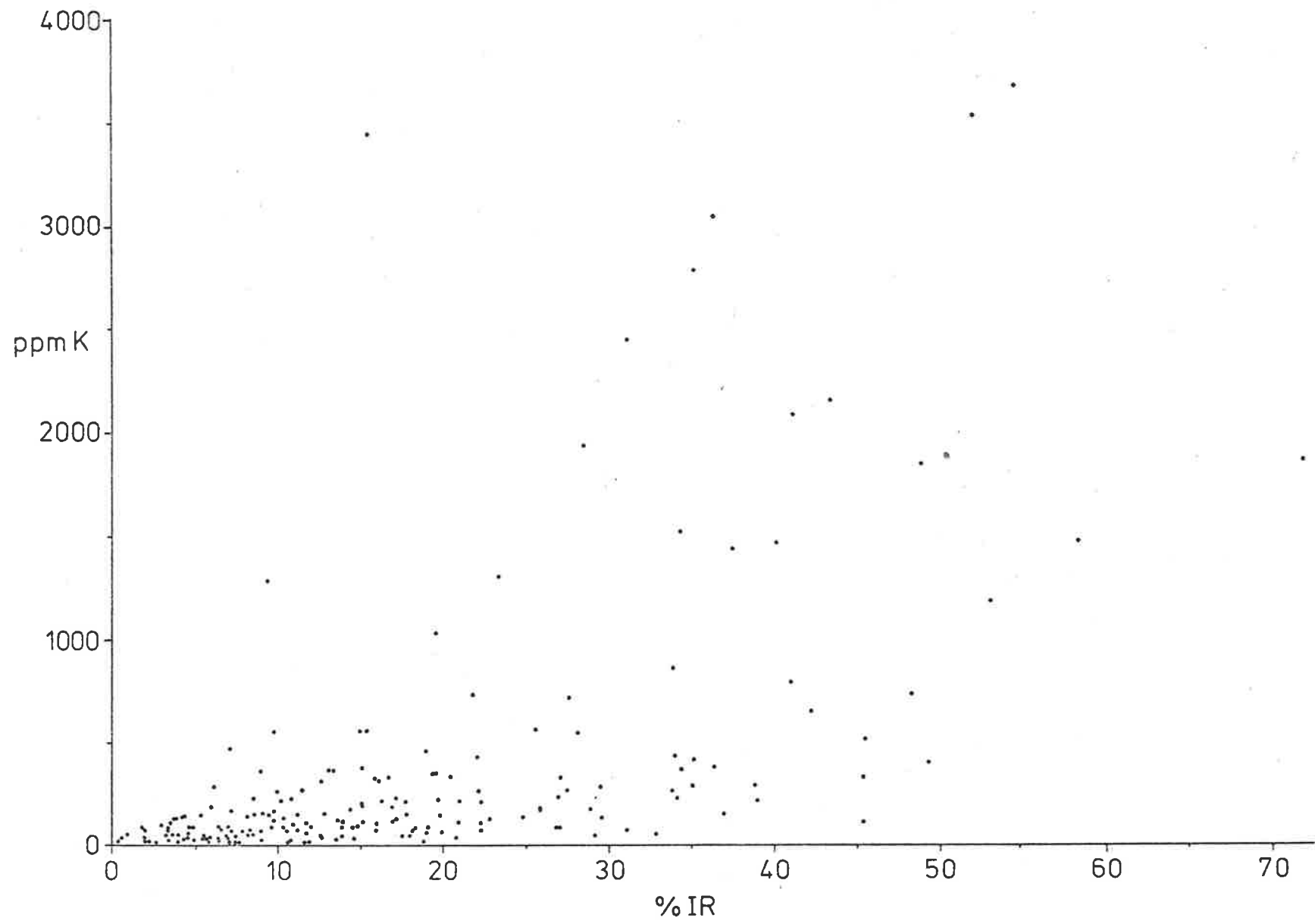
AOU79

Figure 10.7. Frequency distribution of Na contents for dolomite facies of each formation (A-E) and magnesite facies (F).



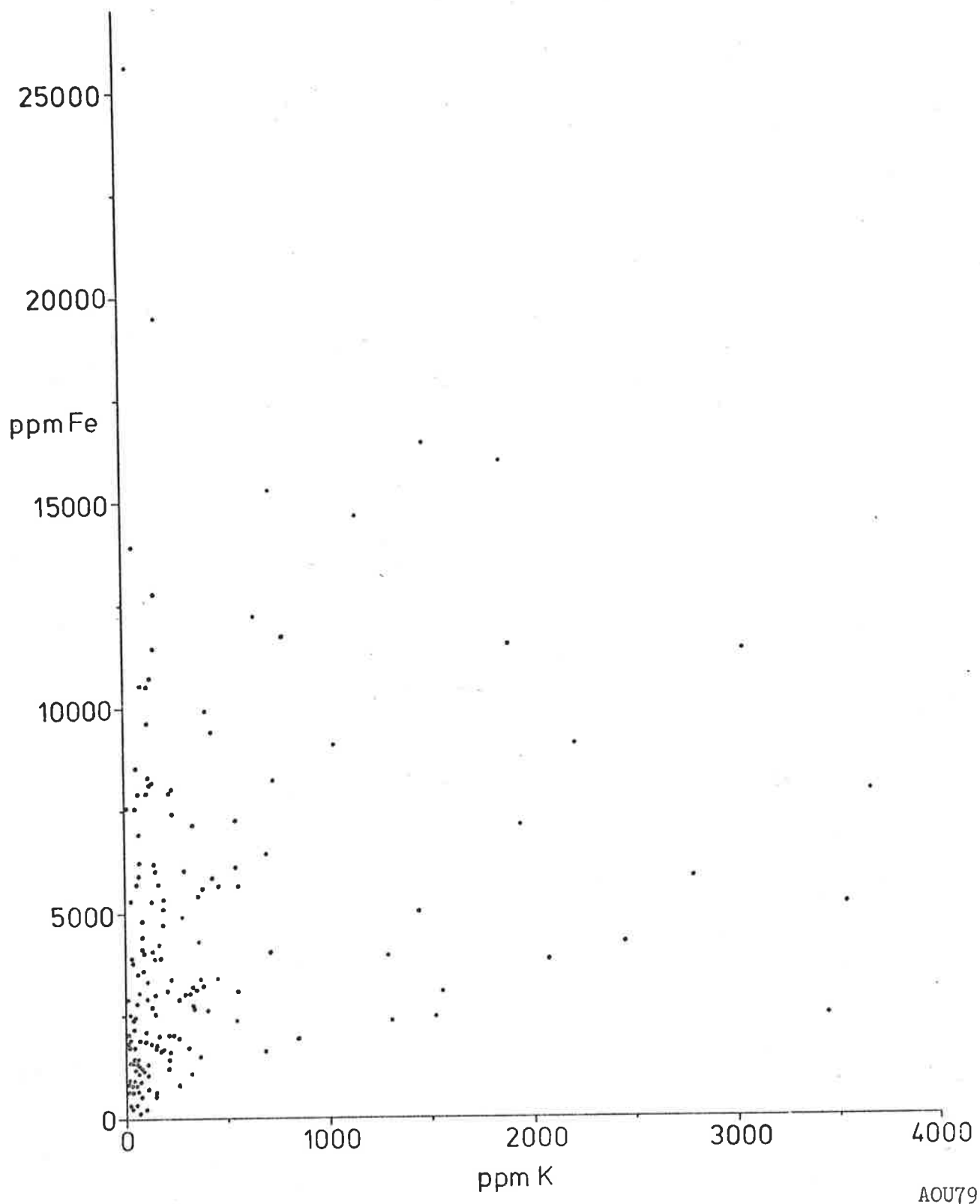
AOU79

Figure 10.8. Frequency distribution of K contents for dolomite facies of each formation (A-E) and magnesite facies (F).



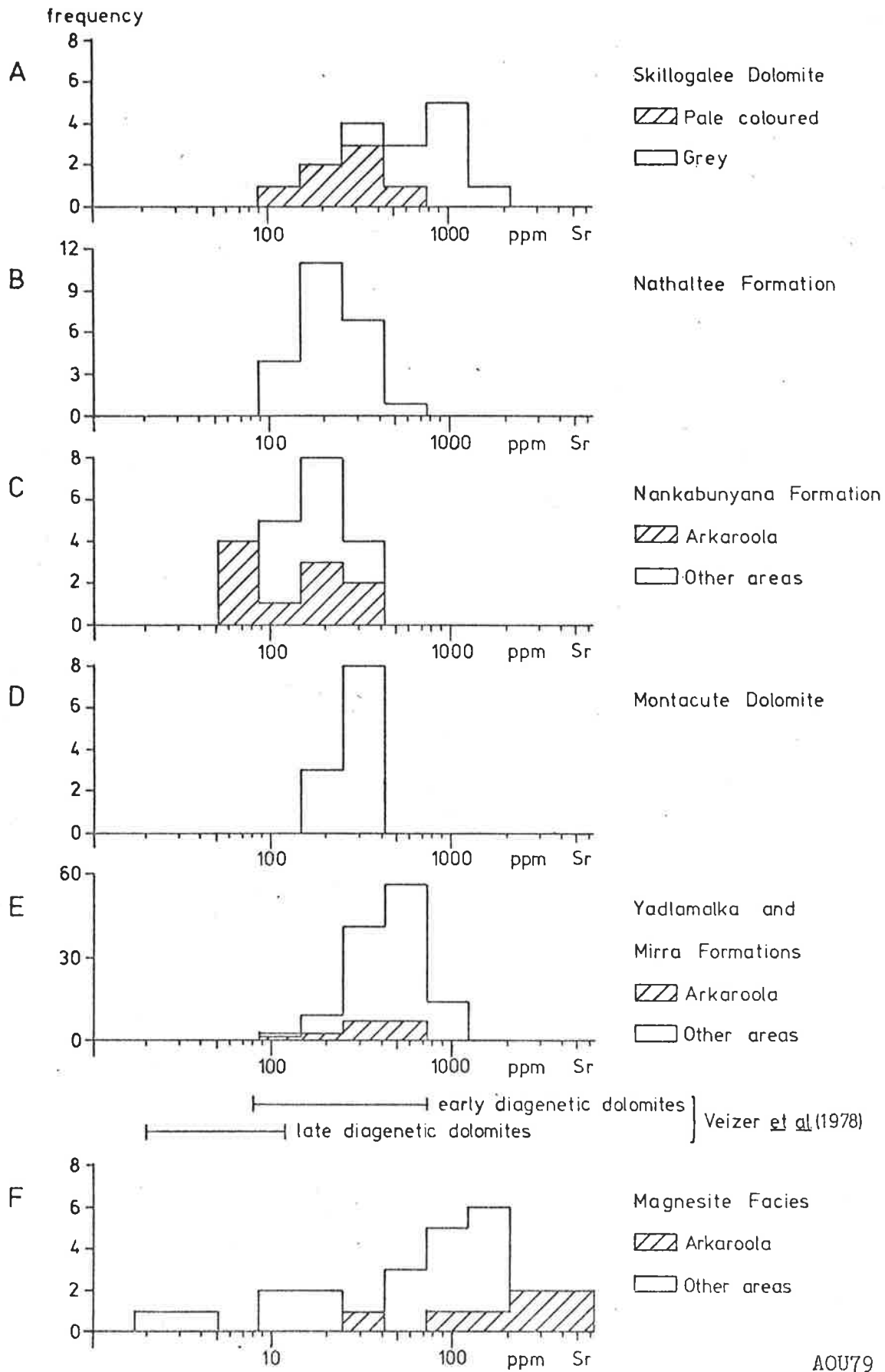
AOU79

Figure 10.9. Plot of K versus IR for all dolomite samples



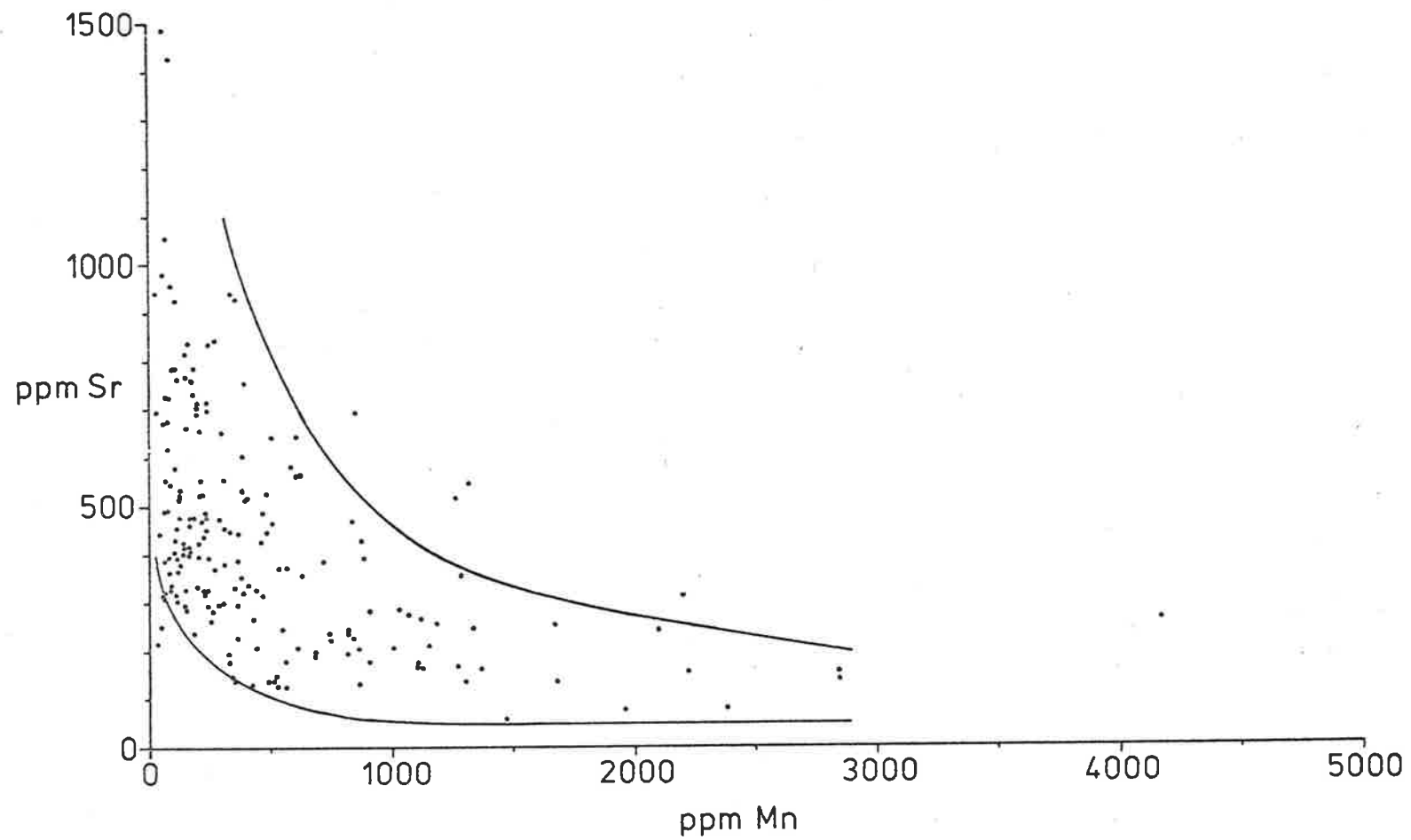
AOU79

Figure 10.10. Plot of Fe versus K for all dolomite samples.



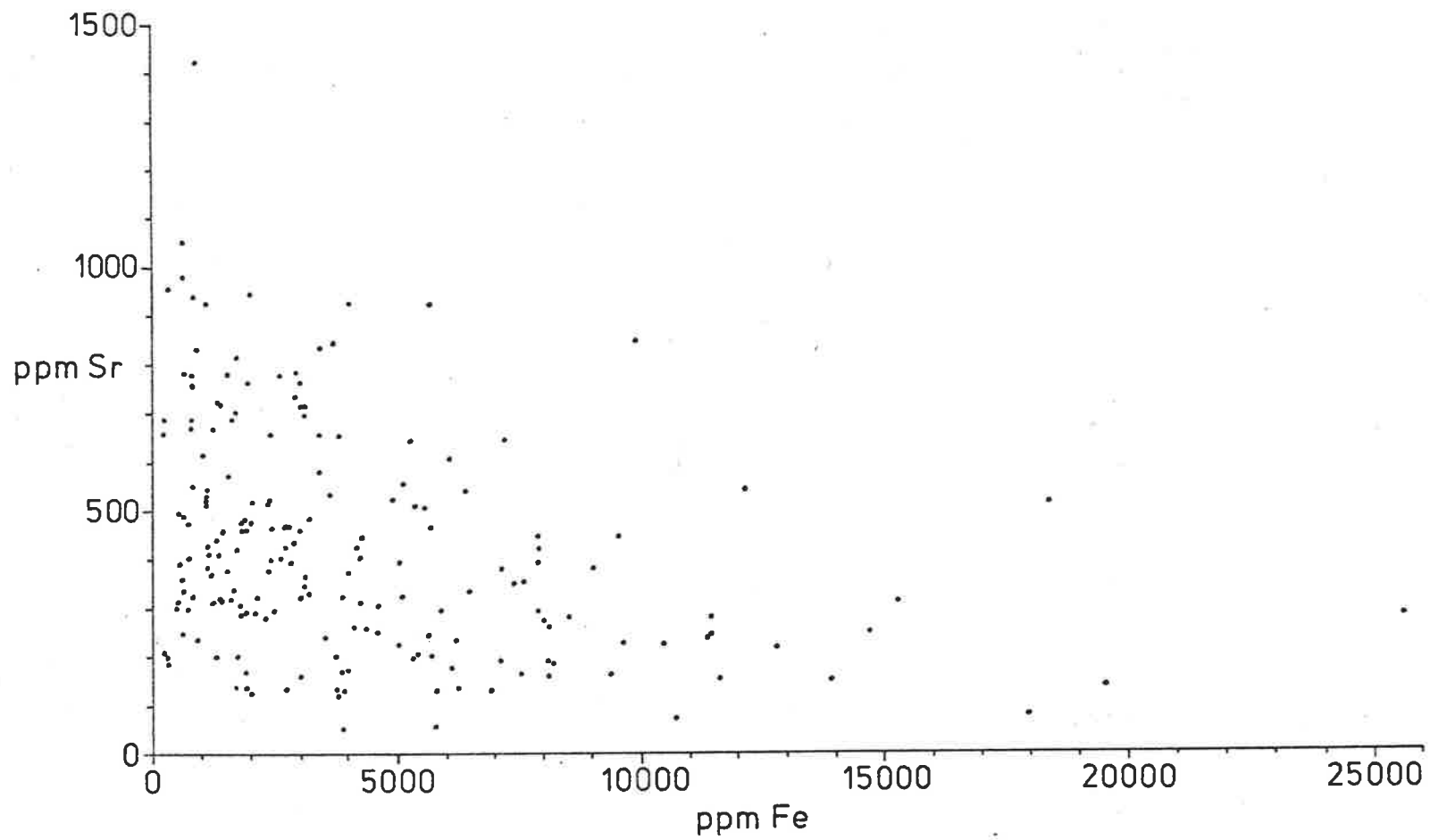
AOU79

Figure 10.11. Frequency distribution of Sr contents of dolomite facies from each formation (A-E) and magnesite facies (F).



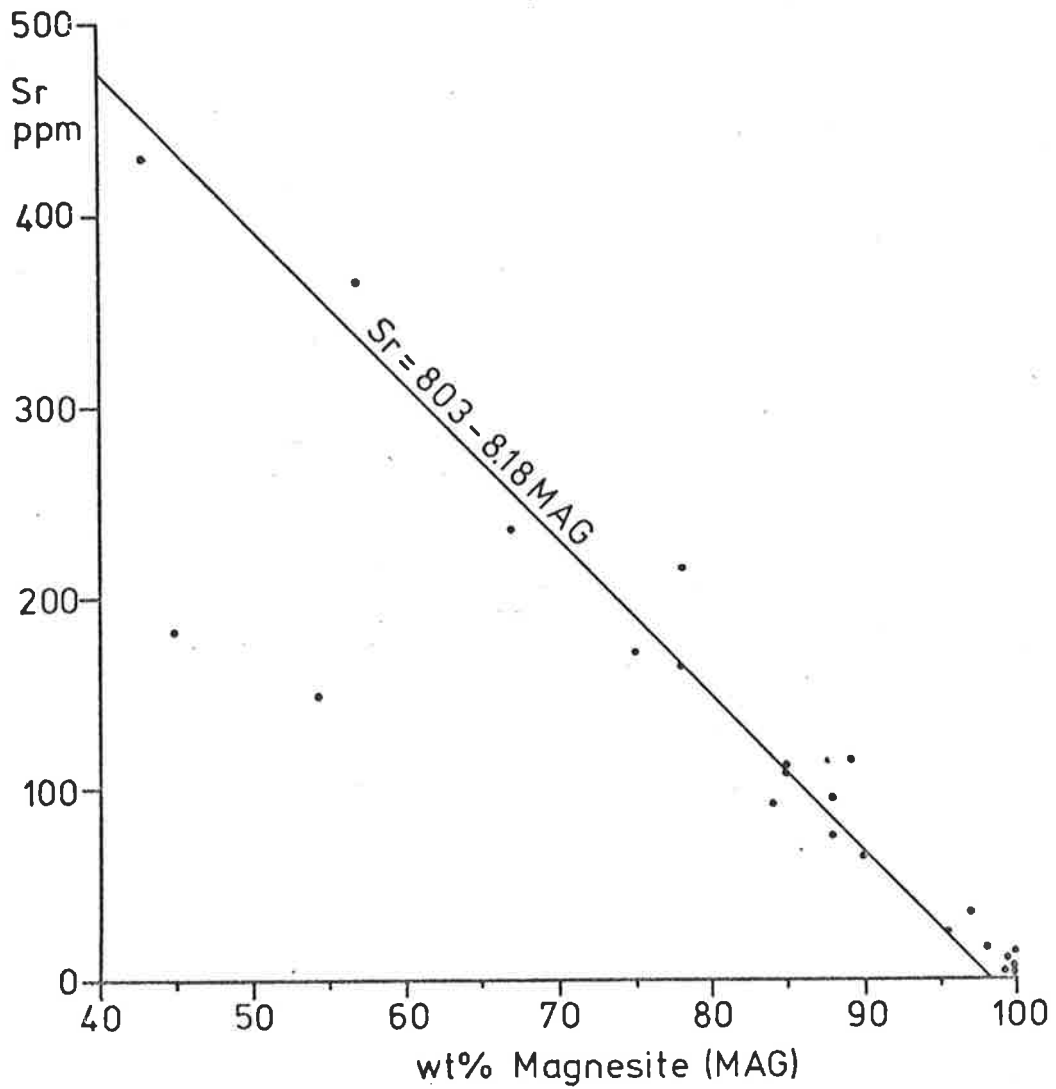
AOU79

Figure 10.12. Plot of Sr versus Mn for all dolomite samples indicating the hyperbolic relationship.



AOU79

Figure 10.13. Plot of Sr versus Fe for all dolomite samples.



AOU79

Figure 10.14. Plot of Sr versus wt % magnesite (as % of total carbonate) in magnesite samples. Regression line was calculated using the reduced major axis method.

Formation/Facies	Location	No. of Samples	IR wt. %		Fe ppm		Mn ppm		Mn/Fe		Na ppm		K ppm		Sr ppm	
			mean	s	mean	s	mean	s	mean	s	mean	s	mean	s	mean	s
Skillogalee pale coloured dolomites	SC, SR	7	12.3	8.1	3589	3331	313	248	0.16	0.2	146	30	107	35	318	170
Dolomite grey dolomites	SC, SR	9	15.2	11.7	2018	3830	243	408	0.17	0.12	242	179	180	188	852	304
Nathaltee Formation	B, PG	5	25.9	16.6	5495	3920	766	139	0.21	0.16	245	94	247	307	213	71
	DC	11	20.6	10.8	5977	2628	1066	506	0.19	0.10	155	70	159	214	197	58
	YDA	7	18.8	18.0	9647	4143	1032	307	0.12	0.03	189	97	349	511	361	101
	mean All areas	23	21.2	14.1	6989	3726	991	401	0.17	0.10	185	88	236	341	250	104
Nankabunyana Formation	CP, MS	8	19.4	3.3	3967	2730	791	414	0.25	0.16	266	134	200	109	202	93
	A	10	22.7	14.4	10385	6863	2136	1658	0.26	0.27	41	24	968	957	153	92
	TM	3	20.8	7.4	9836	3597	1519	1247	0.14	0.06	184	81	136	93	136	28
	mean All areas	21	21.1	10.2	7862	5910	1535	1362	0.24	0.21	147	136	556	761	177	86
Montacute Dolomite	TG	11	10.6	10.6	3749	1669	331	246	0.10	0.06	66	19	364	395	316	89

Table 10.1. Mean values of Insoluble Residue (IR), Fe, Mn, Mn/Fe, Na, K and Sr, for carbonate rocks within the Mundallio Subgroup. Mean and standard deviation(s) are given for different areas of outcrop of each formation. For locations, see Fig. 3.2; continued overleaf.

Formation/Facies	Location	No. of Samples	IR Wt.%		Fe ppm		Mn ppm		Mn/Fe		Na ppm		K ppm		Sr	
			mean	s	mean	s	mean	s	mean	s	mean	s	mean	s	mean	s
Yadlamalka Formation	YE	14	15.8	7.7	4045	2310	282	159	0.07	0.03	141	49	366	238	525	258
	B, PG	8	13.5	14.1	2410	1753	213	102	0.10	0.03	174	38	109	65	542	361
	MC	12	11.5	12.7	1767	1575	168	113	0.12	0.06	122	31	73	98	455	350
	DC	10	9.8	11.6	2288	2621	296	372	0.14	0.06	186	48	75	57	457	215
	YT	4	28.5	15.6	5662	3108	511	302	0.09	0.02	145	47	487	196	858	302
	J	3	19.6	8.1	2684	1413	199	109	0.08	0.01	148	11	126	45	554	233
	YD	14	14.7	14.6	2435	2375	201	135	0.12	0.07	142	48	88	83	367	158
	YDA	3	6.2	4.7	2064	1316	237	161	0.12	0.02	125	25	100	43	407	249
	CP, MS	11	15.5	11.4	2522	1987	263	227	0.11	0.04	151	48	128	87	455	138
	A	12	31.2	15.0	4589	3222	465	548	0.11	0.08	54	55	1946	1376	464	122
	EP	5	36.4	25.0	11097	6765	1367	981	0.12	0.02	135	54	726	766	258	74
	TM	7	17.8	9.5	2840	1744	285	170	0.12	0.08	143	72	100	91	412	126
WR, CO	8	16.5	12.3	1478	974	176	164	0.14	0.13	157	37	140	160	592	154	
Mirra Formation	MI, R	8	25.4	10.0	3176	1493	371	111	0.15	0.10	107	53	500	494	641	145
	NW	4	11.7	3.1	3121	1845	399	231	0.13	0.03	38	8	267	126	636	74
	All Areas	123	17.8	14.1	3221	3034	326	378	0.11	0.07	133	58	380	716	501	214
Magnesite Facies	All areas excluding	26	15.5	12.0	4367	3596	251	249	0.06	0.03	90	41	433	852	133	82
	Arkaroola	19	11.6	7.5	3332	3290	155	138	0.05	0.02	105	32	99	122	81	67

Table 10.1 continued.

Facies	No. of Samples		IR	Fe	Mn	Mn/Fe	Na	K	Sr
Mudstones	78	mean	20.9	3637	349	0.11	130	496	517
		s	14.3	2873	335	0.06	59	792	201
Stromatolitic Dolomite	11	mean	12.0	2033	214	0.11	138	94	502
		s	10.3	1343	178	0.04	65	97	288
Intraclastic Grainstones	8	mean	19.8	6308	800	0.13	121	610	410
		s	7.8	5715	886	0.09	61	1143	158
Other Grainstones	17	mean	14.8	1882	177	0.12	154	101	587
		s	13.0	1820	118	0.07	55	170	288
Massive Diagenetic Dolomites	9	mean	2.7	854	134	0.15	134	45	278
		s	2.0	506	112	0.06	52	23	49

Table 10.2. Mean values and standard deviation(s) of Insoluble Residue (IR, in wt.%), Fe, Mn, Mn/Fe, Na, K and Sr (ppm) for the major dolomite facies within the Yadlamalka and Mirra Formations.

A. Skillogalee Dolomite, pale coloured dolomites, n = 7

	IR	Fe	Mn	Na	K	
Fe	-.194					
Mn	-.212	.925				LV (95%) = .755
Na	-.551	-.377	-.376			LV (99.9%)= .951
K	.230	-.083	.139	.057		
Sr	-.273	-.604	-.238	.074	-.238	

B. Skillogalee Dolomite, grey dolomites, n = 9

	IR	Fe	Mn	Na	K	
Fe	.874					
Mn	.827	.990				LV (95%) = .666
Na	.314	-.041	-.109			LV (99.9%)= .898
K	.763	.944	.930	-.021		
Sr	-.232	-.416	.465	.033	-.455	

C. Nathaltee Formation, n = 23

	IR	Fe	Mn	Na	K	
Fe	.394					LV (95%) = .423
Mn	.387	.562				LV(99.9%)= .65
Na	.619	.290	-.126			
K	.835	.603	.364	.659		
Sr	.261	.323	.089	.399	.434	

Table 10.3. Correlation coefficients, continued overleaf.
 LV (95%) is the limiting value at 95% confidence level,
 and LV (99.9%) the limiting value at 99.9%.

D. Nankabunyana Formation, n = 21

	IR	Fe	Mn	Na	K	
Fe	.155					
Mn	.165	.555				LV (95%) = .433
Na	-.036	-.448	-.423			LV (99.9%) = .665
K	.583	.019	-.174	-.341		
Sr	-.067	.316	-.191	.018	-.173	

E. Montacute Dolomite, n = 11

	IR	Fe	Mn	Na	K	
Fe	.223					
Mn	-.207	.502				LV (95%) = .602
Na	-.022	.214	-.093			LV (99.9%) = .847
K	.934	.307	-.407	.029		
Sr	.439	-.140	-.637	.083	.301	

F. Yadlamalka and Mirra Formations, n = 123

	IR	Fe	Mn	Na	K	
Fe	.638					
Mn	.433	.860				LV (95%) = .27
Na	-.010	-.051	-.100			LV (99%) = .176
K	.584	.403	.333	-.217		
Sr	-.014	-.213	-.270	-.015	-.057	

Table 10.3 continued.

G. All Dolomite Samples, n = 195¹

	IR	Fe	Mn	Na	K	
Fe	.483					
Mn	.296	.734				LV (95%) = .137
Na	.126	-.059	-.118			LV (99%) = .182
K	.580	.292	.153	-.153		
Sr	-.036	-.335	-.407	.076	-.053	

H. All Magnesite Samples, n = 26

	IR	Fe	Mn	Na	K	Sr
Fe	.508					
Mn	.367	.801				LV (95%) = .38
Na	-.138	-.298	-.519			LV (99.9%) = .597
K	.858	.487	.412	-.215		
Sr	.656	.325	.541	-.267	.653	
MAG	-.524	-.528	-.590	.507	-.587	-.590

I. Magnesite Samples, Excluding Arkaroola Area, n = 19

	IR	Fe	Mn	Na	K	Sr
Fe	.515					
Mn	.451	.942				LV (95%) = .456
Na	.138	-.028	-.187			LV (99.9%) = .693
K	.526	.578	.553	.045		
Sr	.290	.203	.440	.298	.185	
MAG ²	-.364	-.201	-.320	-.318	-.145	-.843

Table 10.3 continued.

1. Includes one sample from the Castambul Formation.
2. MAG is the percent magnesite of the total carbonate.

MODERN	Behrens and Land, 1972	Baffin Bay	840 - 970 ppm Sr
		Laguna Madre	850 ppm
		supratidal	620 - 640 ppm
		Persian Gulf	640 ppm
	Land, 1973	Jamaica	3000 \pm 700 ppm
	Muller and Wagner, 1978 ¹	Lake Balaton	360 - 620 ppm
ANCIENT	Shearman and Shirmohammadi, 1969	French Jura	110 - 200 ppm
	Veizer and Demovic, 1974	Mesozoic of the Carpathians	
		early diagenetic	524 \pm 56 ppm
		intermediate	102 ppm
		late diagenetic	53 ppm
	Land <i>et al.</i> , 1975	Eocene, Egypt	90 ppm
		Ordovician, Canada	81 ppm
	Al-Hashimi, 1976	Carboniferous, England	132 \pm 46 ppm
	Veizer and Compston, 1976	River Wakefield Subgroup	440 - 700 ppm
		"Skillogalee Dolomite"	
		= Nathaltee Fm.	150, 230 ppm
		"Skillogalee Dolomite"	
		= Yadlamalka Fm.	290, 310, 440 ppm
		Auburn Dolomite	20, 20, 50 ppm
		Bitter Springs Fm.	50 - 70 ppm
Supko, 1977	Miocene-Pliocene, Bahamas	170 ppm	
Veizer <i>et al.</i> , 1978	Palaeozoic, Canada	66 - 216 ppm	

Table 10.4. The Sr contents of some modern and ancient dolomites.

1. These sediments are mixtures of protodolomite and high magnesium calcite.

Marinoan	0.7074 \pm 0.0002
Sturtian	0.7074 \pm 0.0003
Mundallio Subgroup	0.7090 \pm 0.0004 ¹
River Wakefield Subgroup	0.7106 \pm 0.0002 ¹
Bitter Springs Fm.	0.7068 \pm 0.0002

Table 10.5. $^{87}\text{Sr}/^{86}\text{Sr} \pm 2\sigma$ in Adelaidean carbonates.

Preferred minimum value. Data from
Veizer and Compston, 1976.

1. The authors believed that these values were too high.

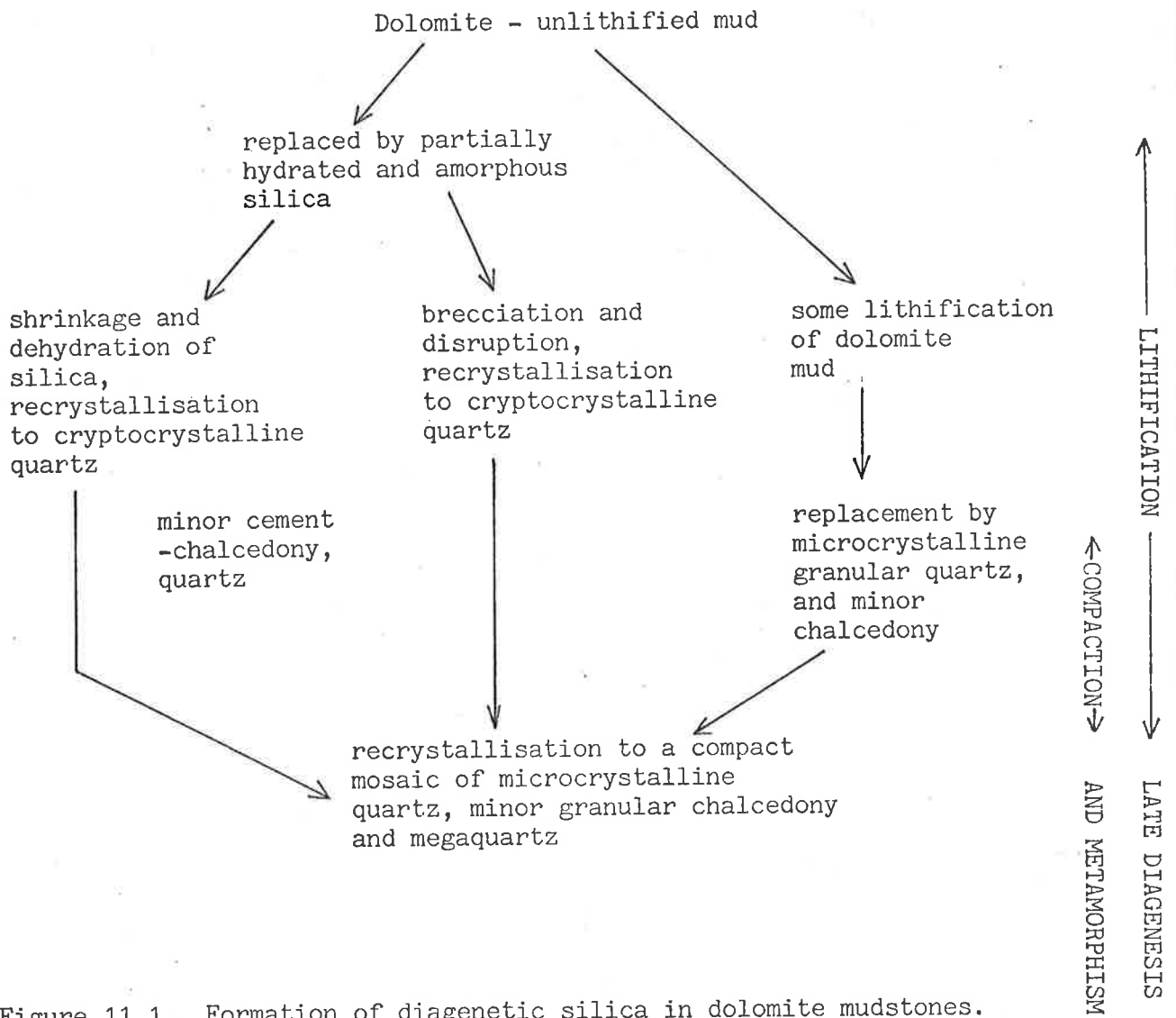


Figure 11.1. Formation of diagenetic silica in dolomite mudstones.

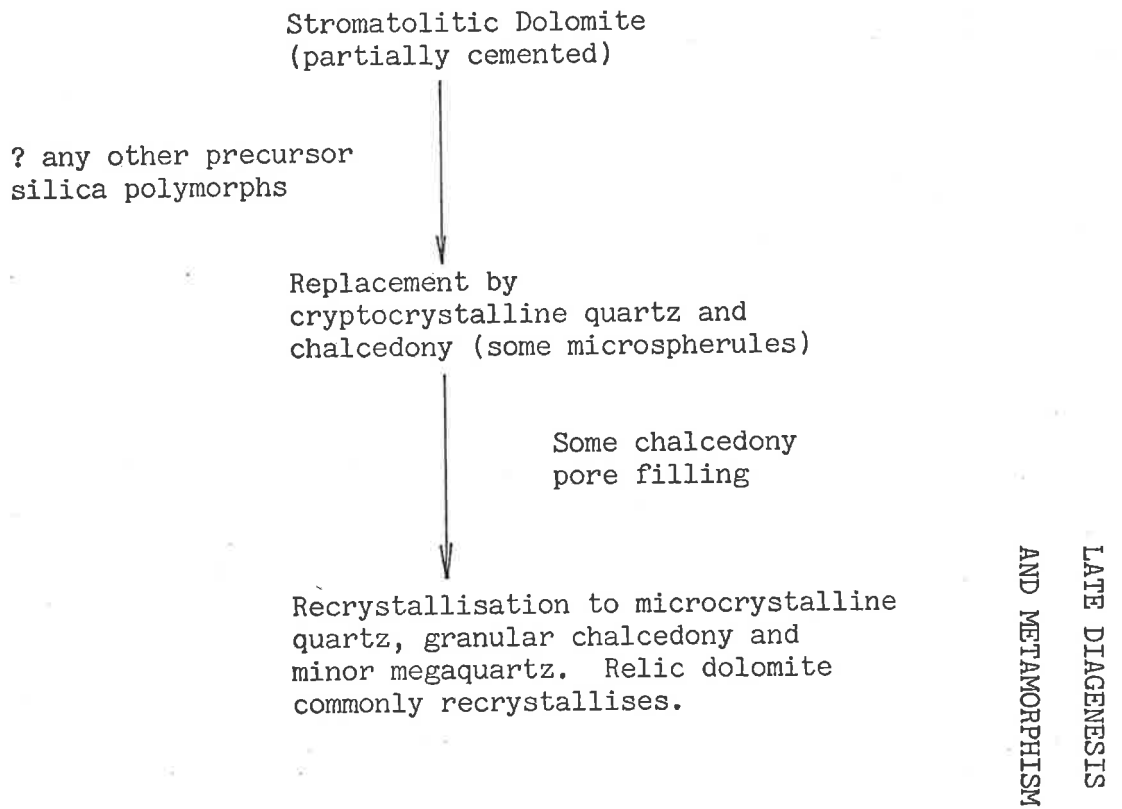


Figure 11.2. Formation of diagenetic silica in stromatolitic dolomites.

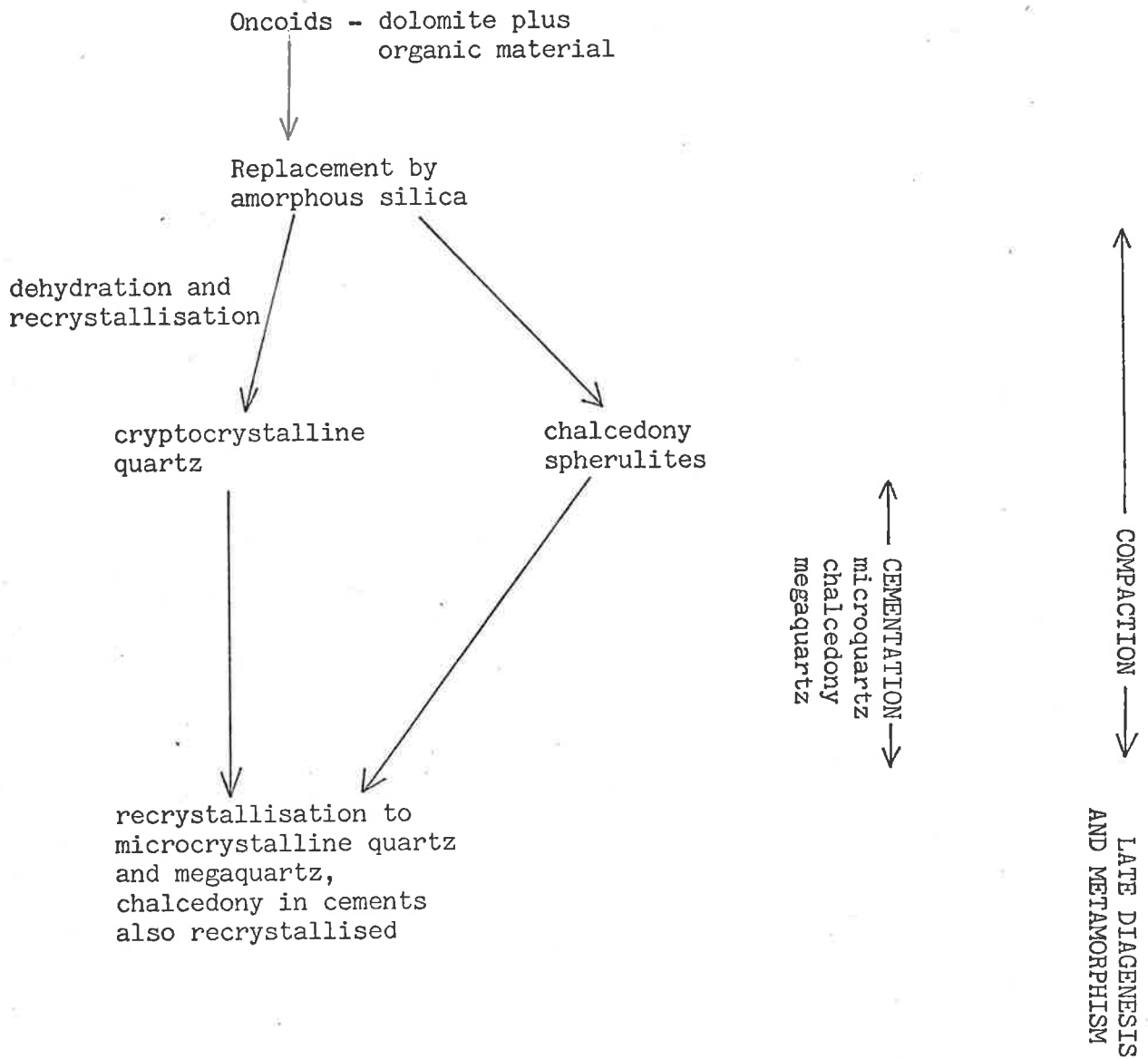
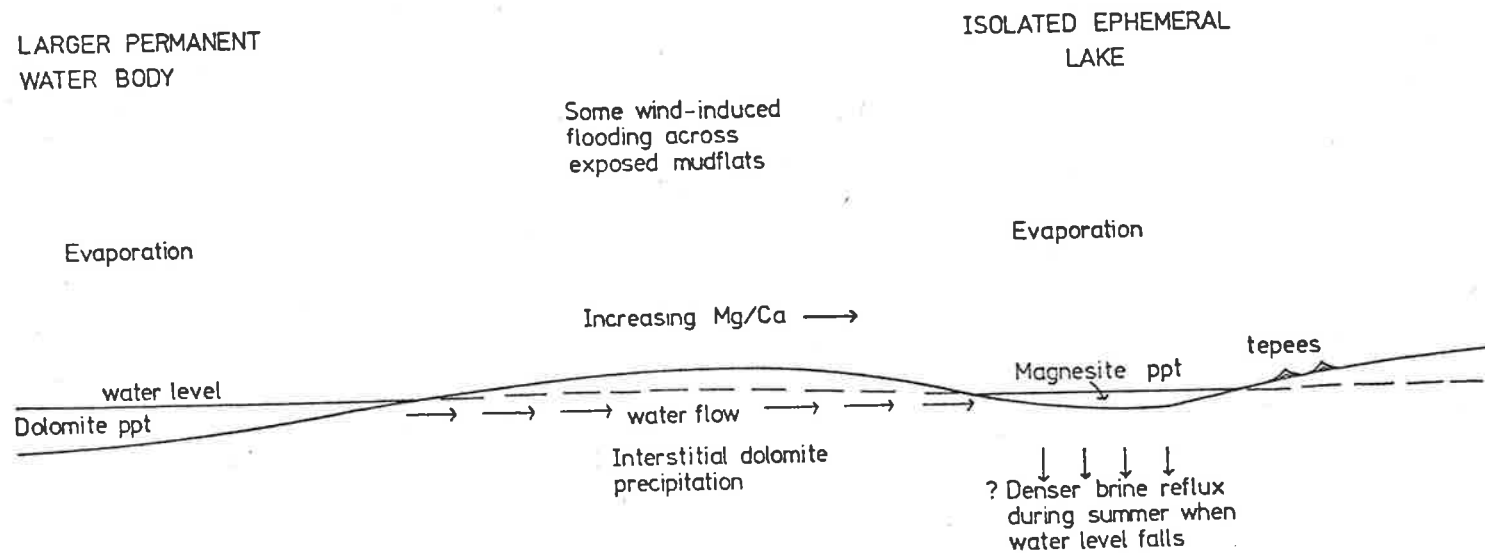


Figure 11.3. Formation of diagenetic silica in dolomite oncoid grainstones.

Figure 12.1. Summary of the major environments of dolomite formation. Modified from Badiozamani (1973) and Wilson (1975).



RKU79

Figure 12.2. Schematic diagram showing the site of magnesite precipitation. Water level may fall below the sediment surface in the ephemeral lake during more intense summer evaporation. Because of vertical exaggeration, gradients of the sediment surface appear much greater than those likely to have been present in the proposed depositional environment.



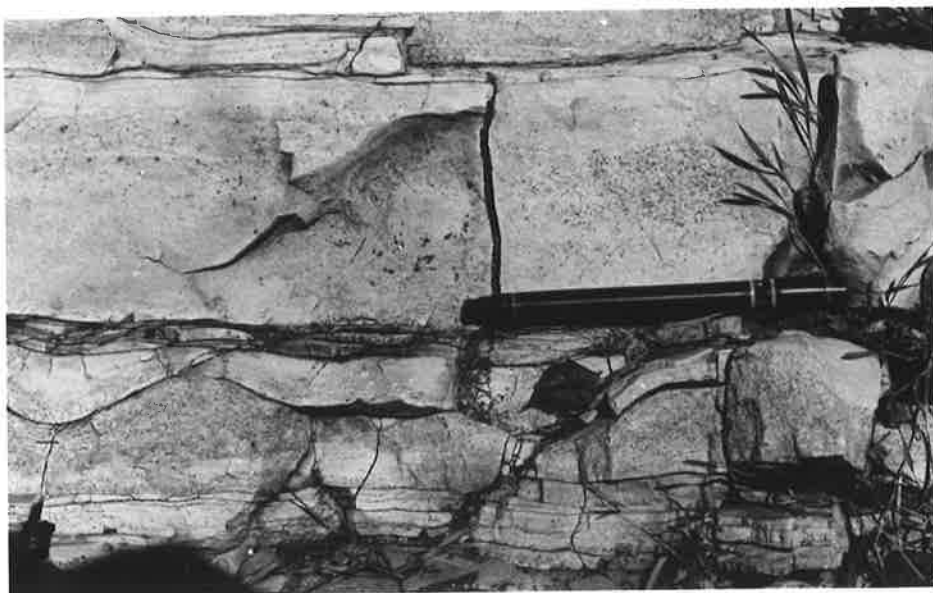
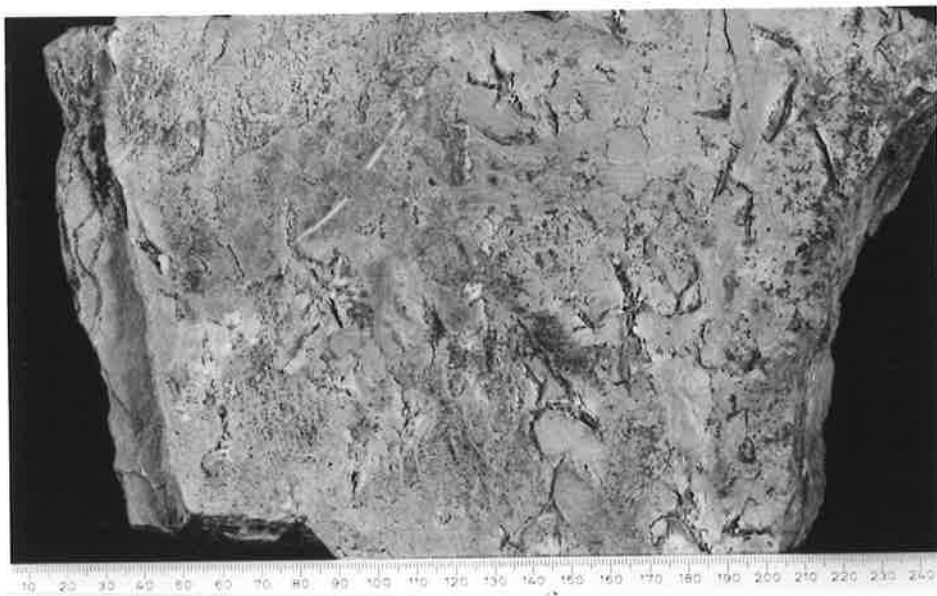
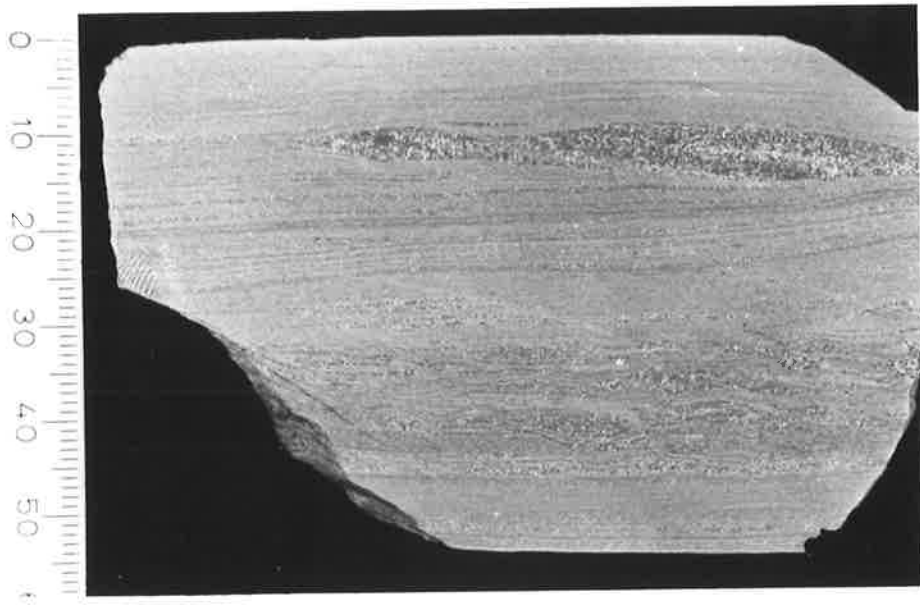


PLATE 4.3

- a. (at left) Massively outcropping biostromes of stromatolitic dolomite interbedded with shales, Unit 2, Nathaltee Formation, Depot Creek (DC).

- b. (at right) Stromatolite microstructure with laminae of homogeneous dolomite mud with scattered quartz silt (base and top) with more grumous textured dolomite in centre. Black grains are iron oxides. Specimen is a columnar stromatolite from Depot Creek (DC). Field of view is 3.3 mm in height.

- c. Coarse-grained, trough cross-bedded sandstone, Unit 3, Nathaltee Formation, Port Germein Gorge (PG). Lens cap is 5.5 cm in diameter.

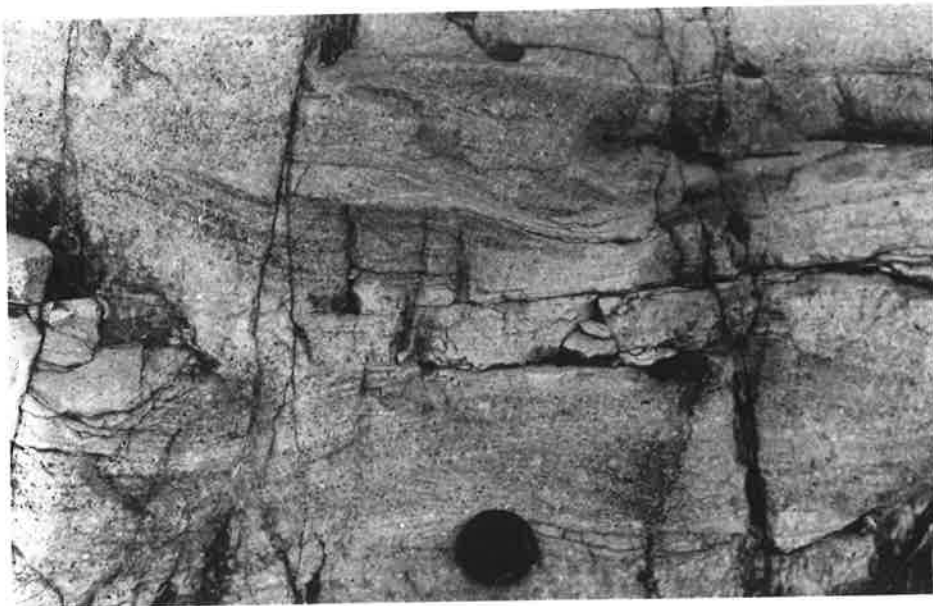
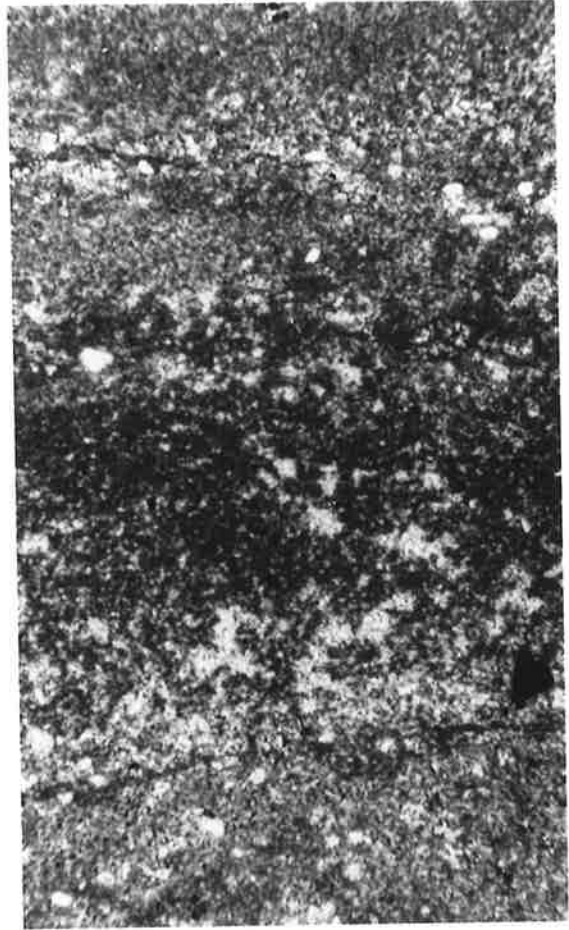




PLATE 4.5

- a. Siltstones with conglomerate filled channels of small pebbles, Unit 1, Nankabunyana Formation, Nudlamutana Hut (NH). Hammer is 33 cm in length.

- b. Cross-bedded sandstone with scattered granules. Shallow trough cross-beds at base of coset overlain by tabular cross-beds, Unit 2, Nankabunyana Formation, Nudlamutana Hut (NH). Hammer is 35 cm in length.

- c. Flat and ripple cross-laminated sandstone. Cross-laminae are erosional into flat laminae, and appear to be formed by wave action, Unit 2, Nankabunyana Formation, Nudlamutana Hut (NH). Pen is 1.2 cm in diameter.

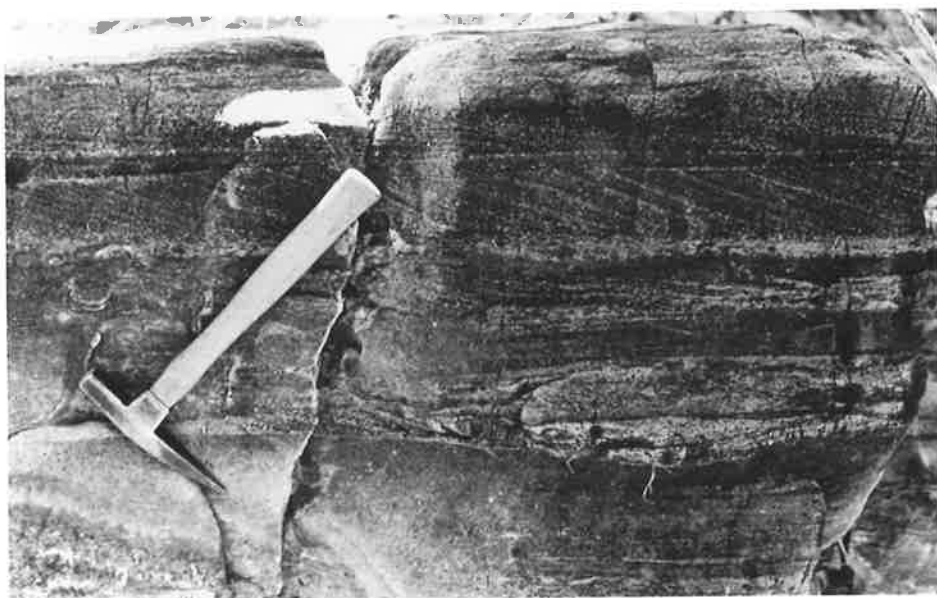
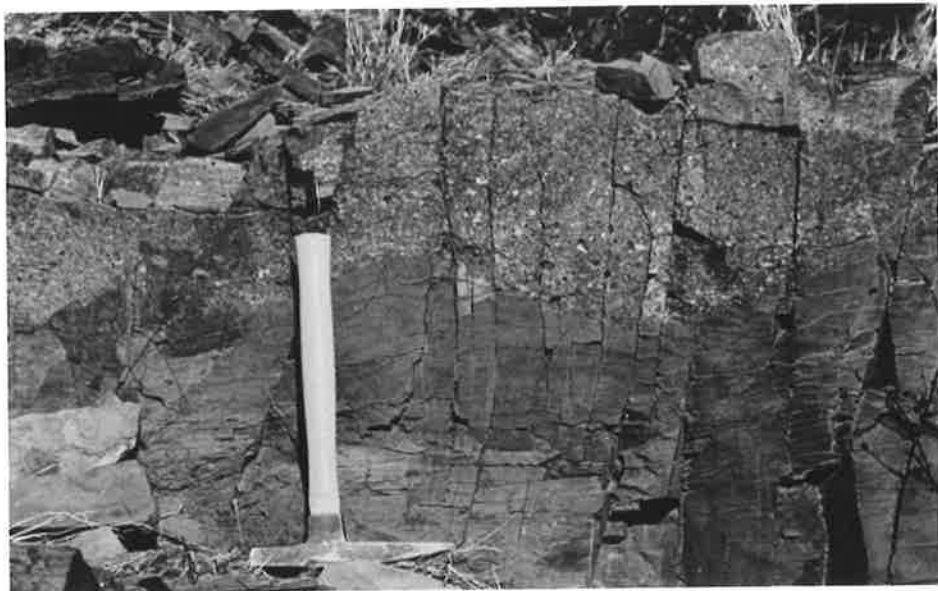


PLATE 4.6

- a. Wavy laminated shale with soft sediment disrupted lamination at left, Unit 2, Nankabunyana Formation, Copley (CP). Lens cap is 5.5 cm in diameter.

- b. (at left) Flat laminated shale with abundant syneresis cracks and disrupted lamination at top, Unit 2, Nankabunyana Formation, Copley (CP). Lens cap is 5.5 cm in diameter.

- c. (at right) Bedding plane of silty dolomite mudstone with rosettes (which also penetrate through lamination) infilled with quartz and dolomite spar, and which may be replaced gypsum crystals, Unit 2, Nankabunyana Formation, Top Mount Bore (TM). Pen is 14 cm in length.

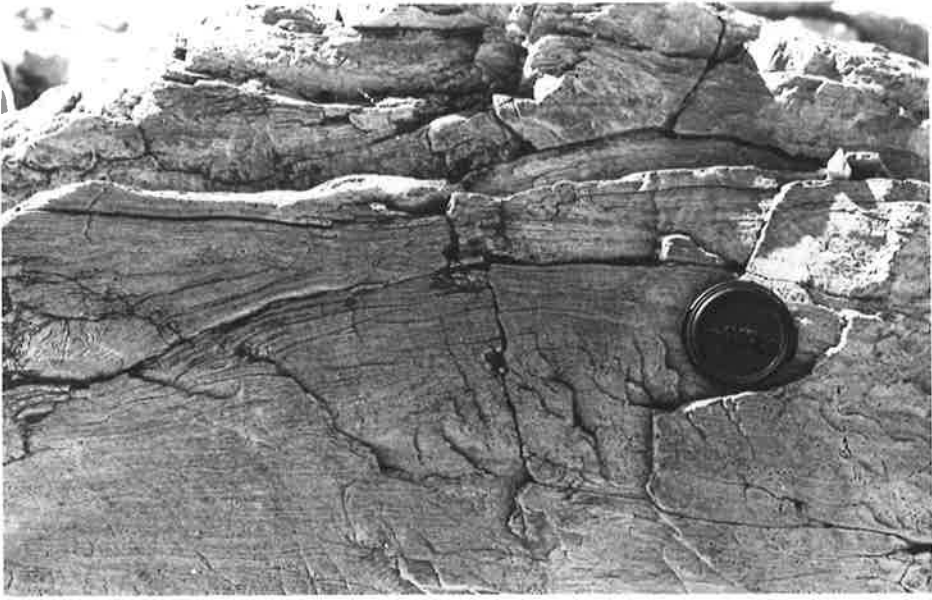


PLATE 4.7

- a. Desiccated and eroded beds of dolomite mudstone, interbedded with coarse-grained sandstone, Unit 2, Nankabunyana Formation, Nudlamutana Hut (NH). Hammer handle is 3 cm in diameter at top.

- b. Cross-bedded, sandy dolomite intraclastic grainstone of sand and granule sized intraclasts, overlain by stromatolitic dolomite consisting of short tuberous columns with sandy interspace sediment, Unit 2, Nankabunyana Formation, West Mount Hut (WM). Stromatolite outcrop is about 40 cm in width.

- c. Part of bioherm of columnar stromatolites, showing stubby, tuberous columns and divergent branching. Note large intraclast derived from erosion of a column at centre right, Unit 2, Nankabunyana Formation, Top Mount Bore (TM). Lens cap is 5.5 cm in diameter.

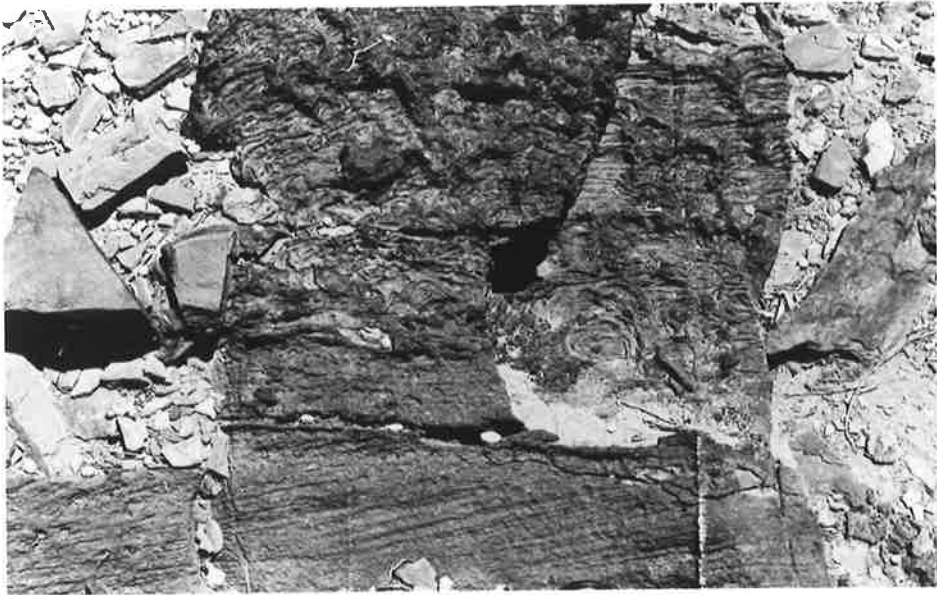


PLATE 4.8

- a. Highly irregular lamination in massively outcropping recrystallised dolomite, Unit 2, Nankabunyana Formation, Nudlamutana Hut (NH). Lens cap is 5.5 cm in diameter.

- b. Massive recrystallised dolomite with indistinct bedding. Vertical zone in centre is infilled with haematite rich sediment. Location as in a. Lens cap is 5.5 cm in diameter.

- c. Thin section of haematite rich sediment containing scattered silt sized dolomite crystals some of which are replaced by quartz (white grains). Location as above. Field of view is 2.0 mm in width.

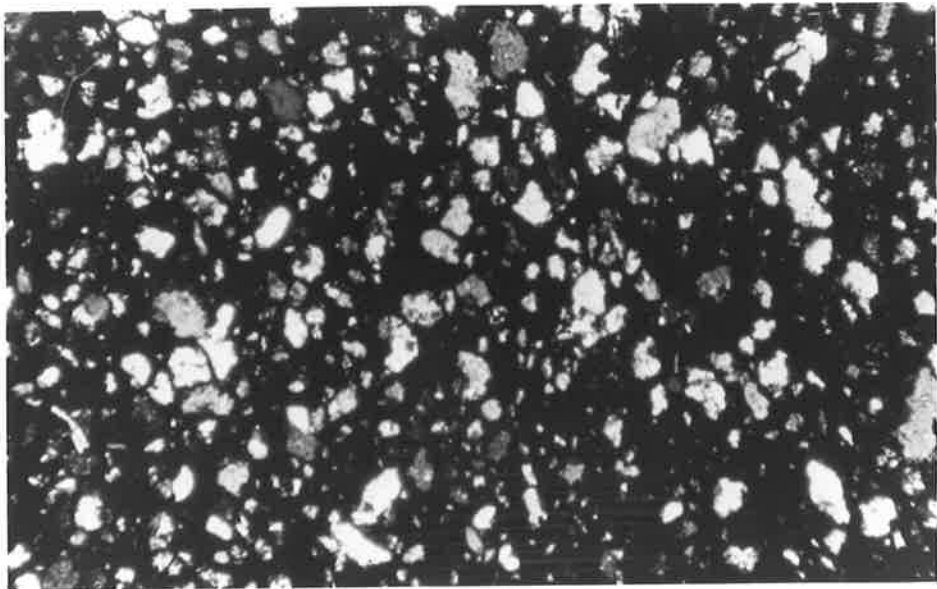
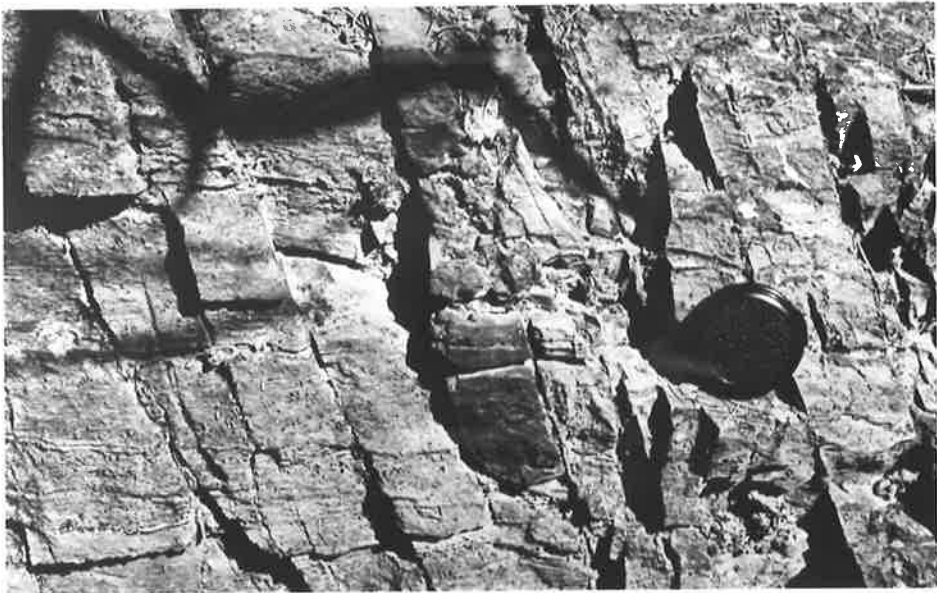
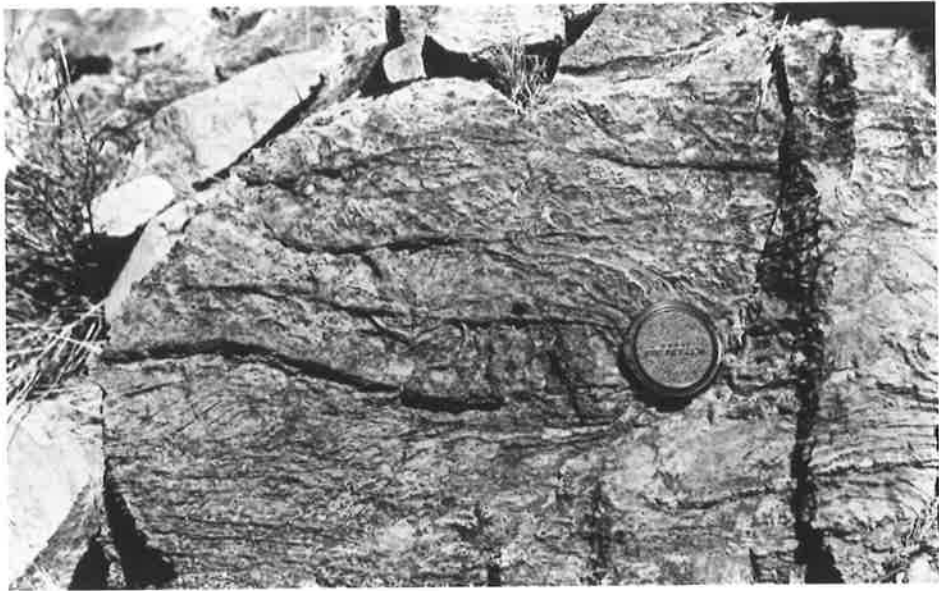


PLATE 4.9

- a. Well laminated shale in which clay laminae contain abundant synaeresis cracks. Slightly darker laminae are silty. Graded laminae are present in centre of specimen and disrupted laminae at base. Specimen from Unit 3, Nankabunyana Formation, Copley (CP). Scale in cm.
- b. Flat, wavy and ripple laminated quartz-cemented sandstone, Unit 3, Nankabunyana Formation, Copley (CP). Pen is 15 cm in length.
- c. Cross-laminated very fine-grained sandstone, in which many sets are erosionally based. Some dolomite rich laminae have weathered out at base, Unit 4, Nankabunyana Formation, Copley (CP). Pen is 8 mm in diameter.

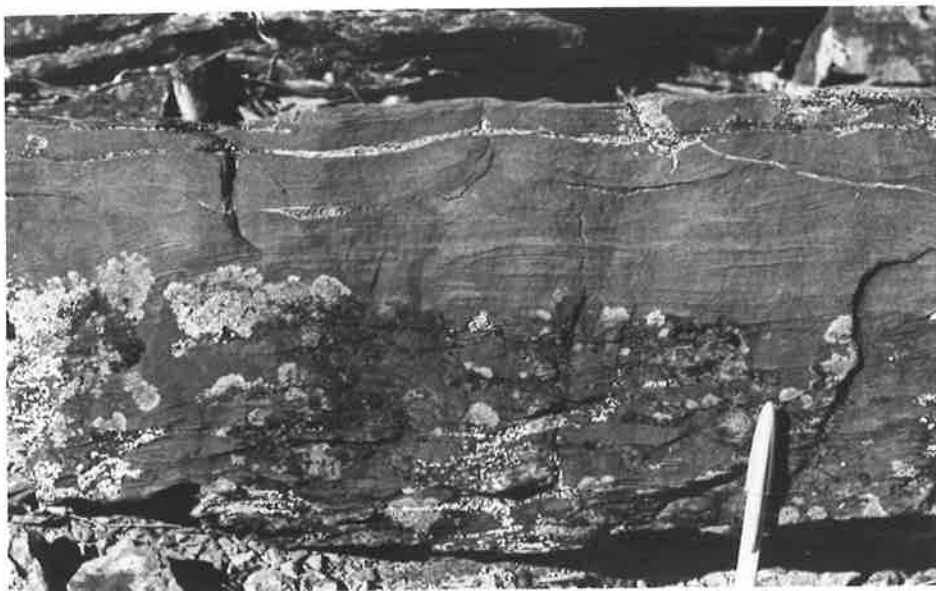
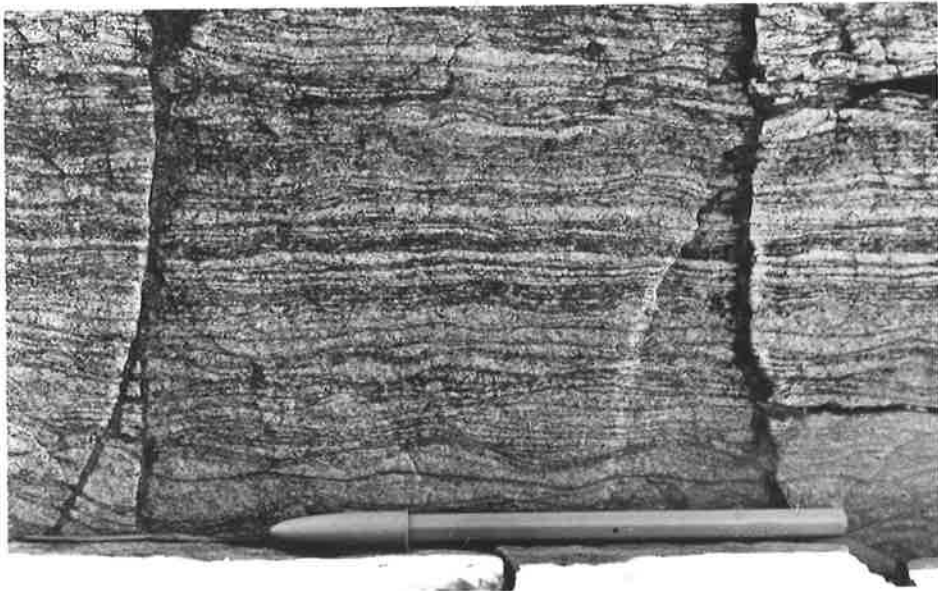
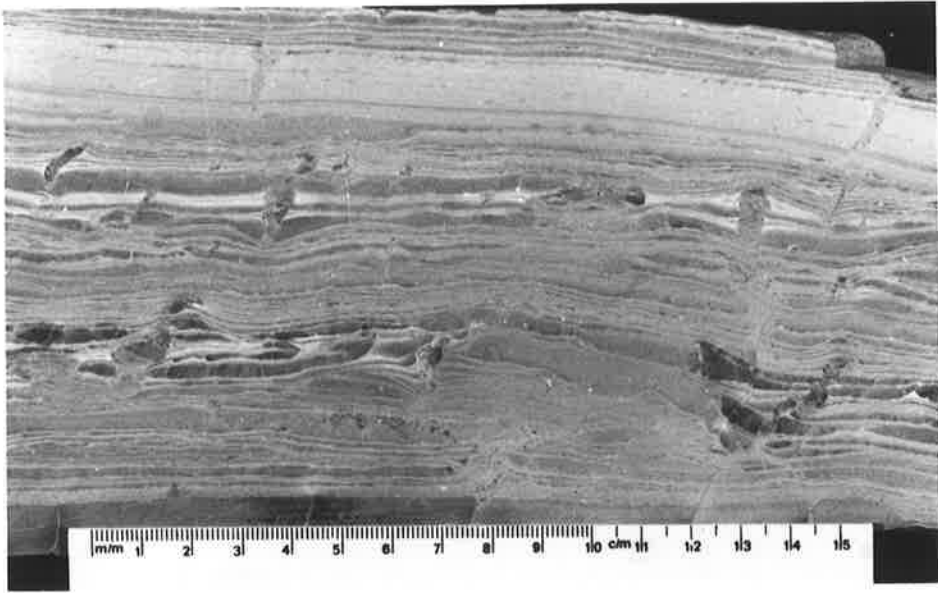


PLATE 4.10

- a. Symmetrical ripple crests with slightly wavy crestlines. Note variable orientation of cross-laminae exposed in ripple troughs, while that related to ripple crests indicates flow from bottom to top. Unit 4, Nankabunyana Formation, Copley (CP). Pen is 8 mm in diameter.
- b. Wavy and ripple cross-laminated very fine-grained sandstone. Cross lamination is variably directed and probably of wave origin. Coarser sand is present as a lag deposit above erosion surface near top (arrowed). Tilterana Sandstone, Mt. Norwest H.S. (NW). Pen is 12 mm in diameter.
- c. Flat lamination (base), gently climbing ripple lamination (centre) and cross-lamination covered by shale laminae (top) in fine-grained sandstone, Tilterana Sandstone, Mt. Norwest H.S. (NW). Pen is 12 mm in diameter.



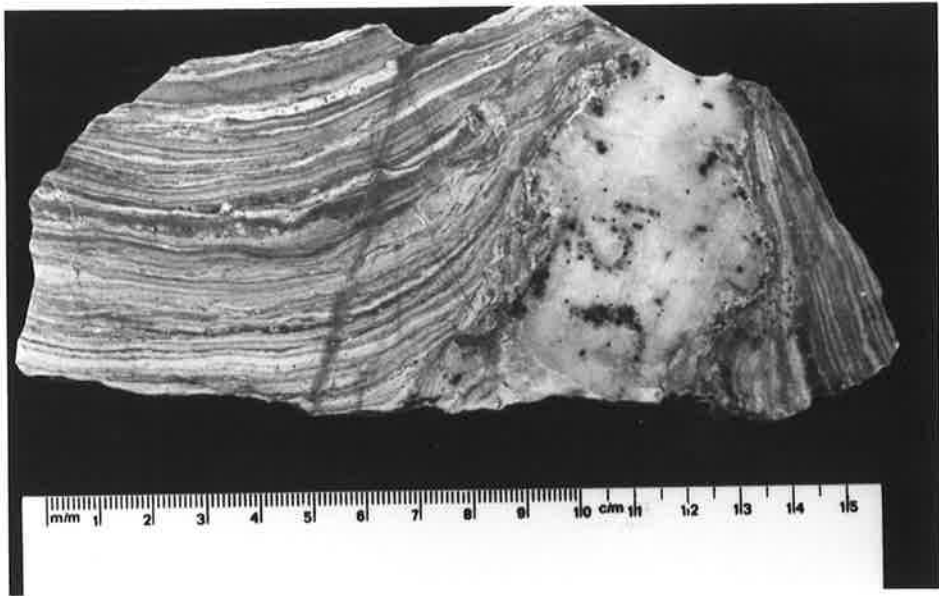
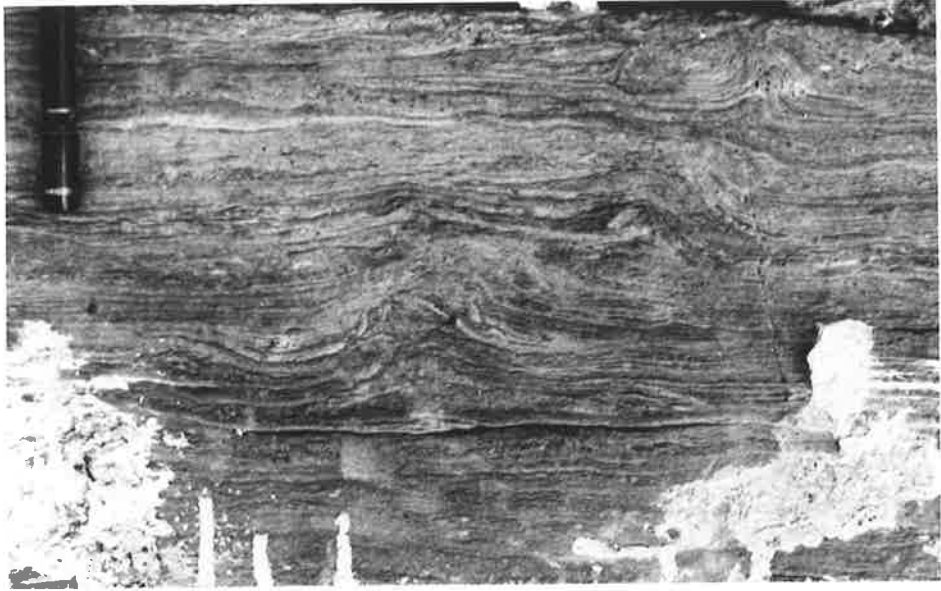


PLATE 5.2

- a. Small tepees in laminated grey dolomite mudstone, Skillogalee Dolomite, west of Tarlee (T). Pen is 12 mm in diameter.

- b. Interlaminated magnesite (cream) and dolomite (grey) mudstone, cut and disrupted by white chert nodule now consisting of recrystallised polygonal quartz. Specimen from the Skillogalee Dolomite, River Wakefield, west of Rhynie (RW). Scale in cm.

- c. Dolomitic sandstone with slightly asymmetrical ripples whose troughs are infilled by grey dolomite mudstone (flaser bedding), Skillogalee Dolomite, Dutton's Trough H.S. (DT). Pen is 14 cm in length.



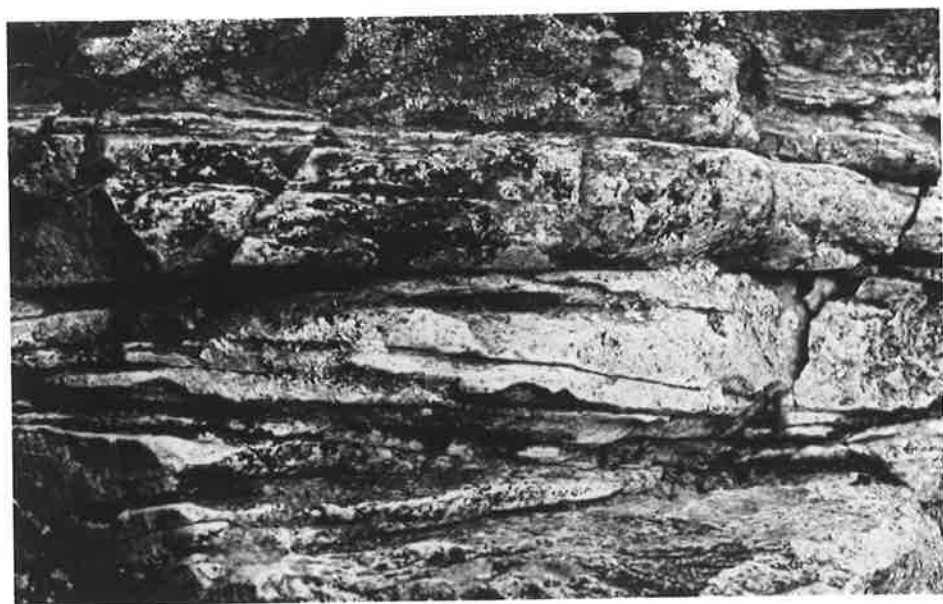
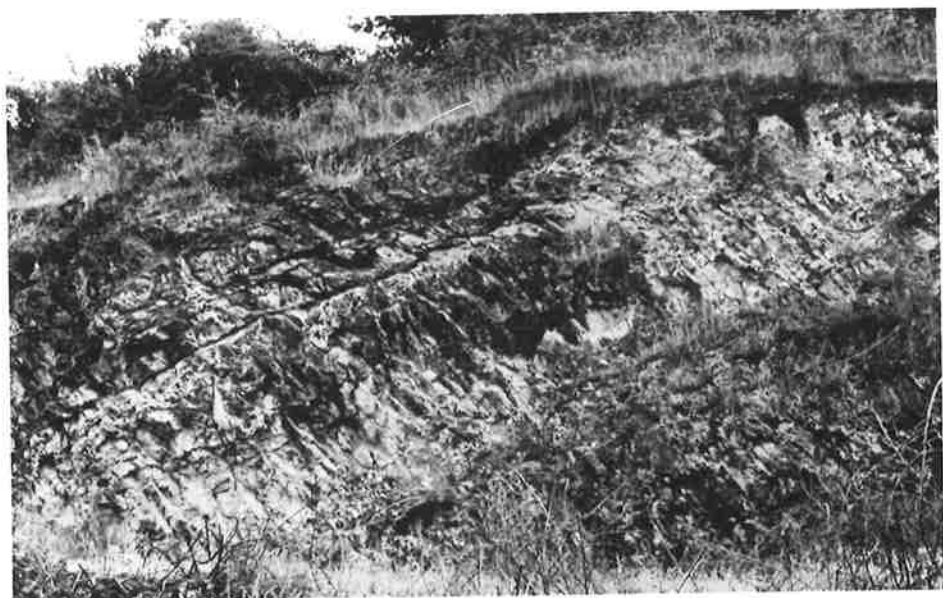


PLATE 6.1

- a. Flat laminated and thinly bedded dark-grey dolomite mudstone, forming a flaggy outcrop. Note truncated laminae immediately to left of hammer head, and elongate lenses of black chert, Yadlamalka Formation, Yednalue (YD). Hammer is 35 cm in length.

- b. Wavy laminated, more massively outcropping dark-grey dolomite mudstone, Yadlamalka Formation, Depot Creek (DC). Pencil is 17 cm in length.

- c. Dark-grey dolomite mudstone with thin coarse-grained sandstone interbeds, small slump fold in centre and disrupted lamination at top, Yadlamalka Formation, Mundallio Creek (MC). Pen is 14 cm in length.

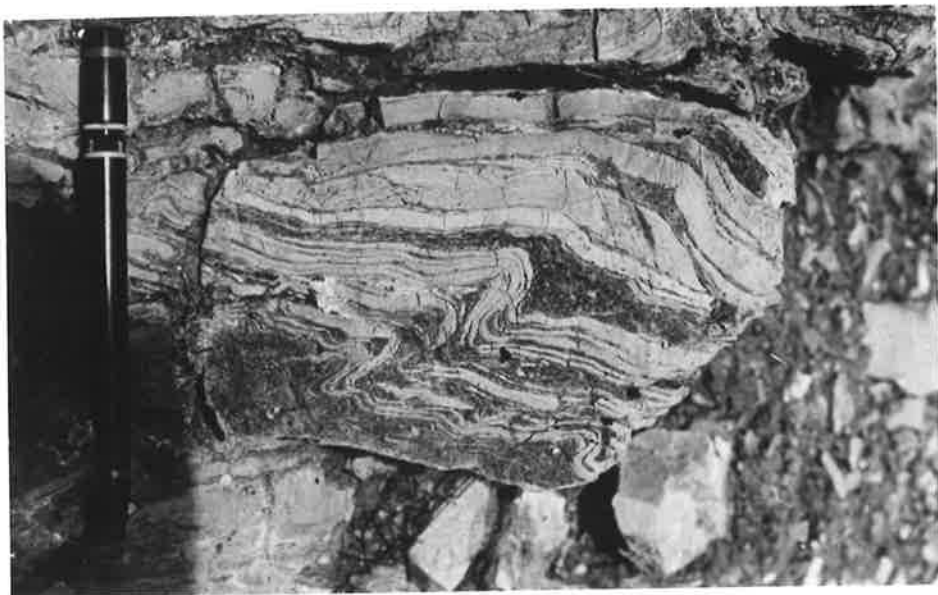
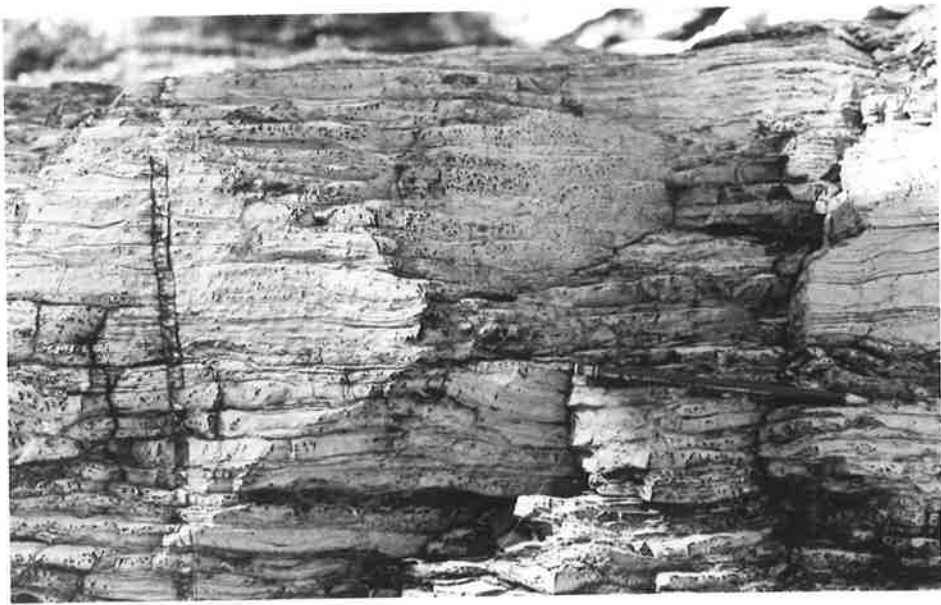
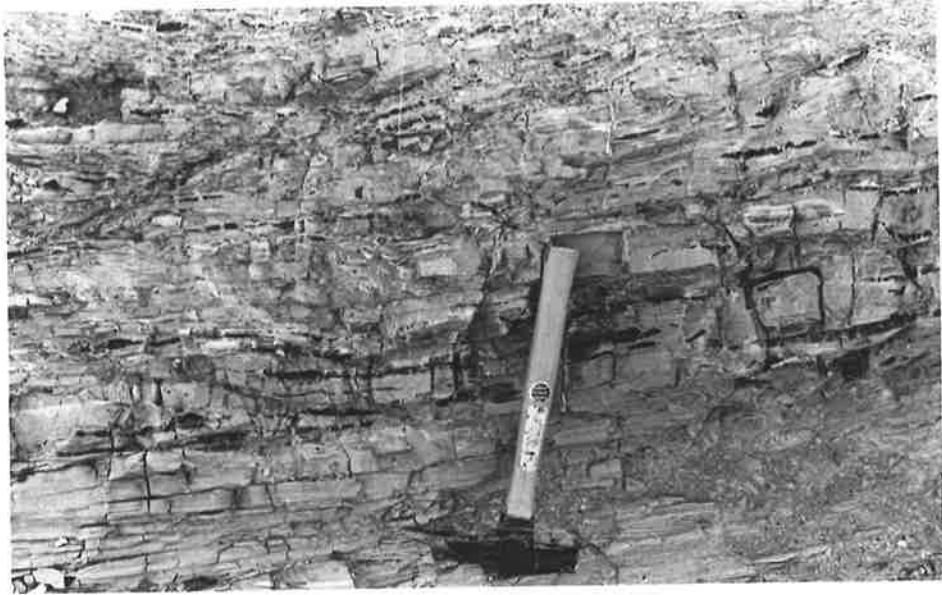


PLATE 6.2

- a. (at left) Dolomite mudstone with graded laminae containing scattered quartz silt grains and coarser dolomicrospar at base of laminae, Specimen from the Yadlamalka Formation, Copley (CP). Field of view is 3.2 mm in length.
- b. (at right) Grumous textured dolomite mudstone containing carbonaceous, micritic clots in a matrix of microspar and some clear fine spar, scattered quartz grains at top. Specimen from the Yadlamalka Formation, West Rischbieth (WR). Field of view is 2 mm in length.
- c. Disrupted dark-grey dolomite mudstone, with fractured and deformed lamination. Pale laminae are silty. Specimen from the Mirra Formation, Mt. Norwest H.S. (NW). Scale in cm.

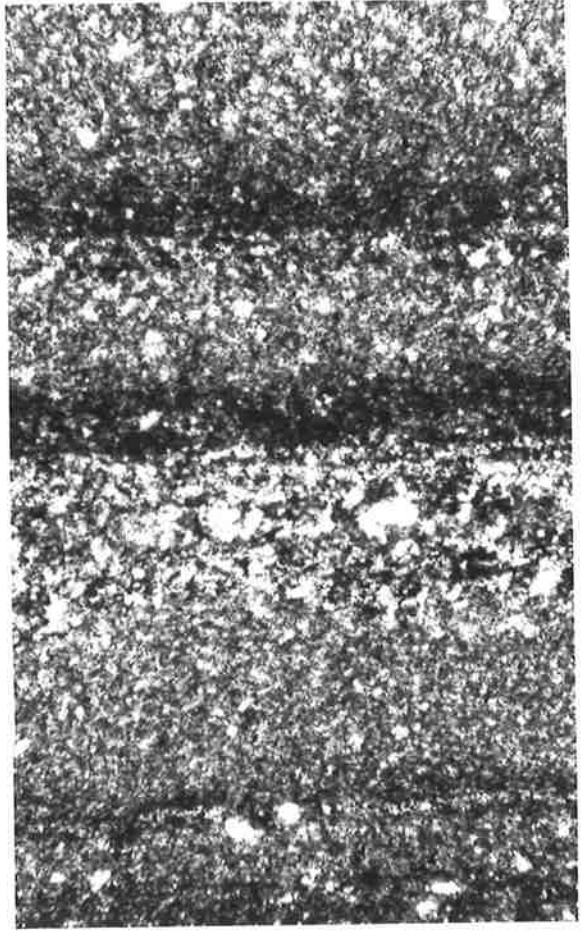
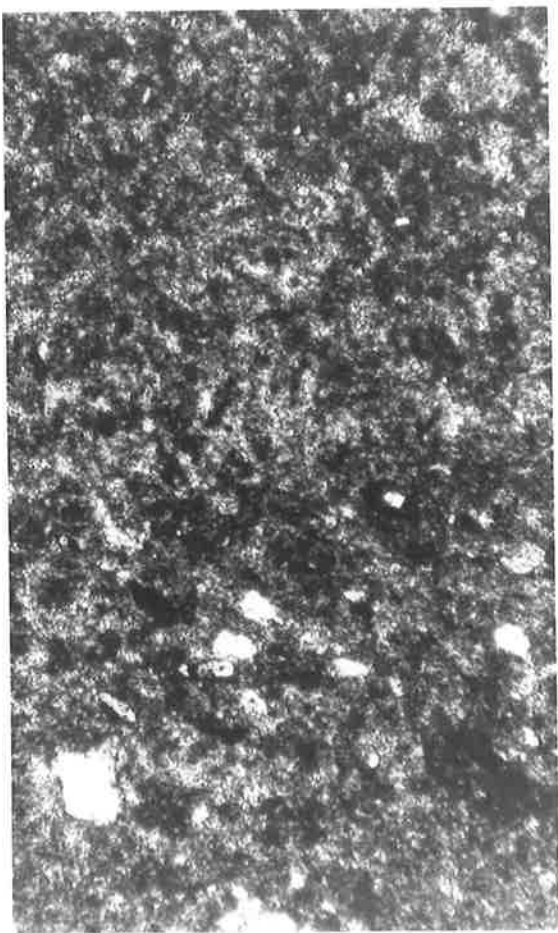
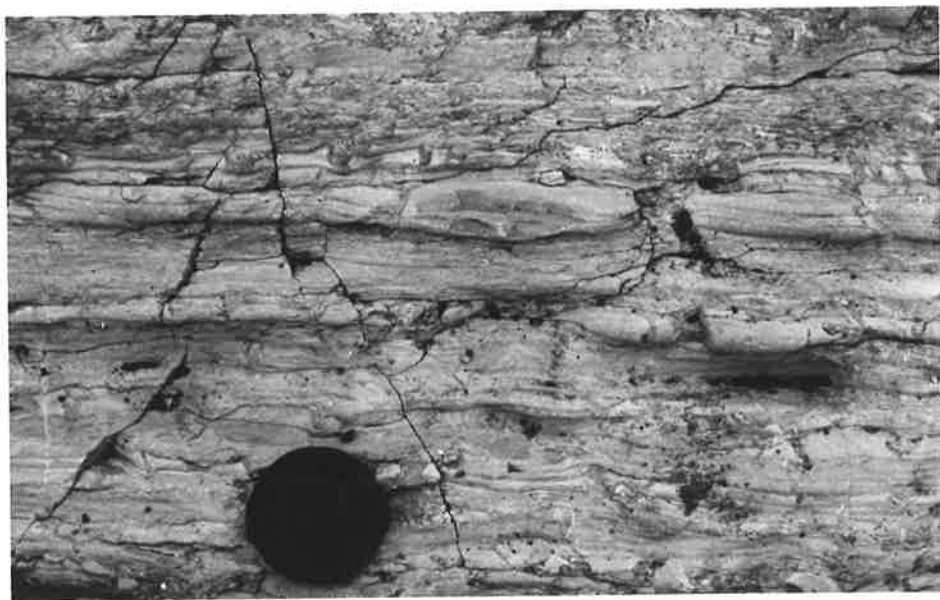
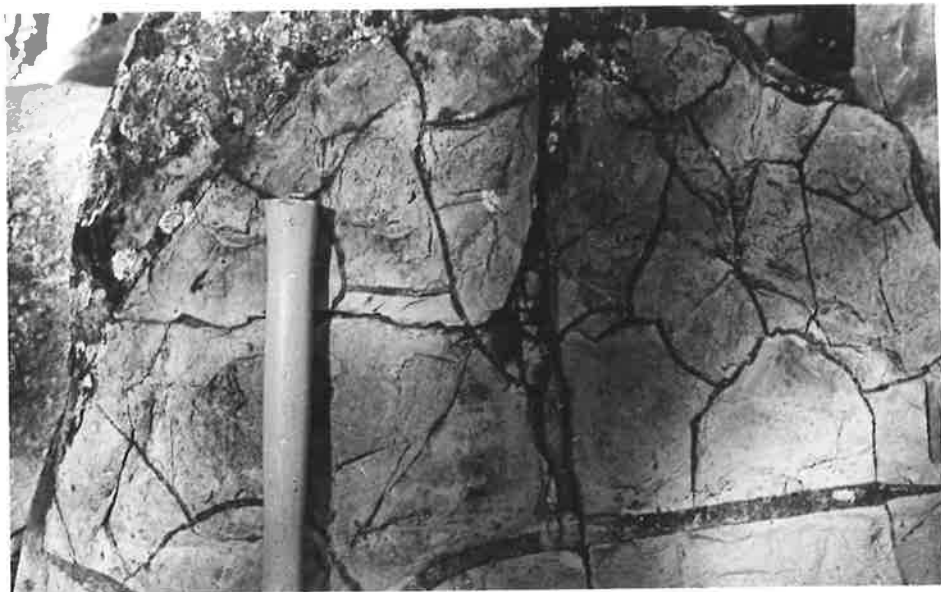


PLATE 6.3

- a. Polygonal desiccation cracks infilled with fine-grained sand in dark grey dolomite mudstone, Yadlamalka Formation, Yednalue Anticline (YDA). Hammer handle is 3 cm in diameter.

- b. Thin desiccated beds of dolomite mudstone which are sometimes eroded to produce intraclasts in the overlying silty dolomite laminae. In grey dolomite mudstone, Yadlamalka Formation, Yednalue (YD). Lens cap is 5.5 cm in diameter.

- c. Small eroded tepee in desiccated dolomite mudstone (weathering light grey), underlain and overlain by grey dolomite-cemented very fine-grained sandstones, Yadlamalka Formation, Copley. Lens cap is 5.5 cm in diameter.



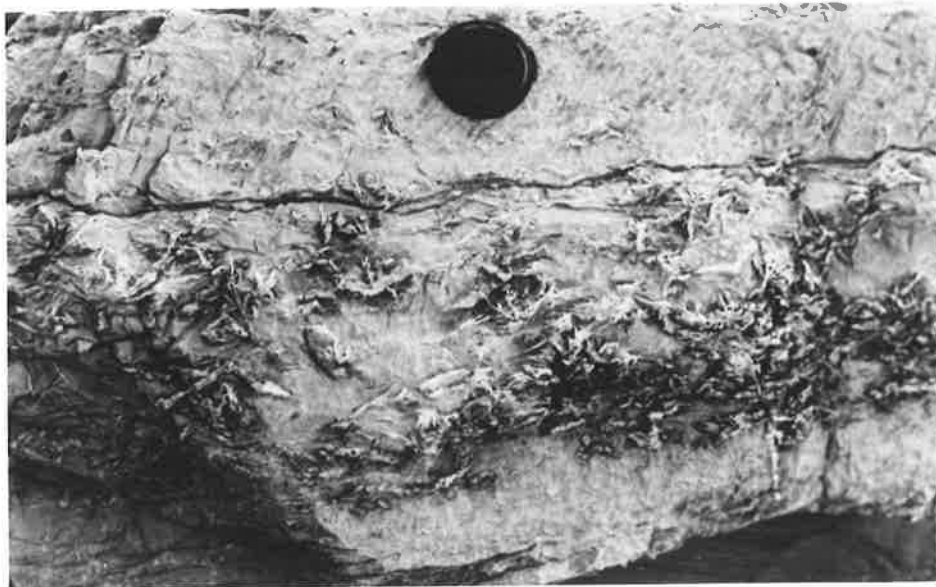
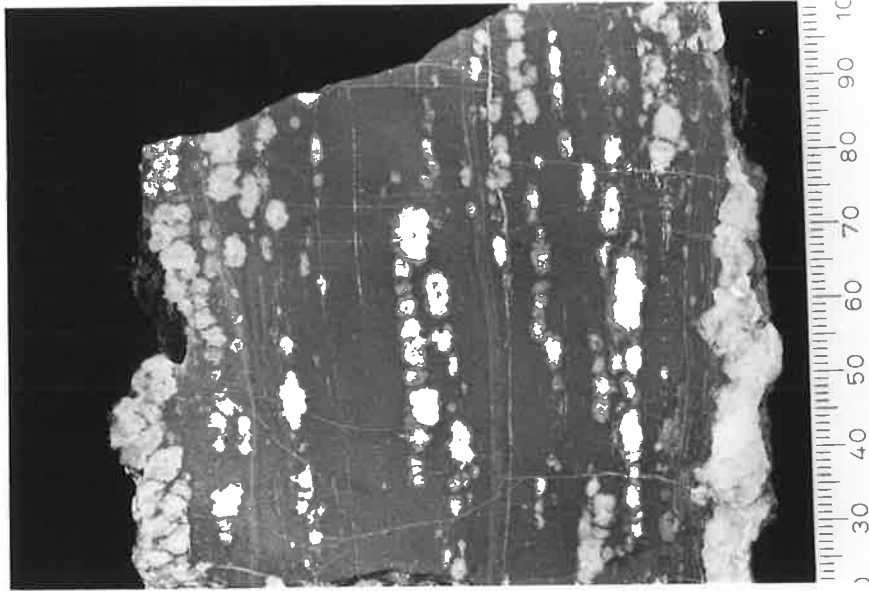


PLATE 6.5

- a. Lenses of sandy intraclastic dolomite in grey dolomite mudstone with sand and granule sized intraclasts, overlain by a fine-grained sandstone with scattered granule sized intraclasts, and larger intraclasts derived from erosion of the underlying dolomite mudstone, Yadlamalka Formation, West Rischbieth (WR). Lens cap is 5.5 cm in diameter.

- b. Medium- to coarse-grained dolomitic sandstone with scattered elongate, angular dolomite intraclasts arranged parallel to bedding, Yadlamalka Formation, Crystal Brook (CB). Hammer head is 18 cm in length.

- c. Extensively silicified oncoïd grainstone (o, chert is black), overlying dolomite mudstone (m). The boundary between the silicified oncoïd grainstone and unsilicified dolomite mudstone is sharp. Yadlamalka Formation, Depot Creek (DC). Pen is 14 cm in length.

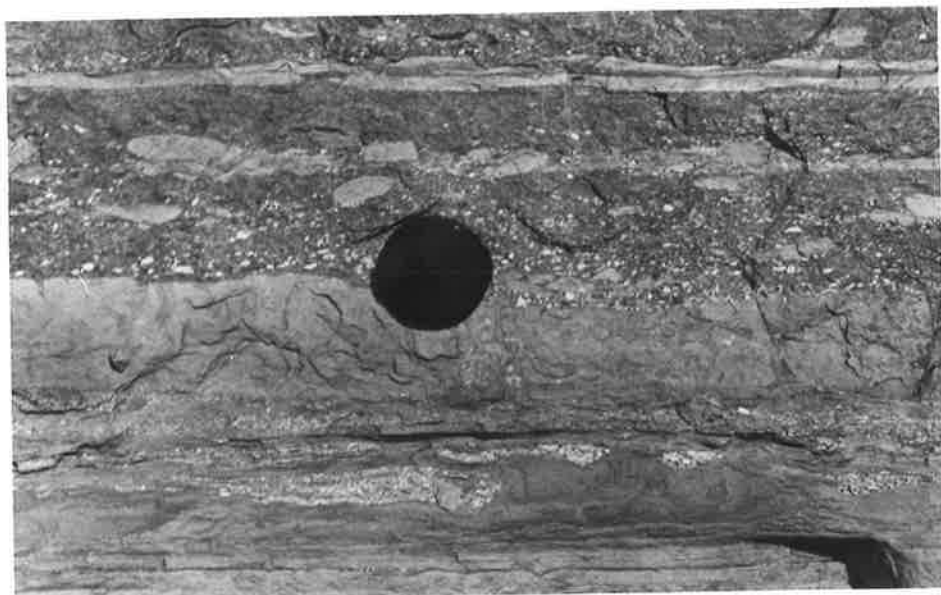


PLATE 6.6

- a. Extensively silicified elongate oncoids, with lenticular lamination which is thickened on the ends of grains and contain fine disseminated carbonaceous material. Scattered very fine dolomite grains are most abundant in the silicified dolomite intraclasts forming nuclei to oncoids (e.g. at right). Larger irregular dolomite grains have formed in the clear quartz cement. Specimen from the Yadlamalka Formation, Copley (CP). Field of view is 2 mm in width.
- b. Silicified oncoids with a vaguely radial pattern defined by disseminated carbonaceous material, and laminae of more even thickness. Oncoid near centre has grown on a more elongate oncoid similar to those in a. above. Specimen from the Yadlamalka Formation, Beetaloo (B). Field of view is 8.5 mm in width.
- c. Silicified massive oncoids with concave and convex margins, and disseminated carbonaceous material. Oncoid at left contains incipient polygonal shrinkage cracks. Specimen from the Yadlamalka Formation, Copley (CP). Field of view is 2 mm in width.

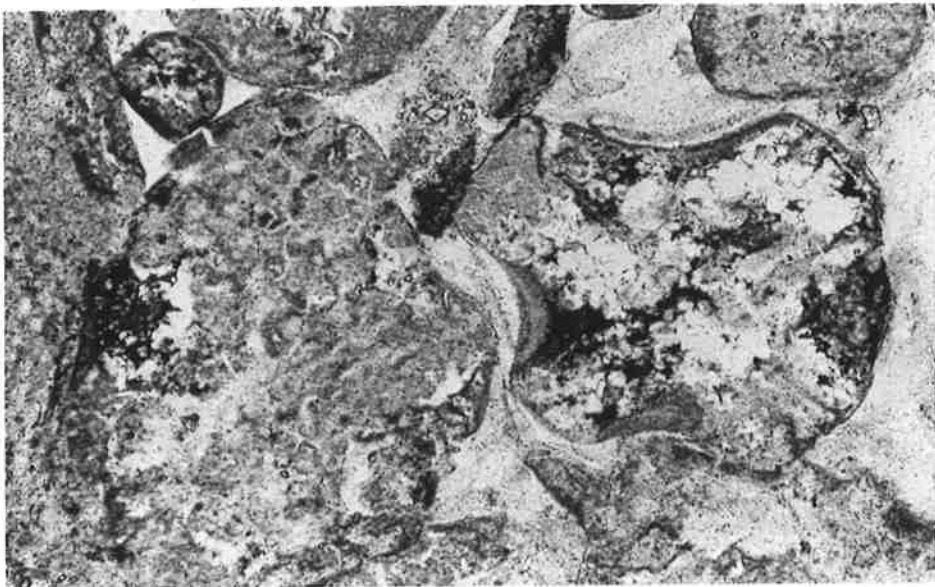
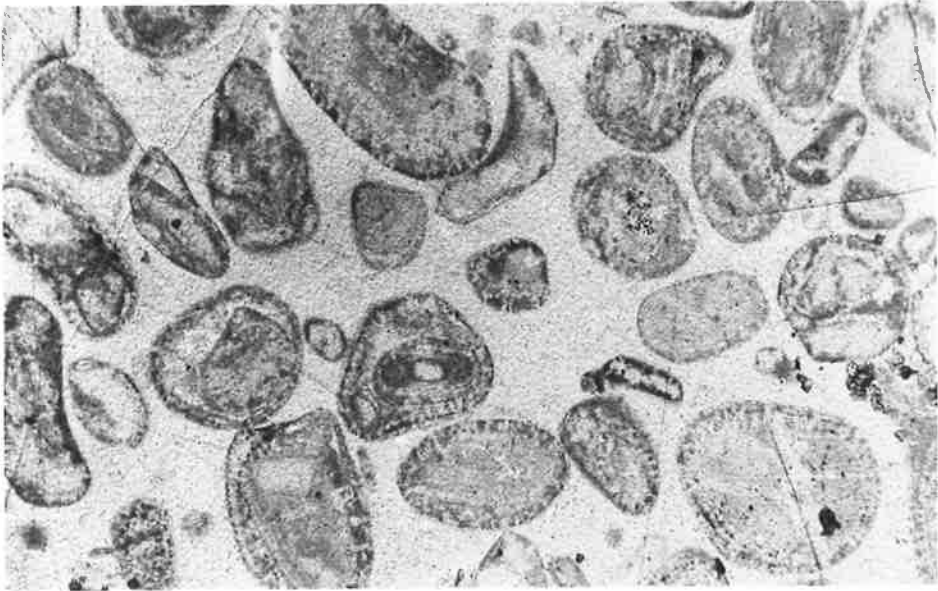


PLATE 6.7

- a. Two isolated broad columnar stromatolites which have grown on an irregular erosional surface on the underlying dolomite mudstone. Part of the columns and interspace sediment have been replaced by black chert. Yadlamalka Formation, Yednalue (YD). Pen is 14 mm in diameter.

- b. Domal and columnar stromatolites in dark-grey dolomite, some divergent branching near lens cap, and flat laminated dolomite at the top. Mirra Formation, Mirra Creek (MI). Lens cap is 5.5 cm in diameter.

- c. Columnar stromatolites in part of a massive biostrome. The columns are very irregular and tuberous, and the interspace sediment is largely dolomite mudstone. Yadlamalka Formation, Yednalue (YD). Pen is 14 cm in length.

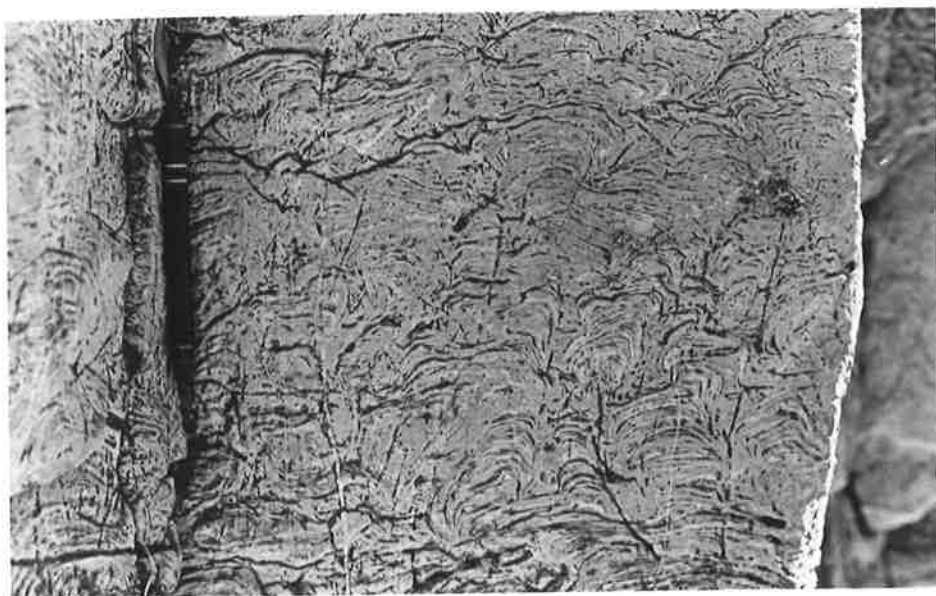
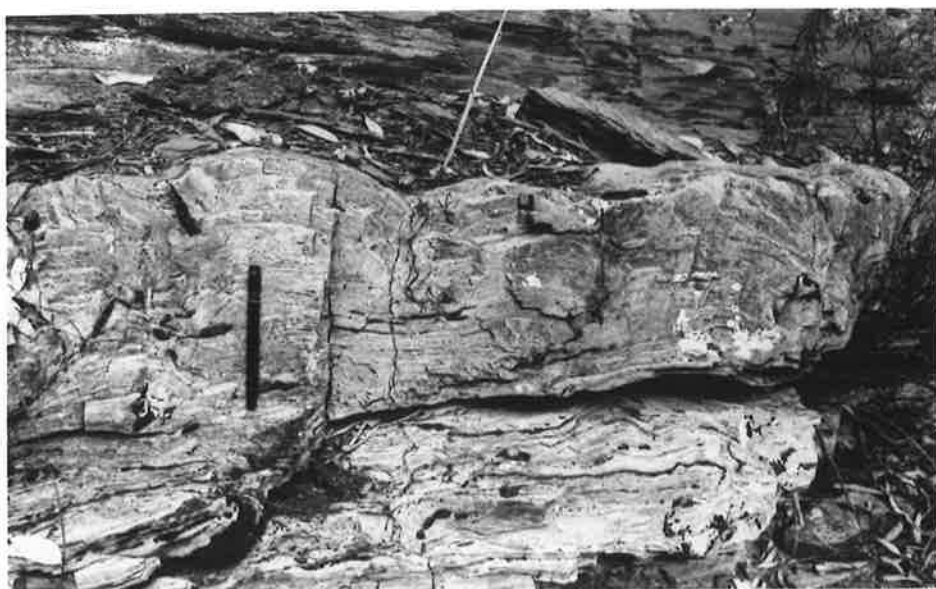


PLATE 6.8

- a. Part of a massive stromatolite biostrome with irregular columnar stromatolites which have grown on an irregular erosion surface. Draping laminae of dolomite mudstone and terrigenous silt (prominent laminae) are present between columns. Yadlamalka Formation, Copley (CP). Pen is 8 mm in diameter.
- b. Small stromatolite bioherms which are aligned, probably by wave or current action, and some isolated domes (cross-sections visible at centre right), overlying dolomite mudstone, Yadlamalka Formation, Depot Creek (DC). Hammer is 45 cm in length.
- c. Horizon of gently domal stromatolites with minor small cross-cutting lenses of black chert, and overlain by a more fissile dolomite mudstone, Yadlamalka Formation, Depot Creek (DC). Pen is 14 cm in length.



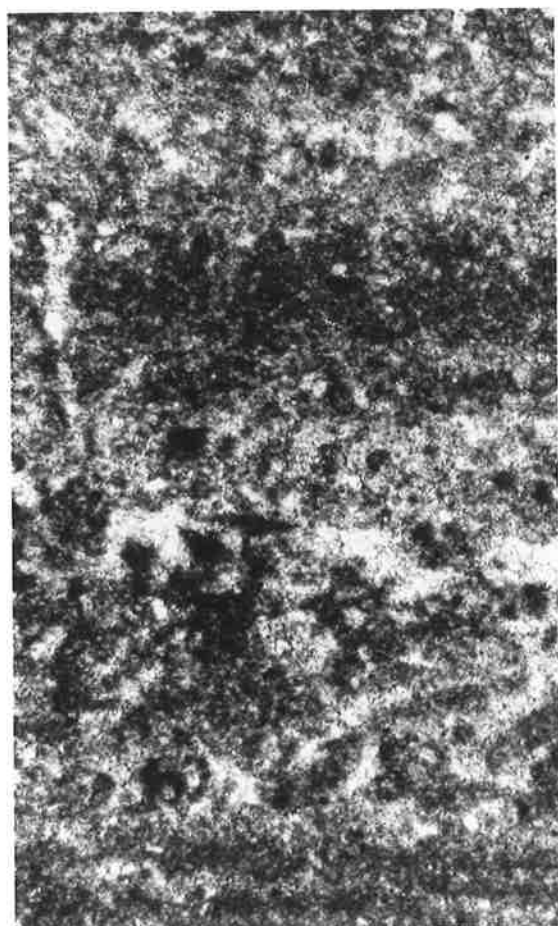
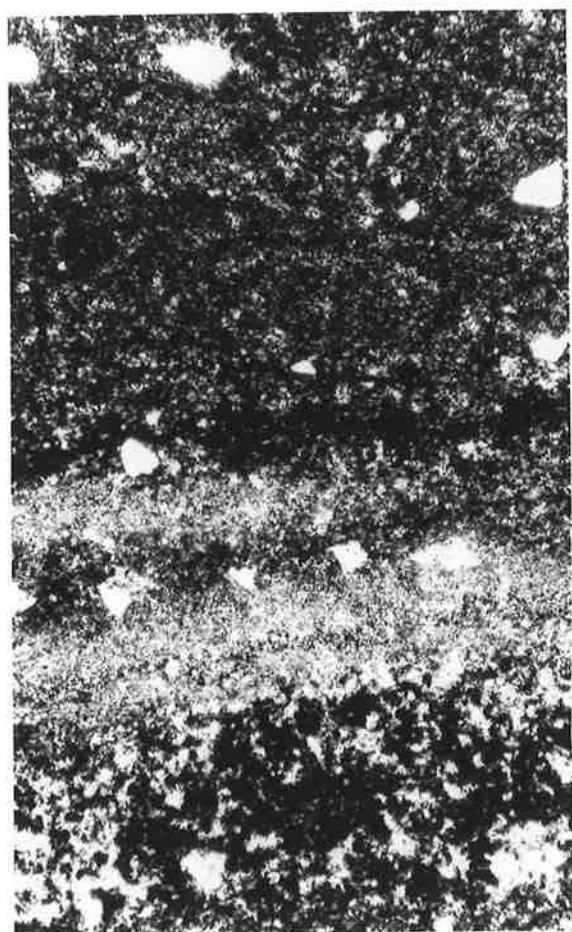
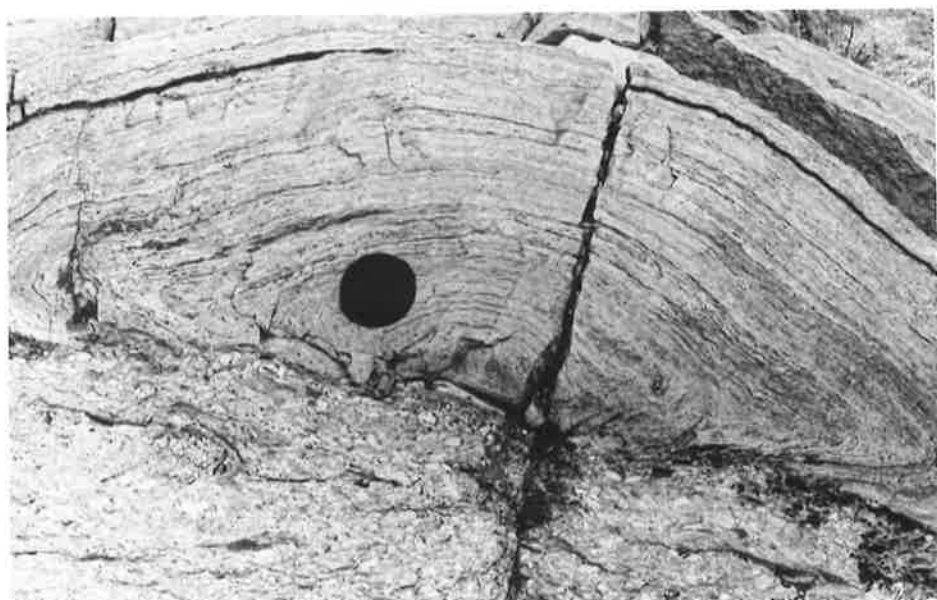


PLATE 6.10

- a. Irregular and rounded clasts of micrite and fine spar, enclosed in a matrix of microspar which may be a dolomite silt. Specimen from a dolomite breccia overlying a massive dolomite, Yadlamalka Formation, Yednalue (YD). Field of view is 8.5 mm in width.
- b. Brecciated dolomite mudstone, with irregular fragments enclosed in an acicular rim cement and blocky spar. Specimen is a massive dolomite from the Yadlamalka Formation, Yednalue. Field of view is 3.2 mm in width.
- c. Very irregular fragments of micrite produced by brecciation of a dolomite mudstone, fragments enclosed in a rim cement and blocky spar. Some micrite fragments partially recrystallised to fine spar (at right). Specimen is a massive dolomite from the Yadlamalka Formation, Yednalue. Field of view is 3.2 mm in width.

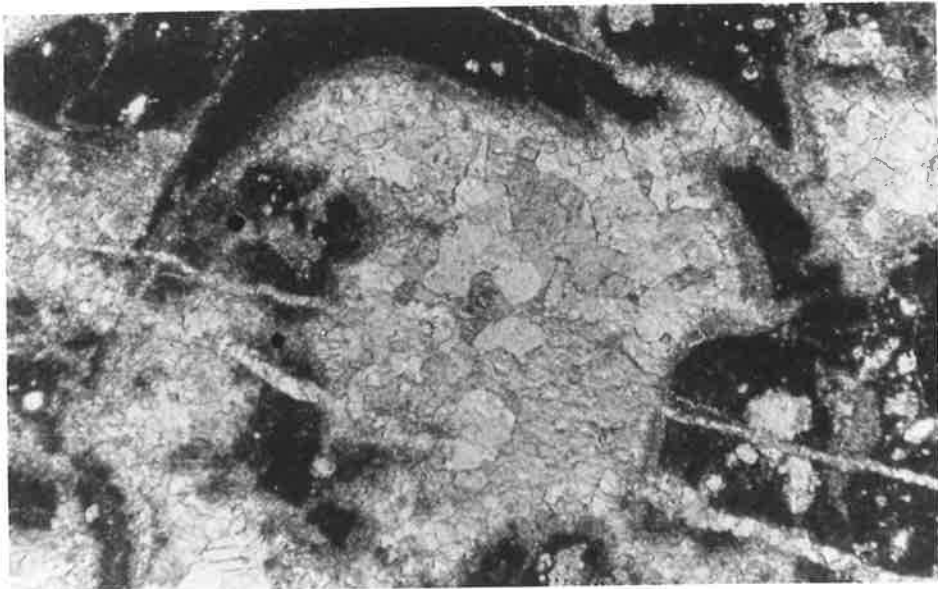
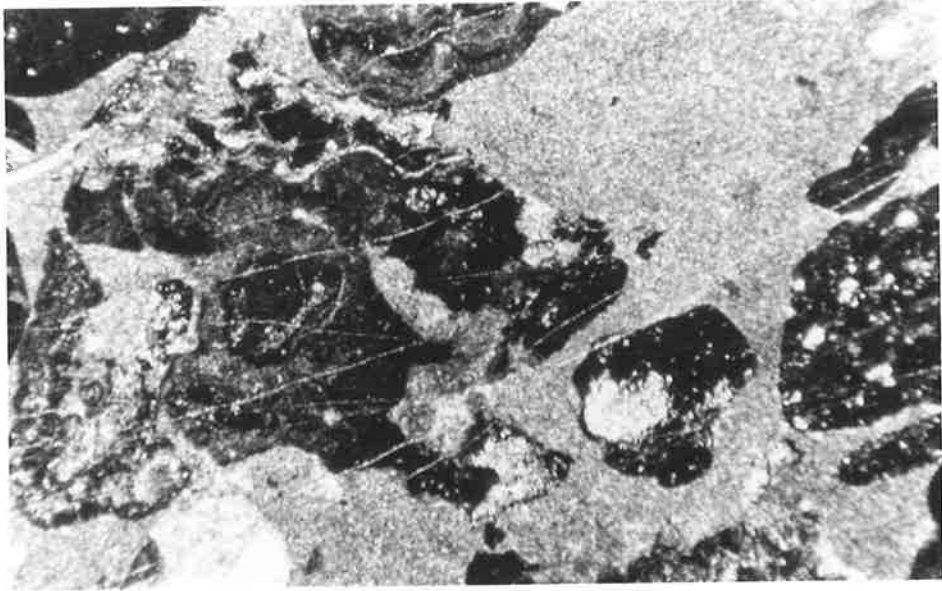


PLATE 6.11

- a. Massive dolomite with a more peloidal texture and large coated grain on a fragment of micrite. Peloids enclosed in clear spar. Specimen from the Yadlamalka Formation, Yednalue (YD). Field of view is 8.5 mm in width.

- b. Massive dolomite consisting of coated grains enclosed in a recrystallised rim cement and clear blocky spar (top right). Specimen from the Yadlamalka Formation, east limb of the Yednalue Anticline (YDA). Field of view is 2 mm in width.

- c. Massive dolomite with peloidal texture in which some peloids are partially recrystallised to microspar (at left). Peloids enclosed in rim cement and blocky spar (at left), but area at right is part of a larger pore infilled with microspar which may be a dolomite silt. Specimen from the Yadlamalka Formation, Yednalue (YD). Field of view is 3.2 mm in width.

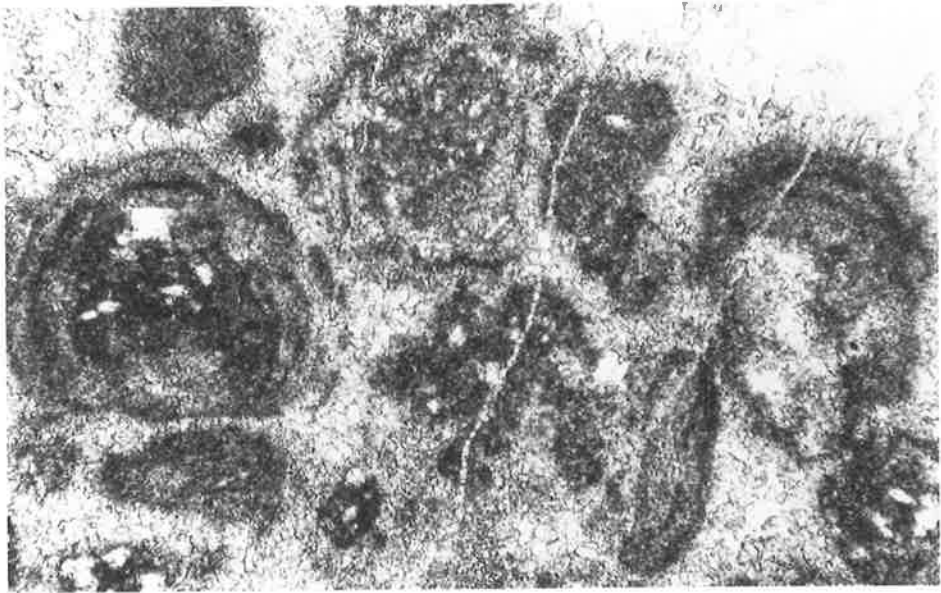
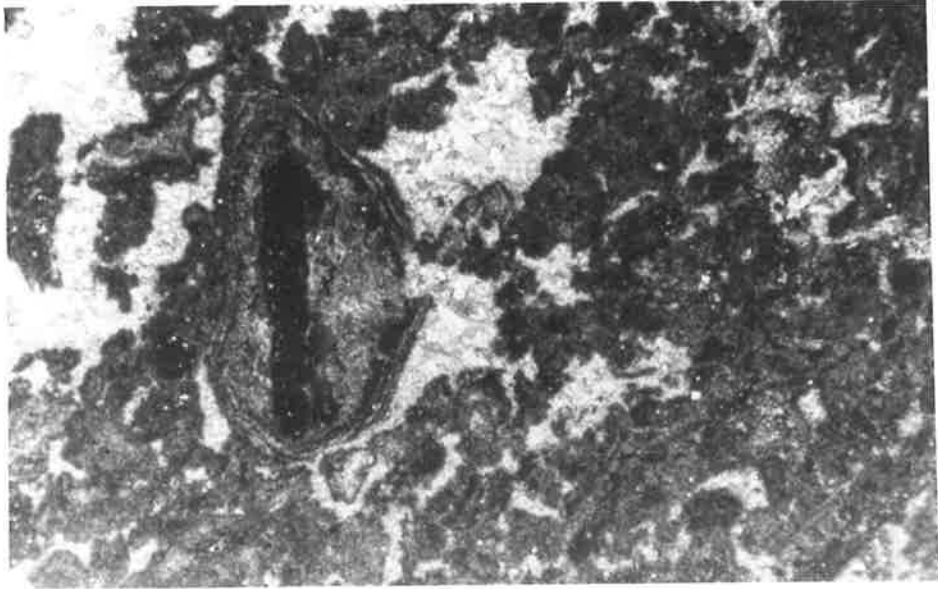
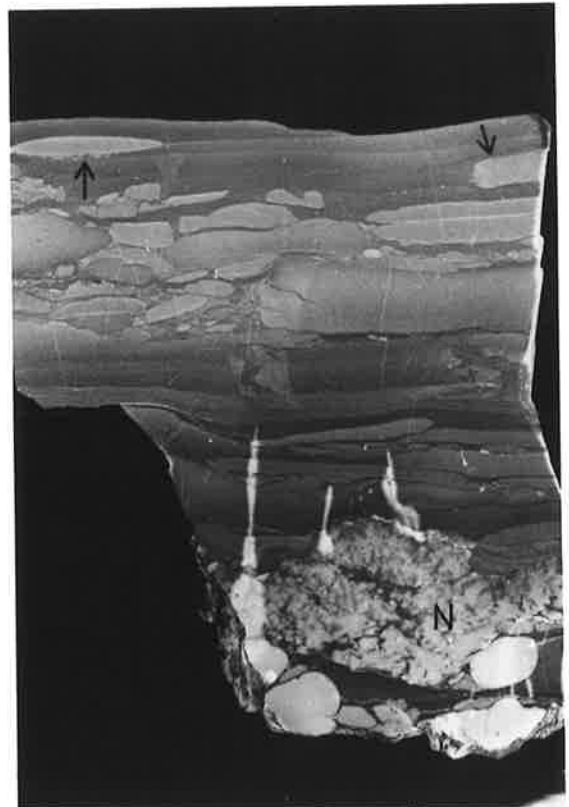


PLATE 6.12

- a. Interlaminated magnesite (light-grey) and dolomite (dark-grey) mudstone with tepees (attenuated by horizontal shortening during folding) which are disrupted in centre. Magnesite intraclasts deposited between tepees which are overlain by dolomite-cemented sandstone. Montacute Dolomite, near Torrens Gorge (TG). Hammer handle at left is 15 cm in length.

- b. (at left) Laminated and thinly bedded magnesite mudstone with horizons of small tepees, and thin intraclastic lenses (I), Yadlamalka Formation, Arkaroola (A). Outcrop is about 25 cm in height.

- c. (at right) Desiccated and eroded magnesite mudstone partly replaced by white, irregular nodular magnesite (N) near base. Rounded white intraclasts at base are the top of an underlying bed of intraclastic magnesite. Lighter grey beds within magnesite mudstone (from which elongate intraclasts derived), appear to have formed by localized cementation of mudstone (see zones arrowed near top of sample). Specimen from the Yadlamalka Formation, Copley (CP). Scale in cm.



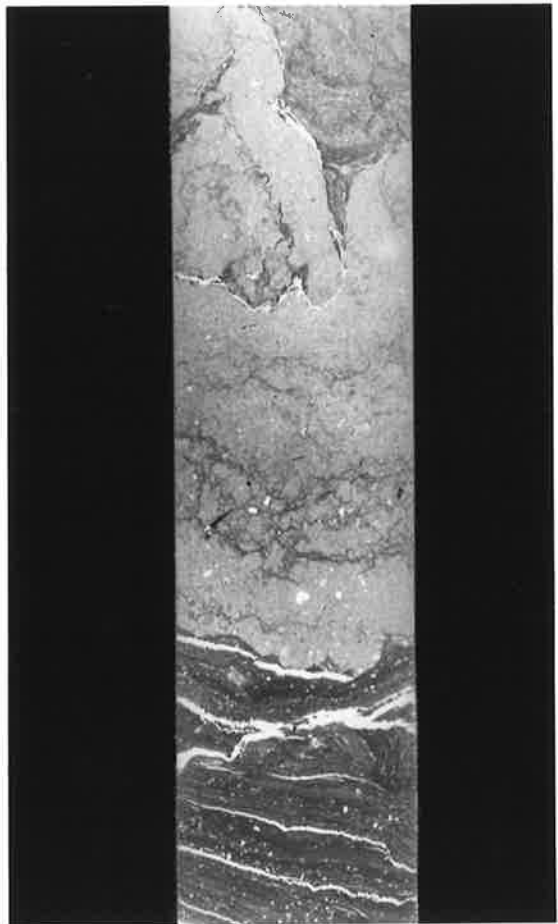
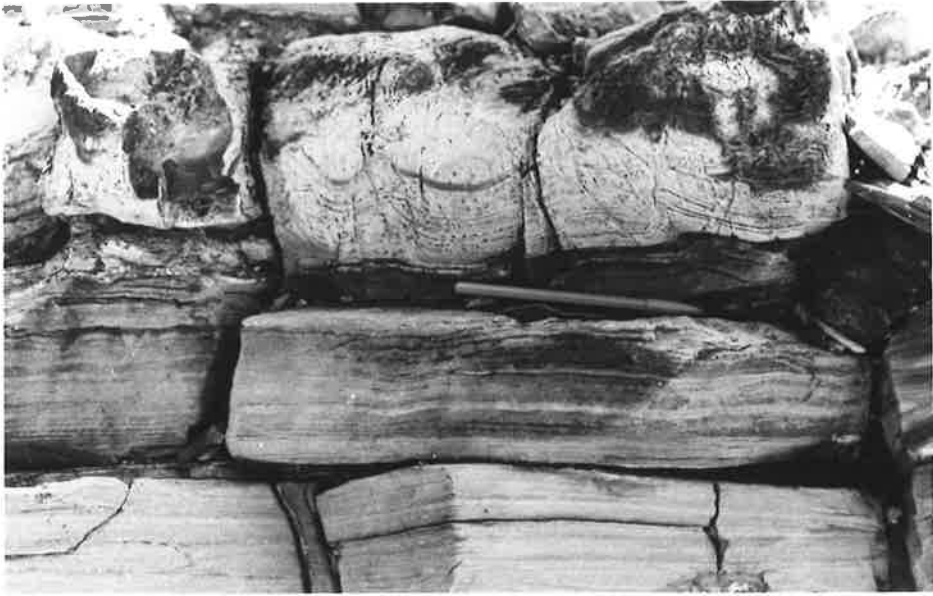
60 70 80 90 100 110 120 130 140 150

PLATE 6.13

- a. Magnesite mudstone (cream coloured outcrop surface) with wavy lamination and possibly small tepees, overlying well laminated dolomite mudstone (grey) with a sharp boundary, Yadlamalka Formation, Copley (CP). Pen is 15 cm in length.

- b. (at left) Nodular magnesite with botryoidal cream coloured nodules. Some elongate intraclasts at centre left. Yadlamalka Formation, Copley (CP). Pen is 15 cm in length.

- c. (at right) Wavy laminated magnesite mudstone (at base of sample) replaced by paler nodular magnesite with thin dark stringers of the host magnesite mudstone. The shape of the nodular magnesite resembles that of nodular anhydrite. White veins at base are talc. Specimen is from the Yadlamalka Formation at Copley (CP) and is 5 cm in length.



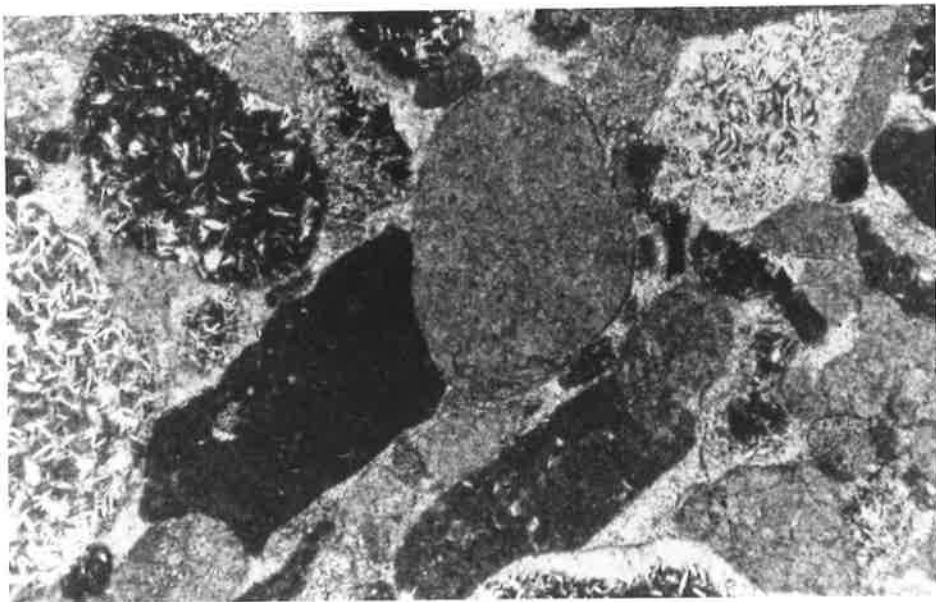
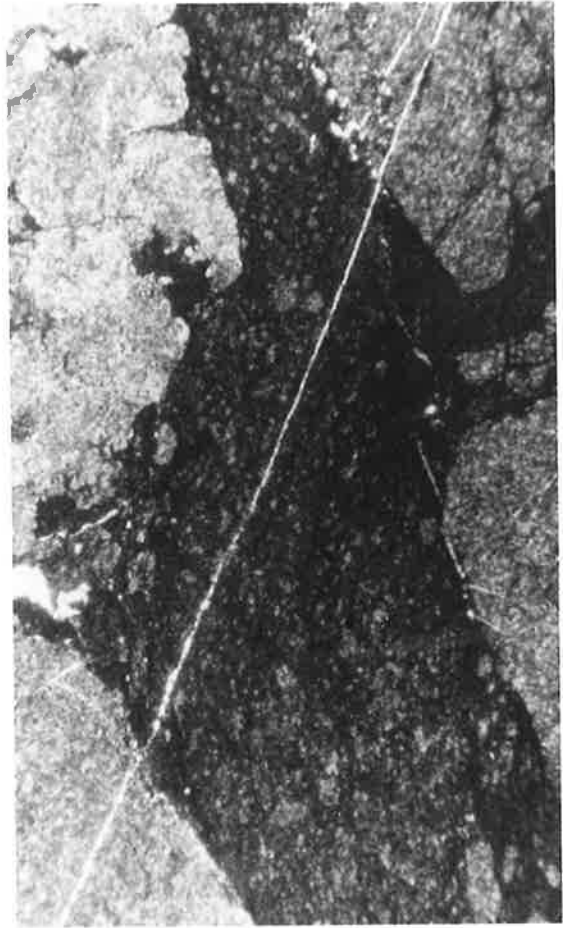
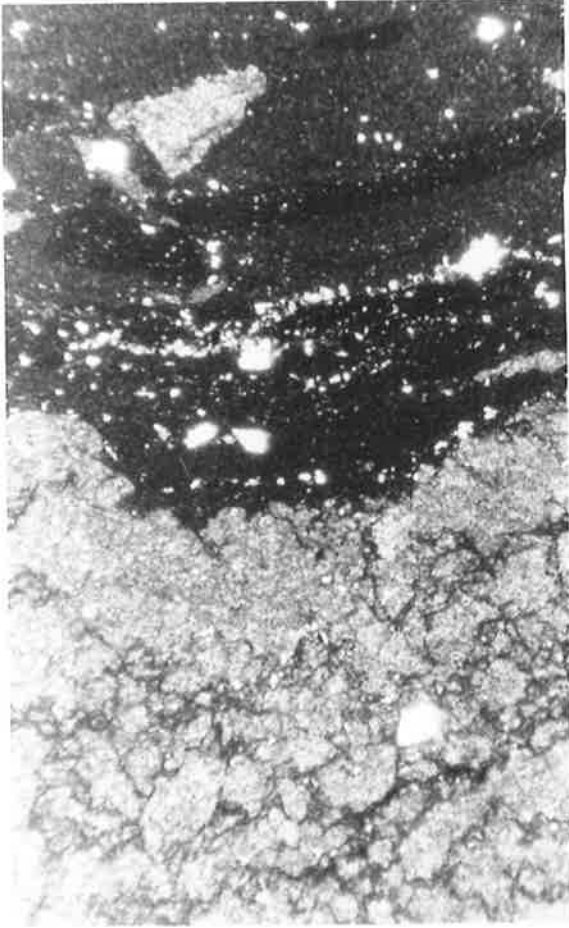


PLATE 6.15

- a. Laminated and thinly bedded magnesite mudstone with small tepees overlain by intraclastic magnesite. This has a bimodal distribution with larger elongate clasts (several cms) which are slightly imbricated, and smaller clasts (less than 1 cm). Yadlamalka Formation, Arkaroola (A). Lens cap is 5.5 cm in diameter.

- b. (at left) Bedded intraclastic magnesite, lower bed has a bimodal distribution of close packed clasts. The larger clasts are elongate, curved, and up to 15 cm in length, the smaller are granule sized. Upper beds contain granule sized intraclasts. Yadlamalka Formation, Copley (CP). Pen is 15 cm in length.

- c. (at right) Intraclastic magnesite with close packed granule sized intraclasts, overlying grey dolomite mudstone at base, and with thin interbeds of dolomite mudstone, and large dolomite intraclast near base. Elongate chert lenses (C) are present in the intraclastic magnesite. Yadlamalka Formation, Depot Creek (DC). Lens cap is 5.5 cm in diameter.

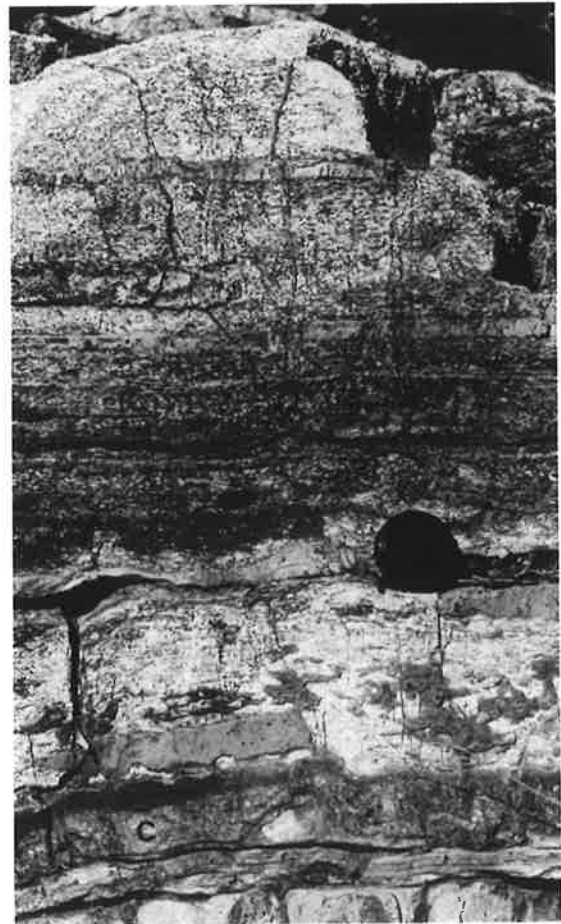
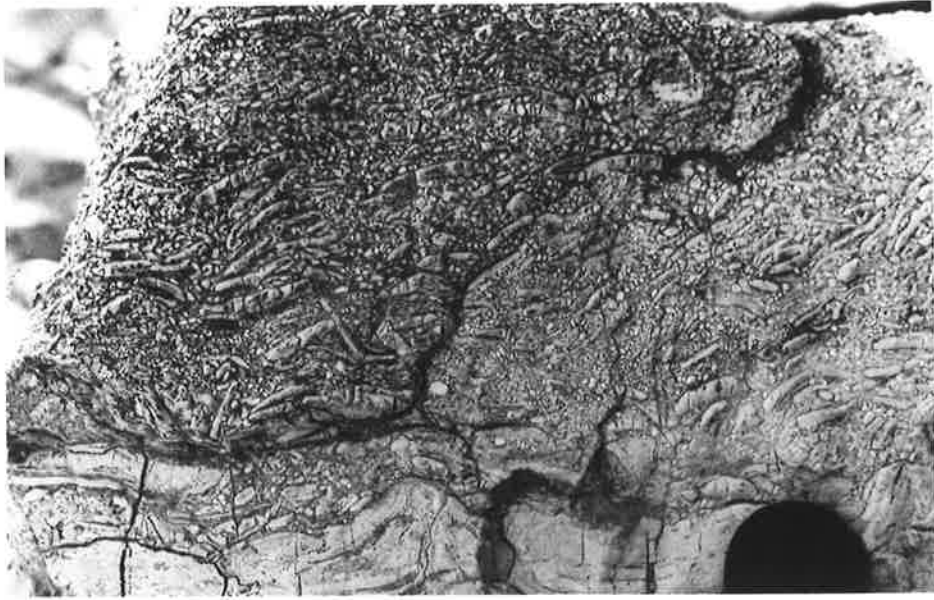


PLATE 6.16

- a. Bedded intraclastic magnesite with variable clast size and content of sandy matrix between adjacent beds, some of which have an open framework. Intraclasts are elongate, while others are more irregular and equidimensional (in bed to left of hammer). Yadlamalka Formation, Depot Creek (DC). Hammer is 33 cm in length, up is to left.

- b. Ripple cross laminated intraclastic magnesite with granule sized intraclasts, Yadlamalka Formation, West Rischbieth (WR). Pen is 14 cm in length.

- c. Inverse graded intraclastic magnesite with very close packed intraclasts at the base, and a greater amount of sandy matrix associated with the coarser intraclasts at the top. Some intraclasts have an irregular shape. Yadlamalka Formation, Depot Creek (DC). Pen is 14 cm in length.



PLATE 6.17

- a. Outcrop of thinly bedded dolomitic sandstone with differential weathering of the more dolomitic interbeds. Symmetrical ripple marks on bedding plane in centre. Yadlamalka Formation, Beetaloo (B).

- b. Sandstone with flat bedding and shallow trough cross-beds with laminae tangential to the lower bounding surface. Yadlamalka Formation, Port Germein Gorge (PG). Lens cap is 5.5 cm in diameter.

- c. Flat and ripple cross-laminated fine-grained sandstone with a coarser grained bed near the base. Cross-lamination at top has symmetrical, rounded ripple profiles with off-shoots, indicating a wave-formed origin, while that in the centre is more asymmetrical. Yadlamalka Formation, Yednalue (YD). Pen is 14 cm in length.

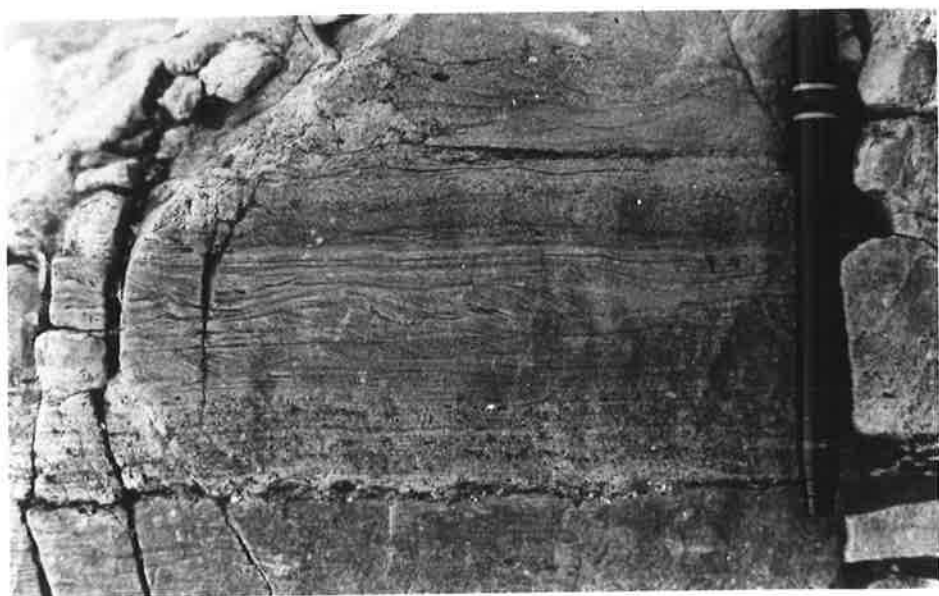


PLATE 6.18

- a. Medium-grained dolomitic sandstone with quartz and feldspar grains enclosed in a dolomitic cement which is replacing the margins of grains. Specimen from the Yadlamalka Formation, Depot Creek (DC). Field of view is 2 mm in width (crossed polars).

- b. Very fine-grained sandstone with scattered peloids of dolomite micrite, enclosed in dolomite cement. Because of the presence of partial quartz overgrowths and replacement of grains on margins by dolomite, the boundaries of the original detrital grains are largely obscured. Specimen from the Yadlamalka Formation, Nudlamutana Hut (NH). Field of view is 0.8 mm in width (plane light).

- c. Flat and low angle lamination in a very fine-grained dolomitic sandstone, eroded by ripple cross lamination which consists of interwoven, erosionally based, scoop-shaped sets, probably formed by wave action. Yadlamalka Formation, West Rischbieth (WR).

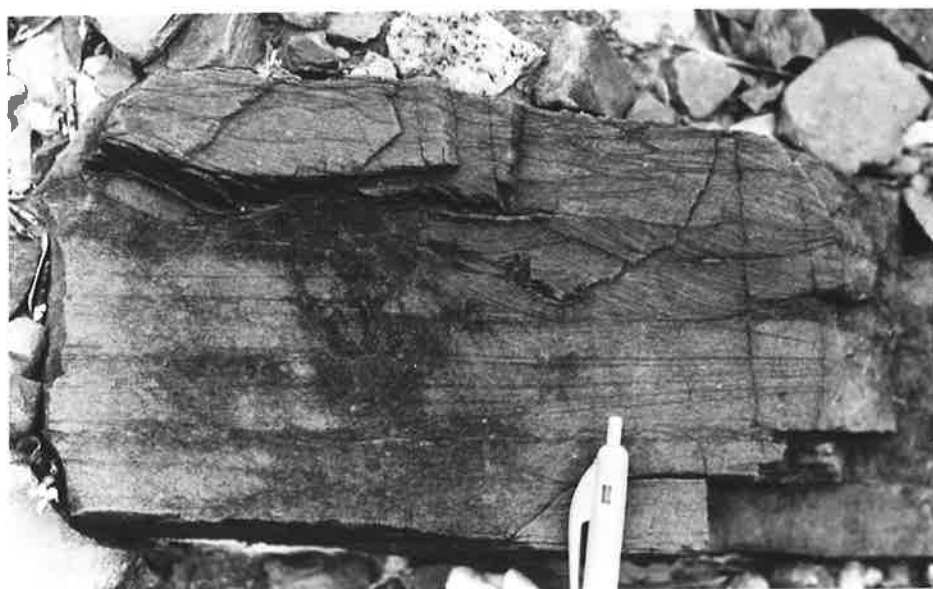
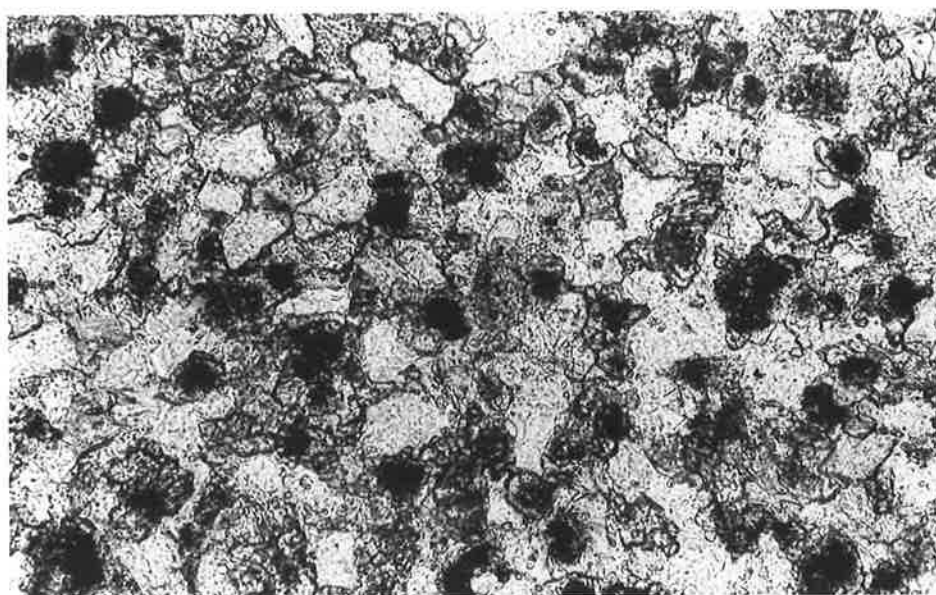
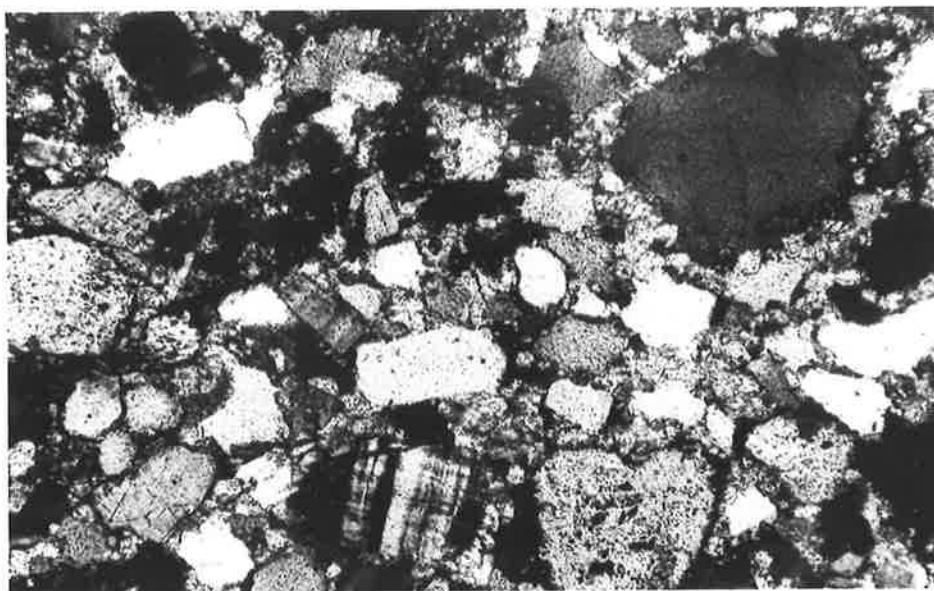




PLATE 9.1

- a. (at left) Dolomite mudstone containing alternating laminae of fine and coarse microspar, the coarser laminae contain scattered quartz silt. Specimen is from the Yadlamalka Formation, Yednalue (YD). Field of view is 2 mm in height.
- b. (at right) Dolomite mudstone overlain by peloidal dolomite with micritic, carbonaceous stained peloids some of which have sharp boundaries, and scattered quartz silt grains, grading up into a less distinct peloidal texture. Specimen is from the Mirra Formation, Mt. Norwest H.S. (NW). Field of view is 2 mm in height.
- c. Wavy laminated magnesite mudstone. The grain size is micritic, with little grain size variation between adjacent laminae. White grains are authigenic albite. Specimen from the Yadlamalka Formation, Copley (CP). Field of view is 2 mm in width.

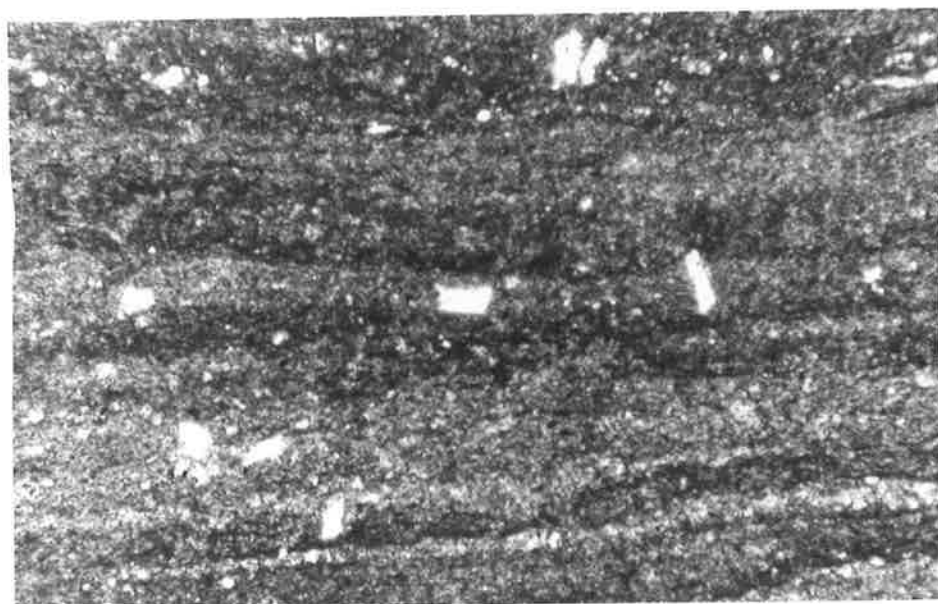
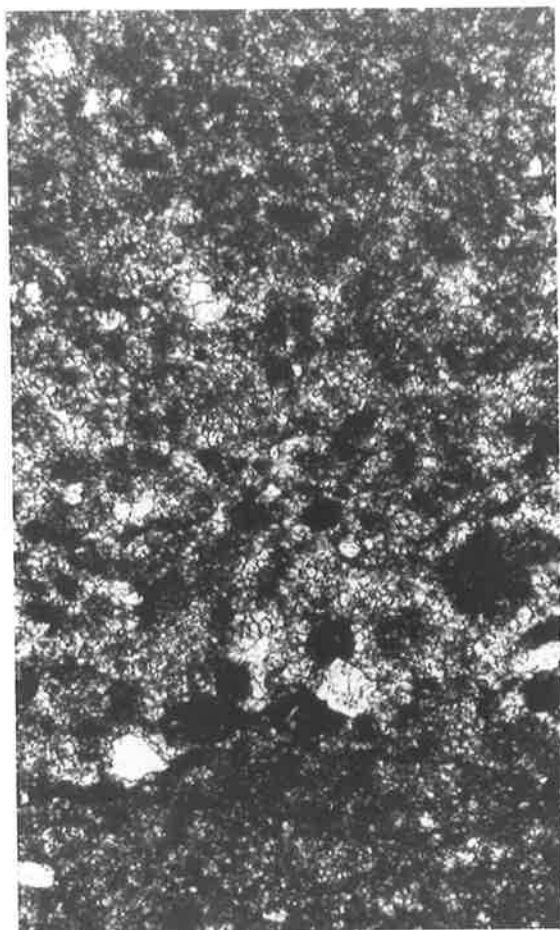
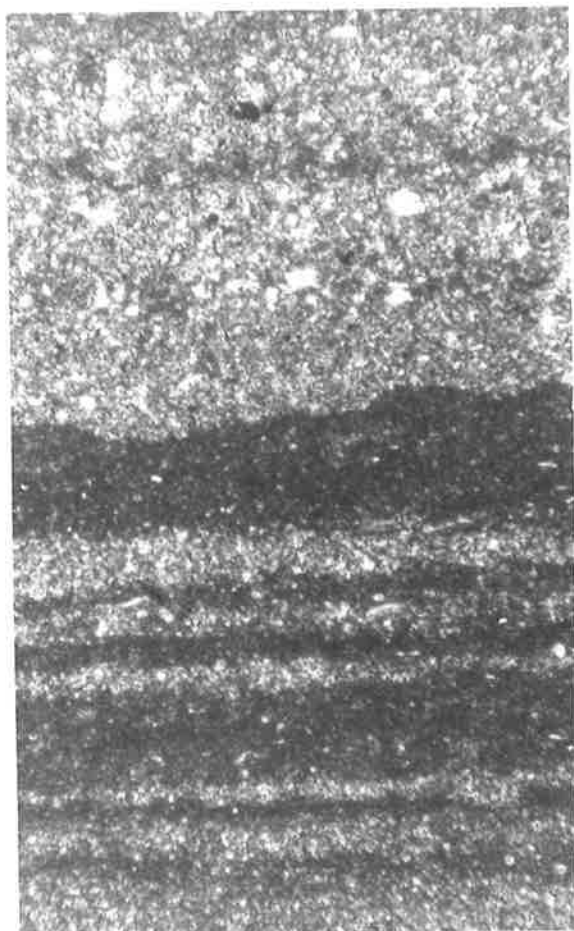


PLATE 9.2 (SEM PHOTOGRAPHS)

- a. (at left) Fracture surface of dolomicrospar with irregular dolomite grains and small clay flakes (arrowed). Specimen is from the Nathaltee Formation, Port Germein Gorge (PG).
- b. (at right) Dolomicrospar (surface of sample polished, and etched in HCl) of interlocking grains with straight and curved grain boundaries and flaky clay mineral at top right. Specimen is from the Nathaltee Formation, Yednalue Anticline (YDA).
- c. (at left) Fracture surface of fine dolomicrospar with a compact mosaic of anhedral, polyhedral grains with straight and slightly curved grain boundaries. Specimen is from the Yadlamalka Formation, Copley (CP).
- d. (at right) Fracture surface of fine dolomicrospar with a compact mosaic of anhedral, polyhedral grains many of which have straight grain boundaries. Specimen is from the Nathaltee Formation, Yednalue Anticline (YDA).
- e. (at left) Fracture surface of coarse dolomicrospar with more irregular grains than c. and d. Grains are anhedral, equant to subequant with some fracturing across grains. Specimen is from the Nathaltee Formation, Depot Creek (DC).
- f. (at right) Fracture surface of coarse dolomicrospar, with some fracturing across grains, sometimes along cleavage planes. Specimen is from the Nathaltee Formation, Depot Creek (DC).

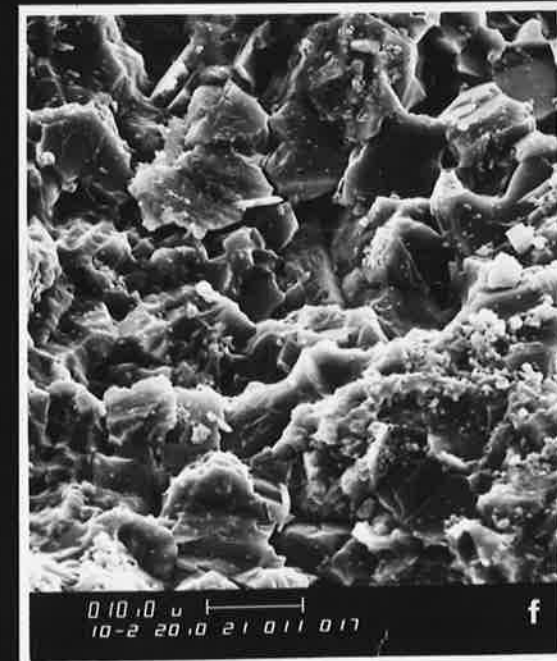
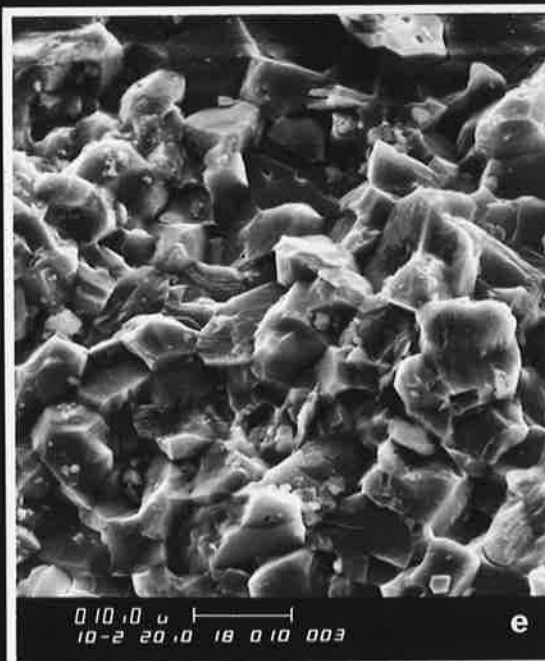
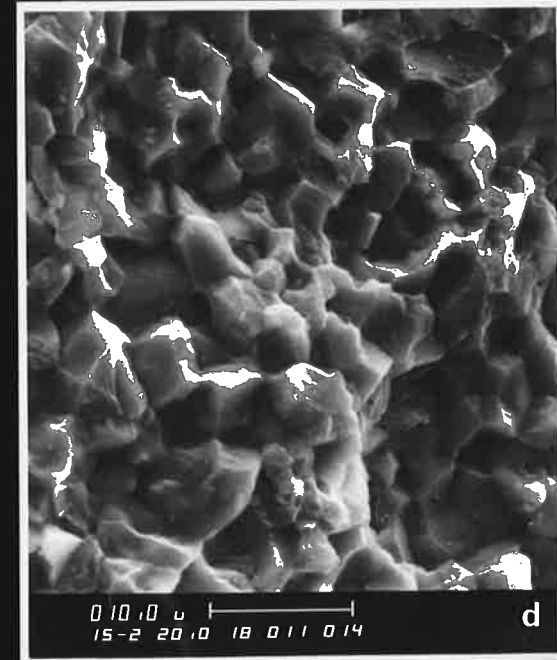
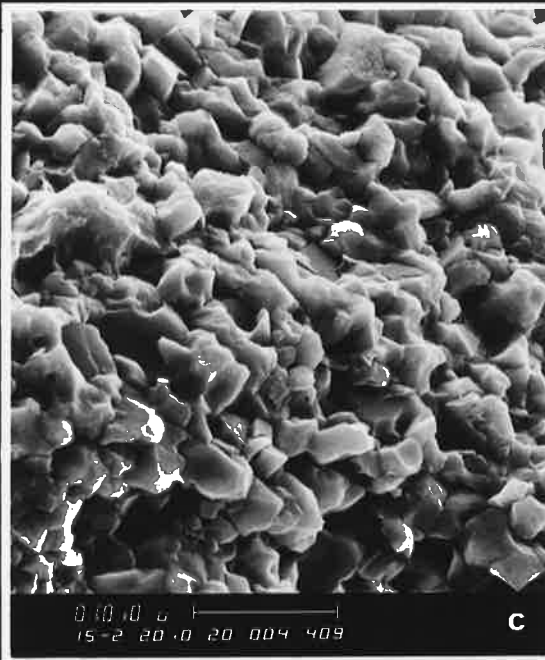
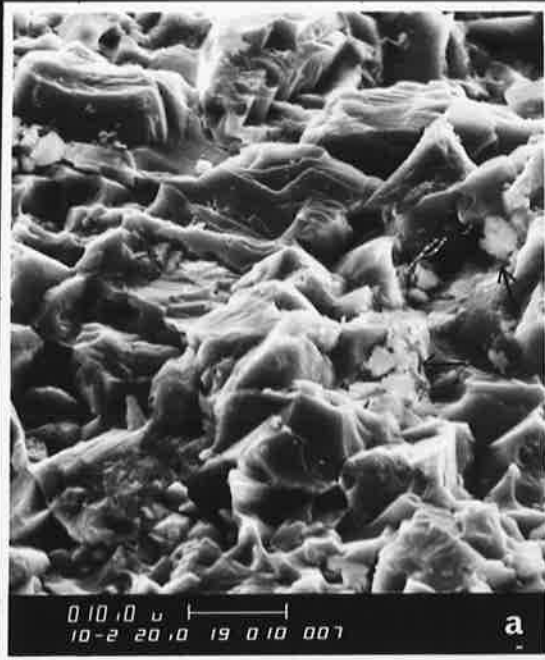


PLATE 9.3 (SEM PHOTOGRAPHS)

- a. (at left) Fracture surface of magnesite mudstone in which the grain size distribution appears bimodal. The finer component is micritic with small rhombs and more anhedral grains, the coarser is a microspar of largely anhedral grains. Specimen is from the Yadlamalka Formation, Copley (CP).
- b. (at right) Fracture surface of magnesite mudstone with a compact mosaic of well-sorted polyhedral grains (coarse micrite) with planar and gently curved faces, similar to dolomicrospars in Plate 9.2c and d. Specimen from the Yadlamalka Formation, Copley (CP).
- c. (at left) Fracture surface of magnesite mudstone consisting of a slightly porous mosaic of fine micrite. Many grains are platy rhombs. Specimen from the Yadlamalka Formation, Copley (CP).
- d. (at right) Fracture surface of nodular magnesite with micritic, well sorted grains which are anhedral to rhombic in shape. Specimen from the Yadlamalka Formation, Depot Creek (DC).
- e. (at left) Polished and acid etched surface of nodular magnesite, with areas of aligned elongate grains, with a variable elongation direction. Some grains have step-like, rhombic boundaries. Specimen from the Yadlamalka Formation, Depot Creek (DC).
- f. (at right) Polished and acid etched surface of nodular magnesite with a texture similar to e. Same specimen as e.

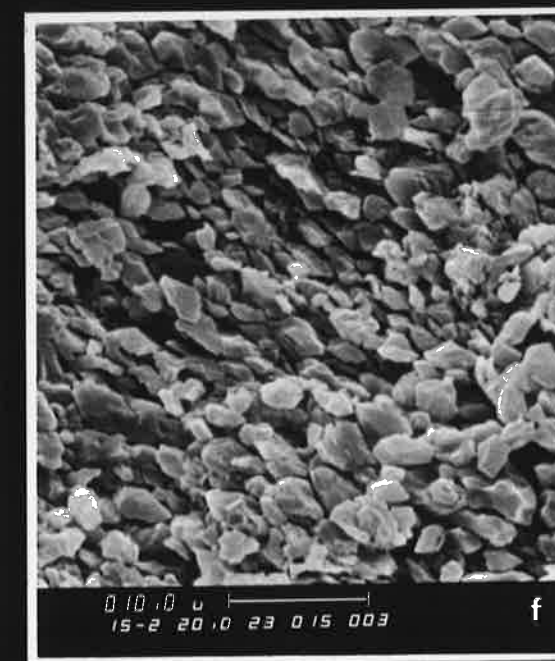
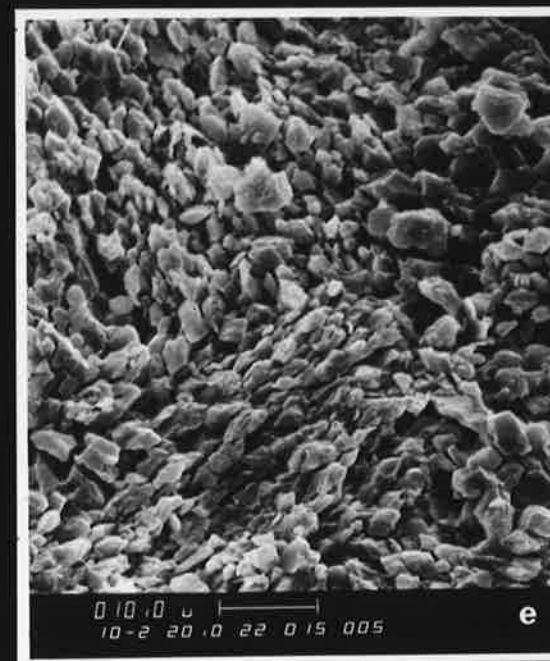
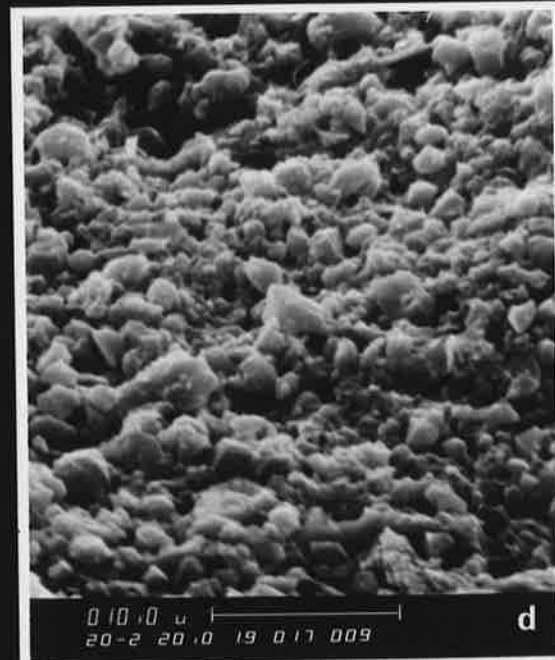
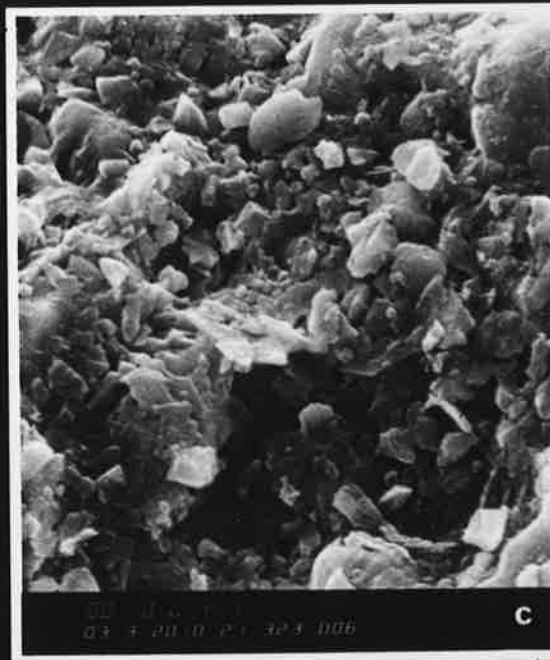
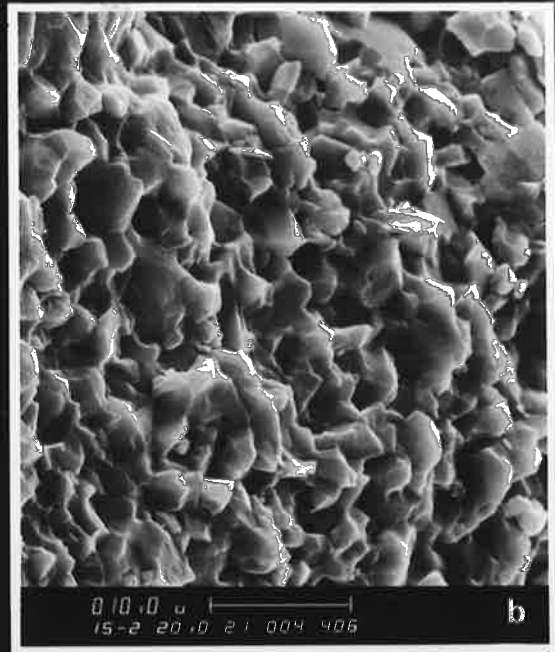
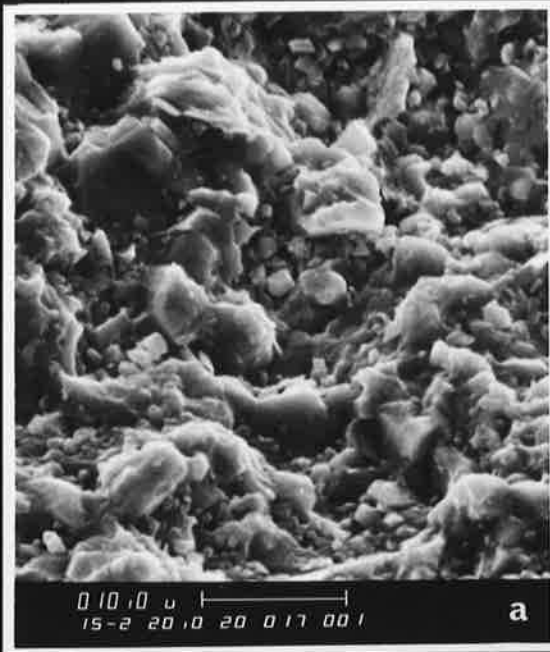


PLATE 11.1

- a. Irregular black chert nodules in massive dark-grey dolomite mudstone enclosed in more fissile, thinly bedded dolomite mudstone. The dolomite has been distorted around the chert nodules (at left). Yadlamalka Formation, Depot Creek (DC). Hammer is 35 cm in length.

- b. Laminated and thinly bedded dolomite mudstone in which lamination has been distorted around the black chert nodules (centre), Yadlamalka Formation, Depot Creek (DC). Pen is 14 cm in length.

- c. Dolomite mudstone in which black chert is located along the bedding plane and within a polygonal network (? desiccation cracks), Yadlamalka Formation, Depot Creek (DC). Lens cap is 5.5 cm in diameter.

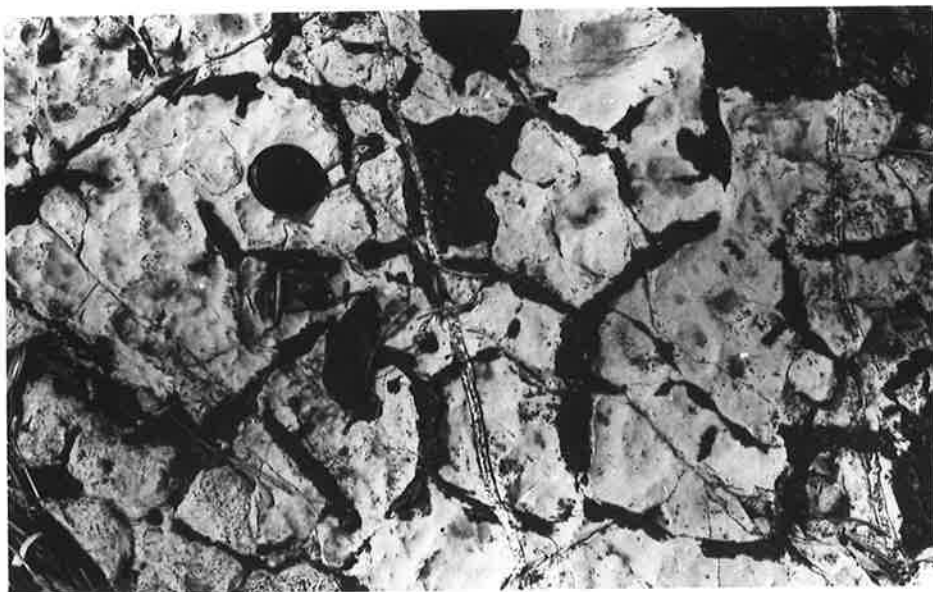
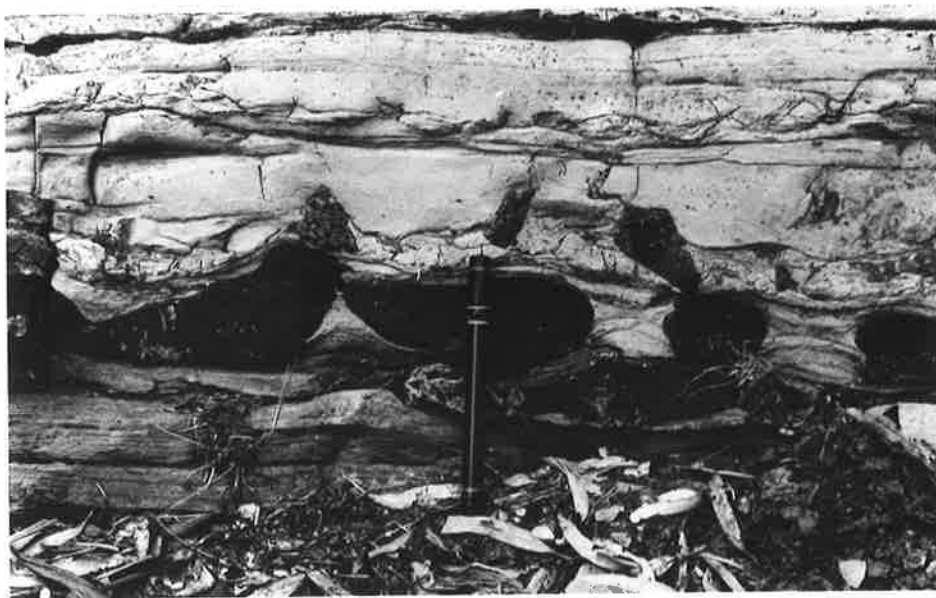


PLATE 11.2

- a. (at left) Bedding plane exposure of domal stromatolites with preferential replacement by black chert along some laminae, Yadlamalka Formation, Depot Creek (DC). Divisions on ruler represent 10 cm.
- b. (at right) Sandy intraclastic dolomite, in which intraclasts in the centre have been replaced by pale-coloured chert. Some intraclasts still have a rim of dolomite (e.g. those arrowed). Specimen is from the Nathaltee Formation, Depot Creek (DC). Scale in cm.
- c. Intraclastic magnesite completely replaced by chert, overlying grey dolomite mudstone, Yadlamalka Formation, Mundallio Creek (MC). Lens cap is 5.5 cm in diameter.

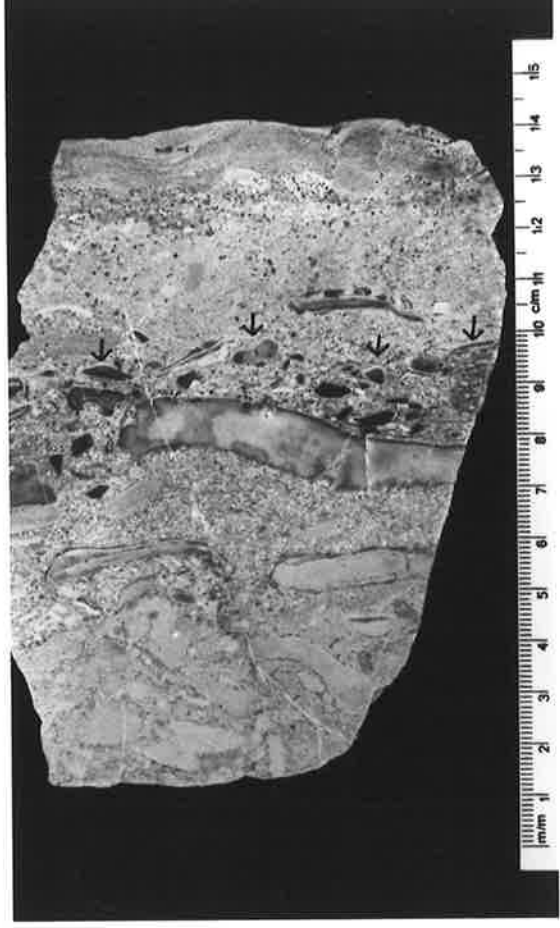


PLATE 11.3

- a. Silicified stromatolitic dolomite with microcrystalline granular quartz (a), and chalcedony with a granular texture and undulose extinction (b) or spherulitic and banded extinction (c). Specimen from the Yadlamalka Formation, Depot Creek (DC). Field of view is 2 mm in width, (crossed polars).
- b. Silicified oncoïd grainstone. Oncoïds replaced by microcrystalline granular quartz (a), and enclosed in a cement of fibrous chalcedony (b) now recrystallised with a slightly granular texture but with the extinction direction oriented perpendicular to oncoïd boundaries, and megaquartz (c). Vein at right (d) contains some fibrous chalcedony. Specimen from the Yadlamalka Formation, Top Mount Bore (TM). Field of view is 2 mm in width (crossed polars).
- c. Silicified dolomite mudstone which has been brecciated and cemented by granular chalcedony and megaquartz. Clasts are replaced by microcrystalline granular quartz, lighter coloured clasts contain more relic dolomite than darker clasts. Sample from the Yadlamalka Formation, Nudlamutana Hut (NH). Field of view is 8.5 mm in width (crossed polars).

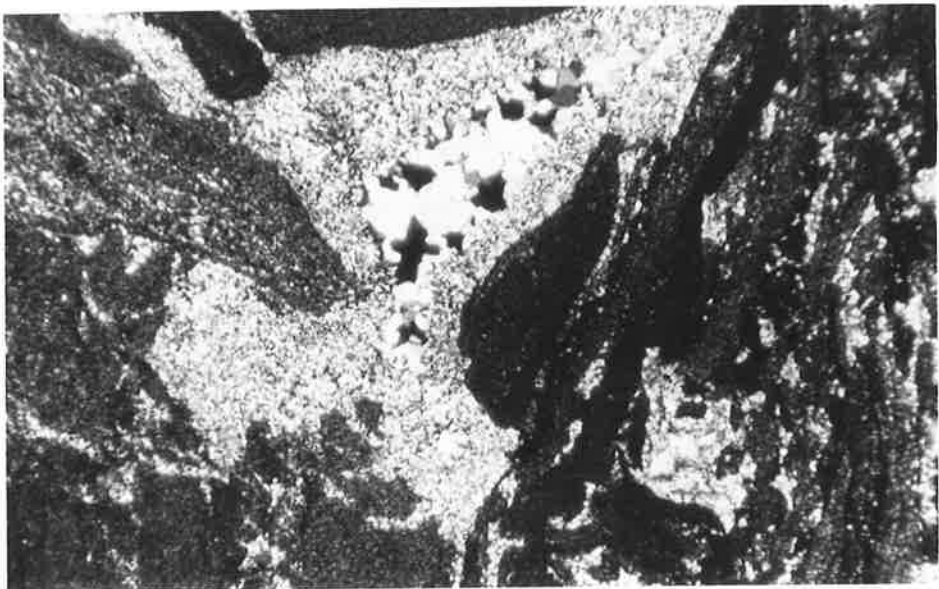
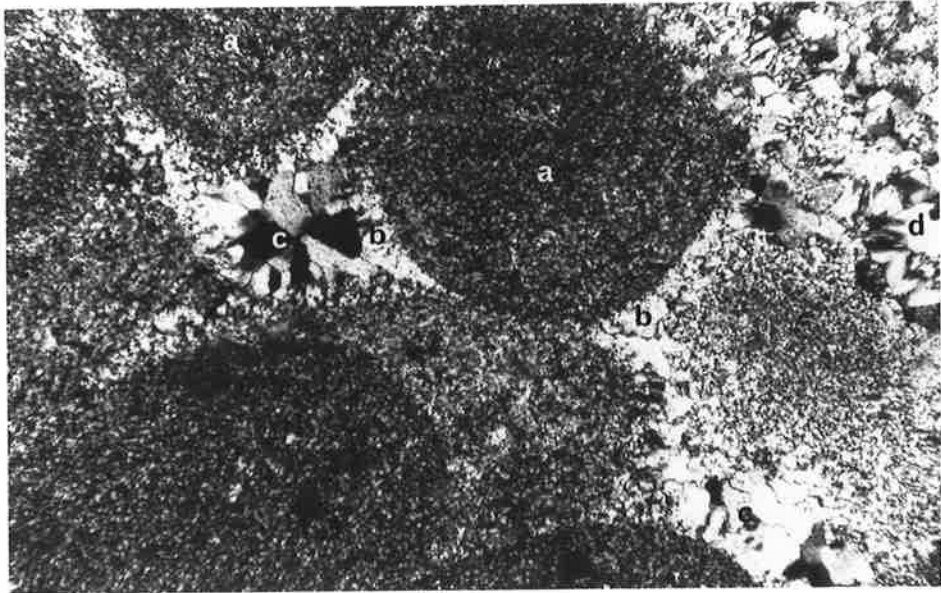
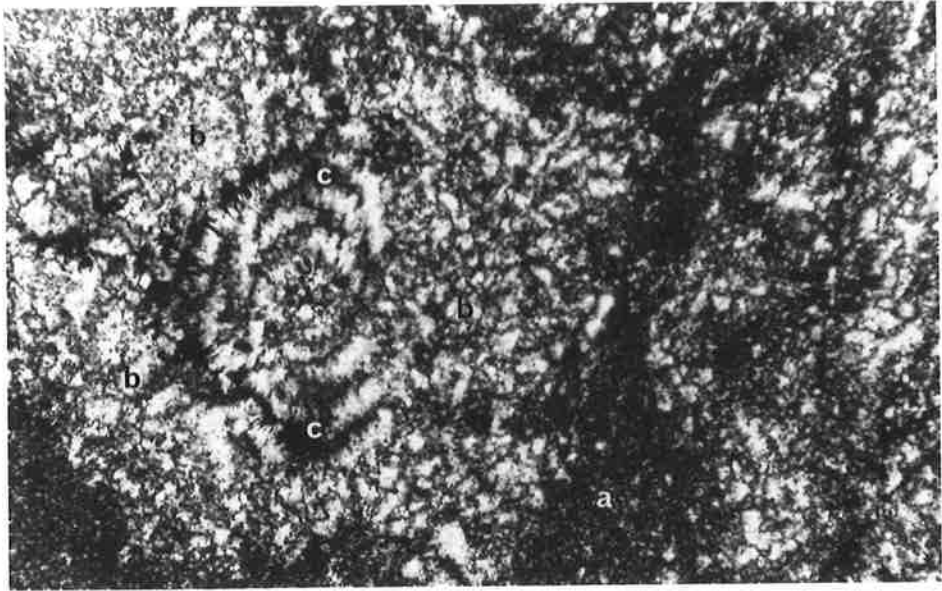


PLATE 11.4

- a. Silicified dolomite mudstone with disseminated fine carbonaceous material. Shrinkage has produced a system of polygonal cracks. The margins are partly coated with dark finely laminated material (e.g. at a), and cracks infilled with clear quartz. Specimen from the Yadlamalka Formation, Arkaroola (A). Field of view is 2 mm in width (plane light).
- b. (at left) Dolomite mudstone at base (lighter), overlain by a laminae replaced by microcrystalline granular quartz (dark) which grades up into unsilicified dolomite at top (light). Some wispy carbonaceous stringers have been preserved in silicified laminae. Specimen from the Yadlamalka Formation, Depot Creek (DC). Field of view is 3.2 mm in height (crossed polars).
- c. (at right) Partly silicified stromatolitic dolomite with wavy carbonaceous laminae in centre. Some silica has grown as spherulitic structures, outlined in carbonaceous laminae and by rims of fine dolomite grains. Specimen from the Yadlamalka Formation, Depot Creek (DC). Field of view is 2 mm in height (plane light).

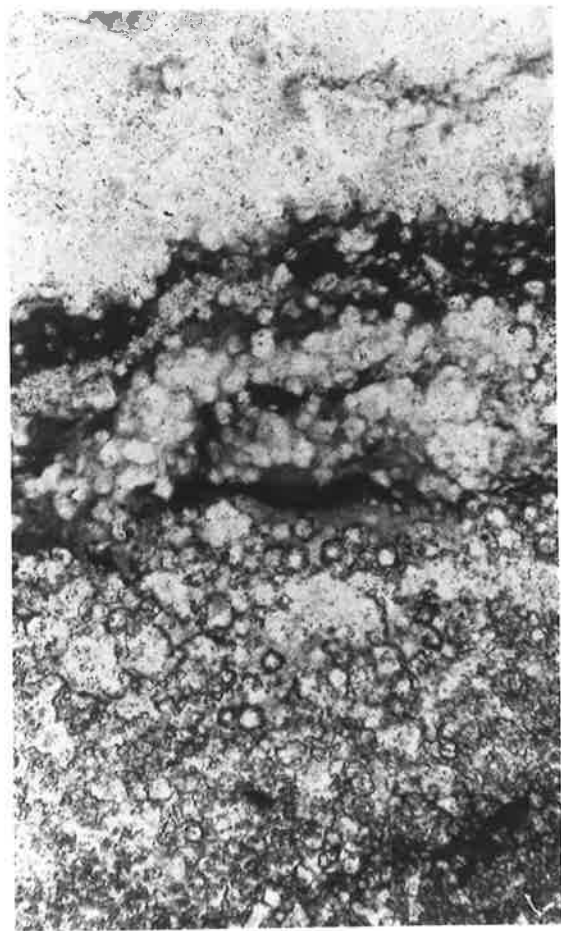
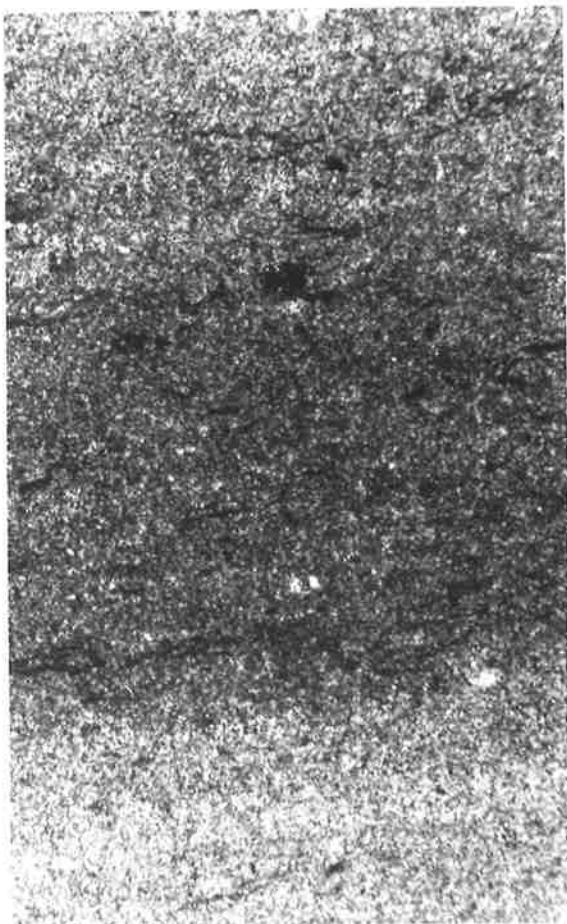
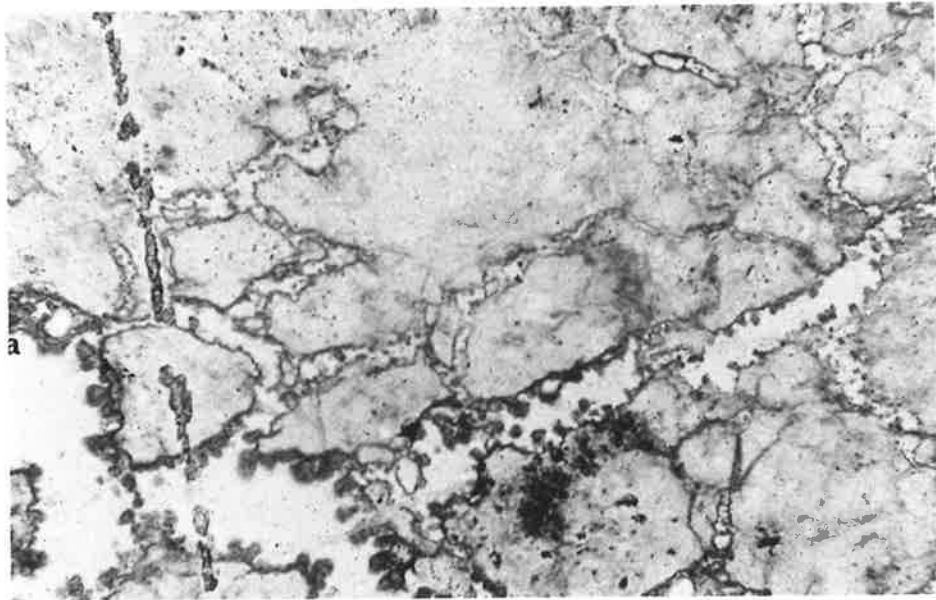


PLATE 11.5

- a. Silicified oncoids enclosed in partly silicified dolomite mudstone. Specimen is from the Yadlamalka Formation, Mundallio Creek (MC). Field of view is 2 mm in width (crossed polars).

- b. (at left) Silicified oncoid grainstone. At the base, oncoids are enclosed in a clear quartz cement, but at the top a cement is not present, and silicified oncoid coatings have been distorted during compaction. Specimen is from the Yadlamalka Formation, Yednalue (YD). Field of view is 2 mm in height (plane light).

- c. (at right) Silicified oncoid grainstone in which oncoid coatings appear isotropic due to the fine grain size of quartz and carbonaceous material. Dolomite intraclasts forming nuclei in some oncoids are only partly silicified. In the uncemented zone at the top, silicified oncoid coatings have been distorted during compaction, cement at base is chalcedony (granular). Specimen is from the Yadlamalka Formation, Depot Creek (DC). Field of view is 3.2 mm in height (crossed polars).

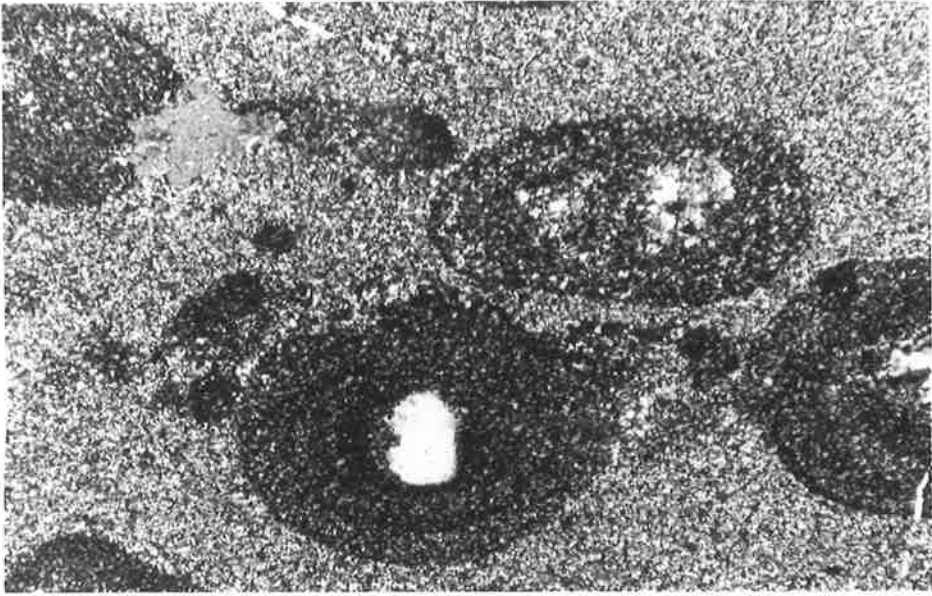


PLATE 11.6

- a. Silicified coated oncoïds. Oncoïd in centre has a magnesite intraclast as nucleus and contains radial shrinkage cracks with carbonaceous material concentrated along the margins of the cracks. Specimen is from the Yadlamalka Formation, Copley (CP). Field of view is 2 mm in width (plane light).

- b. Silicified massive oncoïds in which the silica has recrystallized to clear megaquartz. Microspherular structures outlined by carbonaceous material are preserved in oncoïd at top right. Rim of dolomite grains, some rhombic, has formed on margins of oncoïds after silicification. Specimen is from the Yadlamalka Formation, Depot Creek (DC). Field of view is 3.2 mm in width (plane light).

- c. Silicified oncoïd grainstone in which the large massive oncoïd contains abundant shrinkage cracks infilled by clear quartz. Specimen is from the Yadlamalka Formation, Depot Creek (DC). Field of view is 3.2 mm in width (plane light).

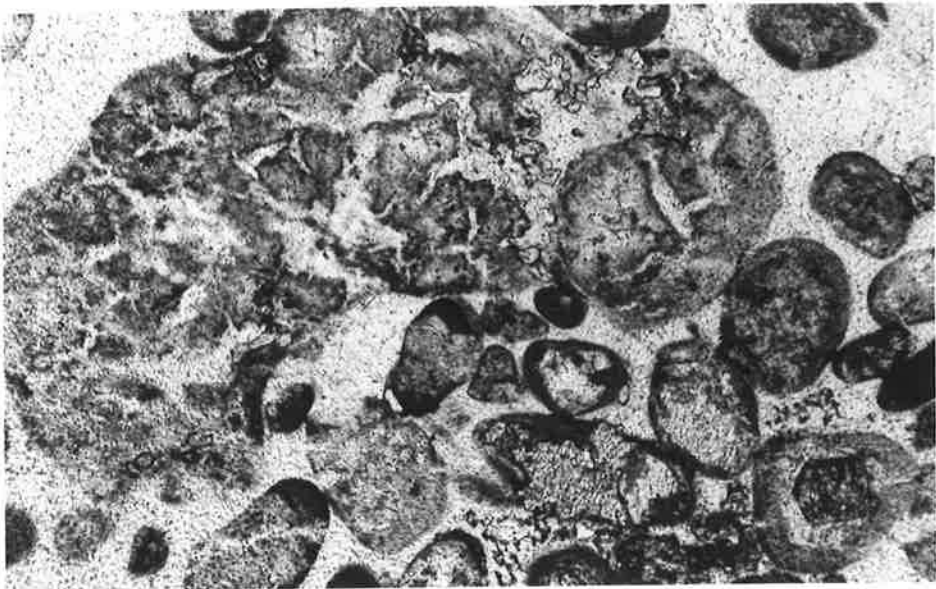
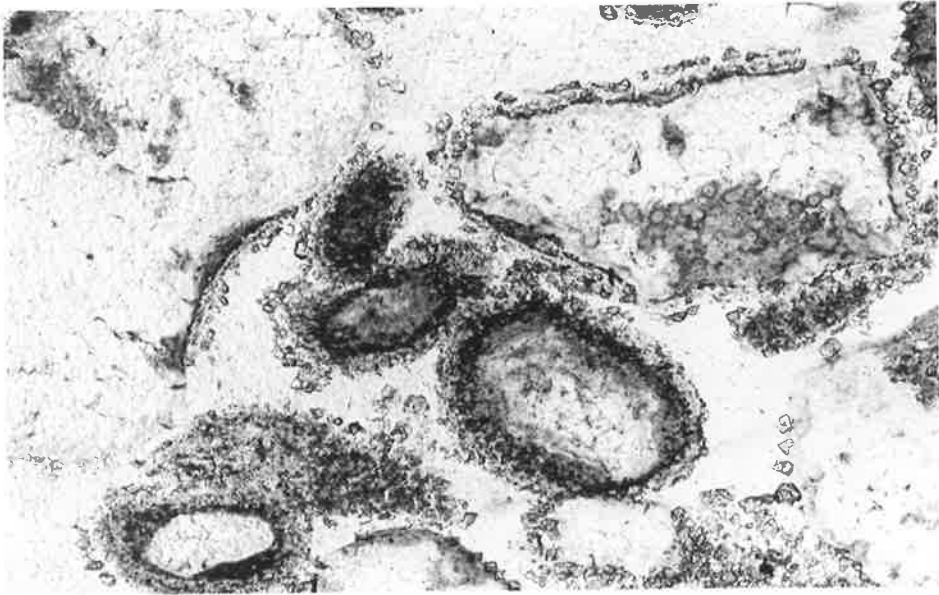
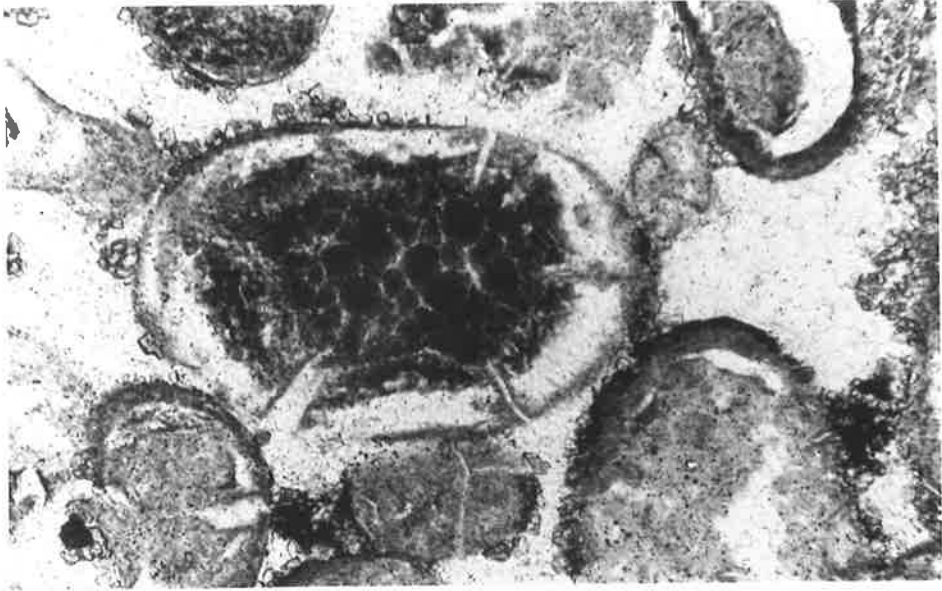


PLATE 11.7

- a. Silicified intraclastic magnesite, with spherular structures at right and left outlined by remnant micritic magnesite. Specimen from the Yadlamalka Formation, Depot Creek (DC). Field of view is 2 mm in width (plane light).

- b. Same area as above with crossed polars, illustrating aggregates of chalcedony spherulites in intraclasts at right and left. Intraclast at centre top replaced by microcrystalline granular quartz.

- c. Silicified intraclastic magnesite in which the intraclastic texture is no longer apparent. Quartz consists of fine and coarse megaquartz, the latter is cloudy at right due to remnant micritic magnesite inclusions. Specimen from the Yadlamalka Formation, Mundallio Creek (MC). Field of view is 3.2 mm in width (crossed polars).

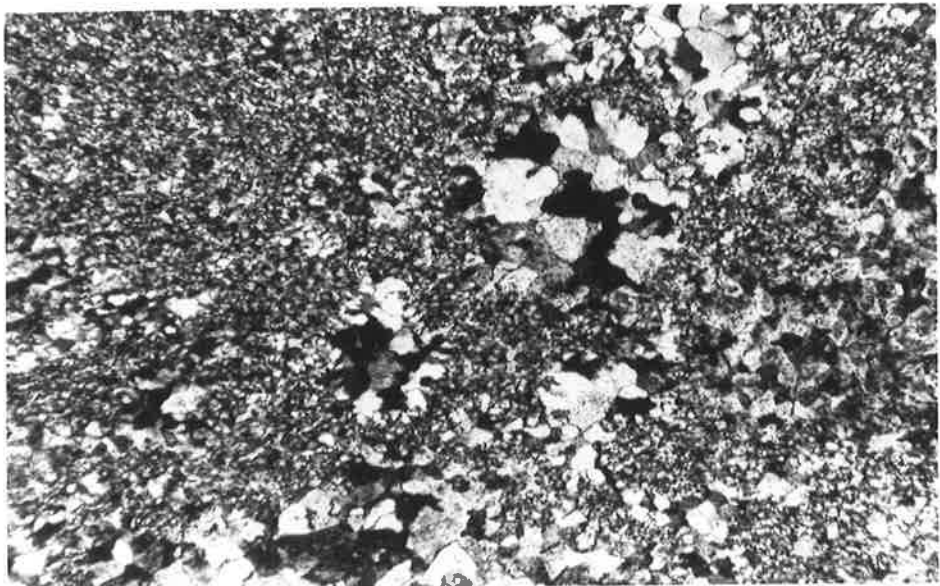
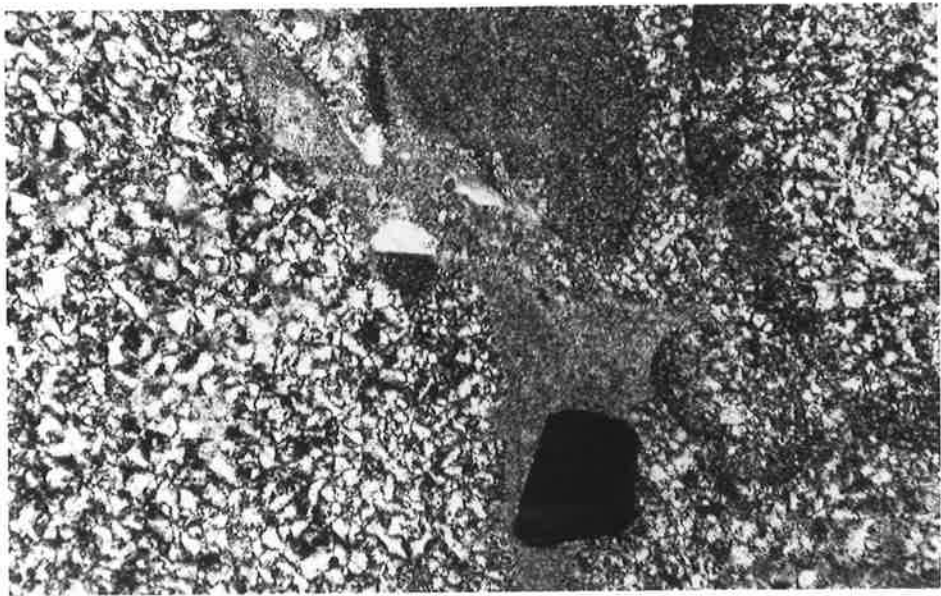
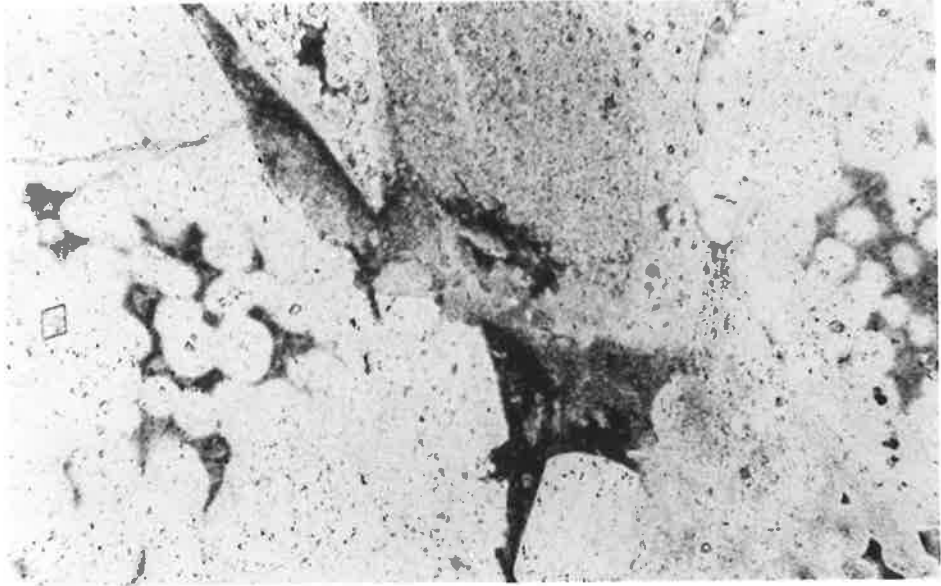


PLATE 11.8 (SEM PHOTOGRAPHS)

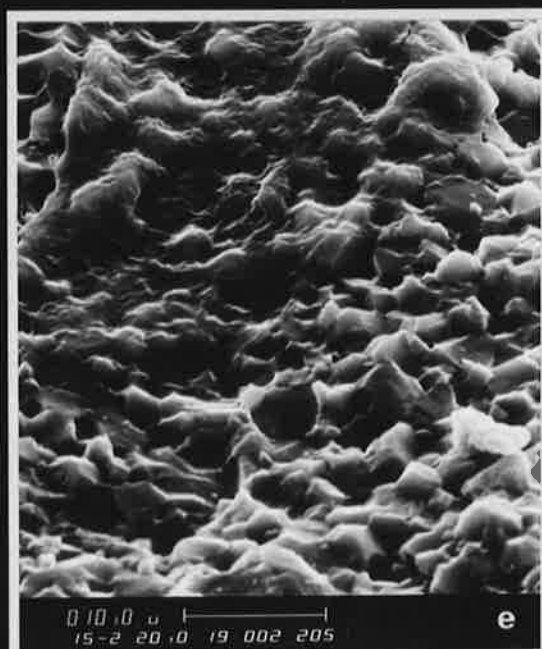
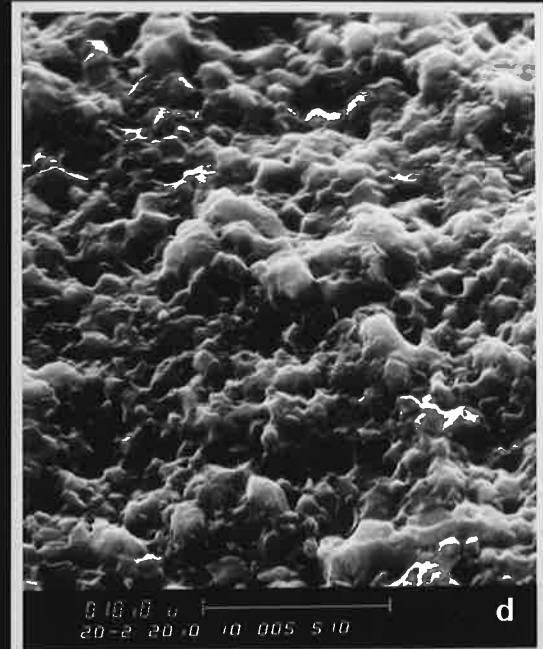
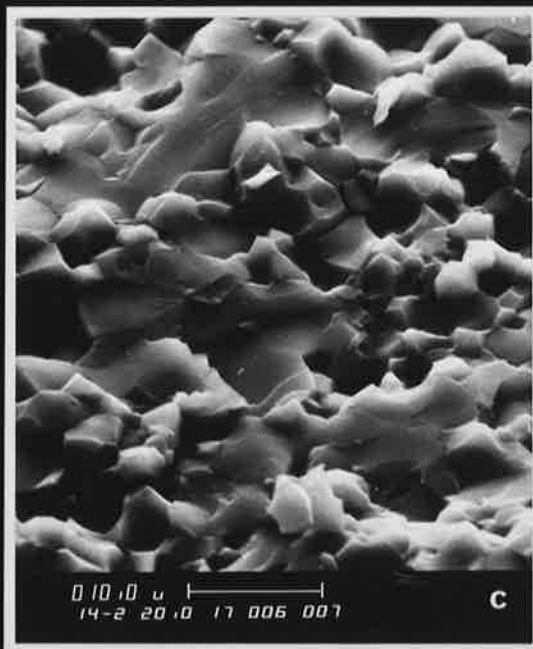
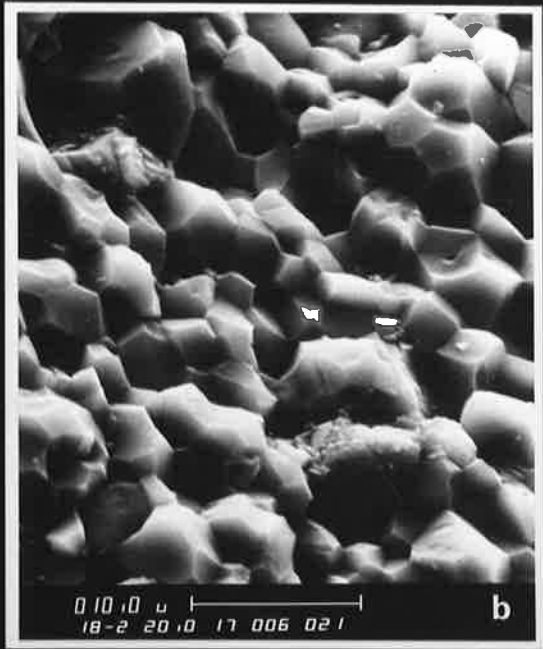
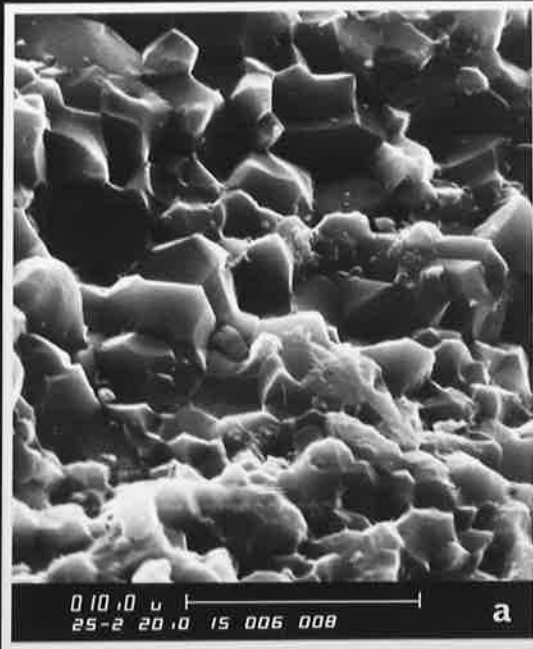
- a. (at left) Fracture surface of microcrystalline quartz with a compact mosaic of regular polyhedral grains with some triple point junctions. Specimen is a silicified dolomite mudstone from the Yadlamalka Formation, Depot Creek (DC).

- b. (at right) Fracture surface of microcrystalline quartz with a texture similar to a. Specimen is a silicified stromatolitic dolomite from the Nathaltee Formation, Depot Creek (DC).

- c. (at left) Fracture surface of microcrystalline quartz on which there has been fracture across grains rather than along grain boundaries because of the strongly interlocking framework. Specimen is a silicified stromatolitic dolomite from the Yadlamalka Formation, Depot Creek (DC).

- d. (at right) Fracture surface of very fine grained microcrystalline quartz with more irregular grains than in a, b and c. Sample is a silicified oncoïd grainstone from the Yadlamalka Formation, Depot Creek (DC).

- e. Fracture surface of microcrystalline quartz much of which has a texture similar to a, b and c, but grades into a cryptocrystalline texture in top left. Specimen is a silicified oncoïd grainstone from the Yadlamalka Formation, Depot Creek (DC).







APPENDIX 1

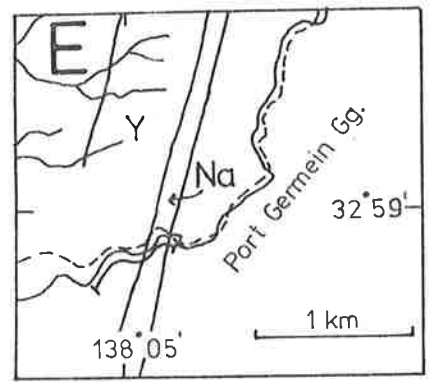
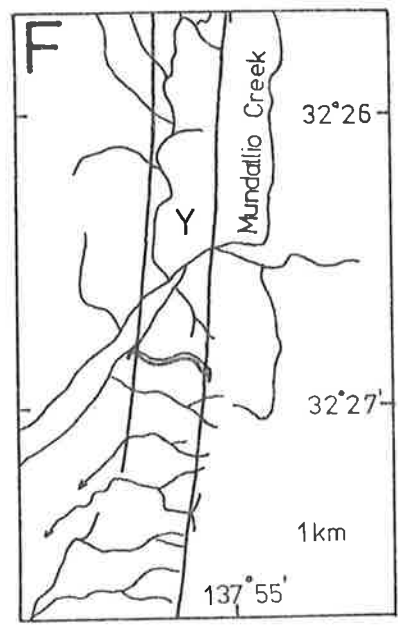
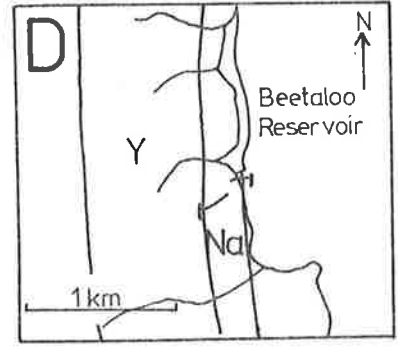
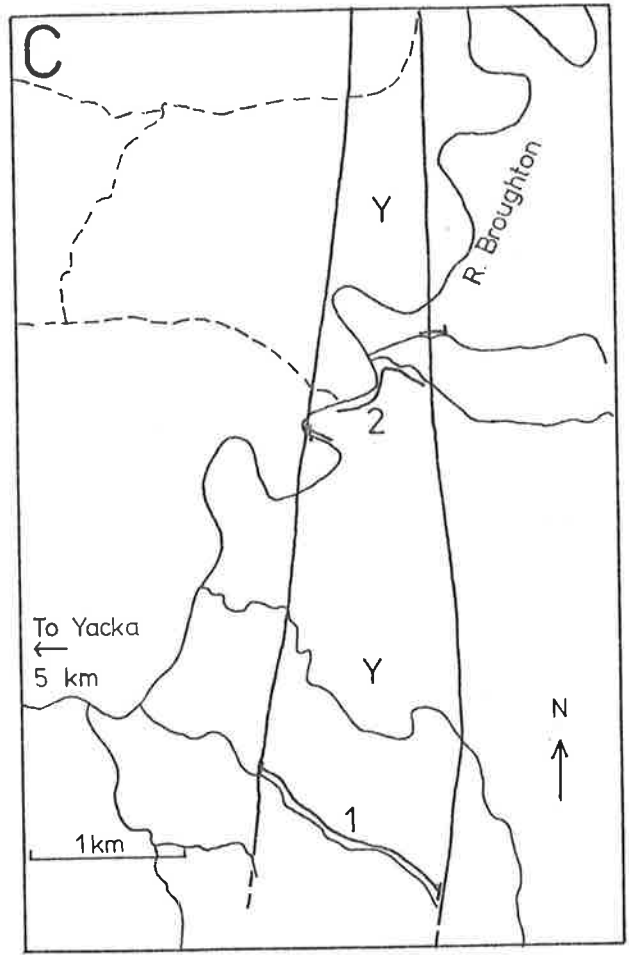
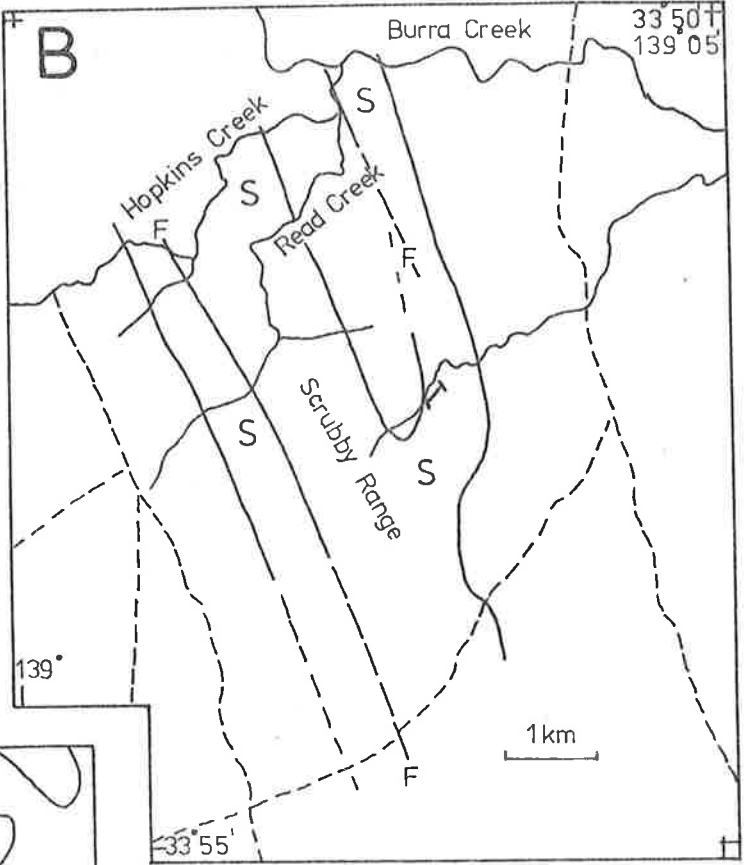
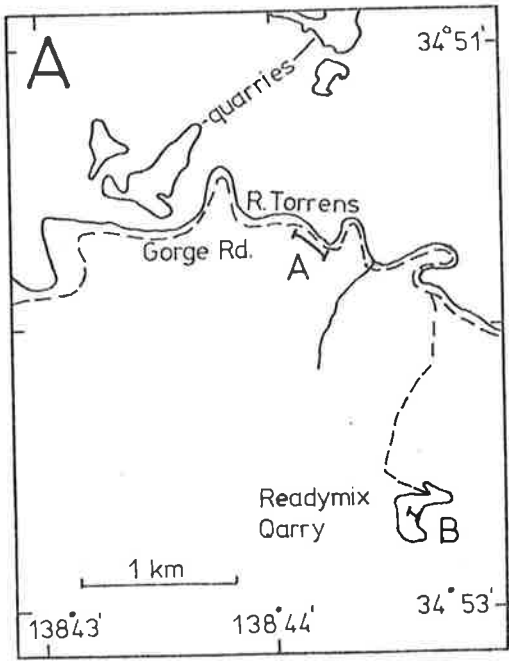
DETAILED LOCATION MAPS OF MEASURED
STRATIGRAPHIC SECTIONS

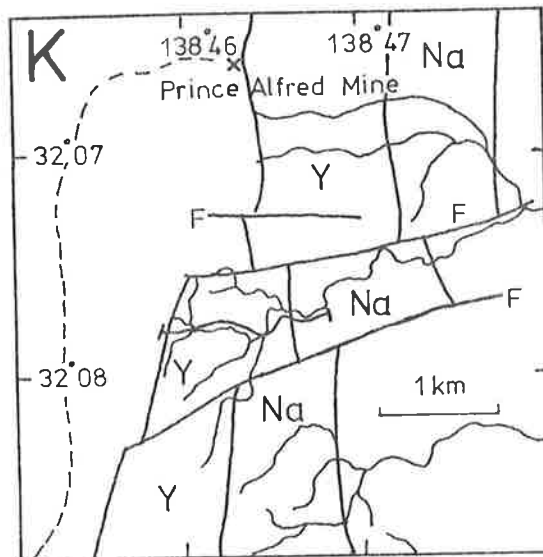
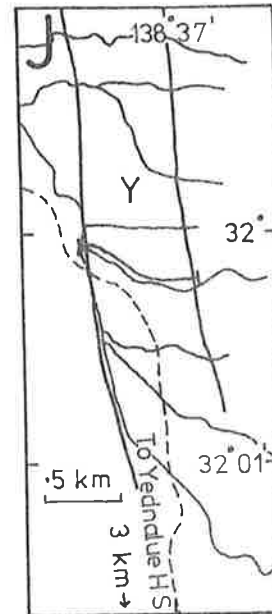
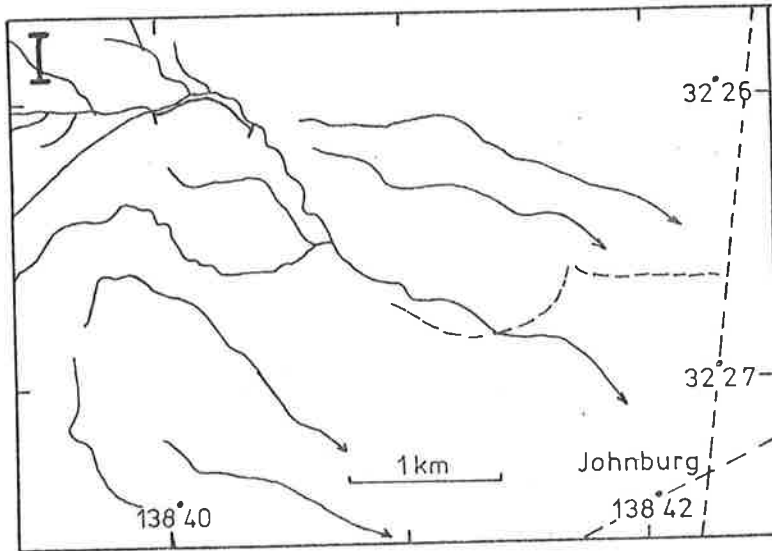
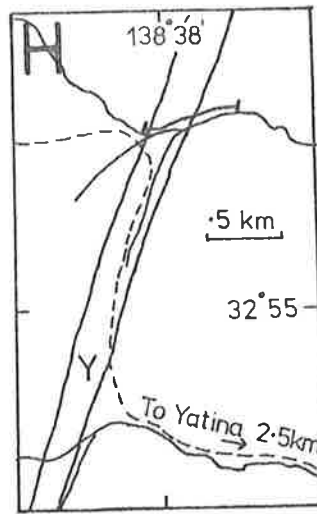
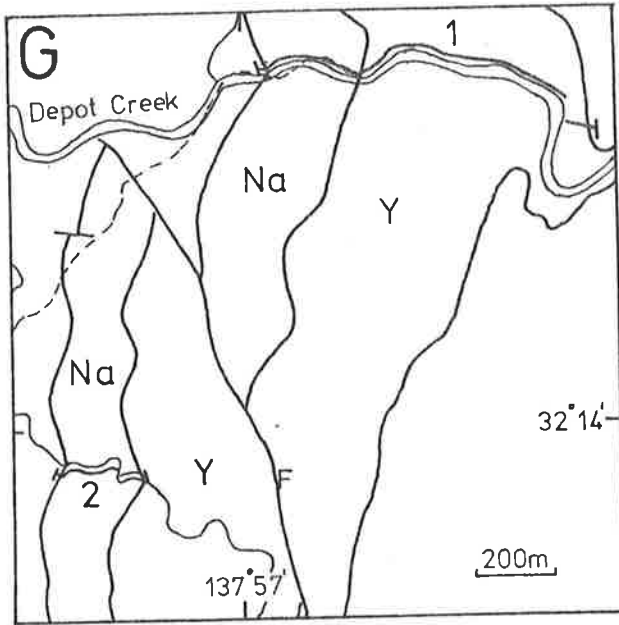
List of Location Maps and Formations Measured in Each Area

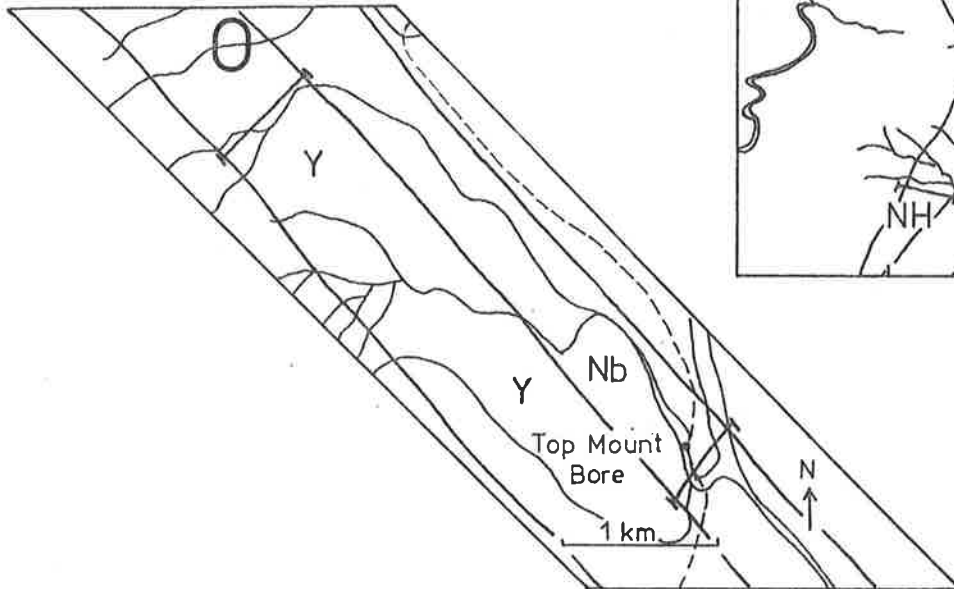
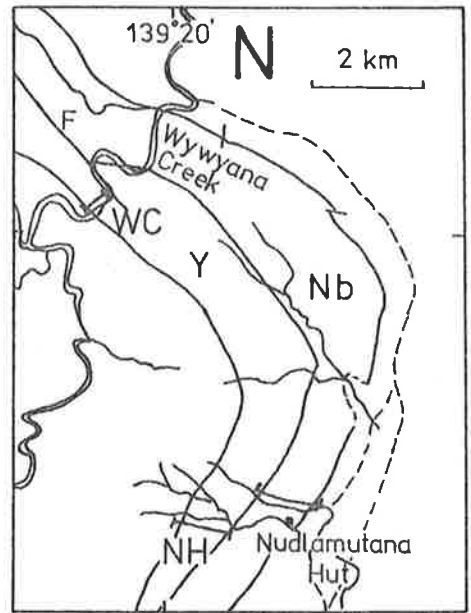
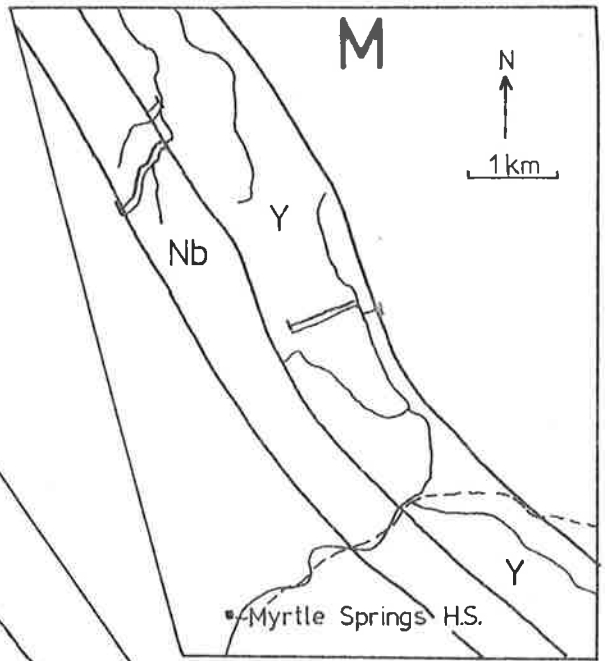
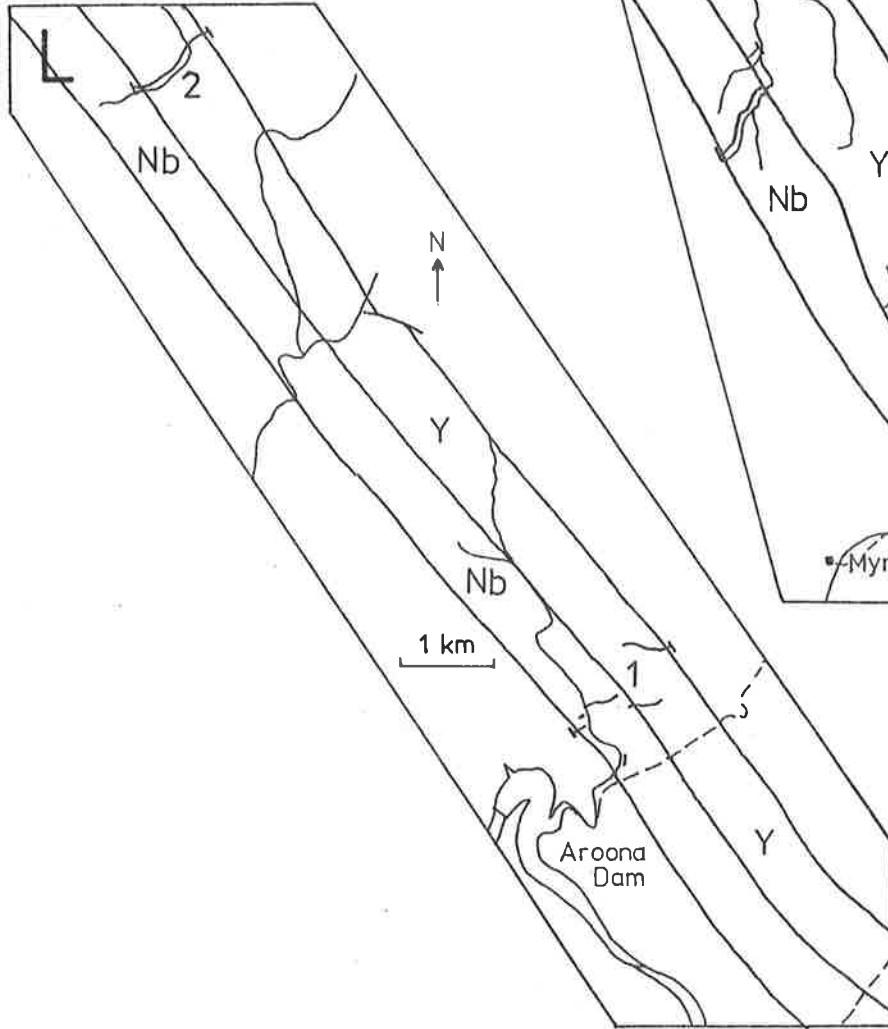
- A. Torrens Gorge (TG) - Montacute Dolomite, see Figure 6.3.
- B. Scrubby Range (SR) - Skillogalee Dolomite (upper part only), see Figure 5.2.
- C. Yacka (east, YE1 and YE2) - Yadlamalka Formation, see Figure 6.4.
- D. Beetaloo (B) - Nathaltee Formation, see Figure 4.1.
- E. Port Germein Gorge (PG) - Nathaltee Formation, see Figure 4.1; Yadlamalka Formation, see Figure 6.4.
- F. Mundallio Creek (MC) - Yadlamalka Formation, see Figure 6.4.
- G. Depot Creek (DC1 and DC2) - Nathaltee Formation, see Figure 4.1; Yadlamalka Formation, see Figure 6.4.
- H. Yatina (YT) - Yadlamalka Formation, see Figure 6.4.
- I. Johnburg (J) - Yadlamalka Formation, see Figure 6.4.
- J. Yednalue (YD) - Yadlamalka Formation, see Figure 6.4.
- K. Yednalue Anticline (west limb, YDA) - Nathaltee Formation, see Figure 4.1; Yadlamalka Formation, see Figure 6.4.
- L. Copley (CP1 and CP2) - Nankabunyana Formation, see Figure 4.11; Yadlamalka Formation, see Figure 6.5.
- M. Myrtle Springs (MS) - Nankabunyana Formation, see Figure 4.11; Yadlamalka Formation; see Figure 6.5.
- N. Arkaroola - Nudlamutana Hut (NH) and Wywyana Creek (WC) - Nankabunyana Formation, see Figure 4.11; Yadlamalka Formation, see Figure 6.5.
- O. Top Mount Bore (TM) - Nankabunyana Formation, see Figure 4.11; Yadlamalka Formation, see Figure 6.5.
- P. West Rischbieth (WR) - Yadlamalka Formation, see Figure 6.5.
- Q. Mirra Creek (MI) - Mirra Formation, see Figure 6.7.
- R. Mt. Norwest H.S. (NW) - Camel Flat Shale and Tilterana Sandstone, see Figure 4.11; Mirra Formation, see Figure 6.7.

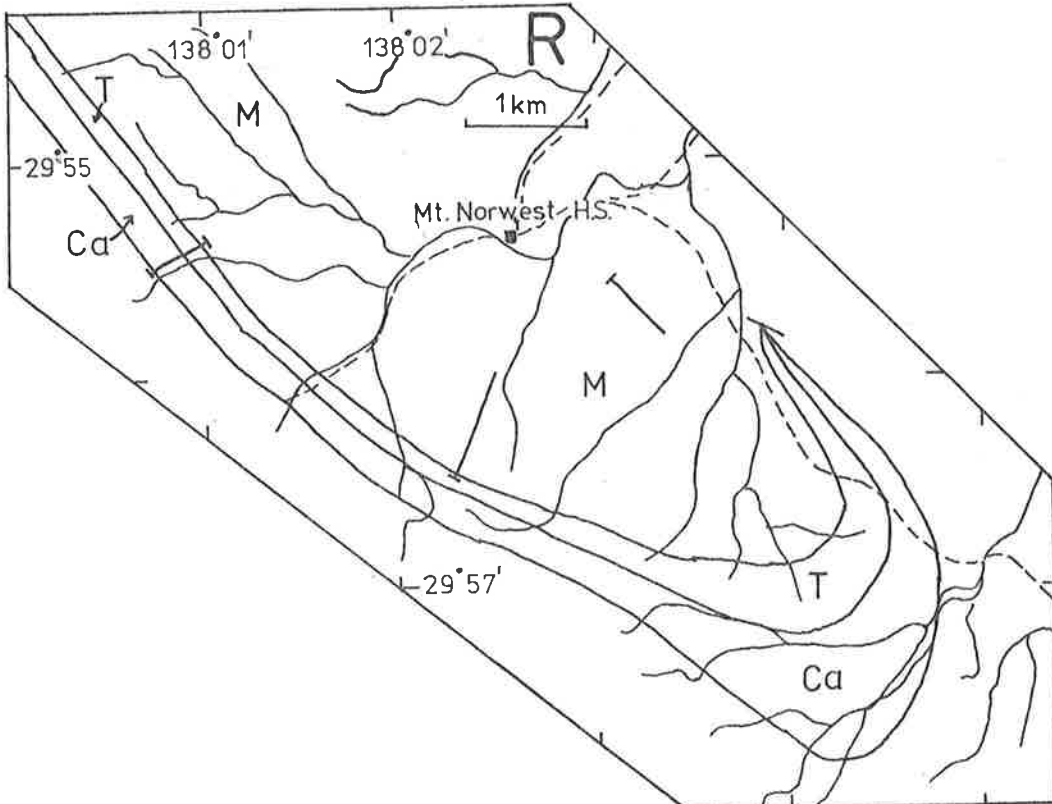
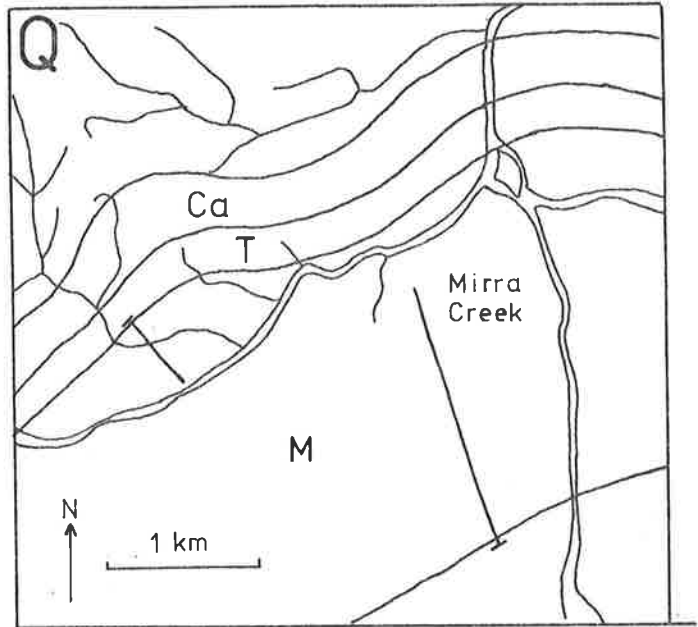
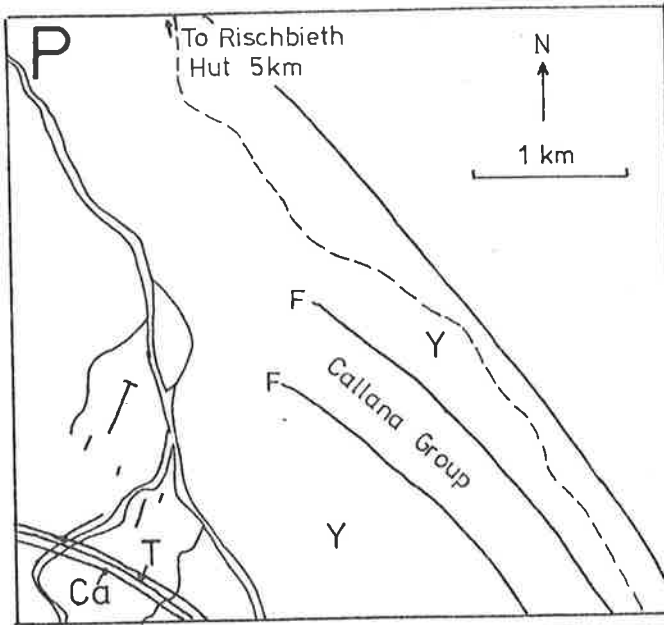
Legend for Location Maps

S	-	Skillogalee Dolomite
Na	-	Nathaltee Formation
Y	-	Yadlamalka Formation
Nb	-	Nankabunyana Formation
Ca	-	Camel Flat Shale
T	-	Tilterana Sandstone
M	-	Mirra Formation
		Measured Section
		Formation Boundary
		Creek
		Road or Track









APPENDIX 2

MARKOV CHAIN ANALYSIS : MATRICES

- Facies
1. Intraclastic Magnesite
 - 2A. Dolomitic, very fine-grained sandstone
 - 2B. Dolomitic, medium-grained sandstone
 3. Dolomite mudstone
 4. Magnesite mudstone
 5. Nodular magnesite
 6. Stromatolitic dolomite
 7. Shales and siltstones
 8. Dolomite grainstones

Example A. COPLEY MAGNESITE DDH1 section

Matrices

Transition Count Matrix

Facies	1	2A	3	4	5	row sum
1	0	20	5	5	1	31
2	11	0	9	2	1	23
3	2	2	0	12	2	18
4	11	1	2	0	7	21
5	8	1	1	2	0	<u>12</u>
						105

Independent Trials Probability Matrix

	1	2A	3	4	5
1	0	.645	.161	.161	.032
2	.478	0	.391	.087	.043
3	.111	.111	0	.667	.111
4	.524	.048	.095	0	.333
5	.667	.083	.083	.166	0

Transition Probability Matrix

	1	2A	3	4	5
1	0	.324	.230	.284	.149
2	.390	0	.207	.256	.134
3	.368	.270	0	.241	.126
4	.381	.286	.202	0	.130
5	.344	.258	.188	.226	0

Difference Matrix

	1	2A	3	4	5
1	0	.321	-.069	-.123	-.117
2	.088	0	.184	-.169	-0.91
3	-.257	-.159	0	.426	-.015
4	.143	-.233	-.107	0	.203
5	.323	-.115	-.100	-.06	0

Test of significance

$$\chi^2 = 111.6$$

$$\text{degrees of freedom} = (n - 1)^2 - n = 12$$

$$\text{limiting value at 95\% confidence level} = 21.03$$

Example B. Copley : Section 1, 0 - 185.4 m

Matrices

Transition Count Matrix

Facies	1	2A	3	4	row sum
1	0	7	34	0	41
2A	4	0	7	0	11
3	30	5	0	5	40
4	5	0	0	0	<u>5</u>
					97

Independent Trials Probability Matrix

	1	2A	3	4
1	0	.17	.829	0
2A	.364	0	.636	0
3	.75	.125	0	.125
4	1	0	0	0

Transition Probability Matrix

	1	2A	3	4
1	0	.214	.732	.089
2A	.453	0	.477	.058
3	.684	.211	0	.088
4	.424	.130	.446	0

Difference Matrix

	1	2A	3	4
1	0	-.044	0.097	-.089
2A	-.089	0	.159	-.058
3	+.066	-.088	0	.037
4	.576	-.130	-.466	0

Test of significance

$$\chi^2 = 108.8$$

$$\text{degrees of freedom} = 5$$

$$\text{limiting value at 95\% confidence level} = 11.07$$

Example C. Copley : Section 1, 209 - 432 m

Matrices

Transition Count Matrix

Facies	1	2A	3	4	row sum
1	0	13	18	0	31
2A	12	0	12	0	24
3	22	7	0	3	32
4	2	0	1	0	3
					<hr/> 90

Independent Trials Probability Matrix

	1	2A	3	4
1	0	.419	.581	0
2A	.5	0	.5	0
3	.688	.219	0	.094
4	.667	0	.333	0

Transition Probability Matrix

	1	2A	3	4
1	0	.339	.525	.051
2A	.545	0	.470	.045
3	.621	.345	0	.052
4	.419	.23	.356	0

Difference Matrix

	1	2A	3	4
1	0	.03	.056	-.051
2A	-.045	0	.030	-.045
3	.067	-.126	0	.042
4	.253	-.23	-.023	0

$$\chi^2 = 81.4$$

degrees of freedom = 5

limiting value at 95% confidence level = 11.07

Example D. Yednalue Section, 0 - 200 m

Matrices

Transition Count Matrix

Facies	1	2B	3	4	6	7	row sum
1	0	7	9	0	4	1	21
2B	1	0	17	0	2	0	20
3	14	11	0	3	5	1	34
4	4	0	0	0	0	0	4
6	1	0	11	0	0	0	12
7	0	1	1	0	0	0	2
							<hr/> 93

Independent Trials Probability Matrix

	1	2B	3	4	6	7
1	0	.33	.429	0	.19	.05
2B	.05	0	.85	0	.1	0
3	.411	.324	0	.09	.235	.265
4	1	0	0	0	0	0
6	.083	0	.917	0	0	0
7	0	.5	.5	0	0	0

Transition Probability Matrix

	1	2B	3	4	6	7
1	0	.292	.472	.042	.153	.028
2B	.274	0	.466	.041	.151	.027
3	.339	.356	0	.051	.186	.034
4	.225	.236	.382	0	.034	.022
6	.247	.259	.419	.037	0	.025
7	.22	.231	.374	.033	.121	0

Difference Matrix

	1	2B	3	4	6	7
1	0	.038	.043	-.042	.037	.022
2B	-.224	0	.384	-.041	-.051	-.027
3	.072	-.032	0	+.039	.049	.231
4	.775	-.236	-.382	0	-.034	-.022
6	-.164	-.259	.498	-.037	0	-.025
7	-.22	.269	.126	-.033	-.121	0

$$\chi^2 = 115.7$$

degrees of freedom = 19

limiting value at 95% confidence level = 31.41

Example E. Depot Creek Section

Matrices

Transition Count Matrix

Facies	1	2B	3	6	7	8	Row sum
1	0	12	41	6	0	1	60
2B	10	0	20	0	1	0	31
3	45	19	0	11	2	5	82
6	2	0	11	0	0	3	16
7	0	2	1	0	0	0	3
8	2	0	8	0	0	0	10
							<u>202</u>

Independent Trials Probability Matrix

	1	2B	3	6	7	8
1	0	.2	.683	.1	0	.017
2B	.326	0	.645	0	.032	0
3	.549	.232	0	.134	.024	.061
6	.125	0	.688	0	0	.188
7	0	.667	.333	0	0	0
8	.2	0	.8	0	0	0

Transition Probability Matrix

	1	2B	3	6	7	8
1	0	.234	.567	.121	.021	.064
2B	.351	0	.468	.099	.018	.053
3	.5	.275	0	.142	.025	.075
6	.323	.177	.430	0	.016	.048
7	.302	.166	.402	.085	0	.045
8	.313	.172	.417	.089	.016	0

Difference Matrix

	1	2B	3	6	7	8
1	0	-.034	.116	-.021	-.021	-.047
2B	-.025	0	.177	-.099	.014	-.053
3	.049	-.043	0	-.008	-.001	-.014
6	-.198	-.177	.258	0	-.16	.14
7	-.302	.501	-.069	-.085	0	-.045
8	-.113	-.172	.383	-.089	-.016	0

$$\chi^2 = 189$$

degrees of freedom = 9

limiting value at 95% confidence level = 31.41

Example F. Depot Creek Section, 0 - 58 m

Matrices

Transition Count Matrix

Facies	1	2B	3	6	8	row sum
1	0	7	4	3	0	14
2B	6	0	14	0	0	20
3	7	13	0	5	1	26
6	1	0	6	0	1	8
8	0	0	2	0	0	2
						<u>70</u>

Independent Trials Probability Matrix

	1	2B	3	6	8
1	0	.5	.286	.214	0
2B	.3	0	.7	0	0
3	.269	.5	0	.192	.038
6	.125	0	.75	0	.125
8	0	0	1	0	0

Transition Probability Matrix

	1	2B	3	6	8
1	0	.357	.464	.143	.036
2B	.28	0	.52	.16	.04
3	.318	.455	0	.182	.045
6	.226	.323	.419	0	.032
8	.206	.294	.382	.118	0

Difference Matrix

	1	2B	3	6	8
1	0	.143	-.178	.071	-.036
2B	.02	0	.18	-.16	-.04
3	-.049	.045	0	.01	-.07
6	-.101	-.323	.331	0	.093
8	.206	-.294	.618	-.118	0

$$\chi^2 = 68.47$$

degrees of freedom = 11

limiting value at 95% confidence level = 17.68

APPENDIX 3
CHEMICAL METHODS

A. WHOLE ROCK ANALYSES : SHALES

Samples were crushed in a small jaw crusher and then ground to approximately 200 # particle size using a Siebtechnik chrome-steel mill. Approximately 6 - 9 gms were ignited at 900°C for 12 hours in order to determine the loss on ignition (LOI). Fused buttons consisting of 280 mg of the ignited powder, 20 mg of sodium nitrate and 1.5 gm of a lithium fluoride flux, were analysed by XRF using a Siemens Sequential Ray Spectrometer, and the major elements determined. Na₂O was measured with a Corning-Eel flame photometer, following overnight dissolution of a known amount of sample in 10 mls of HF and 2 mls of H₂SO₄, and subsequent dilution to 100 mls or 500 mls depending on the concentration.

B. TRACE ELEMENT ANALYSES : CARBONATES

Samples were crushed as above, and 2-5 gm was leached overnight in 30 mls of 20% V/V HCl. Magnesite samples were leached for 48 hours. The solutions were filtered and made up to 250 mls, and the residues dried and weighed. Fe, Mn, Na, K and Sr were measured using a Varian Techtron AA6 Atomic Absorption Spectrophotometer, using the recommended operating conditions. Ca and Mg were added to the calibration standards in amounts appropriate to match them to the unknowns. A further 5 times dilution of solutions was necessary for some measurements. Blank and duplicate samples (for about 15% of total samples) were also run. The average reproducibility is as follows, IR : 4%; Na : 6.5%, K : 4.8%, Mn : 1.3%, Fe : 2.2%, and Sr : 2.3%. Na, K, Fe, Mn and Sr were calculated in ppm on total carbonate (insoluble residue free) basis.

C. DETERMINATION OF WEIGHT PERCENT MAGNESITE

Two samples each containing either magnesite or dolomite as the only carbonate mineral, were mixed in the appropriate proportions in

order to give samples containing 5, 10, 20, 3070, 80, 90, 95 percent magnesite. As all the unknown magnesite samples analysed are fine grained, the dolomite and magnesite samples used for calibration were from the Yadlamalka Formation, rather than reagent grade samples which would be more dissimilar to the unknowns. X-Ray diffraction traces of these sample mixtures were run on a Phillips X-Ray Diffractometer using a cobalt tube and iron filler, at 30 kV and 30 Ma, with a scan speed of $\frac{1}{2}^{\circ}$ /min, chart speed of 1 cm/min and a pulse rate of 400 or 1000 cps.

Values of $\frac{\text{ht Mag}}{\text{ht Mag} + \text{ht Dol}}$ for the [104] peaks of both magnesite and dolomite were measured for each sample (5 runs per sample), and plotted against weight % magnesite (Fig. A3.1). Although measurement of peak area, or counts of peak height intensity for a fixed time interval, would give more accurate measurements of peak intensity than peak heights, the method used is more rapid. X-Ray diffraction traces of unknowns were run under the same conditions, and compared with the calibration curve in order to determine the weight % magnesite. The results are given in Appendix 4B.

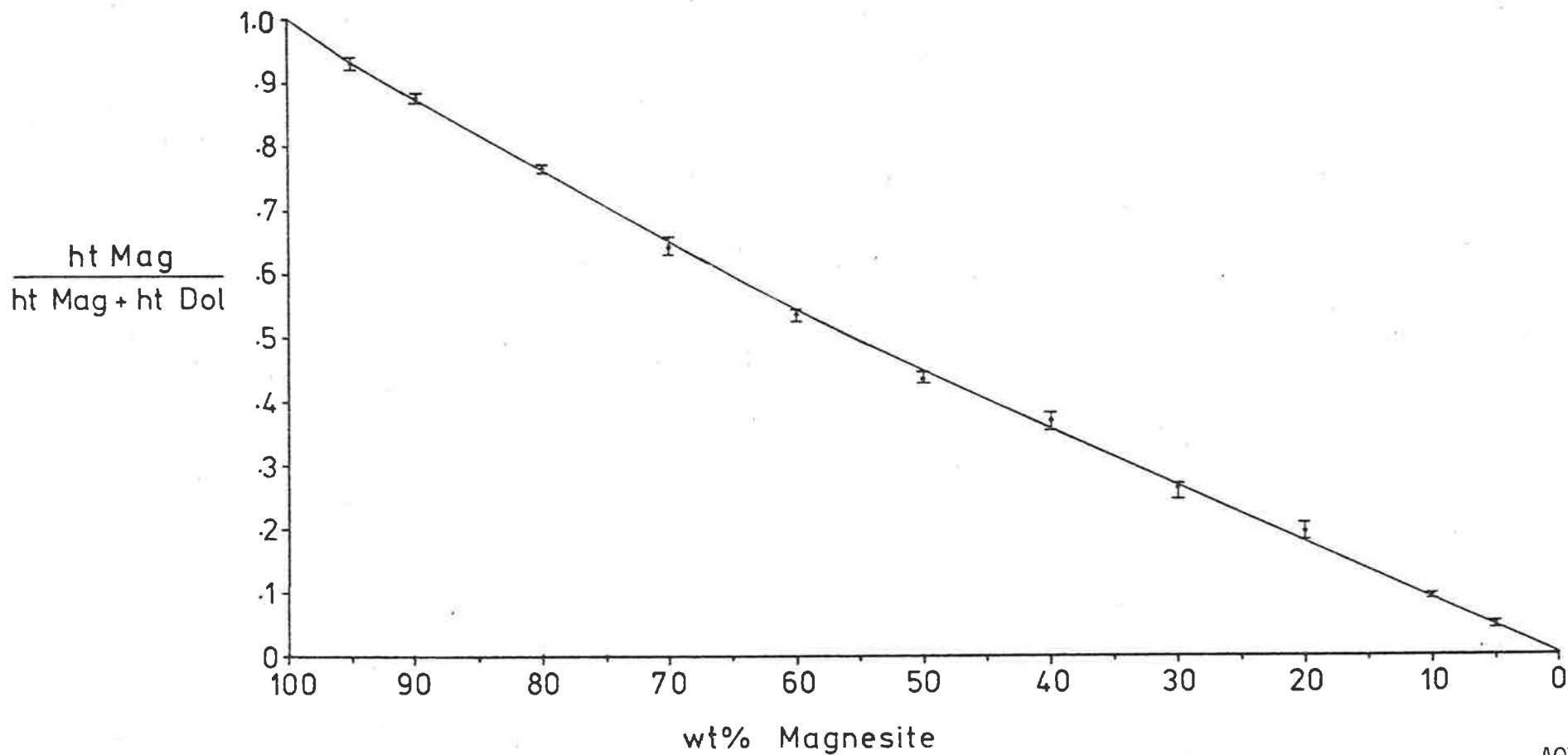


Figure A3.1. Calibration curve for the determination of wt % magnesite from the [104] peak heights of dolomite and magnesite. Bars show the range of values measured for the known mixtures of magnesite and dolomite.

APPENDIX 4

GEOCHEMICAL DATA : CARBONATE FACIES

Letters in sample numbers indicate their locations as in Figure 3.2.

A. Dolomite Facies

Skillogalee Dolomite

Sample No	Lithology	IR	Fe	Mn	Mn/Fe	Na	K	Sr
<u>- pale coloured dolomites</u>								
SC018	White recrystallised dolomite	4.8	5072	377	0.074	177	60	229
SC020	" " "	9.8	9695	745	0.077	114	117	234
SR006	" " "	12.8	534	68	0.127	189	150	313
SR017	Pink recrystallised dolomite	18.2	3964	503	0.127	135	154	137
SR025	White recrystallised dolomite	3.0	266	163	0.613	155	100	663
SR033	" " "	26.8	1165	71	0.061	109	84	388
SR066	White stromatolitic dolomite	10.4	4426	262	0.059	145	90	262
<u>- grey dolomites</u>								
SC009	Grey recryst. intraclastic dolomite	17.6	949	174	0.183	182	40	837
SC010	Dark-grey dolomite mudstone	10.0	876	120	0.137	281	268	760
SC014	Grey recryst. dolomite mudstone	4.4	624	117	0.188	183	146	786
SC023	" " " "	4.2	728	207	0.284	73	110	409
SR005	Dark-grey calcite mudstone	7.2	161	66	0.410	49	70	1489
SR008	Grey dolomite mudstone	21.0	673	56	0.083	563	103	980
SR020	Dark-grey dol. mudstone-cherty	42.0	12208	1320	0.108	207	652	544
SR022	" " " "	17.0	1107	106	0.096	500	113	923
SR026	" " " "	13.6	835	23	0.028	139	121	940

Nathaltee Formation - Unit 1

Sample No	Lithology	IR	Fe	Mn	Mn/Fe	Na	K	Sr
DC006	Grey dolomite mudstone	11.6	3511	549	.156	335	60	241
DC007	Light-grey dolomite mudstone	19.2	4654	1168	.251	139	86	254
DC013	Grey peloidal grainstone	7.8	6977	866	.124	109	71	131
DC016	Dark-grey stromatolitic dolomite	18.4	4146	442	.107	149	83	267
DC105	Grey dolomite mudstone	19.8	6272	1310	.209	79	141	134
DC109	Dark-grey dolomite mudstone	15.2	3358	572	.170	145	117	123
YDA049	Dark-grey oncoid grainstone	9.5	12803	1159	.091	129	156	221
YDA082	Dark-grey recrystallised dolomite	19.8	7977	860	.108	166	224	426
YDA087	Dark-grey oncoid grainstone	4.9	4099	578	.141	136	87	373
YDA088	Dark-grey oncoid gr. and dol. mudstone	11.9	7560	1295	.171	202	16	356
YDA090	Dark-grey dolomite mudstone	11.2	11488	1340	.117	121	144	249
YDA091	Dark-grey dolomitic siltstone	58.3	16408	1270	.077	400	1485	515
YDA092	Dark-grey dolomite mudstone	15.9	7195	725	.101	170	333	384

Nathaltee Formation - Unit 2

Sample No	Lithology	IR	Fe	Mn	Mn/Fe	Na	K	Sr
DC019	Light-grey dolomite mudstone	41.0	11774	2229	.189	192	797	157
DC022	" " " "	29.6	8188	1125	.137	188	128	269
DC024	Buff stromatolitic dolomite	11.0	7598	1279	.168	123	50	169
DC094	Dark-pink stromatolitic dolomite	37.0	3023	1367	.452	84	147	182
DC122	Buff stromatolitic dolomite	16.0	6243	821	.132	158	73	236
PG005	Buff dolomite mudstone	27.0	10510	864	.082	254	84	224
B013	Yellow-pink calcite mudstone	34.5	1606	750	.467	259	369	321
B015	Yellow-pink dolomite mudstone	48.2	8209	815	.099	389	732	193
B017	Yellow-pink stromatolitic dolomite	13.5	5374	870	.162	151	28	201
B018	Light-grey oncoid grainstone	6.4	1778	532	.229	173	20	124

Nankabunyana Formation

Sample No	Lithology	IR	Fe	Mn	Mn/Fe	Na	K	Sr
A014	Brown recrystallised dolomite	5.5	3970	1480	.373	10	34	58
A015	Light-grey recrystallised dolomite	18.0	25616	4184	.163	82	46	281
A022	White dolomite mudstone	34.0	5829	5754	.987	36	425	51
A024	White recrystallised dolomite	3.7	10769	1967	.183	11	130	78
A025	Grey dolomite mudstone	22.1	9431	1113	.118	17	423	166
A027	Dark-grey dolomite mudstone	48.8	16005	2385	.149	59	1854	78
A030	Grey stromatolitic dolomite	21.7	15329	2209	.144	32	735	313
A066	White recrystallised dolomite	9.4	3915	1058	.270	50	1296	174
A095	White dolomite mudstone	35.2	5863	516	.088	55	2793	137
A101	Yellow-brown dolomite mudstone	28.5	7127	689	.095	57	1942	197
CP022	Brown-pink stromatolitic dolomite	20.0	7934	899	.113	81	62	394
CP067	Brown dolomite mudstone	16.8	2673	617	.231	156	332	204
CP077	Light-grey dolomite mudstone	15.1	1738	353	.203	385	187	145
CP078	Brown dolomite mudstone	22.1	1982	626	.316	190	263	145
CP085	" " "	16.3	2090	432	.207	450	217	130
CP096	" " "	20.5	2743	1683	.614	239	337	137
CP098	Red dolomite mudstone	24.9	4060	905	.223	415	139	176
CP099	Light-grey dolomite mudstone	19.1	8528	816	.096	208	60	284
W003	Light-grey intraclastic grainstone	12.6	13969	2954	.211	98	52	155
W004	Buff dolomite mudstone	22.8	8131	697	.086	194	121	197
W011	Light-grey dolomite mudstone	27.0	7409	906	.122	259	236	207

Montacute Dolomite

Sample No.	Lithology	IR	Fe	Mn	Mn/Fe	Na	K	Sr
TG006	Dark-grey dolomite mudstone	6.2	3076	247	.080	80	299	324
TG012	" " " "	7.2	5707	446	.078	59	473	209
TG014	" " " "	15.0	2395	93	.039	62	554	364
TG018	" " " "	3.8	2784	150	.054	50	131	428
TG020	Dark-grey recrystallised dolomite	19.2	2633	176	.067	40	347	404
TG025	Grey intraclastic grainstone	3.6	1377	278	.202	88	111	284
TG030	Dark-grey dolomite mudstone	6.0	4777	369	.077	80	192	388
TG031	" " " "	6.6	5992	316	.053	96	74	298
TG035	Dark-grey recrystallised dolomite	9.0	5475	1006	.184	48	360	205
TG040	Dark-grey dolomite mudstone	38.6	5053	215	.043	77	1441	396
TG042	Dark-grey dolomite mudstone	2.0	1969	348	.177	51	19	173

Yadlamalka Formation

Sample No	Lithology	IR	Fe	Mn	Mn/Fe	Na	K	Sr
YE014	Dark-grey dolomite mudstone	8.6	1676	104	.062	82	233	782
YE021	" " " "	15.3	3122	240	.077	224	554	700
YE024	" " " "	7.2	2052	136	.066	119	167	521
YE028	Grey intraclastic grainstone	15.2	5391	397	.074	165	195	511
YE029	Dark-grey dolomite mudstone	28.4	7254	604	.083	146	545	645
YE030	Light-grey dolomite mudstone	34.2	2034	336	.165	182	235	943
YE042	Grey dolomite mudstone	13.2	4300	234	.054	201	366	451
YE048	Dark-grey intraclastic grainstone	10.8	3438	303	.088	174	225	656
YE051	Dark-grey intra. gr. and dol. mudstone	9.2	1743	147	.084	110	159	815
YE061	Dark-grey dolomite mudstone	19.6	3170	200	.063	106	352	715
YE063	Dark-grey recrystallised dolomite	17.7	1467	118	.080	47	209	456
YE064	Dark-grey dolomite mudstone	12.6	3065	170	.055	104	318	465
YE070	Pink dolomite mudstone	9.8	6148	574	.093	139	546	180
YE072	Dark-grey dolomite mudstone	19.8	9060	498	.055	174	1030	448
YT004	" " " "	11.5	2903	185	.064	123	266	733
YT007A	Light-grey silty dolomite mudstone	49.3	9993	873	.087	215	400	850
YT015	Dark-grey dolomite mudstone	25.6	5704	627	.110	123	564	923
YT017	" " " "	27.6	4046	359	.089	119	718	927
J006	Grey oncolid grainstone	13.9	1148	96	.084	149	90	549
J007	Grey dolomite mudstone	28.9	3931	314	.080	159	177	323
J010	Dark-grey dolomite mudstone	16.0	2973	187	.063	137	112	789
YD004	Light-grey dolomite mudstone	16.8	5134	217	.042	81	186	557
YD008	Dark-grey dolomite mudstone	21.0	3164	382	.121	193	209	348
YD009	Dark-grey stromatolitic dolomite	10.8	2522	246	.098	104	21	295
YD012	" " " "	29.2	2473	145	.059	96	44	401
YD015	Massive diagenetic dolomite	1.0	1465	393	.268	114	59	320
YD016	" " " "	6.8	859	160	.186	89	44	328
YD017	" " " "	3.7	666	97	.146	210	57	336
YD018	" " " "	4.0	655	51	.077	117	18	251
YD019	" " " "	.6	381	42	.110	192	47	206
YD020	" " " "	3.4	966	189	.196	99	68	238
YD022	" " " "	.4	290	43	.148	197	23	223

Yadlamalka Formation (cont.)

Sample No	Lithology	IR	Fe	Mn	Mn/Fe	Na	K	Sr
YD025	Dark-grey dolomite mudstone	32.8	1464	87	.059	199	51	725
YD030	" " " "	29.5	6104	390	.064	143	291	608
YD032	Dark-grey oncolid grainstone	45.3	7950	370	.047	157	111	297
YDA059	Dark-grey dolomite mudstone	5.3	2585	251	.097	153	150	393
YDA061	" " " "	11.2	3040	390	.128	104	74	754
YDA074	Massive diagenetic dolomite	2.0	567	69	.122	118	77	308
PG021	Grey dolomite mudstone	22.3	2167	296	.137	235	105	294
PG023	Dark-grey dolomite mudstone	9.0	1951	298	.153	170	71	474
PG024	" " " "	8.5	1370	155	.113	213	44	414
PG026	" " " "	45.5	6450	372	.058	173	512	446
PG028	" " " "	5.6	2809	236	.084	164	45	476
B021	Dark-grey oncolid grainstone	5.8	995	95	.095	167	19	1423
B026	Dark-grey oncolid gr. and dol. mudstone	4.6	1116	115	.103	166	39	430
B028	Dark-grey oncolid grainstone	7.0	2421	137	.057	106	38	380
MC027	Light-grey dolomite mudstone	22.3	6053	403	.067	151	68	337
MC029	Dark-grey dolomite mudstone	4.4	1930	155	.080	103	24	297
MC031	Buff dolomite mudstone	8.2	2176	234	.108	121	41	325
MC032	Grey dolomite mudstone	3.3	1266	108	.085	139	78	317
MC033	Grey recrystallised dolomite	7.4	771	121	.157	140	16	301
MC034	Grey dolomite mudstone	22.3	1285	65	.051	155	205	672
MC036	Massive diagenetic dolomite	2.7	1838	160	.087	69	10	291
MC037	Grey dolomite mudstone	5.6	638	73	.114	170	33	1057
MC038	Dark-grey dolomite mudstone	5.9	823	199	.242	118	38	783
MC040	Orange, silty dolomite mudstone	45.4	3242	358	.110	80	333	332
MC041	Dark-grey dolomite mudstone	7.7	850	71	.084	121	11	691
MC044	Light-grey dolomite mudstone	2.2	331	74	.224	91	20	191
DC029	Dark-grey dolomite mudstone	39.0	8112	1134	.140	153	213	162
DC033A	" " " "	18.2	5668	825	.146	223	66	246
DC041	" " " "	4.0	3112	274	.088	149	57	369
DC058	Grey ooid grainstone	6.4	396	91	.230	122	27	958
DC064	Dark-grey stromatolitic dolomite	3.2	517	82	.159	213	48	497
DC088	" " " "	1.8	1569	112	.071	227	97	579

Yadlamalka Formation (cont.)

Sample No	Lithology	IR	Fe	Mn	Mn/Fe	Na	K	Sr
DC091	Dark-grey dolomite mudstone	14.0	1565	114	.073	228	117	392
DC126	Dark-grey stromatolitic dolomite	5.0	565	88	.156	125	23	395
DC128	Dark-grey dolomite mudstone	4.6	620	71	.115	166	83	494
DC132	Dark-grey oncoid grainstone	2.0	760	171	.225	255	24	475
CP030	Dark-grey dolomite mudstone	27.5	7438	835	.112	166	265	355
CP044	Dark-grey dolomite mudst. and pel. gr.	10.2	1832	137	.075	170	212	479
CP047	Dark-grey peloidal grainstone	38.8	2410	134	.056	118	284	515
CP058	Grey stromatolitic dolomite	8.2	4287	476	.111	99	140	316
CP083A	Dark-grey dolomite mudstone	14.8	1953	150	.077	202	98	768
CP087A	" " " "	7.0	3630	387	.107	114	86	532
CP089A	" " " "	9.0	879	103	.117	99	27	328
CP106	" " " "	9.7	886	75	.085	141	87	552
CP108	Dark-grey peloidal grainstone	31.2	2376	225	.095	195	76	470
CP118	Dark-grey dol. mudstone and pel.gr.	6.5	1412	238	.169	203	98	321
CP120	Dark-grey oncoid grainstone	7.5	638	133	.208	241	43	365
A044	Dark-grey recrystallised dolomite	36.3	11419	2102	.184	23	3043	242
A055	Dark-grey dolomite mudstone	52.0	5173	448	.087	88	3538	327
A056	" " " "	41.2	3842	217	.056	55	2093	658
A061	" " " "	43.4	9093	313	.034	78	2160	380
A062	Dark-grey intraclastic grainstone	15.5	2453	843	.344	19	3440	467
A064	Dark-grey dolomite mudstone	31.1	4294	315	.073	39	2453	405
A098	" " " "	11.6	2012	189	.094	15	13	480
A098M	Dark-grey intraclastic grainstone	18.9	2919	234	.080	18	10	438
A116	Dark-grey dol. mudstone-dolomite ss.	54.5	7908	335	.042	213	3680	450
A122	Dark-grey dolomite mudstone	23.3	2347	217	.092	23	1304	658
A144	Dark-grey oncoid grainstone	12.0	1183	139	.117	36	92	534
A146	Dark-grey dolomite mudstone	34.3	2435	224	.092	43	1522	525
A189	Grey intraclastic grainstone	25.9	19555	2854	.146	86	179	138
A190	Grey ooid grainstone	17.2	8033	1075	.134	124	230	279
A193	Grey dolomitic sandstone	53.0	14719	1665	.113	187	1180	255
A194	" " " "	71.8	11508	1040	.090	195	1864	284

Yadlamalka Formation (cont.)

Sample No	Lithology	IR	Fe	Mn	Mn/Fe	Na	K	Sr
A195	Grey intraclast grainstone	14.3	1672	201	.120	83	178	336
W021	Grey oncoid grainstone	13.9	1769	466	.263	116	43	425
W023	Grey dolomite mudstone	10.3	1873	184	.098	81	128	467
W029	Grey dolomite mudstone	7.1	1314	43	.033	223	18	443
W031	Light-grey dolomite mudstone	20.8	3814	360	.094	49	38	136
W035	Grey ooid grainstone	12.7	1182	214	.181	217	41	523
W036	Brown-grey dolomite mudstone	25.8	4212	208	.049	104	170	423
W038	" " " "	33.9	5715	519	.091	211	265	466
W052	Dark-grey dolomite mudstone	36.4	3228	241	.075	86	380	466
W062	" " " "	11.7	1048	86	.082	152	110	613
W063	" " " "	35.2	2649	185	.070	155	409	780
W065	" " " "	10.6	816	85	.104	126	13	674
W136	Grey dol. mudstone-intraclastic gr.	10.5	1225	543	.443	200	66	372
W137	Grey stromatolitic dolomite	8.3	1188	162	.136	189	77	414
W143	Grey pel. and oncol. grainstone	4.3	280	34	.121	165	27	690
W147	Grey stromatolitic dolomite	14.6	1393	68	.049	186	36	728

Mirra Formation

Sample No	Lithology	IR	Fe	Mn	Mn/Fe	Ma	K	Sr
W045	Yellow-grey dolomite mudstone	35.2	4956	492	.099	118	268	525
W048	Grey dolomite mudstone	27.1	1176	404	.344	153	322	516
W088	Dark-grey dolomite mudstone	33.9	1911	471	.246	192	858	485
W091	" " " "	19.0	3455	249	.072	79	457	839
W093A	Dark grey dol. mudst. and pel. grst.	40.1	3098	244	.079	143	1570	716
W095	Dark-grey stromatolitic dolomite	14.5	3717	286	.077	56	82	845
W105	Dark-grey dolomite mudstone	17.2	5307	510	.096	46	128	648
W114	" " " "	15.9	1791	310	.173	67	312	556
W127	Dark-grey pel. grst. and dol. mudstone	9.7	1659	201	.121	30	164	691
W131	Dark-grey peloidal grainstone	8.6	1775	197	.111	48	151	708
W152	Dark-grey dolomite mudstone	15.1	5603	590	.105	35	384	580
W153	Dark-grey stromatolitic dolomite	13.4	3447	609	.177	39	368	564

B. Magnesite Facies

All samples are from the Yadlamalka Formation, except SC019 which is from the Skillogalee Dolomite.

Sample No	Lithology	IR	Fe	Mn	Mn/Fe	Na	K	Sr	% Magnesite
SC019	Magnesite - dolomite mudstone	15.8	4284	302	.070	113	147	150	54
YE056	Cream intraclastic magnesite	13.8	3650	207	.057	87	311	11	99
YE057	Grey magnesite mudstone	25.5	7145	245	.034	125	475	108	85
MC008	Cream intraclastic magnesite	3.4	1448	72	.050	83	33	0	100
DC097	Grey nodular magnesite	1.0	3477	218	.063	64	29	5	100
DC125	Cream nodular magnesite	2.8	974	86	.088	62	56	14	100
YDA060	Grey magnesite mudstone	19.2	13990	625	.045	87	266	172	75
CP007	" " "	19.1	3059	105	.035	130	84	75	88
CP049	Cream intraclastic magnesite	25.4	2480	119	.048	121	50	93	84
CP056	Dark-grey magnesite mudstone	16.4	3228	129	.040	85	28	22	96
CP081A	Grey magnesite mudstone	11.3	7639	221	.029	164	50	62	90
CP110	Cream intraclastic magnesite	8.3	3706	146	.039	80	63	19	98
CP120A	Cream magnesite mudstone	7.7	1079	48	.044	100	8	2	99
CP125	Cream intraclastic magnesite	41.0	607	40	.066	112	93	219	78
A017A	Grey magnesite mudstone	25.4	3283	634	.193	23	705	562	93
A045	Light-grey magnesite-dolomite mudst.	49.6	7938	499	.063	105	3294	431	43
A047	Light-grey intraclastic magnesite	41.1	9973	485	.049	65	2714	237	67
A048	" " " "	33.0	7754	367	.047	31	1909	365	57
A060	Disrupted grey magnesite mudstone	12.1	4996	248	.050	38	126	37	97
A141	Grey magnesite mudstone	17.0	4816	214	.044	33	343	96	88
W053	Cream intraclastic magnesite	18.0	3110	173	.056	54	15	141	78
W072	" " "	6.6	845	35	.041	111	45	118	89
Q074	Grey magnesite mudstone	7.1	963	53	.055	156	41	111	85
W138	Cream intraclastic magnesite	9.8	1002	73	.073	130	28	158	67
W142	" " "	5.5	616	53	.086	146	50	63	86

APPENDIX 5

REPRINT OF PAPER

"Stratigraphy and depositional environments of the Mundallio Subgroup (new name) in the late Precambrian Burra Group of the Mt. Lofty and Flinders Ranges" by Robin K. Uppill.

Published in

Transactions of the Royal Society of South Australia,
Volume 103, Part 2, pages 25-43.

REPRINTED FROM

Transactions of the Royal Society of South Australia

Vol. 103, Pt. 2, pp. 25-43

STRATIGRAPHY AND DEPOSITIONAL ENVIRONMENTS OF
THE MUNDALLIO SUBGROUP (NEW NAME) IN THE LATE
PRECAMBRIAN BURRA GROUP OF THE MT LOFTY AND
FLINDERS RANGES

By ROBIN K. UPPILL

ADELAIDE
February, 1979

Uppill, R.K. (1979). Stratigraphy and depositional environments of the Mundallio subgroup (new name) in the late Precambrian Burra group of the Mt Lofty and Flinders Ranges *Transactions of the Royal Society of South Australia*, 103(2), 25-43.

NOTE:

This publication is included in the print copy
of the thesis held in the University of Adelaide Library.